Identification and evaluation of the driving mechanisms like bioavailability for xenobiotics degradation optimization in wastewater treatment

Glenda Cea-Barcia

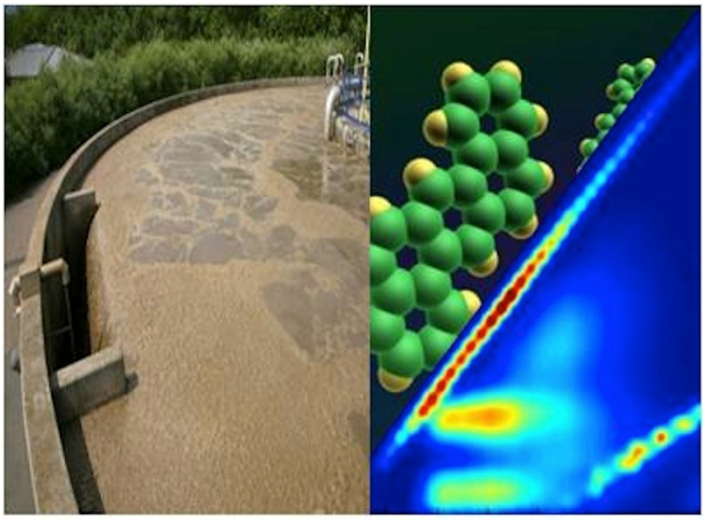

Identification and evaluation of the driving mechanisms like bioavailability for xenobiotics degradation optimization in wastewater treatment

Identification des mécanismes qui gèrent la disponibilité des micropolluants organiques en vue de l'optimisation de leur dégradation au sein d'écosystèmes épuratoires

PhD thesis 2012

Glenda Edith CEA-BARCIA

ALIMENTATION
AGRICULTURE
ENVIRONNEMENT

SCIENCES ET TECHNIQUES DU LANGUEDOC

T H E S E

pour obtenir le grade de

DOCTEUR DE L'UNIVERSITE MONTPELLIER II

Formation Doctorale : Génie des procédés.
Ecole Doctorale : Sciences des Procédés-Sciences des Aliments

présentée et soutenue publiquement

par

Glenda Edith CEA-BARCIA
Ingénieur en Biochimie

le 29 Mai 2012

Titre :

Identification des mécanismes qui gèrent la disponibilité des micropolluants organiques en vue de l'optimisation de leur dégradation au sein d'écosystèmes épuratoires

JURY

M^{me} **C. ALBASI**
Directrice de Recherche, CNRS , Rapporteur
M^{me} **T. GORNER**
Maitre de conférences, Université de Lorraine , Rapporteur
M. **A. GRASMICK**
Professeur, Université de Montpellier II , Examinateur
M^{me} **M. CASELLAS**
Maitre de Conférences ENSIL , Examinateur
M. **Y. DUDAL**
Docteur, Envolure , Invité
M^{me} **H. CARRERE**
Directrice de Recherche, INRA Narbonne , CoDirectrice de thèse
M^{me} **D. PATUREAU**
Directrice de Recherche, INRA Narbonne , Directrice de Thèse

Résumé: Les micropolluants organiques (MPO) tels que les HAPs, PCBs et NP sont sous la surveillance étroite des différentes agences de santé et de l'environnement à cause de leurs effets toxiques, cancérigènes et perturbateurs endocriniens sur les organismes vivants. Dans l'environnement, ils se retrouvent dans le sol, les aquifères, les eaux usées, et en raison de leurs propriétés hydrophobes, ces MPO sont principalement associés aux compartiments matière organique dans les boues d'épuration et les sédiments de rivières. La digestion anaérobie, procédé de stabilisation des boues, présente un potentiel pour l'abattement de ces composés. Les deux principaux mécanismes qui régissent l'abattement dans ces conditions des MPO sont le cométabolisme et la biodisponibilité. Leur double influence est évaluée dans ce travail, avec un focus fort sur l'étude des interactions MPO-matrice, la détermination de la distribution des MPO dans les compartiments physiques de la matrice (libre, sorbé à la matière dissoute et colloïdale (DCM) et sorbé aux particules) et avec une caractérisation fonctionnelle, physique et chimique détaillée de la matrice. Pour cela, des réacteurs anaérobies continus et batch ont été mis en œuvre avec des boues de caractéristiques différentes. L'abattement des MPO varie considérablement en fonction des caractéristiques des boues s'expliquant soit par des variations du niveau de cométabolisme, soit par les différents niveaux de biodisponibilité ; ceci suggère qu'une caractérisation détaillée de la matrice boue pourrait aider à prévoir les niveaux d'abattement des MPO. Par ailleurs, les cinétiques en batch montrent que l'abattement des MPO est associé aux premières étapes de la digestion anaérobie, conjointement à leur transfert du compartiment des particules vers le compartiment aqueux. L'abattement des MPO s'observe simultanément dans les trois compartiments libre, sorbé à la DCM et sorbé aux particules. Il est aussi noté l'importance du compartiment DCM sur l'abattement des MPO de haut poids moléculaire. Les coefficients de partage K_{DOC} et K_{part} ont été calculés pour étudier les interactions MPO-matrice. Ces données couplées à celles de caractérisation fonctionnelle de la matrice par fluorescence 3D ont permis de construire un modèle explicatif et prédictif des interactions MPO-matrice à l'aide de la méthode de régression partielle des moindres carrés (PLS). Il a été constaté que le compartiment type acide humique a un rôle important dans les interactions MPO-matrice, principalement dans la phase aqueuse, et dans la phase particulaire, les protéines complexes régissent les interactions. Enfin, des modèles PLS explicatifs et prédictifs d'abattement total des MPO ont été construits. Il en ressort que l'abattement des MPO est favorisé par tous les paramètres du cométabolisme (abattement des divers compartiments matière) et par la concentration des MPO en phase aqueuse ce qui tenterait à confirmer que ce compartiment correspond au compartiment biodisponible. Le modèle prédictif basé sur les caractéristiques des boues initiales a identifié les concentrations initiales de MPO (libre et sorbé à la DCM) et le compartiment type protéines comme les variables les plus importantes qui permettent de prédire l'abattement total des MPO. Cette étude contribue ainsi à mieux comprendre la répartition des MPO dans les matrices boue, et son implication dans le devenir des MPO, de prévoir cette répartition par une caractérisation fonctionnelle de la matrice et de proposer des stratégies pour optimiser l'abattement des MPO au cours de la digestion anaérobie.

Mots-clés: Biodégradation, biodisponibilité, cométabolisme, micropolluants organiques, fluorescence 3D, sorption, PLS.

Abstract: Organic micropollutants (OPs) such as PAHs, NP and PCBs, are nowadays looked as environmental pollutants by environmental and health agencies because of their toxic, carcinogenic and endocrine disrupting effect on living organisms. Within the environment, they can deposit to soil, water bodies and sewage system and due to their hydrophobic properties, they are mainly associated with hydrophobic compartments such as organic matter in sewage sludge. Anaerobic digestion has been shown as a potential biological process for removing these compounds. The two main mechanisms that govern their anaerobic removals are the cometabolism and the bioavailability. In this work, cometabolism and bioavailability influences were evaluated focusing mainly on the study of the OP-organic matrix interactions, the determination of the OPs distribution among the physical compartments (free, sorbed to dissolved and colloidal matter (DCM) and sorbed to particles) combined with a detailed physical, chemical and functional matrix characterization. For this, continuous and batch anaerobic reactors were fed with different sludge samples. It was found that the OPs removals varied greatly as a function of sludge characteristics and that greater or lesser removal might be explained either by variations in cometabolism or by different levels of bioavailability, suggesting that a detailed characterization of the feed may help to predict the OPs removals. Additionally, batch kinetics demonstrated that OPs removals are coupled to the first step of the anaerobic digestion, jointly to the OPs transfer from the particles to the aqueous compartment. The OPs are simultaneously removed from the three physical compartments (free, DCM and particles). Moreover, it was highlighted the importance of the DCM fraction on the removal of the high molecular weight OPs. K_{DOC} and K_{part} partition coefficients were calculated to study the OP-organic matrix interactions coupled to a functional characterization by 3D fluorescence of the matrix in order to construct an explicative and predictive model of the OP-organic matrix interactions using partial least square regression (PLS). It was found that the humic acid-like compartment has a great role in the OP-organic matrix interactions mainly in the aqueous phase, and in the particulate phase, the complex proteins govern the interactions. Finally, explanatory and predictive PLS models of total OPs removals were constructed. It was concluded that OPs removals are favored by all cometabolic parameters (substrates removals) jointly to the aqueous OPs concentration which tends to confirm that this compartment corresponds to the bioavailable one. The predictive model based on the initial sludge characteristics, identified the initial OPs concentrations (free and DCM), representing the bioavailability, and the protein-like, representing the cometabolism influence, as the most important variables that predict the total OPs removals. This study contributes to better understand the OPs distribution among the sludge compartments and its role in the fate and removal of the compounds, to predict this distribution through matter functional characterization and to propose strategies in order to optimize the OPs removals under anaerobic conditions.

Keywords: Biodegradation, bioavailability, cometabolism, organic micropollutants, 3D fluorescence, sorption, PLS.

Remerciements

Je remercie chaleureusement mes encadrantes **Dominique Patureau** et **Hélène Carrère**. Merci pour votre disponibilité, votre confiance, votre patience et votre compréhension dans les moments difficiles et pour m'avoir offert l'opportunité de travailler au LBE. Vous ne pouvez pas imaginer tout ce que j'ai appris avec vous, merci !!.

Je remercie le **CONICYT du Gouvernement du Chili** pour son financement et m'avoir donné l'opportunité de me perfectionner.

Je remercie **Jean-Philippe Steyer** pour m'avoir accueillie dans son laboratoire, pour avoir mis à ma disposition les moyens nécessaires à ce projet de thèse.

Je remercie aussi les scientifiques du LBE qui m'ont aidé au cours de ce travail: **Eric Latrille et Nadine Delgenès.** Merci aussi à **Maialen Barret** et à **Mathieu Muller** pour m'avoir formé aux premières étapes de ce travail.

Je remercie les scientifiques de l'Institut des Sciences Moléculaires de l'Université de Bordeaux 1, CNRS, **Hélène Budzinski et Edith Parlanti** pour m'avoir donné l'opportunité de travailler dans leur laboratoire et d'apprendre des nouvelles techniques. Merci **Karyn** et **Marie** pour m'avoir formé et pour votre aide.

Je remercie les membres du jury **Claire Albassi** et **Tatiana Gorner**, rapporteurs, et **Alain Grasmick**, **Magali Casellas** et **Yves Dudal**, une mention particulière pour ces deux derniers pour m'avoir suivie et conseillée lors des comités de thèse.

Je remercie les professeurs **Andrés Illanes** et **Andrés Markovits** de la « Escuela de Ingeniería Bioquímica de la Pontificia Universidad Católica de Valparaíso » d'avoir contribué à ma formation scientifique et de m'avoir soutenue pour l'obtentionde ma bourse.

Finalement, je remercie chaleureusement mes anciens et nouveaux amis et tous les personnes avec qui j'ai partagé ces quatre années au LBE: Liliana, j'ai gagné une grande copine, je te porterai toujours dans mon coeur, « gracias chinita!! », Sarah, c'est vrai….c'est incroyable comme tu peux avoir plus de points communs avec quelqu'un qui habite à l'autre bout de la planète qu'avec ton voisin, Virginie, Xin Mei, Abi et Denisse, je suis très heureuse de vous avoir connues. Merci à mes collègues de bureau pour tous les bons moments partagés et pour votre aide: Florian, Carlos et Quentin; à mes collègues de Doctorat: Charly, Amel et Florence. Julian, Fred, Doña Elia, Salome, Sarita, Ganesh, Angeles, Cristina, Rim, Helen, Ivette, Andres, Kim, Doris, Cynthia, Elodie, Bea, etc…j'ai de très jolis souvenirs du bon temps partagé avec vous à Narbonne. Merci Juan pour m'avoir aidée à arriver au LBE. Merci Cristina, ma copine depuis toujours, pour m'avoir encouragé à faire une thèse à l'étranger et pour ta fidélité… toutes les sorties et réunions avec Christoph en Belgique vont me manquer.

Je suis arrivée depuis Chili en France pour faire une thèse et sans imaginer je croiserais un mexicain qui a changé mon chemin,…..cette réussite est aussi à toi « **mi pochonguito** », merci pour ton courage et pour croire en moi.

Mais tout cela n'aurait pas été possible sans toi…..Ce travail est dédié à mon père **Roque Cea Cordova**. Tu vois…j'ai réussi !!

Résumé

Les micropolluants organiques (MPO) tels que les HAPs, PCBs et NP sont sous la surveillance étroite des différentes agences de santé et de l'environnement à cause de leurs effets toxiques, cancérigènes et perturbateurs endocriniens sur les organismes vivants.

Les MPO sont majoritairement d'origine anthropique, même si certains peuvent être produits naturellement (HAPs issus de la combustion incomplète de matières organiques). Ils sont présents dans les déversements de pétrole brut, la combustion de combustibles fossiles, et dans la formulation d'une grande variété de lubrifiants, peintures, détergents, pesticides, résines, produits chimiques ménagers, produits de soins personnels et produits pharmaceutiques.

Une grande variété de ces substances est présente à très faible concentration (ng/L à µg/L) dans notre environnement. Transportés par l'air et les eaux, les MPO se retrouvent dans les sols, les cours d'eau et les eaux usées. Certains d'entre eux, du fait de leur faible solubilité dans l'eau et de coefficients de partage octanol-eau élevés, sont principalement associés à des matrices hydrophobes telles que la matière organique des boues d'épuration et des sédiments de rivières ou les lipides des organismes vivants. Ainsi, en raison de leur potentiel de bioaccumulation, leur persistance et leur toxicité, les études scientifiques se sont focalisées sur leurs sources et leurs devenirs, afin de quantifier leur entrée, leur concentration dans les divers compartiments de l'environnement (air, sol, eau), leur concentration dans les organismes vivants et leur effet toxique, et les processus et les dynamiques de dissipation (volatilisation, adsorption, dégradation chimique, biodégradation).

Les stations d'épuration des eaux usées peuvent être considérées comme un point de convergence pour divers MPO et jouer un rôle important dans la chaîne de diffusion de ces composés dans l'environnement. Dans ces systèmes, les composés hydrophobes sont simplement transférés ou sorbés sur les boues d'épuration produites lors du traitement des eaux usées, et leur élimination est souvent incomplète dans les procédés de traitement des boues. Les boues d'épuration, riches en matières organiques, sont majoritairement utilisées comme engrais et conditionneur de sol sur les terres agricoles françaises. Toutefois, l'application directe de ces boues contenant des MPO peut entraîner une contamination potentielle des sols et des eaux souterraines. Avant leur apport, les boues d'épuration sont traitées par plusieurs procédés afin d'assurer leur stabilisation, la digestion anaérobie est l'un de ces procédés de stabilisation des boues.

La digestion anaérobie présente plusieurs avantages, elle permet (i) la réduction des matières solides, (ii) une production d'énergie renouvelable sous la forme de biogaz et (iii) un abattement partiel des MPO concentrés dans les boues.

Différents mécanismes d'abattement des MPO dans les boues contaminées ont été identifiés en condition anaérobie. Ils dépendent des propriétés physico-chimiques des MPO, ainsi que des caractéristiques des boues et de l'état biologique du système. En effet, les deux principaux

mécanismes proposés dans la littérature qui régissent l'abattement anaérobie des MPO sont le cométabolisme (*ie* les interactions entre métabolisme des MPO et métabolisme des matières organiques de la boue en lien avec le potentiel microbiologique) et la biodisponibilité des MPO (*ie* les interactions entre matières organiques des boues et MPO).

L'objectif de cette thèse était d'évaluer les influences respectives de ces deux processus cométabolisme et biodisponibilité sur le devenir de micropolluants organiques dans le procédé de digestion anaérobie des boues. À cette fin, les approches expérimentales se sont concentrées principalement sur les interactions étroites entre les MPO et la matrice des boues.

Tout d'abord, l'influence des caractéristiques des boues sur les abattements des MPO a été évaluée dans des réacteurs anaérobies continus, mettant en évidence les effets conjoints et souvent indissociables entre les deux processus. Ensuite, la distribution des MPO dans les compartiments physiques des boues est étudiée à la fois sur des mélanges initiaux et au cours de cinétiques batch anaérobies de dégradation de MPO. Enfin, les interactions MPO-matrice sont étudiées au travers des phénomènes de sorption et de la distribution des MPO, combinés à une caractérisation physique, chimique et fonctionnelle détaillée de la matrice boue, ceci afin de mieux comprendre et identifier les principaux mécanismes qui régissent la biodisponibilité des MPO en vue d'optimiser leur dégradation.

Le manuscrit se divise en six chapitres.

Dans **le chapitre I**, le sujet de thèse est introduit et les objectifs sont énoncés. Les publications et les présentations orales issues de ces travaux sont listées.

Le chapitre II est dédié à la revue bibliographique.
Afin de replacer ce projet de thèse dans son contexte, la problématique de gestion des boues d'épuration ainsi que le positionnement du procédé de méthanisation face à cette problématique sont tout d'abord détaillés dans cette synthèse bibliographique.
La production, le traitement et l'élimination des boues d'épuration dans les systèmes d'épuration des eaux usées restent un problème environnemental grandissant. Les systèmes de traitement font face à des quantités d'effluents qui ne cessent d'augmenter, du fait de la croissance de la population et des activités. Leur fonctionnement génère donc des quantités croissantes de boue.
Les systèmes d'épuration des eaux usées traitent la matière organique et les nutriments présents dans les effluents industriels et domestiques. Les traitements les plus courants sont constitués de traitements primaires et secondaires qui produisent respectivement des boues primaires et secondaires. En général, indépendamment de l'origine des boues, les boues d'épuration contiennent 95% d'eau et 5% de matière sèche, et cette matière sèche est généralement constituée de matières organiques, de nutriments, de microorganismes, de métaux et de MPO.
Les MPO se retrouvent dans les boues à des teneurs variables allant de 0,001 à 10 mg/kg $_{DM}$ pour les hydrocarbures aromatiques polycycliques et les polychlorobiphényls jusqu'à 100 mg/kg $_{DM}$ pour les nonylphénols. Ces trois familles de MPO choisis dans cette étude sont toutes classées perturbateurs endocriniens par l'une ou l'autre des agences environnementales.
Des résultats récents ont démontré que certains HAPs, NPs et les PCBs présents à de faibles concentrations dans des boues secondaires et mixtes peuvent être dégradés dans des conditions méthanogènes. La biodégradation des MPO peut se produire via des mécanismes

différents: les MPO sont utilisés comme unique source d'énergie et de carbone pour la croissance des microorganismes ou bien la biodégradation des MPO dépend de la transformation métabolique d'un autre substrat primaire, qui est la source de carbone et d'énergie. Ce mécanisme est appelé cométabolisme. Différentes études ont montré que des consortia anaérobies peuvent croître avec des HAP de faible poids moléculaire et des NPs comme seule source de carbone. A l'inverse, la biodégradation des HAPs de haut poids moléculaire n'est possible que lorsqu'elle est combinée à d'autres voies métaboliques. Ce cométabolisme peut être stimulé par l'addition d'un substrat facilement biodégradable. Cependant, le principal mécanisme d'élimination des MPO hydrophobes des eaux usées est la sorption sur la fraction solide des boues. Ce phénomène de sorption des MPO à la matière organique conditionne directement la biodisponibilité des composés.
Cette revue montre que dans le contexte de matrices boues d'épuration contaminées par des MPO, le comportement des MPO est conditionné par une série de rétroactions et d'interactions complexes entre les différents composants du système qui sont MPO / microorganismes / matrice. D'une part, la paire matrice/microorganismes détermine le métabolisme basal de la communauté microbienne, ici anaérobie, en termes de voies métaboliques empruntées, de flux de carbone et d'énergie et d'accepteurs finaux d'électrons. Enfin, un lien direct s'établit entre le métabolisme basal de la communauté et la dégradation des MPO : le cométabolisme permet de coupler le métabolisme thermodynamiquement peu favorable des MPO au métabolisme basal, pour le rendre favorable. Les interactions physico-chimiques entre les MPO et la matrice (paire MPO/matrice), en termes de sorption, sont susceptibles d'influer sur la biodisponibilité des MPO aux microorganismes, et par conséquent sur leur biodégradation. Or, ces interactions varient selon les différentes origines des matrices et les compartiments physiques considérés de la matrice boue (phases particulaire et aqueuse) qui pourraient générer des comportements différents des MPO au sein du système. Considérant que des MPO contenus dans la phase aqueuse sont biodisponibles, différents auteurs ont étudié les interactions MPO-matière dissoute et colloïdale, afin d'identifier les principales molécules qui régissent le comportement des MPO dans cet environnement. Ceci suggère que la matière dissoute et colloïdale pourrait jouer un rôle important dans la biodisponibilité des MPO (liée à la nature de ces matières), à la fois en tant que substrat cométabolique et dans la distribution des MPO entre les compartiments physiques de la matrice. Enfin, la paire MPO/microorganisme définit un potentiel microbiologique par la présence d'organismes directement impliqués dans la dégradation anaérobie des MPO dans des conditions méthanogènes.
Pour comprendre la dynamique et optimiser le devenir des MPO au sein des systèmes épuratoires, ce réseau complexe d'interactions entre les trois composants sera considéré et décortiqué tout au long de ce manuscrit.

Le chapitre III regroupe l'ensemble des méthodes et des protocoles expérimentaux utilisés pour mener à bien les objectifs de cette thèse.

Le chapitre IV est dédié à l'étude de l'influence du cométabolisme et de la biodisponibilité des polluants sur l'élimination des MPO. Les abattements des MPO ont été mesurés en réacteurs anaérobies semi-continus alimentés avec différents types de boues d'épuration. Le panel de boues sélectionnées est suffisamment large pour *a priori* obtenir des comportements MPO et des cinétiques de réaction divers. En effet, les caractéristiques physico-chimiques de la boue digérée, et donc l'affinité des MPO pour ce digestat, dépendent de la matrice initiale d'alimentation. En outre, les rendements de transformation de la matrice dépendent également

de sa composition, de son accessibilité et de sa biodégradabilité. Ainsi, biodisponibilité et cométabolisme des MPO sont confrontés. Les résultats ont montré que les abattements des MPO par digestion anaérobie varient considérablement en fonction des caractéristiques des boues d'alimentation. Selon le réacteur, l'élimination plus ou moins grande peut être expliquée soit par des variations de cométabolisme ou par différents niveaux de biodisponibilité des MPO. Cependant, les résultats suggèrent qu'une caractérisation détaillée de l'alimentation, en particulier de la fraction aqueuse, peut aider à prédire l'abattement des MPO.

Le chapitre V est dédié aux cinétiques d'élimination des MPO en conditions anaérobies. Les abattements des MPO ont été mesurés dans des réacteurs batch alimentés avec différents mélanges de boues, mais inoculés avec le même consortium anaérobie adapté aux MPO. L'objectif était ici de mieux comprendre l'influence de la biodisponibilité sur les abattements des MPO au travers de l'étude du rôle de la concentration et de la nature de la matière dissoute et colloïdale sur la distribution des MPO dans les trois compartiments physiques de la boue, soit le compartiment libre, sorbé à la matière dissoute et colloïdale et sorbé aux particules. Les concentrations totales, aqueuses et libres des MPO ont été mesurées tout au long des expériences en utilisant la technique SPME-solid phase microextraction. Ainsi, les cinétiques des abattements des MPO dans les trois compartiments physiques de la boue ont été obtenues pour chaque mélange de boues.

Les cinétiques des abattements des MPO dans les réacteurs batch ont montré que les abattements des MPO sont couplés aux premières étapes d'hydrolyse et d'acidogenèse de la digestion anaérobie. Ces abattements sont conjoints à un transfert des MPO du compartiment particulaire vers le compartiment aqueux lors de l'hydrolyse des particules. Ce transfert des MPO permet l'élimination apparente et simultanée des concentrations libre, sorbée à la matière dissoute et colloïdale et sorbée aux particules. De plus, les résultats soulignent l'importance de la matière dissoute et colloïdale sur l'élimination des MPO de haut poids moléculaire qui est directement liée à la concentration initiale des MPO sorbés à ce compartiment. Cependant, même si un niveau élevé de cette concentration implique un fort abattement de cette concentration, l'élimination totale des MPO n'est pas uniquement régie par le compartiment dissout et colloïdale, mais l'est également par le flux cométabolique généré par l'hydrolyse de la matrice et par les phénomènes de transfert des MPO d'un compartiment à l'autre.

Le chapitre VI est dédié à l'étude des interactions MPO-matrice et leur influence sur l'élimination des MPO. Les coefficients de partition K_{DOC} et Kpart, c'est à dire les affinités respectives des MPO pour la matière dissoute et colloïdale et les particules, ont été calculés en utilisant les résultats SPME. Ces coefficients sont bien corrélés avec les Kow des MPO, mais sont différents entre les boues. Ils ont donc été utilisés pour construire un modèle explicatif et prédictif de ces interactions MPO-matrice avec la méthode statistique de régression partielle des moindres carrés (PLS). Les autres données explicatives choisies sont des données biochimiques et de caractérisation fonctionnelle par fluorescence 3D de la fraction aqueuse. Il a été constaté que les compartiments de type acides humiques-like et mélanoïdines-like ont un grand rôle dans les interactions MPO-matrice dans la phase aqueuse. Cette caractérisation de

la phase aqueuse par fluorescence 3D a également été utilisée pour expliquer et prédire l'affinité des MPO pour le compartiment de particules. Pour ce compartiment, en plus du compartiment matière du type acides humiques-like, les protéines complexes régissent les interactions MPO-matrice. Cependant, cette caractérisation fonctionnelle de la phase aqueuse n'est pas suffisante pour expliquer les interactions entre tous les MPO et la fraction particulaire, ce qui rend nécessaire une caractérisation plus détaillée de cette fraction afin de déterminer quel type de matière organique particulaire interagit avec les MPO. Le modèle prédictif de K_{DOC} présente quant à lui une très bonne précision en utilisant cette méthode simple et non-destructive de caractérisation fonctionnelle.

Des modèles PLS explicatifs et prédictifs des abattements totaux des MPO ont aussi été construits. Il en ressort que l'élimination des MPO est favorisée par tous les paramètres cométaboliques (élimination des substrats). La variable « concentration aqueuse des MPO » est elle aussi très fortement corrélée aux abattements, ce qui tend à confirmer que ce compartiment correspond au compartiment biodisponible. Le modèle prédictif PLS a été construit à partir d'une caractérisation plus détaillée initiale et en tenant compte de l'influence de la biodisponibilité (via la distribution initiale des MPO dans les trois compartiments matriciels). Les distributions initiales des MPO ont été identifiés comme les variables les plus importantes qui permettent de prédire les abattements totaux des MPO, avec une influence positive des concentrations « libre » et « matière dissoute et colloïdale » et négative de la concentration « particules ». Des paramètres de caractérisation des boues, les compartiments matière de type protéines-like, acides humiques-like et mélanoïdines-like présentent les plus grandes influences. Ces paramètres peuvent influer soit sur la biodisponibilité par affinités variables des MPO pour les différents compartiments soit indirectement sur le flux cométabolique.

De façon générale, ce sont la nature et la taille des colloïdes du compartiment aqueux qui participent aux interactions MPO-matrice. En effet, il a été montré en couplant SPME et filtration/ultrafiltration que les colloïdes de grande taille contribuent principalement à la sorption des MPO dans le compartiment aqueux.

Enfin, le chapitre VII reprend les diverses conclusions et ouvre ce travail sur des perspectives générales.

En général, deux principaux paramètres participent dans les interactions MPO-matrice: la nature et la taille des molécules. Ce dernier a été attesté par le couplage filtration/ultrafiltration-SPME. Il a été montré que les colloïdes de grande taille contribuent principalement à la sorption des MPO dans le compartiment aqueux. En ce qui concerne la nature des molécules, trois groupes fonctionnels jouent un rôle important sur les interactions MPO-matrice ainsi que sur l'influence cométabolique: les protéines-like, les acides humiques-like et les mélanoïdines-like. En outre, ces interactions MPO-matrice régissent principalement les abattements des HAPs de haut poids moléculaire démontrant que la biodisponibilité et la biodégradation de ces composés dépend directement de leurs interactions avec la matière organique (substrat métabolique). Toutefois, le transfert des MPO des particules vers le

compartiment aqueux est identifié comme le principal facteur limitant les abattements totaux des MPO, lui-même dépendant principalement du flux cométabolique (hydrolyse de la fraction particulaire) et des phénomènes de sorption / désorption.

De plus, dans cette étude, deux techniques innovantes qui n'ont pas été utilisé auparavant dans les boues d'épuration ont été testées: la SPME et AF^4. En effet, ces deux techniques sont habituellement appliquées à des échantillons aqueux de faible charge organique, issus de rivières ou de lacs. Elles ont été appliquées avec succès à des échantillons aqueux de boue avec une forte concentration en matière organique avec, dans le cas de la SPME, la mesure des concentrations de MPO libres, sorbés à la matière dissoute et colloïdale et sorbés aux particules et dans le cas d'AF4, la séparation des colloïdes en fonction de leur taille.

List of abbreviations and symbols

Dimension

d	Days
g	Gram
kg	Kilogram
L	Liter
mg	Milligram
ng	Nanogram
µg	Microgram

Abbreviations

Name	*Description*	*Dimension*
AD	Anaerobic Digestion	
AF^4	Asymmetrical flow field-flow fractionation	
COD	Chemical Oxygen Demand	g_{O2}/L
$C_{OP,free}$	Free OP concentration	µg/L or ng/L
$C_{OP,DCM}$	Sorbed to dissolved and colloidal matter OP concentration	µg/L or ng/L
$C_{OP,aqu}$	Aqueous OP concentration	µg/L or ng/L
$C_{OP,part}$	Sorbed to particles OP concentration	µg/L or ng/L
Cx	Cross flow	
DCM	Dissolved and Colloidal Matter	
DM	Dry matter	g/L
DOC	Dissolved organic carbon	g/L or kg/L
DOM	Dissolved organic matter	
EEM	Excitation-emission matrix	
EPA	U.S. Environmental Protection Agency	

EPS	Extrapolymeric Substances	
eq-BSA	Serum albumin equivalents	g eqBSA/gTOC or g eqBSA/gDOC
eq-EEP	Extractable petroleum ether equivalent	g eqEEP/gTOC
EU	European Union	
FFF	Field-flow fractionation	
F4	Chemical Oxygen Demand < 1kDa	(%)
GC	Gas Chromatography	
HLSS	High loaded secondary sludge	
HLSS-1kDa	High loaded secondary sludge with 1kDa DCM	
LLSS	Low loaded secondary sludge	
HRT	Hydraulic retention time	t
HPCD	Hydroxypropyl-β-cyclodextrin	
IARC	International Agency for Research on Cancer	
JEA	Japan Environment Agency	
Kd	Sorption coefficient	
Kow	Octanol-water partition coefficient	
K_{DOC}	DOC/free partitioning coefficients	L/gDOC
K_{part}	POC/free partitioning coefficients	L/gPOC
MS	Mass spectrometry	
NMR	Nuclear magnetic resonance	
NP	Nonylphenol	
NPE	Nonylphenol Polyethoxylates	
NP1EO	Nonylphenol Monoethoxylate	
NP2EO	Nonylphenol Diethoxylate	
NPEC	Nonylphenoxy Carboxylic Acid	

PAHs	Polycyclic Aromatic Hydrocarbons	
PCBs	Polychlorinated Biphenyls	
PS	Primary Sludge	
POC	Particulate organic carbon	g/L or kg/L
OM	Organic matter	
OPs	Organic micropollutants	
OSPAR	Oslo and Paris Commission	
SS	Secondary Sludge	
SOM	Solid organic matter	
SPE	Solid phase extraction	
SPME	Solid phase microextraction	
TE	Trace Elements	
TOC	Total organic carbon	g/L or kg/L
TS	Total Solids	g/L or kg/L
USEPA	United States Environmental Agency	
UKEA	United Kingdom Environment agency	
VFAs	Volatile Fatty Acids	g/L
WWF	World Wildlife Fund	
WWTP	Wastewater Treatment Plants	

Table of contents

List of figures

List of tables

I. GENERAL INTRODUCTION

Introduction and objectives

Organic micropollutants are nowadays looked as environmental pollutants by environmental and health agencies because of their toxic, mutagenic, carcinogenic and endocrine disrupting effects on living organisms, mainly on aquatic ecosystems and humans.

Organic micropollutants are mainly formed during human activities such as crude oil spillage, fossil fuel combustion, and are present in the formulation of a large variety of lubricants, paints, detergents, pesticides, resins, household chemicals, personal care products and pharmaceuticals.

A huge variety of these substances are present at very low concentration (ng/L to µg/L) in our environment. Through the air and runoff after rainy events, the organic micropollutants can deposit to soil, water bodies and sewage system. For some of them, due to their low water solubility and high octanol-water partition coefficients, they are mainly associated with hydrophobic compartments such as the organic matter in sewage sludge and river sediments or the lipids in biota. Indeed, due to their persistence, bioaccumulation potential and their toxicity, different scientific studies have focused on their sources and fate, i.e., to minimize their input, their concentration in various environmental compartments (air, soil, water), organisms bioconcentration, processes and dynamic of dissipation (volatilization, adsorption, chemical degradation, biodegradation).

The wastewater treatment plants are considered as a point of convergence for various organic micropollutants and play an important role on the chain of dissemination of these compounds through the environment. A large amount of various organic micropollutants, especially the hydrophobic compounds, are transferred or sorbed to the sewage sludge produced during wastewater treatment, and their elimination is often incomplete in the sludge treatment processes. Sewage sludge could be of great advantage if used in farmland as fertilizer and soil conditioner. However, the direct application of this sludge containing micropollutants on agricultural fields may cause a potential contamination of the soil and groundwater. Before their disposal, sewage sludge can be treated by several processes in order to ensure their stabilization and sanitation, being the anaerobic digestion, one of the most used processes.

The anaerobic sludge digestion presents several advantages, it allows (i) an efficient reduction of solids, (ii) a production of renewable energy in the form of biogas and (iii) a partial removal of the organic micropollutants concentrated in the sludge.

Different mechanisms of organic micropollutants removals in contaminated sludge under anaerobic conditions have been identified. They depend on their physicochemical properties, as well as the sludge characteristics and the operating condition of the biological process. Indeed, the two main mechanisms that govern their anaerobic removal are the cometabolism and the bioavailability.

The objective of the thesis was to evaluate the influences of cometabolism and bioavailability on organic micropollutants fate in sludge anaerobic digestion process. For this purpose,

experimental and scientific approaches were focused mainly on the tight interactions between the organic micropollutants and the sludge matrix. First, the influence of sludge characteristics on the organic micropollutants removals is evaluated, confronting the cometabolism and bioavailability influences. After, the organic micropollutants distribution among the physical sludge compartments jointly to their removals kinetics is determined and studied. Finally, the organic micropollutants-sludge matrix interactions are studied through the sorption phenomena and the organic micropollutants distribution combined with a detailed physical, chemical and functional matrix characterization in order to better understand and identify the key mechanisms that govern the organic micropollutants bioavailability on ways to optimize their degradation.

The chapter II is dedicated to the literature review, the chapter III is dedicated to the experimental and analytical mythologies used, the chapter IV shows an initial approach to study the cometabolism and bioavailability influences, the chapter V is a more detailed study of these aspects showing the removals kinetics among the different physical compartment and the chapter VI presents the link between OPs removals and a detailed characterization of the sludge matrix.

List of publications, submitted articles, oral presentations and posters:

Barret M., **Cea Barcia G.**, Guillon A., Carrère H., and Patureau D. (2010). *Influence of feed characteristics on the removal of micropollutants during the anaerobic digestion of contaminated sludge*. Journal of Hazardous Materials 181, 241-247.

Barret M., Delgadillo-Mirquez L., Trably E., Braun F., **Cea-Barcia G**., Steyer J.P. and Patureau D. (2011). *Trace organic contaminant removal under anaerobic conditions: 15 years of experience.* Pedosphere, Accepted.

Cea-Barcia G., Carrère H., Steyer J.P. and Patureau D. (2012*). Evidence for PAH and NP removal coupled to the first steps of anaerobic digestion in sewage sludge*. Chemosphere, Submitted.

Oral Presentations:

"PAH biodegradation kinetics under anaerobic conditions: link between sorption, bioavailability and cometabolism". 5th European Bioremediation Conference, July 2011, Chania, Crete, Greece.

"Biodegradation of PAHs during the anaerobic digestion of sludge: modeling the limitations by bioavailability and cometabolism". 12th World Congress on Anaerobic Digestion (AD12), November 2010, Guadalajara, México.

Poster:

Florence Braun, **Glenda Cea-Barcia** and Liliana Delgadillo-Mirquez. *Approche intégrée et pluridisciplinaire de la dégradation des perturbateurs endocriniens dans un procédé modèle*

de digestion anaérobie de boues urbaines. June, 2011. Journée de l'ED Sciences des Procédés, Sciences des Aliments, Montpellier, France.

Cea Barcia Glenda, Carrère Hélène, Budzinski Hélène, Le Menach Karyn, Patureau Dominique. *Role of dissolved and colloidal matters on the distribution and the removal of PAH in sewage sludge.* June 25-27th 2012, Santiago De Compostela (Spain). EcoSTP/ Ecotechnologies for Wastewater Treatment.

II. Literature Review

II.1 Production, treatment and disposal of sewage sludge

II.1.1 Sludge production: wastewater treatment plants

The wastewater treatment plant (WWTP) removes the organic matter and the nutrient present in runoff, industrial and domestic effluents. The most common municipal wastewater treatments are constituted of primary and secondary treatments.

The primary treatment consists of removing a substantial amount of the suspended solids from wastewaters. The secondary treatment consists of bio-oxidizing the remaining organic suspended solids and the dissolved organic matter. The Figure II-1 shows the diagram of a conventional activated sludge plant followed by anaerobic digestion of sludge. It consists of screening, grit removal, primary clarification and secondary treatment. The thick solids are removed by screening and the sand is removed by the grit removal system. The primary clarification removes most of the suspended solids and produces the primary sludge. The primary effluent is mixed with the return activated sludge. The mixture flows to the aeration tank where the remaining organic matter is biodegraded under aerobic conditions, and then the final clarifier removes the biological solids (return and waste activated sludge). The effluent from the final clarifier may be disinfected to kill pathogenic organisms and then discharged to the receiving body of water. The waste activated sludge, named secondary sludge, is mixed with the primary sludge and sent to the anaerobic digester for biodegradation of organic solids. The digested sludge is dewatered, for example, by centrifugation or vacuum filtration, and the dewatered sludge is either thermally treated, or used as soil fertilizer, or disposed in a sanitary landfill, or mixed with green waste for composting.

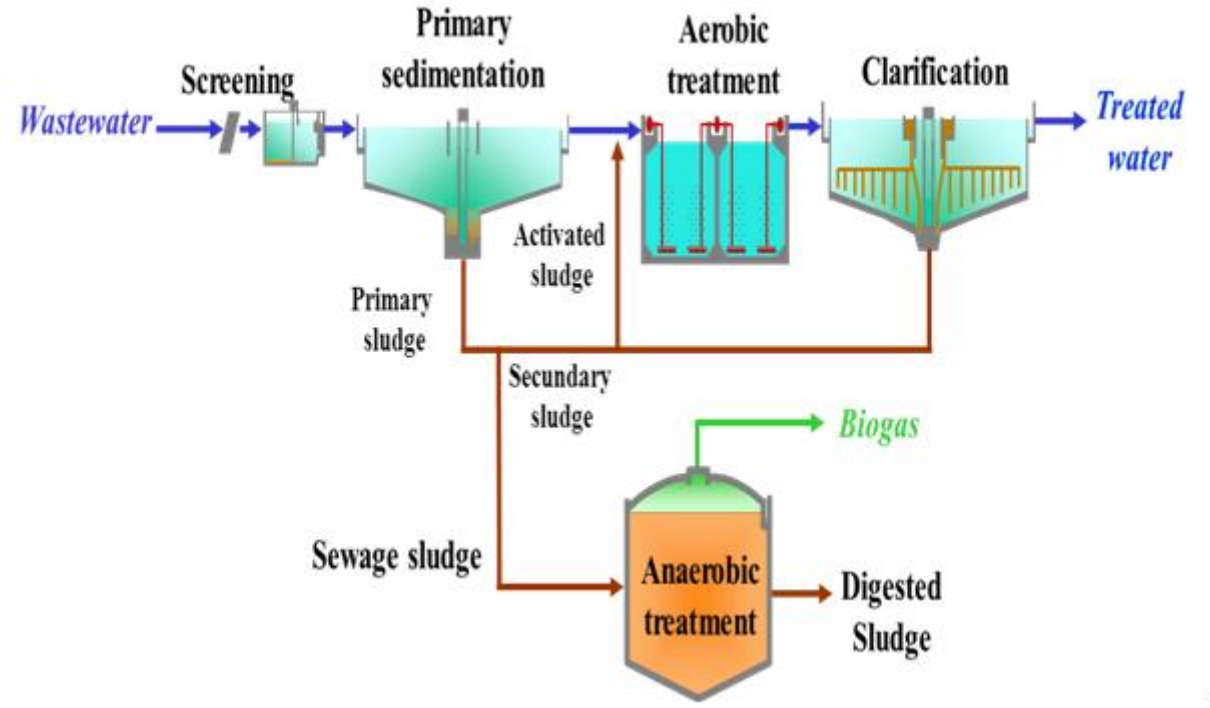

Figure II-1: Conventional wastewater treatment plant system.

II.1.2 Sewage sludge characteristics

II.1.2.1 Sludge physicochemical characteristics

To treat and dispose of the sewage sludge produced from wastewater treatment plants it is important to know their physicochemical characteristics. The characteristics vary depending on the origin of the sludge and the type of process. The sewage sludge can be classified into three types of sludge: primary, secondary and mixed sludge (primary and secondary). Primary sludge that comes from the primary clarifier has a high organic content since it is mainly composed by untreated organic matter, therefore, has a high potential to be biodegraded. Secondary sludge that comes from the final clarifier and that corresponds to waste activated sludge is mainly made of biomass and refractory matter from the aerobic treatment. Its potential to be biodegraded depends on the sludge retention time of the secondary treatment (sludge stability).

In general, regardless of sludge origin, the sewage sludge contains 95% of water and 5% of dry matter, and this dry matter is usually made of organic matter (measured as volatile solids), nutrients, microorganisms, metals and micropollutants. Typical data on the chemical composition of untreated sludge samples are reported in Table II-1. The organic matter contents mainly extracellular polymers and effluents polymers such as cellulose and humic acids and large quantities of proteins.

Table II-1: Typical chemical composition and properties of untreated sludge (Metcalf and Eddy, 1991)

Item	Untreated primary sludge, range	Untreated secondary sludge, range
Total dry solids (TS), %	2.0-8.0	0.83-1.16
Volatile solids (% of TS)	60-80	59-88
Grease and fats (% of TS)		
Ether soluble	6-30	-
Ether extract	7-35	5-12
Protein (% of TS)	20-30	32-41
Nitrogen (N, % of TS)	1.5-4	2.4-5.0
Phosphorus (P_2O_5, % of TS)	0.8-2.8	2.8-11.0
Potash (K_2O, % of TS)	0-1	0.5-0.7
Cellulose (% of TS)	8-15	-
Iron (not as sulfide)	2-4	-
Silica (SiO_2, % of TS)	15-20	-
pH	5-8	6.5-8.0
Alkalinity (mg/L as $CaCO_3$)	500-1500	580-1100
Organic acids (mg/L as HAc)	200-2000	1100-1700

The sewage sludge has high concentrations of different kinds of microorganisms (from 5 to 20% of total dry matter), such as bacteria (1012 to 1013 bacteria/g), protozoa and fungus. The

rest 80 to 95% is made of extrapolymeric substances (EPS). EPS are extracellular organic matter, such as bacterial secretions and bacterial lysis products, or molecules coming from the raw wastewater that are adsorbed on microorganisms. (Nielsen et al., 2004). They are made of mainly polysaccharides and proteins, and in lower quantities of humic substances, uronic acids, phospholipids and nucleic acids (Frolund et al., 1996). The main functions of the EPS are the formation and stabilization of flocs structure, water retention, sorption of exogenous compounds and hydrolytic activity (Laspidou and Rittmann, 2002). The flocculation process is explained by interactions between functional groups of EPS negatively charged and divalent cations. The EPS functional groups are ionizable groups such as carboxylic, phosphoric, sulfonic, amines and hydroxyl, that give a global negative charge to the floc. This negatively charged floc interacts with cations such as Ca^{2+} and Mg^{2+} that serve as bridges between the EPS and the microbial surface. These interactions favor the aggregation and stabilization of the matrix formed by EPS and microorganisms (Sobeck and Higgins, 2002). Thus, EPS, microorganisms, filamentous bacteria and metallic cations form flocs and microflocs through electrostatic interactions, and a complex sludge structure is constituted.

Figure II-2 shows a typical morphology of conventional activated sludge, in which filaments are observed (Figure II-2 a and b). The scanning electron microscopy reveals that the sludge had a very loose and irregular three-dimensional structure (Figure II-2 c). The typical floc sizes are in the range 10-70 µm with floc densities in the range 1.015-1.034 g/cm^3. A strong correlation between floc density and size has been reported. The specific floc surface area (typically 100-200 m^2/g dry sludge) is one to two orders of magnitude higher than the corresponding geometric floc surface area, indicating a porous floc structure (Andreadakis, 1993; Tay et al., 2001).

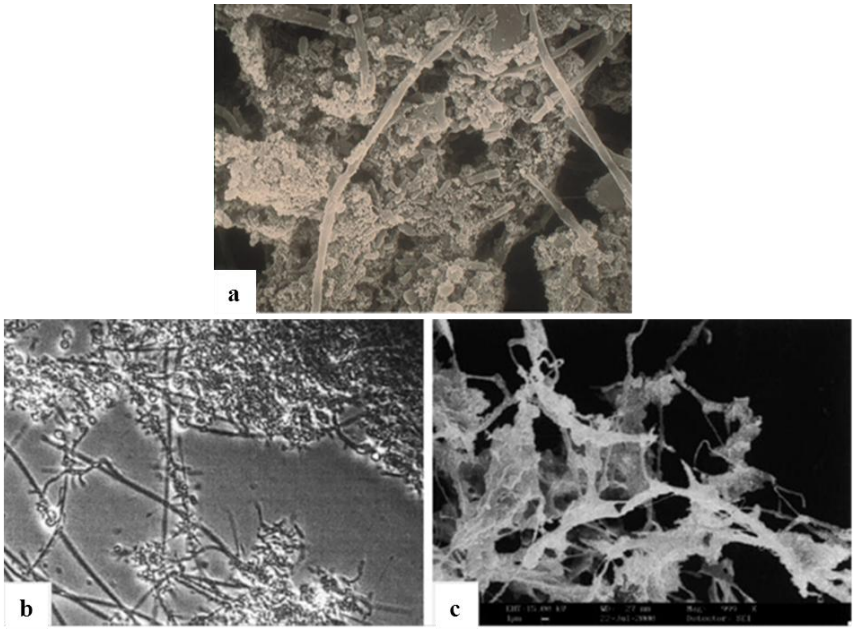

Figure II-2: Morphology of activated sludge flocs. (a) Optical microscopy 5000X; (b) optical microscopy of activated sludge; (c) scanning electron microscopy of activated sludge (Tay et al., 2001).

The sludge can be fractionated according to three phases or physical compartments: particulate, colloidal and soluble. The flocs correspond to the particulate phase and the rest of the matter can be located in the colloidal and soluble phase. The colloids are solids microscopically dispersed in a solvent (water) with sizes from 1 nm to 1 mm, which have, among other characteristics, an important specific area and usually, a negative electrostatic charge (Degrémont, 1989; Lead and Wilkinson, 2006). The colloidal matter consists of a heterogeneous mixture of polydisperse inorganic and organic components. Major inorganic colloids are often dominated by iron oxides, whereas the colloidal organic matter is mainly composed of humic substances and EPS. Colloidal stability is controlled by coagulation and flocculation processes, depending on the size, the shape and the relative concentration of colloidal components (Buffle et al., 1998).

Distinguishing these three compartments is complicated. The criterion most used is the compounds size by membrane separation. However, the size to separate the colloidal phase varies greatly among different authors (McCarthy and Zachara, 1989). For this reason, the sludge compartments are separated according to the French standard norm NF EN 872 of suspended matter by filtration at 1.2 µm on microfiber filter. The compounds lower than 1.2 µm are commonly called "soluble matter" even if this phase includes colloidal matter. This approach is acceptable due to the similar physical behavior of the colloids and the soluble matter.

II.1.2.2 Presence of micropollutants in the sludge

Sewage sludge can contain some micropollutants, which might show adverse effects on the ecosystem. Indeed, chemical pollution in rainfall-runoff and wastewater resulting from atmospheric washout, erosion of building materials, traffic emissions, pesticides application, industrial production, use of household chemicals, personal care products and pharmaceuticals are numerous sources for trace elements (TE) (Table II-2), organo-metallic pollutants and man-made organic micropollutants (OPs) found in WWTP that end up in sewage sludge. The main groups of OPs, usually named xenobiotics or persistent organic pollutants, are the polycyclic aromatic hydrocarbons, polychlorinated biphenyls, pesticides, dioxins, detergent derivates (nonylphenol), etc. As a consequence, some countries have already implemented cut-off values for these compounds found in sewage sludge and EU has proposed a draft for modifying the Sewage Sludge Directive of 1986. The Sewage Sludge Directive of 1986 already limited the level of TE for sewage sludge spreading: as a consequence, since application of the Directive, the level of TE has sharply decreased essentially due to source action. In the case of emerging contaminants such as organotins, their presence in sewage sludge has been frequently demonstrated: up to 1700 and 750 µg (Sn)/kg of dry sludge for total organotins and triorganotins respectively. For the OPs, a broad variation of the levels is found in the literature due to diverse analytical methodologies and variability of the wastewater and sludge treatment processes, from 0.001 to 10 mg/kg_{DM} for polycyclic aromatic hydrocarbons (Abad et al., 2005; Blanchard et al., 2004; Bodzek and Janoszka, 1999), 100 mg/kg_{DM} for nonylphenol (Aparicio et al., 2007; Fountoulakis et al., 2005) and 0.1 mg/kg_{DM} for polychlorinated biphenyl (Katsoyiannis and Samara, 2004).

However, it seems that some compounds have very high levels (detergents and plasticizers) with medium toxicity and persistence and some others low levels (halogenated or not hydrocarbons, pesticides, flame retardant, pharmaceuticals) but high toxicity and persistence.

Table II-2: Typical metal trace element content in sewage sludge (Metcalf and Eddy, 1991)

	Dry sludge mg/kg
Metal	**Median**
Arsenic	10
Chromium	500
Copper	800
Iron	17000
Lead	500
Mercury	6
Nickel	80
Zinc	1700

II.1.3 Treatment and disposal of sewage sludge

II.1.3.1 Stages of sewage sludge treatment

The sewage sludge requires different treatments before use and disposal in order to reduce its fermentative potential, volume, and to eliminate pathogens. These treatments consist of four main stages (Metcalf and Eddy, 1991).

Thickening (concentration): Thickening is a physical procedure used to increase the solids content of sludge by removing a portion of the liquid fraction. In general, the sludge volume can be reduced until five-fold. Typical sludge-thickening methods are: gravity settling, flotation, centrifugation and gravity belts.

Stabilization: Sludge is stabilized to reduce pathogens, eliminate offensive odors and inhibit, reduce, or eliminate their fermentative potential. The main operations or methods used for sludge stabilization are biological reduction of organic matter, chemical oxidation of organic matter, and the application of heat to disinfect or sterilize the sludge. The biological processes used for sludge stabilization are the anaerobic digestion, aerobic digestion and composting. The most sustainable stabilization technology according to a life cycle analysis is the anaerobic digestion due to the energy production (Suh and Rousseaux, 2002).

Conditioning: Sludge is conditioned expressly to improve its dewatering characteristics. The two most commonly used methods involve the addition of chemicals and heat treatment. Both chemicals and heat treatment coagulate the solids, break down the gel structure, and consequently, reduce the water affinity of sludge solids. Conditioning is used before mechanical dewatering systems such as vacuum filtration and centrifugation.

Dewatering: Dewatering is a physical unit operation used to reduce the moisture content of sludge. This operation is required normally prior to the sludge incineration, composting and

landfilling to reduce leachate production at the landfill site. The dewatering processes include vacuum filters, centrifuges, drying beds, among others.

II.1.3.2 Stabilization of sewage sludge by anaerobic digestion

General aspects

Anaerobic digestion is one of the oldest processes used for the stabilization of sludge. The anaerobic digestion may be defined as the process in which microorganisms degrade the organic matter without oxygen into a variety of end products including methane (CH_4) and carbon dioxide (CO_2), and new cells. The anaerobic digestion consists of four stages (Figure II-3) where different microbial populations participate: (1) hydrolysis, (2) acidogenesis, (3) acetogenesis, and (4) methanogenesis.

Stages of anaerobic digestion

Hydrolysis: The most important components in sludge are polymeric compounds such as carbohydrates, proteins and lipids. The anaerobic digestion process begins with the hydrolysis of these compounds into monomers that are available for other microorganisms (Batstone et al., 2002)

Different groups of fermentative bacteria are capable to degrade complex polymeric compounds into oligo- and monomers by excreting extracellular enzymes. The proteolytic bacteria produce proteases to catalyze the hydrolysis of proteins into amino acids, the cellulolytic and xylanolytic bacteria produce cellulases and/or xylanases to degrade cellulose and xylan to glucose and xylose respectively, and finally the lipolytic bacteria produce lipases to degrade lipids to glycerol and long chain fatty acids.

In the case of the anaerobic digestion of sludge and solid waste, the hydrolysis is the limiting step due to the high content of complex polymers.

Acidogenesis: The acidogenesis is the process where the hydrolysis products are converted to carbon dioxide, hydrogen, alcohols and volatile fatty acids (VFAs) such as acetic, propionic, butyric, etc. by fermentative bacteria.

In an optimal anaerobic digestion process, most of the hydrolysis products are transformed to methanogenic substrates (hydrogen, carbon dioxide and acetate). However, a significant part (approx. 30%) is transformed into metabolic intermediates (other fatty acids and alcohols).

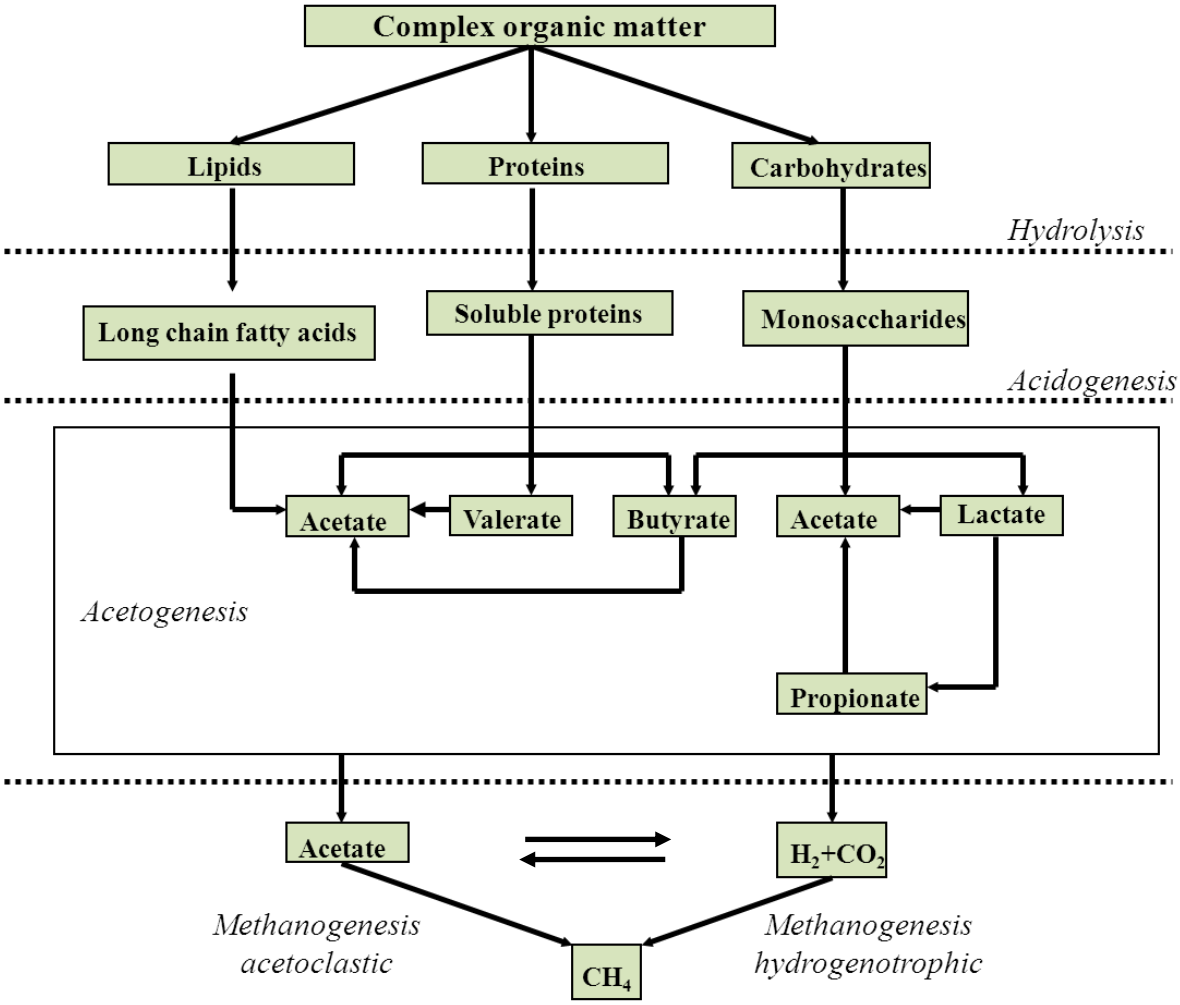

Figure II-3: Stages of anaerobic digestion.

Acetogenesis: The metabolic intermediates are converted to acetic acid, hydrogen and carbon dioxide by three different groups of *Bacteria*: hydrogenic acetogenic (syntrophic bacteria), homoacetogenic and sulfatoreductive (Ahring, 2003).

Overall, the reactions of acetogenesis are slow, and subjected to the phenomena of inhibition by hydrogen. The acetogenesis is thus achieved efficiently in the presence of hydrogen consuming microorganisms such as Homoacetogens, Sulfatoreductors and Methanogens (Delbes, 2000). The balance of interactions on the hydrogen transfer between species is an important factor for the stability of the microbial consortium.

Methanogenesis: The methanogenic microorganisms (strict anaerobic *Archaea*) convert the acetic acid, hydrogen and carbon dioxide into methane. The two main metabolic pathways, attributed to the *Archaea* are the following:

Archaea methanogenic acetoclastic: $CH_3COOH \longrightarrow CO_2 + CH_4$

Archaea methanogenic hydrogenotrophic: $CO_2 + 4H_2 \longrightarrow 2H_2O + CH_4$

The most important methane precursor is acetate (70%), while the remaining is formed from H_2/CO_2. Only the genera *Methanosarcina* and *Methanosaeta* can degrade the acetate into methane and a number of *Methanosarcina* species can transform the hydrogen as well as acetate. Substrates of less quantitative importance for methanogenic are: formate, methanol, methylsulfides, methylamines and some higher alcohols.

Because Methanogens are the most sensitive microorganisms of the anaerobic digestion consortium (inhibition by the VFAs and ammonia), they govern the overall operation of the process (Trably, 2002).

Operational and environmental conditions

To maintain an anaerobic treatment system, the *Bacteria* and *Archaea* must be in a state of dynamic equilibrium. To accomplish this, the reactors contents should be without dissolved oxygen and free of inhibitory concentrations of constituents such as heavy metals, sulfides and ammonia. Also, the pH of the aqueous environment should range from 6.6 to 7.6. Sufficient alkalinity should be present to ensure that the pH will not drop below 6.2 because the Methanogens cannot function below this point. When digestion is proceeding satisfactorily, the alkalinity will normally range from 1000 to 5000 mg/L, and the VFAs will be less than 250 mg/L. A sufficient amount of nutrients, such as nitrogen and phosphorus, must also be available for the growth of the microbial community. Temperature is another important environmental parameter. The optimum temperature ranges are the mesophilic, 30 to 38°C, and the thermophilic, 49 to 57°C. In the case of free biomass digester, the hydraulic retention time (HRT) should be of the magnitude of slower species (methanogens) to avoid washing out the reactor. In general, this corresponds to approximately 20 days in mesophilic conditions.

II.1.3.3 Disposal of sewage sludge

Regulation for sludge disposal

Every year, wastewater treatment plants generate millions of tons of residual sludge worldwide. In the last years, the progressive implementation of the directives 91/271/EEC and 98/15/EEC concerning urban wastewater treatment has increased the number of wastewater treatment plants operating in the European Union (EU) and consequently the quantities of sewage sludge requiring disposal. Nowadays, the three most common final destinations of sewage sludge are incineration, landfills and land application (Figure II-4) (Aparicio et al., 2009).

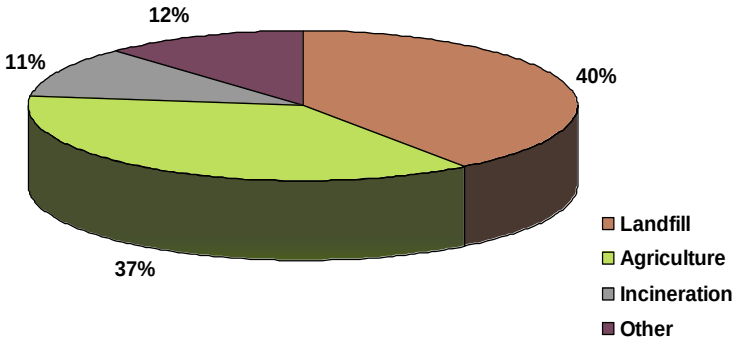

Figure II-4: Sewage sludge disposal routes in Europe in 2003 (Aparicio et al., 2009).

In France, the land application of sludge represents 57 % of the final destination. However, it must be ensured the safety of sludge to the ecosystems in which they are introduced since microorganisms, plants and animals inhabit the concerned soil. This safety must be effective both in physico-chemical and biological terms. The ordinance of January 8, 1998 (French norm) sets limits and cumulative concentrations after ten years for the sum of 7 PCBs, and for fluoranthene, benzo(b)fluoranthene and benzo(a)pyrene (1.2, 7.5, 4 and 3 mg/m^2 respectively).

In the EU Directive 86/278/EEC of June 1986, limit values of the total amount of several TE were established for land application of sludge, but no limit values for OPs in sludge were fixed. In 2000, the EU published the third draft of a future sludge directive entitled ‘‘Working document on sludge” (Table II-4) where more restricted concentration limit values for TE are fixed and where, concentration limit values for some OPs are included.

Table II-3: Limit values for concentrations of organic micropollutants in sludge for use on land.

Micropollutants	Limit values (mg/kg_{DM})
AOX[1]	500
LAS[2]	2 600
DEHP[3]	100
NPE[4]	50
PAH[5]	6
PCB[6]	0.8
PCDD/F[7]	100[8]

[1] Sum of halogenated organic compounds. [2] Linear alkylbenzene sulphonates. [3] Di(2-ethylhexyl)phthalate. [4] Nonylphenol and nonylphenolethoxylates with 1 or 2 ethoxy groups. [5] Sum of the following polycyclic aromatic hydrocarbons: acenapthene, phenanthrene, fluorene, fluoranthene, pyrene, benzo(bjk)fluoranthene, benzo(a)pyrene, benzo(ghi)perylene, indeno(1, 2, 3-c,d)pyrene. [6] Sum of the polychlorinated biphenyls components number 28, 52, 101, 118, 138, 153 and 180. [7] Polychlorinated dibenzodioxins/ dibenzofuranes. [8] (ng TE/kg_{DM}).

Ultimate disposal of sludge

Thermal processess: Incineration of sludge involves the total or partial conversion of organic matter to oxidized end products, carbon dioxide and water by thermal oxidation. Other thermal processes are the wet-air oxidation, the partial oxidation and volatilization of organic matter by pyrolysis and the starved-air combustion to end products with energy content. The advantages of incineration are: maximum volume reduction, destruction of pathogens and energy recovery potential. Disadvantages are: high capital and operating cost, a previous dewatering stage is necessary (more energy costs), the residuals produced (air emissions) may have adverse environmental effects, and disposal of residuals, which are classified as hazardous wastes, may be uncertain and expensive (Metcalf and Eddy, 1991).

Land application: Land application of stabilized sewage sludge is defined as the spreading of sludge on or just below the soil surface. Sludge may be applied to agricultural land, forest land, and disturbed and dedicated land disposal sites. In the three cases, sludge is used as a valuable resource to improve the characteristics of the land. Sludge also serves as a partial replacement for expensive chemical fertilizers. However, sludge tends to concentrate OPs with low water solubility and high adsorption capacity. The spreading of this contaminated sludge may induce the transfer of the OPs to crops and to enter to the food chain, and they can also be carried by runoff into aquatic systems (Metcalf and Eddy, 1991).

Landfill: A sanitary landfill is used for disposal of sludge, grease, grit and other solids. The landfill method is most suitable if it is also used for disposal of other solid wastes of the community. The wastes are deposited in a designated area, compacted in place. Landfilling of sewage sludge is forbidden in France since July 2002.

II.2 The organic micropollutants

II.2.1 Definition and characteristics

According to the OSPAR Convention (Convention for the Protection of the Marine Environment of the North-East Atlantic), an **environmental contaminant** is “any substance found in a place where it is not normally”, however this definition does not explain the concept of "pollutant" used by environmental scientists. Moriarty (1983) defines a **pollutant** as “a substance in larger amounts than in natural conditions and resulting from human activity”. In this context, the definition of pollutant most widely used is: “a biological, chemical or physical alterative that beyond a certain threshold, and sometimes under certain conditions, developed negative impacts on all or part of an ecosystem or environment in general”. This is equivalent to define the pollutant as a contaminant of one or more compartments of the ecosystem (air, water, soil) and/or organism (which may be human) and that affects the ecosystem, beyond a threshold or norm. Based on this definition of pollutant, it is possible to define the term **micropollutant** as a pollutant present in very small quantities in the environment, either in the order of µg/L or ng/L, but still much higher than in natural

conditions. It is possible to distinguish between inorganic micropollutants or TE (metals) and organic micropollutants (OPs) such as pesticides, drugs, biocides, etc.

Among the OPs, some are persistent. These persistent OPs are compounds that are resistant to environmental degradation through chemical, biological, and photolytic processes. Because of this, they have been observed to persist in the environment, to be capable of long-range transport, bioaccumulate in human and animal tissue, biomagnify in food chains, and to have potential significant impacts on human health and the environment. The Stockholm Convention is an international environmental treaty, signed in 2001 and effective from May 2004, that aims to eliminate or restrict the production and use of the persistent OPs. The Table II-4 shows the listing of OPs in the Stockholm Convention, which are classified according to the compounds that their production and use have to be eliminated, restricted, and their unintentional releases reduced.

Table II-4: Listing of persistent OPs in the Stockholm Convention 2001.

Production elimination	**Production restriction**	**Reduction of unintentional production**
Aldrin	DDT	Polychlorinated dibenzo-p-dioxins (PCDD)
Chlordane	Perfluorooctane sulfonic acid, its salts and perfluorooctane sulfonyl fluoride	Polychlorinated dibenzofurans (PCDF)
Chlordecone		Hexachlorobenzene (HCB)
Dieldrin		Pentachlorobenzene
Endrin		Polychlorinated biphenyls (PCB)
Heptachlor		
Hexabromobiphenyl		
Hexabromodiphenyl ether and heptabromodiphenyl ether		
Hexachlorobenzene (HCB)		
Alpha hexachlorocyclohexane		
Beta hexachlorocyclohexane		
Lindane		
Mirex		
Pentachlorobenzene		
Polychlorinated biphenyls (PCB)		
Tetrabromodiphenyl ether and pentabromodiphenyl ether		
Toxaphene		

Specific effects of OPs can include cancer, allergies and hypersensitivity, damage to the central and peripheral nervous systems, reproductive disorders, and disruption of the immune system. Some OPs are also considered to be endocrine disrupters, which, by altering the hormonal system, can damage the reproductive and immune systems of exposed individuals as well as their offspring; they can also have a developmental effect. The U.S. Environmental Protection Agency (EPA) has proposed a more detailed definition of these endocrine disrupting compounds: "an endocrine disrupter is an exogenous agent that interferes with the synthesis, secretion, transport, binding, action, or elimination of natural hormones in the body which are responsible for the maintenance or homeostasis, reproduction, development and or behavior" (Kavlock et al., 1996). Table II-5 includes a wide list of chemicals and OPs that have already been classified as endocrine disrupters by organizations worldwide.

Due to their low water solubility and high octanol-water partition coefficients (Kow), the OPs are mainly associated with hydrophobic compartments such as the organic matter in sewage sludge and river sediments or the lipids in living organisms (bioaccumulation). In the bioaccumulation process, the OPs are readily absorbed in fatty tissue. Fish, predatory birds, mammals, and humans are high up the food chain and so absorb the greatest concentrations.

II.2.2 The organic micropollutants studied

Among these OPs, some of them are often found in sewage sludge: the polycyclic aromatic hydrocarbons (PAHs), the polychlorinated biphenyls (PCBs) and the nonylphenols (NPs) (Abad et al., 2005; Aparicio et al., 2007; Fountoulakis et al., 2005; Katsoyiannis and Samara, 2004). In this work, we focused on NPs as representing detergent derivates, 13 representatives of the family of PAHs and 7 PCBs representing the persistent OPs. The point in common between these three families of compounds is that they are classified as endocrine disrupting compounds by most of the international organizations (Table II-5).

II.2.2.1 The organic micropollutants in the WWTP

Within WWTP, if OPs concentrations are followed only in the water line, it is possible to find high removal levels, such as 98% of PAHs and 75% of PCBs (Blanchard et al., 2004; Katsoyiannis and Samara, 2004). However, if the sludge line is analyzed, high concentrations of OPs are found in primary or secondary sludge. This suggests that the OPs removal from wastewater involves mainly a sorption mechanism. In fact, it was reported that the main mechanism for the removal of PAHs and PCBs from wastewater was sorption, and significant elimination is only observed for PAHs of low molecular weight (Blanchard et al., 2004; Katsoyiannis and Samara, 2004; Manoli and Samara, 1999).

II.2.2.2 Nonylphenol

NPs are degradation products of nonylphenol polyethoxylates (NPEs), compounds that belong to the alkylphenols family and that are used in the formulation of a large variety of lubricants, paints, detergents, pesticides and resins (Tolls et al., 1994). NPEs end up to the WWTP and they are removed during biological wastewater treatment. However, the overall yield of

biodegradation is limited due to the formation of biorefractory metabolites, including NPs, nonylphenol mono- and diethoxylates (NP1EO, NP2EO) and nonylphenoxy carboxylic acids (NPEC) (Ahel et al., 1994; Corvini et al., 2006). The presence of NPs was widely reported in surface water, groundwater, atmosphere, sewage sludge-amended soils and food.

Table II-5. List of compounds classified as endocrine disrupters by various organizations: UKEA (United Kingdom Environment Agency), USEPA (United States Environmental Protection Agency), OSPAR (Oslo and Paris Commission), JEA (Japan Environment Agency) and WWF (World Wildlife Fund).

Compound	UKEA	USEPA	OSPAR	JEA	WWF
Steroids					
Ethinyl estradiol	X		X		
17β-estradiol	X		X		
Estrone	X		X		
Mestranol			X		
Diethylstilbestrol	X		X	X	X
Alkylphenols					
Nonylphenol	X	X	X	X	X
Nonylphenol ethoxylate	X				
Octylphenol	X	X	X	X	
Octylphenol ethoxylate	X				
Polyaromatic compounds					
Polychlorinated biphenyls (PCBs)	X	X	X	X	X
Brominated flame retardants				X	X
Polycyclic aromatic hydrocarbons (PAHs)		X	X		
Organic oxygen compounds					
Phtalates	X	X		X	X
Bisphenol A	X	X		X	X
Pesticides					
Atrazine	X	X		X	X
Simazine	X	X		X	X
Dichlorvos	X				
Endosulfan	X	X		X	X
Trifluralin	X	X			X
Demeton-S-methyl	X				
Dimethoate	X				X
Linuron					X
Permethrin	X	X		X	
Lindane	X	X	X		X
Chlordane	X			X	X
Dieldrin	X	X		X	X
Hexachlorobenzene	X			X	X
Pentachlorophenol	X	X		X	X
Others					
Dioxins and furans	X		X	X	X
Tributyltin	X	X	X	X	

The degradation of NPEs into metabolites in the WWTP is shown in the Figure II-5. NP1EO and NP2EO are NPs hydrophobic intermediates concentrated in the sewage sludge, finding levels close to 100 mg/kg_{DM} for NPs (Aparicio et al., 2007; Fountoulakis et al., 2005). The NPEC are hydrophilic NPs intermediates, and according to Ahel et al., (2009), these compounds are found in the treated water and in the soluble phase of sewage sludge. Normally in the WWTP, the sewage sludge is stabilized by anaerobic digestion and it was reported that this anaerobically treated sewage sludge contained extraordinarily high concentrations of NPs. This phenomenon suggests that the transformation of NP1EO, NP2EO and NPEC into NP is strongly favored under anaerobic conditions (Corvini et al., 2006; Giger et al., 1984).

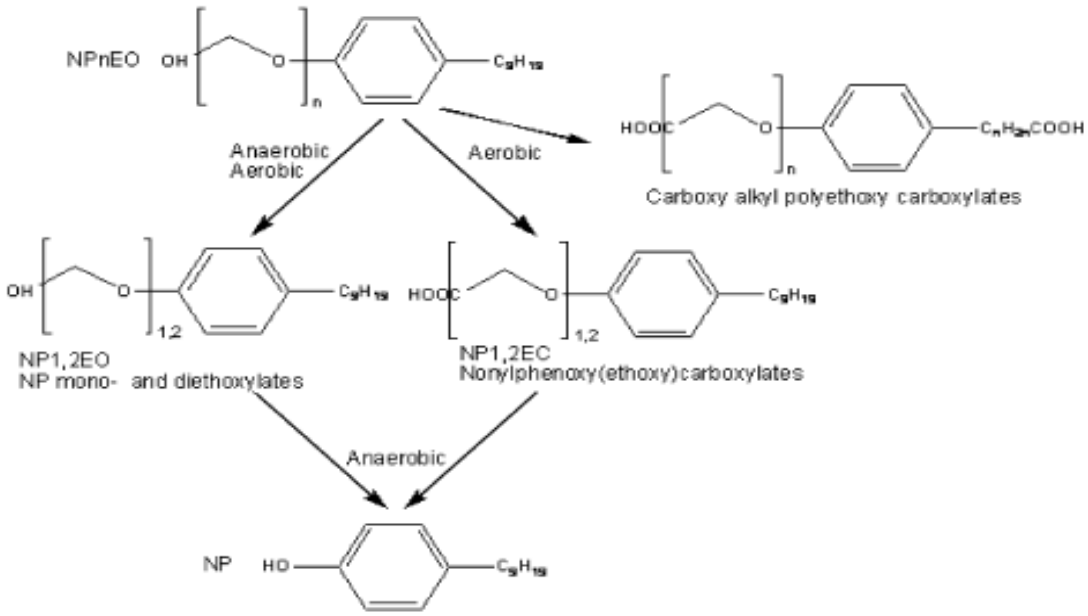

Figure II-5: Degradation of NPEs in the WWTP (Corvini et al., 2006).

Due to the nonyl chain, NP is hydrophobic (log Kow = 5.76) and its hydroxyl group gives it amphiphilic properties (with both hydrophilic and hydrophobic moieties). These characteristics suggest that the NP sorption to different matrix and the physicochemical interactions between the molecule and matrix are favored.

NPs has been shown to have a toxic and endocrine disrupting effect on wild life organisms and humans and its bioaccumulation in aquatic species is widely known. (Ekelund et al., 1990; Soto et al., 1991).

Because of its high persistence in the environment and its high endocrine disrupting effect, NP is a priority OPs.

II.2.2.3 Polycyclic aromatic hydrocarbons

PAHs are a class of organic compounds with two or more fused benzene rings in linear, angular, or cluster structural arrangements (Figure II-6). PAHs are mainly formed during human activities such as fossil fuel combustion, waste incineration, coal gasification, and petroleum refining (Lu et al., 2011). Through the air and runoff after rainy events, the PAHs can deposit to soil, water bodies and wastewater treatment system (Wada et al., 2005; Welker 2005).

PAHs are ubiquitous in natural environments and easily accumulate in soil, sediment and sewage sludge due to their low water solubility and high hydrophobicity, and their complex chemical structure which limit their availability to biodegradation. The physical properties of 13 PAHs are presented in the Table II-6.

Within WWTP, a broad variation of PAHs levels in sewage sludge is found in the literature due to the diverse analytical methodologies and the different origins of the wastewater and sludge treatment processes (Table II-7).

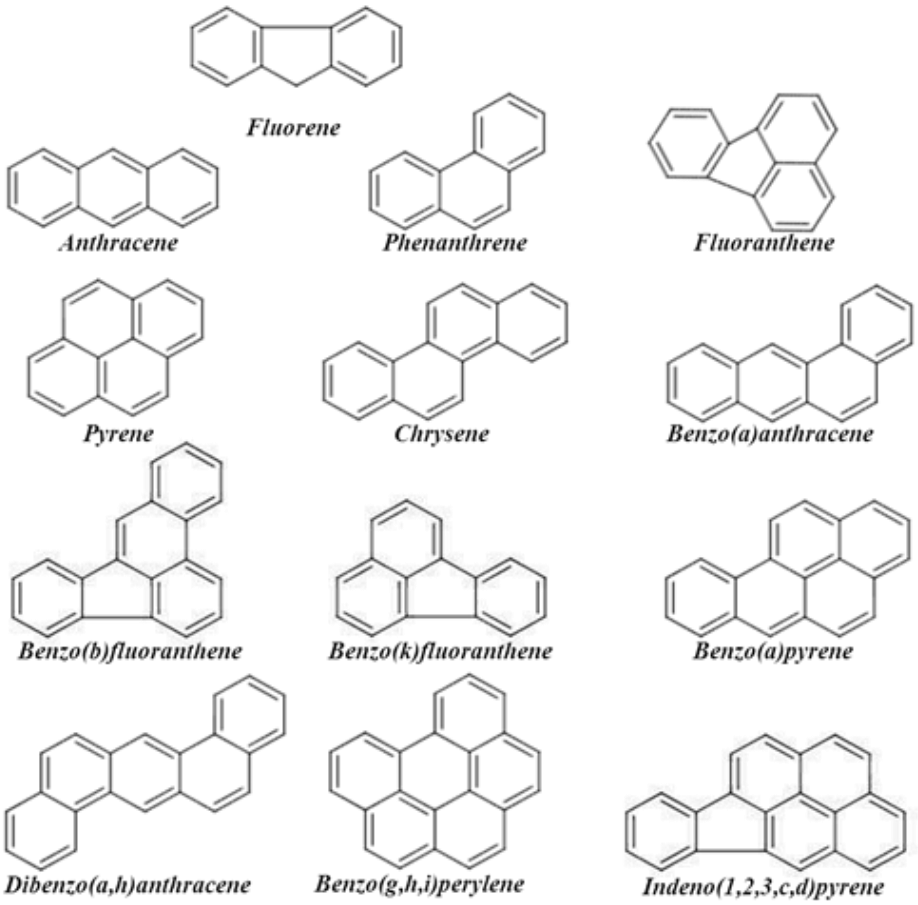

Figure II-6: Structure of the 13 polycyclic aromatic hydrocarbons priority according to the United States Environmental Protection Agency (USEPA).

Table II-6: Physical properties of PAHs (Shuttleworth and Cerniglia, 1995; Feix et al., 1995).

Compound	Molecular weight	Water solubility (25°C mg L^{-1})	Log Kow	Half-life in soil
Fluorene	166	1.68	4.18	30-60 d
Phenanthrene	178	1.0	4.46	2-200 d
Anthracene	178	0.045	4.5	2-20 m
Fluoranthene	202	0.206	4.9	30-60 d
Pyrene	202	0.132	4.88	1-5 y
Benzo(a)anthracene	228	0.0094	5.63	1-3 y
Chrysene	228	0.0018	5.63	1-3 y
Benzo(b)fluoranthene	252	0.0015	6.04	1-2 y
Benzo(k)fluoranthene	252	0.0080	6.21	2-6 y
Benzo(a)pyrene	252	0.0016	6.06	2-20 m
Dibenzo(a,h)anthracene	278	0.0050	6.86	1-2 y
Benzo(g,h,i)perylene	276	0.0007	6.78	1-2 y
Indeno(1,2,3,c,d)pyrene	276	0.0002	6.58	1-2 y

d: days; m: months; y: years.

Table II-7: PAHs concentrations measured in sewage sludge (mg/kg_{DM})

	Poland (Bodzek and Janoszka, 1999)	Poland, Industrial wastewater (Bodzek and Janoszka, 1999)	Paris (Blanchard et al., 2004)	Spain (Abad et al., 2005)	China (Cai et al., 2007)
Sludge number/samples	**3/1**	**5/1**	**1/3**	**22/9**	**11/1**
Fluorene	nm	nm	nm	PAHs Sum 5.3	0.08 – 2.7
Phenanthrène	3.5 – 11.0	6.0 – 6.4	nm		0.05 – 6.6
Anthracene	1.4 – 2	0.4 – 1.4	nm		0.07 – 6.1
Fluoranthene	2.0 – 8.0	5.2 – 6.0	1.1		<0.001 – 8.0
Pyrene	2.4 – 6.5	5.0 – 7.1	nm		0.08 – 4.3
Benzo(a)anthracene	2.4 – 3.4	6.8 – 11.1	nm		<0.001 – 8.3
Chrysene	nm	nm	nm		<0.001 – 4.0
Benzo(b)fluoranthene	nm	nm	0.24		<0.001 – 2.9
Benzo(k)fluoranthene	nm	nm	nm		0.007 – 7.0
Benzo(a)pyrene	1.6 – 2.8	8.0 – 10.2	0.37		0.007 – 6.6
Dibenzo(a,h)anthracene	<0.001	2.6 – 2.7	nm		<0.001 – 0.2
Benzo(g,h,i)perylene	<0.001	1.2	nm		<0.001 – 0.6
Indeno(1,2,3,cd)pyrene	<0.001	2.8 – 3.0	nm		<0.001 – 0.5

nm: not measured

PAHs are nowadays looked as priority environmental pollutants by environmental and health agencies because of their toxic, mutagenic and carcinogenic effect on living organisms and humans through the food chain (Samanta et al., 2002).

II.2.2.4 Polychlorinated biphenyls

PCBs are persistent OPs chlorinated aromatic compounds that are characterized by high physical and chemical stability. PCBs are composed of a biphenyl core substituted with 1–10 chlorine atoms, resulting in a class of theoretically 209 compounds. Some of them are on Figure II-7. Because of their thermal stability and high dielectric constant, PCBs have been used for a variety of industrial applications, including lubricants, dielectric fluids, and plasticizers. PCBs were manufactured widely during a half century (from 1929 to the 1970s) and an estimated 1.5 million tons of PCB have been produced worldwide. Because of their toxicity and persistence in the environment, PCBs have been banned in most countries since 1979.

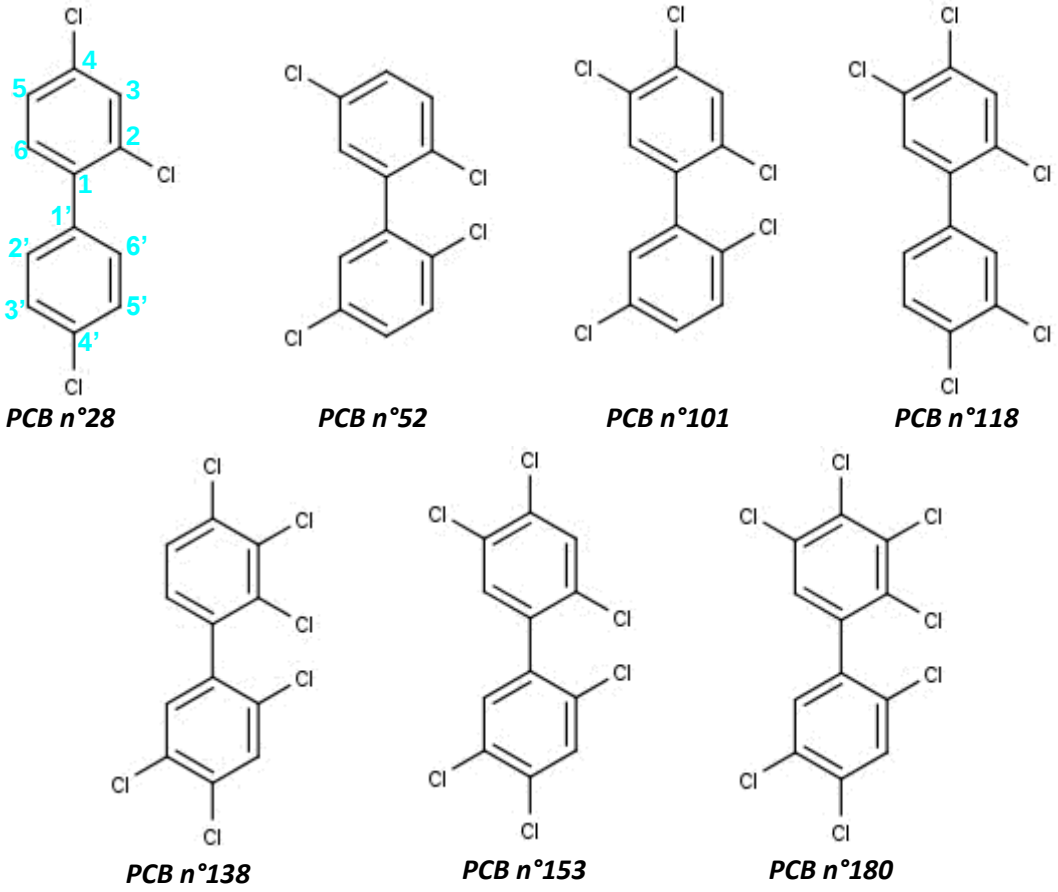

Figure II-7: Structure of the 7 polychlorinated biphenyls priority according to the USEPA.

Local manufacture, usage, spill, and improper disposal of PCBs have led to extensive environmental contamination. Because of their high volatility and stability, PCBs have been largely dispersed by atmospheric transport. The higher-chlorinated PCBs, with log Kow above 6, are associated with particulate matter in soils and sediments; lower-chlorinated PCBs, with lower log Kow, exist in gaseous phase and can be transported over longer distance.

Today, PCBs are still emitted from several sources, such as leaks of existing equipment (e.g., electrical capacitors and ballasts), volatilization from contaminated sediments, and sewage sludge soil application. PCBs are highly hydrophobic, leading to their bioaccumulation in living organisms. Plants constitute the major route of entry of PCBs in the food chain (Van Aken et al., 2010). The PCBs concentrations in sewage sludge according to different authors are presented in the Table II-8.

Table II-8: PCBs concentrations in sewage sludge (mg/kg_{DM}).

Compound	(Katsoyiannis and Samara, 2004)	(Blanchard et al., 2004)	(Abad et al., 2005)	(Kohli et al., 2006)
PCB 28	nd – 0.10			
PCB 52	0,14 – 0.71			
PCB 10	0,02 – 0.41			
PCB 118	nd – 0.07	PCBs sum	PCBs sum	PCBs sum
PCB 138	nd – 0.06	0.15	nd – 0.60	0.03 – 0.32
PCB153	nd – 0.05			
PCB 180	0.06 – 0.30			

nd: not detected

Chronic exposure to PCBs induces serious neurobehavioral, immunological, reproductive, and endocrine disorders in humans. According to the USEPA and International Agency for Research on Cancer (IARC), PCBs are suspected to be carcinogenic in animals and humans and are listed as priority OPs.

II.3 Removal mechanisms of NPs, PAHs and PCBs

II.3.1 Fate and behavior of OPs in natural matrix

OPs tend to accumulate in the soil, sediment and sludge matrices, and they may be removed by biodegradation or biotransformation, leaching and volatilization, or they may accumulate within living organisms or be retained or sequestered by the mineral and organic matter fractions (Figure II-8).

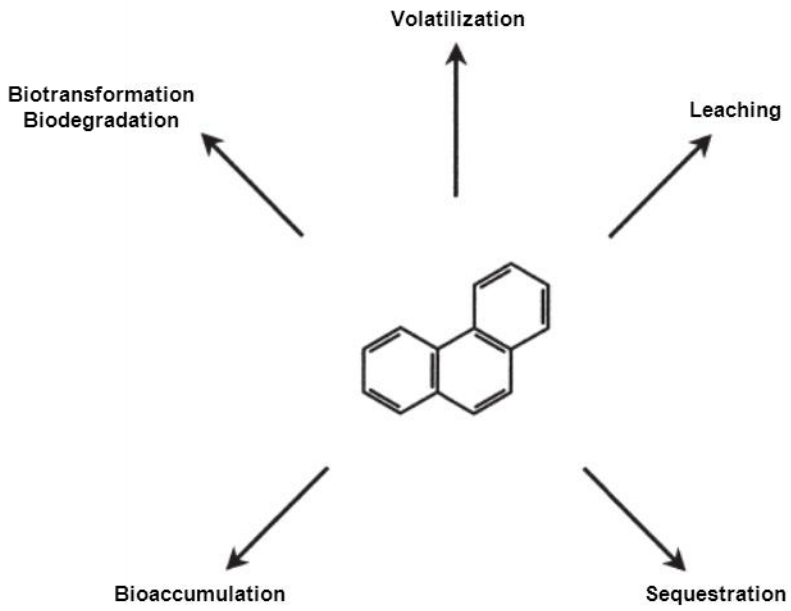

Figure II-8: Putative fate and behavior of a hydrophobic OP (phenanthrene) in soil (Semple et al., 2003).

The fate and behavior of OPs in organic matrices are controlled by several factors including the mineral and organic matter content of the matrix and the OPs physico-chemical properties (e.g. aqueous solubility, polarity, hydrophobicity, lipophilicity and molecular structure). Hydrophobic and lipophilic OPs that are poorly soluble in water, have a low vapor pressure and a recalcitrant molecular structure, are retained strongly within the matrix (Semple et al., 2003).

OPs can be removed from the matrix at varying rates. Figure II-9 describes the theoretical removal curves for three classes of contaminants: A represents a water-soluble, highly mobile, easily biodegradable contaminant; B represents the biphasic behavior of most contaminants, where removal is occurring, however, as the time of contact increases between the matrix and contaminant, the rate and extent of removal decrease; and C represents the slow removal of a highly intractable chemical.

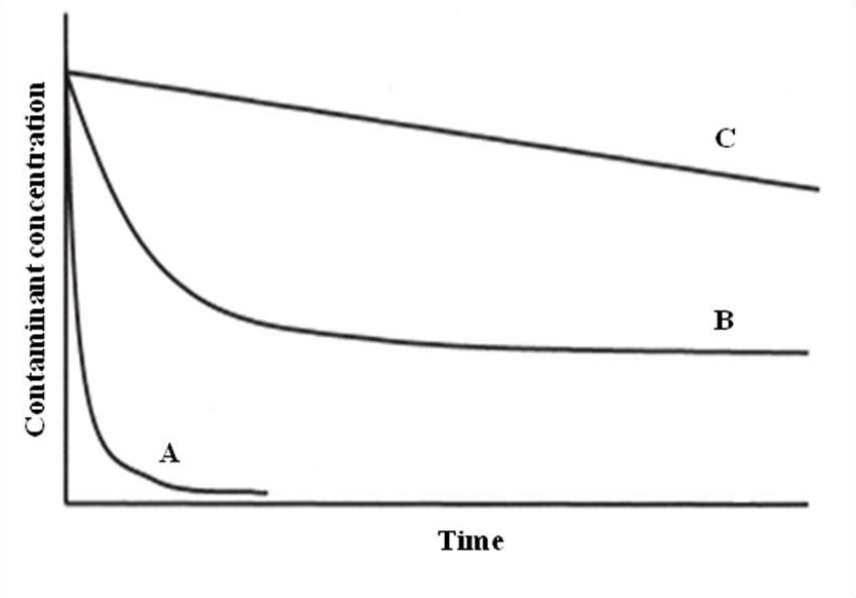

Figure II-9: Theoretical loss curves for three classes of contaminants: A, a water-soluble contaminant; B, a representation of most contaminants in soils; C, a highly recalcitrant chemical (Semple et al., 2003).

In general, the main removal mechanisms of OPs linked to soil and sludge matrices are volatilization, biodegradation and sequestration. Below, all removal mechanisms are briefly explained.

Volatilization is the conversion of a solid or liquid into a gas. Vapor pressure is an important factor in determining whether an OP will volatilize. Compounds with a high vapor pressure at normal temperature are often referred to as volatile. Environmental factors such as high temperature, low relative humidity and air movement tend to increase volatilization. Normally, an OP adsorbed to matrices is less likely to volatilize.

Some microorganisms have a naturally occurring microbial catabolic diversity to degrade, transform or accumulate a huge range of compounds including OPs such as PAHs, PCBs and pharmaceutical substances. **Biodegradation** is the oxidation of organic matter by microorganisms or other biological means to obtain carbon and energy for growth. Organic matter can be degraded aerobically with oxygen, or anaerobically, without oxygen. A term related to biodegradation is biomineralization, in which organic matter is converted into mineral carbon (CO_2 and CH_4). In the following section the OPs biodegradation will be more detailed. Another related concept to biodegradation is **biotransformation**. OPs biotransformation is the transformation of OPs by microorganisms or other biological means into intermediary metabolites or cosubstrates (Ghasemi et al., 2011). For example, an important pathway of PAHs biodegradation is through biotransformation, which results in increased aqueous solubility (Jørgensen et al., 2008).

Another transformation mechanism is the **photodegradation** or photochemical oxidation. Photodegradation is known to occur for OPs in solution, in pure solid form or adsorbed onto solid substrates. Exposure of aromatic compounds to light produces partially oxidized

intermediates which are more susceptible to the biodegradation than parent compounds (Lehto et al., 2000).

If an OP linked to a matrix is not completely removed by volatilization or biodegradation, the phenomenon of **sequestration** has to be considered. The main mechanisms involved in the sequestration are the sorption and diffusion, which are interactions between the pollutant and the mineral and organic solid fractions within the matrix. The nature of the matrix and the OPs physico-chemical properties largely determine the rate and extent of the sequestration phenomenon. In soil matrix, OPs generally exhibit two kinetic stages within the soil. Initially, a portion of the contaminant can be sorbed quickly (in minutes to a few hours), whereas the remaining fraction is sorbed more slowly over weeks or months. The initial rapid sorption is generally governed by hydrogen bonding and Van der Waals forces, mechanisms that are expected to occur instantaneously upon contact of the OPs with the soil surface. Then, the slow sorption is governed by covalent bonds generating a stable almost irreversible incorporation into the soil. These OP-residues in the soil are named non-degraded or bound residues because they are not available to microorganisms biodegradation; therefore they are not bioavailable (Semple et al., 2003). Sequestration has been reported by different authors as one of the abiotic mechanisms of OPs removal in soils (Northcott and Jones, 2001; Schlebaum et al., 1998).

In soils, **leaching** refers to the solubilization of compounds in water, due to rain and irrigation. Leaching is an environmental concern because it contributes to groundwater contamination. As water from rain, flooding, or other sources seeps into the ground, it can dissolve chemicals such as OPs, fertilizers, animal manure components and biocides and carry them into the underground water supply.

Bioaccumulation refers to the accumulation of compounds, such as pesticides, OPs, or other organic chemicals in a living organism. Bioaccumulation occurs when an organism absorbs a substance at a rate greater than that at which it is lost or biodegraded or eliminated by the organism.

Thus, volatilization, sequestration, leaching and bioaccumulation are mobility mechanisms of OPs because they are not really eliminated. The only mechanisms that remove the OPs of the environment are the biodegradation and photodegradation.

II.3.2 OPs biodegradation

OPs biodegradation, which is also referred as bioremediation, can occur aerobically, anoxically or anaerobically. Bioremediation consists in the use of microorganisms to degrade (destroy or render harmless) pollutants present in wastes. Bioremediation of OPs-contaminated soils, sediments, sludge and water can be treated by *in situ* and *ex situ* methods. Landfarming is an *in situ* treatment for soils, which focuses upon stimulating the indigenous microorganisms in the soil by providing nutrients, water and oxygen. Composting and bioreactors are *ex situ* treatments that benefits from being more subject to monitoring and control (Bamforth and Singleton, 2005).

OPs biodegradation follows two main mechanisms: the first involves the use of OPs as sole carbon and energy source for the growth of the microorganisms and the second involves a co-metabolism with other carbon sources, and where the biodegradation of OPs is not used for cellular growth (Van Aken and Bhalla, 2011; Wilson and Jones, 1993). The co-metabolism mechanism will be discussed more extensively in the next section.

Most of the previous studies have focused on the aerobic degradation of OPs due to the higher degradation rate and more easily cultivable aerobic pure bacteria compared with anoxic/anaerobic biodegradation. However, due to energetic advantages and the fact that most contaminated environments are anoxic or anaerobic (Lu et al., 2011), anaerobic biodegradation of OPs will be more extensively detailed in this work.

II.3.2.1 Aerobic conditions

Numerous aerobic bacteria that utilize **PAHs** as carbon and energy source in the presence of oxygen have been isolated. The main PAHs degradation mechanism for the aerobic bacteria is the initial oxidation of the benzene ring by the action of dioxygenase enzymes to form cis-dihydrodiols. These dihydrodiols are dehydrogenated to form dihydroxylated intermediates, which can then be further metabolized via catechols to carbon dioxide and water (Bamforth and Singleton, 2005).

Degradation of PAHs by aerobic bacteria under controlled conditions has been successfully applied in *ex situ* treatments of PAHs (Eriksson et al., 2003; Yuan et al., 2000). Regarding the different types of contaminated-matrix, PAHs aerobic biodegradation has been already widely studied in the case of highly contaminated soils and sediments, but not sufficiently in low contaminated environment like sewage sludge (Quantin et al., 2005; Wilson and Jones, 1993; Yuan et al., 2001). In this aspect, Trably and Patureau (2006) showed that the low PAH-contaminated sewage sludge can be successful treated under aerobic conditions.

In the case of NPs, biodegradation was reported in sediments, soils and sewage sludge-amended soils (Corvini et al., 2006; Chang et al., 2005a). However, most of these experiments were assessed in *ex situ* treatments under aerobic conditions. *Sphingomonas* sp and *Pseudomonas* sp, aerobic NP-degrading bacteria were isolated by different authors: *Sphingomonas* sp can grow on NP as a sole carbon and energy source and display the highest degradation capacity (Corvini et al., 2006; Gabriel et al., 2005; Yuan et al., 2004).

Bacterial biodegradation of PCBs has been extensively reviewed in the literature (Pieper and Seeger, 2008; Van Aken and Bhalla, 2011; Vasilyeva and Strijakova, 2007). Two major metabolic routes are known (anaerobic and aerobic) which involve different microorganisms and PCBs molecules (higher and lower chlorinated). Higher chlorinated are transformed by anaerobic reductive dechlorination, generating lower chlorinated that are susceptible to aerobic oxidation, potentially resulting in full mineralization of the molecule. PCBs aerobic biodegradation involves hydroxylation, sometimes coupled with the removal of chlorine atoms from the biphenyl ring, followed by ring cleavage and oxidation of the resulting compounds. The full aerobic mineralization of PCBs would generate only innocuous

chemicals, such as CO_2, Cl^-, and H_2O. In general, PCBs with three or fewer chlorine atoms per molecule are easily degraded by the aerobic pathway, and the ones with five or more are recalcitrant molecules.

II.3.2.2 Nitrate-reducing and sulfate-reducing conditions

Nitrate-reducing bioremediation has been shown to be an attractive alternative to aerobic bioremediation, since nitrate has a better electron-accepting capacity than oxygen.. Several studies were conducted to apply nitrate-reducing conditions in remediation of **PAH-contaminated** sediments (McNally et al., 1998), soils (Eriksson et al., 2003; Dou et al., 2009), and sludge (Chang et al., 2003) by enriched cultures as well as PAHs degradation in pure cultures (Rockne et al., 2000; Weissenfels et al., 1990). The results of PAHs degradation in sewage sludge under nitrate-reducing conditions showed that the degradation rates were much lower than those under sulfate-reducing and methanogenic conditions, even if the redox potential of nitrate was higher (Chang et al., 2003). In addition, Yuan and Chang (2007) reported that PAHs degradation in river sediments was inhibited under nitrate-reducing conditions compared with that under sulfate-reducing conditions.

The feasibility of PAHs degradation under sulfate-reducing conditions has been demonstrated in a number of investigations (Chang et al., 2003; Lei et al., 2005; Lu et al., 2011; Zhang and Young, 1997). Moreover, it was found that PAHs biodegradation under sulfate-reducing conditions had a long lag phase which might be attributed to the high concentration of PAHs in sediments (Lei et al., 2005; Zhang and Young, 1997).

Some studies have demonstrated that the PAHs biodegradation by pure cultures under nitrate and sulfate reducing conditions occur and different bacteria have been isolated and identified as PAHs degraders. Rockne et al. (2000) isolated three pure bacterial cultures from a highly enriched denitrifying consortium with the ability to grow anoxically in liquid culture with naphthalene as the sole source of carbon and energy in the presence of nitrate. Phylogenetic analyses identified two denitrifing bacteria: *Pseudomonas stutzeri* and *Vibrio pelagius.* In the same way, Weissenfels et al. (1990) identified from a PAH-degrading mixed culture the bacteria *Alcaligenes denitrificans* as fluoranthene degrader. Musat et al. (2009) isolated the bacteria *Deltaproteobacteria NaphS3b* from a marine sediment as naphthalene degrader under sulfate-reducing conditions.

Regarding other aromatic substrates, another study characterized the microbial community structure and *bamA* gene diversity involved in the degradation of toluene and benzoate under denitrifying conditions. The combined analysis of 16S rRNA and bamA genes showed that the species related to genera *Thauera chlorobenzoica*, a proteobacteria, was dominant in toluene and benzoate cultures (Li et al., 2011).

NPs biodegradation under nitrate and sulfate-reducing conditions was investigated by Chang et al. (2004, 2005b). The results show that the NP degradation rates under sulfate-reducing conditions were higher than those under nitrate-reducing and methanogenic conditions, being the sulfate-reducing bacteria the major component of the contaminated-environment. (Chang

et al. (2005b) isolated eight pure bacteria from sludge samples capable of degrading NP anoxically, using it as a carbon source. The two isolates that showed the highest degradation rates were identified as *Bacillus cereus* and *Acinetobacter baumannii*.

NPs biodegradation under nitrate and sulfate-reducing conditions was investigated by Chang et al. (2004, 2005b).

The mechanisms of anaerobic/anoxic PAHs degradation are still under study, and some studies have proposed a pathway for the anaerobic degradation of naphthalene under sulfate-reducing conditions, which is summarized in Figure II-10.

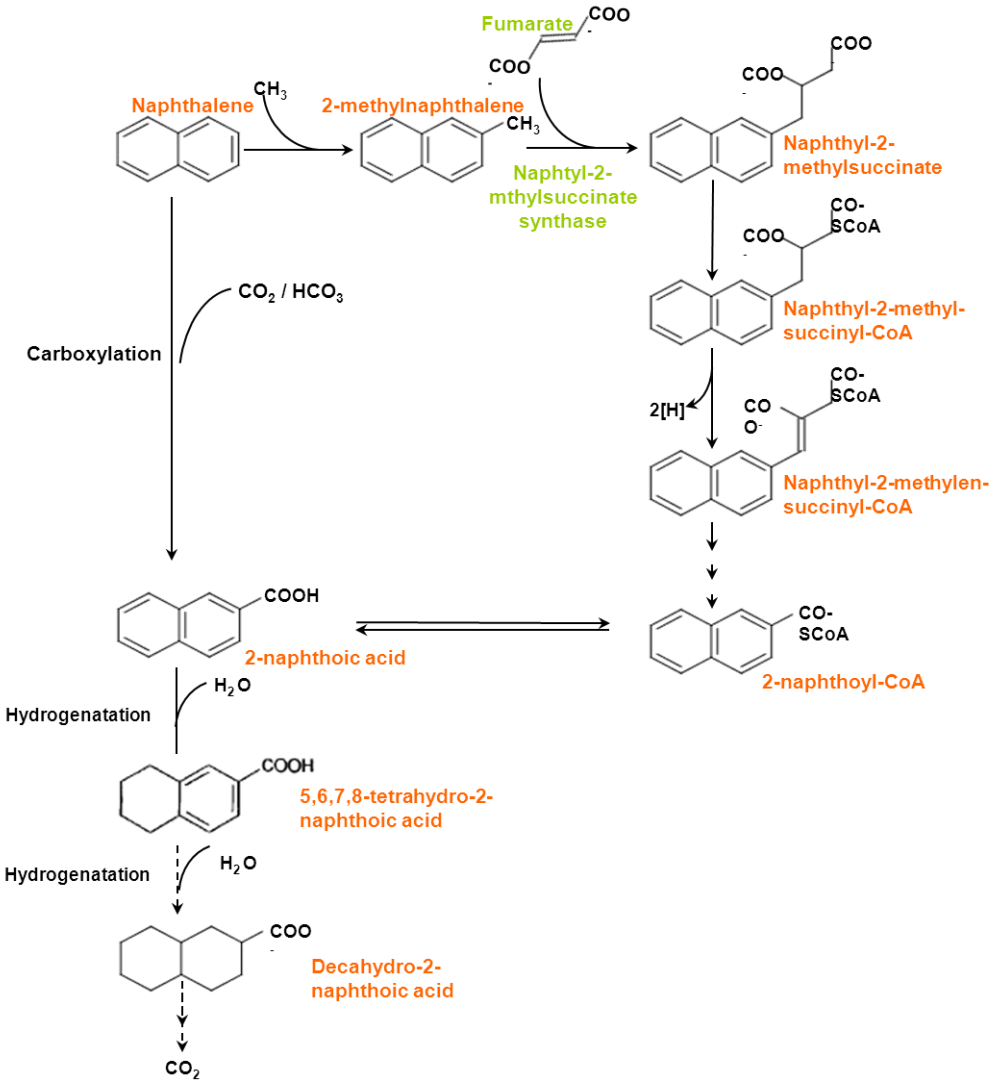

Figure II-10: Simplified pathway proposed for the anaerobic metabolism of naphthalene under sulfate-reducing conditions (Safinowski and Meckenstock, 2006; Zhang and Young, 1997; Zhang et al., 2000).

Zhang and Young (1997), using ^{13}C marking, demonstrated the activation of naphthalene by incorporation of CO_2 into the intermediate 2-naphthoic acid. This intermediate was also

detected by Musat et al. (2009). In addition, a second activation pathway of naphthalene has been demonstrated, initiated by methylation. The enzyme reactions (addition of fumarate and then co-enzyme A, and dehydrogenation) may be afterwards measured analogous to the toluene pathway (Safinowski and Meckenstock, 2006).

The pathways used by anaerobic bacteria of various physiological types for the degradation of monoaromatic compounds such as benzene, toluene, ethylbenzene and p-cresol have been well documented (Gibson and Harwood, 2002). In general, all studies indicate that the initial attack on these compounds is geared to converting them to benzoyl-CoA. Specific and inducible enzymes catalyze several sequential reactions, leading to benzoyl-CoA formation.

In the case of toluene degradation, the initial reaction is the addition of fumarate to the methyl group of toluene, catalyzed by benzylsuccinate synthase. This enzyme has been characterized at both biochemical and molecular level (Figure II-11). The hypothetical further steps are analogous to β-oxidation of α-methyl-branched fatty acids. Once formed, benzoyl-CoA molecule is degraded into acetyl-CoA, which enters in the citric acid cycle (Figure II-12).

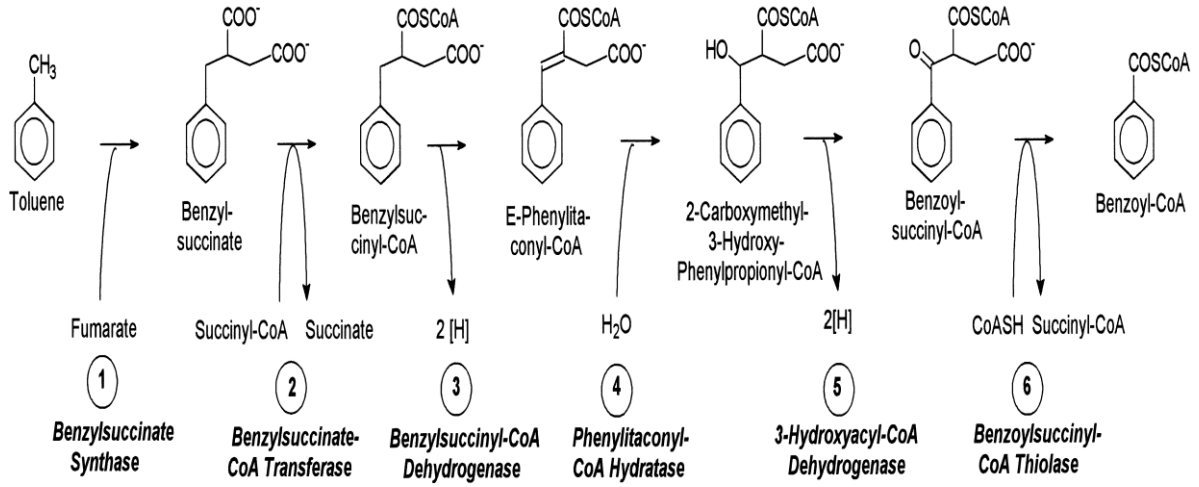

Figure II-11: Proposed pathway of anaerobic degradation of toluene to benzoyl-CoA (Heider et al., 1999).

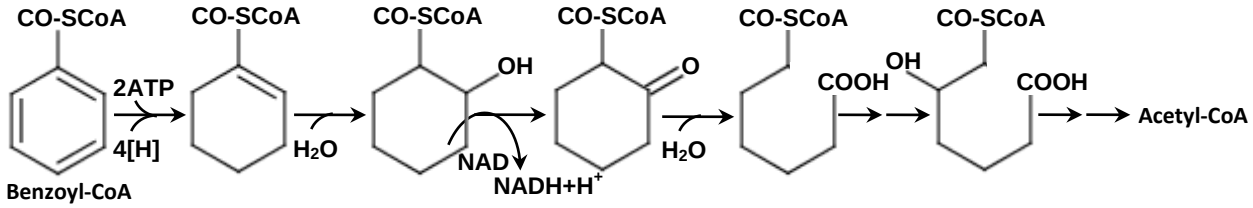

Figure II-12: Pathway of anaerobic degradation of benzoyl-CoA (Gibson and Harwood, 2002).

II.3.2.3 Methanogenic conditions

Methanogenic degradation of OPs has long been considered impossible, but evidence in contaminated surface environments suggests that it can occur. Recent results demonstrated that some PAHs (Bernal-Martinez et al., 2009; Chang et al., 2003; Christensen et al., 2004; El-Hadj et al., 2006; Larsen et al., 2009; Trably et al., 2003), NPs (Chang et al., 2005b; Patureau et al., 2008) and PCBs (Patureau and Trably, 2006; El-Hadj et al., 2007) present at low level in secondary and mixed sludge can be degraded under anaerobic conditions. It appears that this biodegradation is mainly coupled to methanogenic terminal oxidation processes (Chang et al., 2006; Jones et al., 2008). A recent theoretical thermodynamic landscape study showed that the biodegradation of PAHs under methanogenic conditions is an exergonic process; it indicated also that PAHs could be degraded to acetate and H2 coupled to the conversion of these substrates to methane as the optimal pathway (Dolfing et al., 2009). In the same way, Christensen et al. (2004) showed that it is thermodynamically possible to degrade naphthalene under methanogenic conditions, if methanogenic Archaea are available to remove hydrogen produced by oxidation of the PAHs.

According to Heider et al. (1999), several alkylbenzenes, alkanes or alkenes are anaerobically utilized as substrates by several species of denitrifying, ferric iron-reducing and sulfate-reducing bacteria, and another group of anaerobic bacteria that are “proton reducers” that depend on syntrophic associations with methanogens. The stoichiometric equations of oxidation of toluene and naphthalene by anaerobic bacteria, proposed by Heider et al. (1999) and Dolfing et al. (2009) are presented in Table II-9. These proposed routes are thermodynamically feasible only if the steady state concentration of hydrogen (and possibly also of acetate) is kept at a low level. This is achieved by hydrogen and acetate consumption by methanogens.

Regarding the PCBs biodegradation, when an anaerobic environment is deficient in electron acceptors, the halogenated compounds play an important role. Reductive dechlorination, where a chlorine atom is displaced by hydrogen, is involved in the energy metabolism where PCBs serve as electron acceptors for the oxidation of an electron donor, typically an organic substrate. The ability to use halogenated compounds as electron acceptors confers a selective advantage to bacteria, making anaerobic dehalorespiration a widespread biological activity in organochlorine-contaminated ecosystems (Smidt and de Vos, 2004; Van Aken and Bhalla, 2011). Following the removal of one or more chlorines of the higher chlorinated PCBs, the lower chlorinated PCBs are easily oxidized by aerobic bacteria (Van Aken and Bhalla, 2011). Moreover, the removal of lower and higher chlorinated PCBs in sewage sludge under methanogenic conditions has been assessed in ex situ treatments by some authors. Patureau and Trably (2006) obtained a total removal efficiency of 40%; and considering the abiotic losses, they showed that the higher chlorinated PCBs were more efficiently anaerobically biodegraded. El-Hadj et al. (2007) obtained a total PCBs removal efficiency in the range of 59-84% under thermophilic condition, only finding an accumulation of the lower chlorinated PCBs under mesophilic conditions.

Table II-9: Stoichiometric equations of toluene and naphthalene anaerobic degradation coupled to methanogenic as electron acceptor.

Toluene **Heider et al., 1999**	**Naphthalene** **Dolfing et al., 2009**
$C_7H_8 + 9\ H_2O \rightarrow HCO_3^- + 3\ CH_3COO^- + 4\ H^+ + 6\ H_2$	$C_{10}H_8 + 10\ H_2O \rightarrow 5\ CH_3COO^- + 5H^+ + 4\ H_2$
$6\ H_2 + 1.5\ HCO_3^- + 1.5\ H^+ \rightarrow 1.5\ CH_4 + 4.5\ H_2O$	$5\ CH_3COO^- + 5H^+ + 10\ H_2O \rightarrow 10\ CO_2 + 20\ H_2$
$3\ CH_3COO^- + 3\ H_2O \rightarrow 3\ CH_4 + 3\ HCO_3^-$	$24\ H_2 + 6\ CO_2 \rightarrow 6\ CH_4 + 12\ H_2O$
Sum: $C_7H_8 + 7.5\ H_2O \rightarrow 4.5\ CH_4 + 2.5\ HCO_3^- + 2.5\ H^+$	Sum: $C_{10}H_8 + 8\ H_2O \rightarrow 4\ CO_2 + 6\ CH_4$
a	
	$C_{10}H_8 + 10\ H_2O \rightarrow 5\ CH_3COO^- + 5H^+ + 4\ H_2$
	$5\ CH_3COO^- + 5H^+ \rightarrow 5\ CO_2 + 5\ CH_4$
	$4\ H_2 + CO_2 \rightarrow CH_4 + 2\ H_2O$
	Sum: $C_{10}H_8 + 8\ H_2O \rightarrow 4\ CO_2 + 6\ CH_4$
	B

a: Syntrophic acetate oxidation and methanogenesis from CO_2 reduction.

b: Acetoclastic methanogenesis and CO_2 reduction.

II.3.2.4 Cometabolism

OPs biodegradation can occur by different mechanisms: when OPs are used as sole source of energy, carbon, and/or nitrogen for the growth of the microorganisms, and when the OPs biodegradation depends on the metabolic transformation of another primary substrate, which is source of carbon and energy. This mechanism is called cometabolism.

Different studies have shown that anaerobic consortia can grow with PAHs until 4 rings and NPs as sole carbon source (Table II-10). The biodegradation of PAHs over 4 rings under methanogenic conditions was firstly reported by Trably et al. (2003), and is only possible when it is combined with other metabolic routes due to that their degradation is thermodynamically less favorable. This cometabolic mechanism can be stimulated by the addition of a readily biodegradable substrate (Chang et al., 2005b; Chang et al., 2008; Dionisi et al., 2006). Several publications have shown the cometabolism as a possible approach in the degradation of different OPs (Barret et al., 2010c; Chang et al., 2003; Clara et al., 2005; Criddle, 1993; Kocamemi and Çeçen, 2010; Yuan et al., 2001; Zhong et al., 2007).

Table II-10: Microorganism consortiums that can use PAHs and NPs as sole carbon source under anaerobic conditions.

Sole carbon source	Consortium	Oxydo-reduction conditions	Reference
Naphthalene	Enrichment from sediment	Sulfate-reduction	(Galushko, 1999)
	Enrichment from soil	Sulfate-reduction	(Meckenstock et al., 2000)
	Pure culture	Nitrate-reduction	(Rockne et al., 2000)
	Enrichment from sediment	Methanogenic	(Chang et al., 2006)
Anthracene	Enrichment from soil	Sulfate-reduction	(Drazenka Selesi, 2009)
	Enrichment from sediment	Sulfate-reduction	(Rockne and Strand, 1998)
	Enrichment from sediment	Nitrate-reduction	(Rockne and Strand, 2001)
Phenanthrene	Enrichment from sediment	Sulfate-reduction	(Davidova et al., 2007)
	Sediment	Methanogenic	(Chang et al., 2008)
	Enrichment from soil	Sulfate-reduction	(Drazenka Selesi, 2009)
	Enrichment from sediment	Sulfate-reduction	(Rockne and Strand, 1998)
	Enrichment from sediment	Nitrate-reduction	(Rockne and Strand, 2001)
	Enrichment from sediment	Methanogenic	(Chang et al., 2006)
Pyrene	Sediment	Methanogenic	(Chang et al., 2008)
Biphenyl	Enrichment from soil	Sulfate-reduction	(Drazenka Selesi, 2009)
	Enrichment from sediment	Sulfate-reduction	(Rockne and Strand, 1998)
	Enrichment from sediment	Nitrate-reduction	(Rockne and Strand, 2001)
	Enrichment from soil	Sulfate-reduction	(Yang et al., 2008)
	UASB reactor granules	Methanogenic	(Natarajan et al., 1999)

II.4 Bioavailability and bioaccessibility of OPs in organic/mineral matrix

II.4.1 Link between biodegradation, bioavailability and matrix composition

The sorption of OPs occurs in various organic matrices like soil, sediment and sludge because of their low water solubility and high Kow. Different authors suggest that the low yields of biodegradation achieved in these environments are related to their reduced bioavailability. This is influenced latter by a number of physico-chemical processes such as sorption-desorption, diffusion, solubility and sequestration phenomena due to physical and/or chemical interactions (Barret et al., 2010a; 2010c; Chang et al., 2003; Cuypers et al., 2002; Patureau and Trably, 2006; Semple et al., 2003).

In studies with sewage sludge matrices, OPs biodegradation has been improved with the addition of surfactants which increased OPs solubility in the aqueous phase, and therefore enhanced OPs bioavailability (Chang et al., 2003; 2005b; Bernal-Martinez et al., 2005; Fuchedzhieva et al., 2008). In the same context, it was demonstrated that the biodegradation of OPs strongly varied as a function of sludge characteristics which depend on the sludge source. The different sludge matrices induce variable levels of OPs bioavailability (Barret et al., 2010a; Chang et al., 2003; Larsen et al., 2009). However, the variations in the OPs biodegradation might be explained either by different levels of bioavailability or by variations in the cometabolism mechanism, although these two phenomena are difficult to dissociate (Barret et al., 2010a; 2010c).

In general terms, regarding the system OP-matrix, the organic/mineral matrices may interact with OPs by ion exchange, hydrogen bonding, Van der Waals forces, covalent bonds and hydrophilic/hydrophobic interactions (Haitzer et al., 1998). The type of interaction depends of the matrix nature and the physico-chemical properties of OPs. The hydrophobic interactions have been the most described among the interactions OPs-matrix and they are defined as not specific mechanisms of association between a hydrophobic compound and the hydrophobic structures of the matrix (Doll et al., 1999), although they can be more specific and oriented such as the π-π interactions (aromatic ring interactions), which are commonly reversible interactions (Wijnja et al., 2004).

The interactions OP-matrix depend also on environment chemical parameters such as pH and ionic force. The matrix contains ionizable groups such as carboxylic, phosphoric, sulfonic, amines, hydroxyl, etc., which are affected by pH variations, modifying their total charge, and thus the OP-matrix interactions. Additionally, metallic ion concentration may modify the spatial conformation of the matrix, forming or suppressing favorable interaction sites for OPs (Pan et al., 2008).

In aqueous matrix, different authors identify the humic acids (hydrophobic acids) as the molecules that have stronger interaction with hydrophobic contaminants than the fulvic acids, that contain more oxygenated functional groups and less aromatic rings (being thus more hydrophilic) (Lee and Farmer, 1989; Perminova et al., 1999). In the case of PAHs, it was demonstrated that higher is the hydrophilic fraction (carboxylic and hydroxyl) of the

dissolved organic matter (DOM), lower are the PAH-DOM interactions. In fact, it was demonstrated that benzo(a)pyrene has stronger interactions with the hydrophobic acid DOM fraction, which is rich in aromatic structures (McCarthy et al., 1989).

On the other hand, McCarthy and Jimenez (1985) showed that dissolved humic acids can reversibly bind PAHs with an affinity comparable to sediment particles, although binding to dissolved humic acids appears to be more rapid than comparable binding to particles. Additionally, their results suggest that the presence of humic acids or other sorptive components of the DOM can affect the environmental transport and fate of PAHs by competing with suspended particles for the binding of PAHs.

Other studies in aquatic environment about OP-humic acids interactions demonstrated that different sources of dissolved humic acids in natural waters can have different affinities for binding OPs (Carter and Suffett, 1982; Wijayaratne and Means, 1984).

Some authors have studied the behavior of some PAHs and NPs in the composting process. In the case of PAHs, they have suggested that their low mineralization is related to their low bioavailability for microorganism degradation because of their sorption on compost (Carlstrom and Tuovinen, 2003). However, in a recent study, both sorption coefficients (Kd) and mineralization of ^{14}C-labeled of fluoranthene and NP were followed over time (Lashermes et al., 2010). Fluoranthene mineralization was reported only at the end of composting maturation, while that the Kd coefficients were within the same range during the whole composting process. This result suggests that the mineralization of fluoranthene appeared to be less dependent on sorption phenomena than on compost colonization by specific microorganisms to degrade the aromatic structure. In contrast, the highest mineralization of NP was found at the beginning of composting maturation without significant changes in Kd values. Many studies, performed without ^{14}C-labeled NP have found NP dissipation yields during composting higher than 80 % of the initial content (Gibson et al., 2007; Pakou et al., 2009). However, in this study the ^{14}C-labeled mineralization did not exceed 56 %, suggesting that some of the observed NP removal is probably due to the formation of non-extractable or bound residues (Lashermes et al., 2010). According to Semple et al. (2003), in the process of sequestration, covalent bonds are formed with OPs that have similar structures to organic matrix, for example a phenolic structure. This suggests that NP, unlike fluoranthene, could interact with both hydrophilic and hydrophobic fractions of the organic matrix due to its amphiphilic properties, resulting in the formation of less reversible interactions.

II.4.2 Bioavailability and bioaccessibility definitions

According to the previous section, hydrophobic OPs are sorbed into different organic matrices limiting their biodegradation. The two concepts that might explain this phenomenon are the bioavailability and the bioaccessibility of these OPs.

The concept of bioavailability of pollutants is extensively discussed in the scientific community which is focused on the transfer of pollutants from contaminated soils to organisms, which may be terrestrial or aquatic, unicellular or multicellular plants or animals.

If we consider the example of contaminated soils and plants, the transfer of a pollutant in the soil to the plant involves on the one hand, a mobilization and, on the other hand, absorption. For plants, an element is considered bioaccessible when in theory it could be absorbed, but it is not due to physical or time limitations. The concept of bioavailability in plants does not distinguish between the "absorbed pollutant" and the "absorbable pollutant" by the plants (Figure II-13).

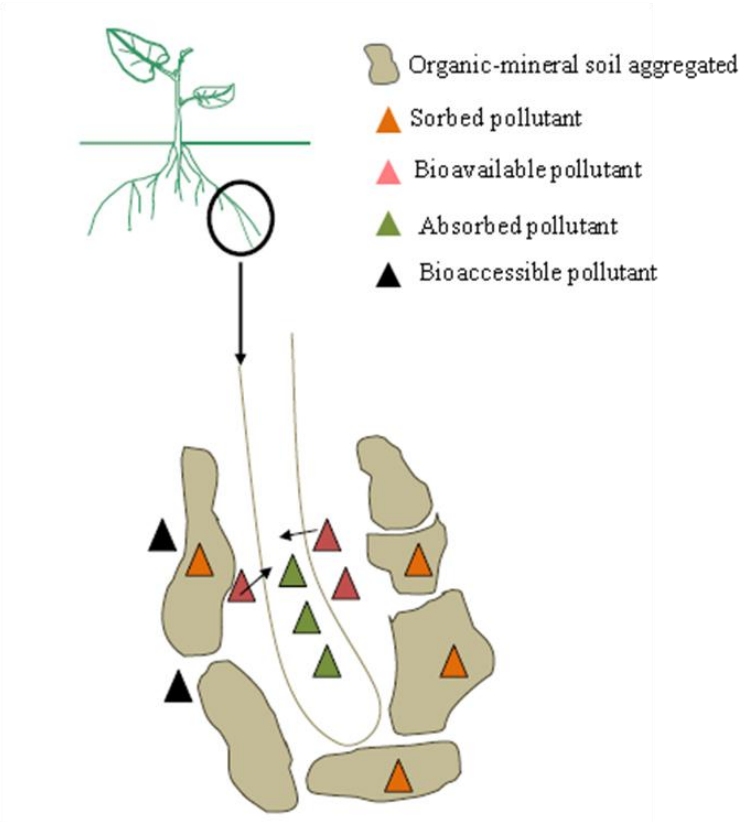

Figure II-13: Illustration of the concepts of bioaccessibility and bioavailability in plants (Denys, 2011).

In the same context as for the plants, other authors have proposed different definitions of these concepts depending on their discipline (e.g. pharmacology, toxicology, environment, etc); however, to have so many definitions creates confusion, therefore we have taken the definition proposed by Semple et al. (2004) for environmental scientists:

- an OP is **bioavailable** when it is freely available to cross an organism's cellular membrane from the medium where the organism inhabits at a given time. Once transfer across the membrane has occurred, storage, transformation, assimilation, or degradation can take place within the organism.

- an OP is **bioaccessible** when is available to cross an organism's cellular membrane from the environment, if the organism has access to the compound. However, the OPs may be either physically removed from the organism or only bioavailable after a period of time. In this context, "physically removed" may refer to a compound that is occluded in organic matrix and therefore is not bioavailable at a given time (Figure II-14).

To better understand the differences between bioavailability and bioaccessibility it is important to consider the timescale. OPs can become bioavailable within the order of seconds from the organic matrix locations, or the organism can move into contact with the OPs. To sum up, bioaccessibility encompasses what is actually bioavailable now and what is potentially bioavailable. Moreover, bioaccessibility comprehends three physical processes: the OP and matrix interactions, transport of OP to organism, and passage across cellular membrane, while bioavailability includes only the last process (Semple et al., 2007).

Additionally, the sequestration concept, which is explained in the section II.3.1, is linked to the irreversible incorporation of an OP into the matrix. Its release may occur over much longer timescales (e.g., years or decades) and may render the OP bioaccessible (Figure II-14).

Within the sludge matrix, the aqueous OPs concentrations are assumed to be bioavailable by some authors (Artola-Garicano et al., 2003; Dionisi et al., 2006; Urase and Kikuta, 2005). However, Fountoulakis et al. (2006) found that a fraction of sorbed-to-particles OPs was also bioavailable to microorganisms. Moreover, the aqueous fraction includes free and sorbed-to-dissolved and colloidal matter (DCM) OPs (Barret et al., 2010a) (Figure II-14). These two sludge compartments are usually not differentiated in literature even if interactions between OPs and DCM are likely to condition their bioavailability (Perminova et al., 2001). Based on the modelling of OPs sorption in sludge (Barret et al., 2010a), Barret et al. (2010b) demonstrated experimentally that the aqueous fraction (free and sorbed-to-DCM OPs) corresponds to the bioavailable sludge compartment.

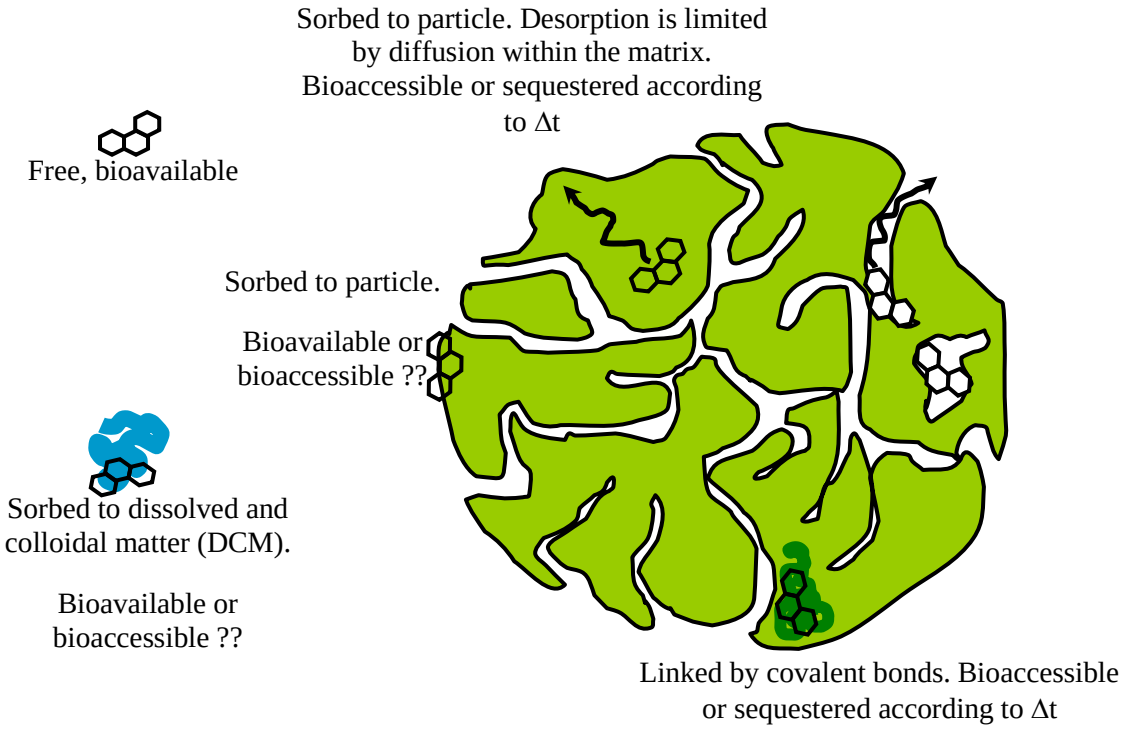

Figure II-14: Summary of possible physical states for phenanthrene in the sludge, and correspondence with biological compartments: bioavailable, bioaccessible and sequestered, inspired by an illustration of Semple et al. (2004).

II.4.3 Methods to study OPs bioavailability

Different chemical and physico-chemical extraction methods are used to estimate the bioavailable and bioaccessible fractions in soils and sediments.

According to Semple et al. (2007), to predict the bioavailability and bioaccessibility of OPs in a matrix, chemical extraction methods need to mimic the capacities of natural microorganisms to access these compounds. Ideally, the extraction procedure should yield the same bioaccessible fraction of OPs as the truly bioaccessible fraction to microorganisms, but it should be noted that chemical extraction and microorganism access to OPs have different time frames and spatial ranges. Hence, in order to predict the bioaccessibility, chemical approaches need to be much faster than the biodegradation itself. The chemical extraction thus needs to be more efficient (higher fluxes) than the microbial substrate acquisition while leaving the same quantity of non-bioaccessible or sequestrated OPs untouched (Figure II-15).

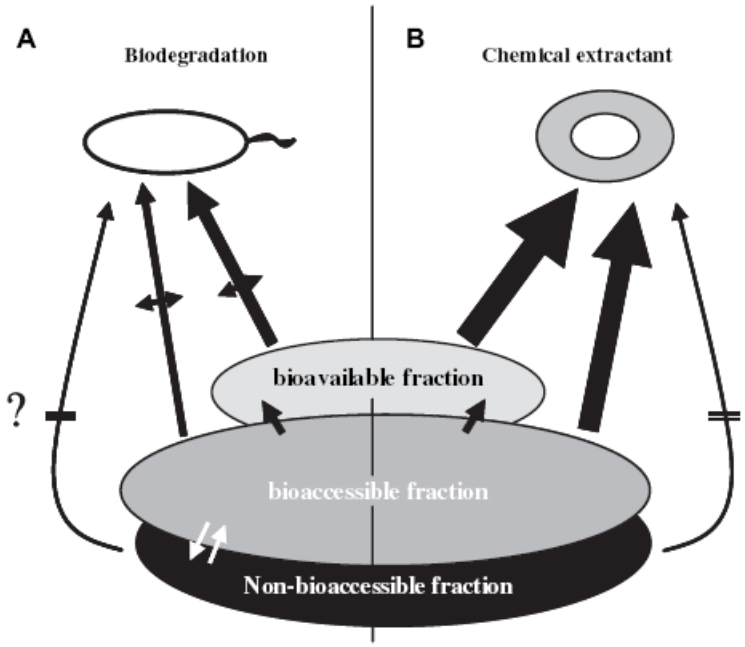

Figure II-15: Schematic view of the OPs fluxes arising from the bioavailable, bioaccessible and non-bioaccessible fractions in a soil matrix in presence of biodegradation (A) and a chemical extractant (B) (Semple et al., 2007). The importance of the fluxes released from the different OPs fractions in soil is visualized by the width of the arrows.

The extraction method most used is the **solid phase extraction (SPE)** in which the OPs have a strong physico-chemical affinity with a solid phase which may consist of adsorbent particles (having microfiber form); thus they are separated or extracted from their environment. A SPE method for the evaluation of PAHs bioavailability is the aqueous-based extraction technique utilizing **hydroxypropyl-β-cyclodextrin (HPCD)**. HPCD is a polymer with a high aqueous solubility because it has hydroxyl functional groups. It also has a hydrophobic organic cavity in the interior, which is approximately 6.5 Å in diameter for β-cyclodextrin. It is therefore possible to form a 1:1 inclusion complex between HPCD and the lightest PAHs, and a 1:2 inclusion complex between two HPCD molecules and the heaviest PAHs. An aqueous solution of HPCD can be used to extract labile matrix-associated PAHs i.e. the bioaccessible fraction while sequestered molecules are not transferred to the aqueous phase. Simultaneous biodegradation tests have demonstrated that HPCD extraction provides a good method for the prediction of PAHs bioavailability (Cuypers et al., 2002; Reid et al., 2000). It was also demonstrated that HPCD extracts NPs and PCBs molecules (Dean and Scott, 2004; Kawasaki et al., 2001).

Tenax TA beads is a SPE method to assess the bioavailability of PAHs and other OPs in sediments and soils, determining the rapidly desorbing fractions. Tenax TA is a porous polymer based on 2,6-diphenyl-p phenylene oxide. Extraction with Tenax TA has been shown to be effective in desorption kinetics experiments due to its high sorption capacity and its rapid compound adsorption from water. However, it was demonstrated that the rapidly desorbing fractions of PAHs extracted by Tenax TA beads are higher than the biodegraded fractions (Cornelissen et al., 1998). This effect was confirmed in another study where Tenax

TA overestimated the 5-6 ring PAHs biodegradation in contrast with the 3-4 ring PAHs biodegradation which was well estimated. (Cuypers et al., 2002).

Solid phase microextraction (SPME), developed by Arthur and Pawliszyn (1990), is a non-exhaustive procedure that has been used for the determination of PAHs concentration in water samples. SPME is an equilibrium extraction method that consists of a fine silica fiber backbone coated with a thin film of organic polymer, e.g., polydimethylsiloxane (PDMS), polyacrylate (PA) to adsorb target compounds from aqueous solutions or the headspace over condensed phases. SPME is used to determine both the free dissolved PAHs concentrations and the concentrations of PAHs associated to dissolved organic carbon (DOC) (Hawthorne et al., 2005). Recently studies have assessed the reliability of SPME in estimating the bioavailability of PAHs in soils. Liu et al. (2010; 2011) showed that SPME measurements were well correlated with the amount of biodegraded naphthalene by indigenous microorganisms in various types of soils. In contrast, to assess pyrene bioavailability, SPME slightly overestimated the biodegraded amount by indigenous and seeded microorganisms.

II.4.4 OPs-organic matrix interactions through sorption

A method to study the OP-OM interactions is the evaluation of the sorption mechanisms by sorption/desorption equilibrium kinetics in aqueous and solid phase (During et al., 2002) or by capillary electrophoresis studying the migration of OPs in a medium containing a ligand e.g. humic acids (Lucio et Schmitt-Koplin, 2006).

Other methods are the study of the spatial localization of OPs into a matrix by X-ray microfluorescence (Chawick Roper et al., 2006), studies by spectrofluorimetry, IR, ^{13}C RMN, etc, to know the interaction between OPs and functional groups, the dialysis and SPME to determine the DOC/water partitioning coefficients (K_{DOC}) to study the interactions between OPs and DOM from different origins (Hawthorne et al., 2005; Poerschmann et al., 1997), among others.

The spectrofluorimetry is also used to measure the rate of binding of OPs to fluorescent DOM by quenching of OP fluorescence (McCarthy and Jimenez, 1985; Pan et al., 2007). Additionally, this technique is used in the functional characterization of DOM and solid organic matter (SOM) and will be more detailed in the following section.

One of the oldest and most used techniques is the dialysis. This allows the physical separation of molecules in solution according to a size criterion. The sample is introduced in a dialysis bag (membrane) which is immersed in ultrapure water. The smaller particles cross through the membrane by diffusion until to achieve an equilibrium in both sides (Spohn et al., 2005). Although the dialysis is a physical separation technique to characterize the DOM, its main use is for the study of interactions between pollutants and DOM. If the threshold of separation is well chosen, it is possible to separate the free OPs that can cross the membrane from the OPs associated to DOM solution. Thus, it is possible to quantify the free OPs concentration in the dialysat and the free and associated OPs concentrations in the retentate, and consequently calculate the K_{DOC} values (Figure II-16).

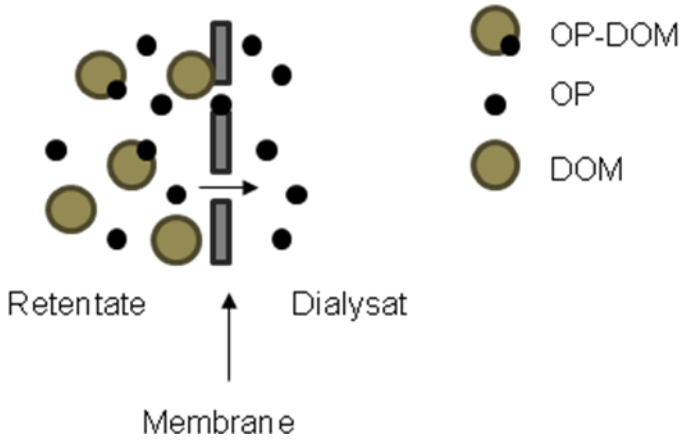

Figure II-16: Process of separation of free OP from OP associated to DOM by dialysis.

Different configurations are used in the studies of interactions OP-DOM by dialysis, but the most used consists of a solution of DOM introduced in the membrane-bag, itself immersed in a solution of free OP (McCarthy and Jimenez, 1985; De Paolis and Kukkonen, 1997). Because the volume of the bag is normally 10 to 100 times lower than the external volume, this configuration prevents a dilution of the OP solution in the dialysat, to use a small sample volume of DOM and an easier quantification of OP in the retentate.

II.5 Organic matter characterization

II.5.1 Characteristics of organic matter from different sources

The natural organic matter (OM) is composed of a number of organic molecules such as proteins, lipids, carbohydrates and the mixture of them. The OM may be synthesized by different organisms and multiple routes, whereby the OM composition depends on its source, localization or its period of study. For these reasons, it is very difficult to characterize exhaustively all the molecules that compose the OM. In general, the OM is characterized by physical, chemical, biochemical and functional techniques. The most used are:

- the spectroscopic techniques (UV-visible, infrared, spectrofluorimetry…) that characterize functional groups and molecules,
- the physical techniques such as size separation (dialysis, ultrafiltration, granulometry, flow field-flow fractionation…),
- the determination of the physical (organic density, mineral density, specific surface area…), physico-chemical and biochemical properties (hydrophobicity index, octanol-water partition coefficient (Kow), separation by affinity resins, Van Soest biochemical fractions…) and,
- analysis of elements and molecules (carbon, oxygen, nitrogen, proteins, lipids, carbohydrates…).

Usually the size separation techniques are combined with the other characterization techniques and with the OPs quantification in order to characterize individually the different OM fractions and to identify the functional groups that govern the OP-OM interactions.

Regarding the typical OM composition from different natural and synthesized sources and different physical states (particulate and soluble), it is common to find different levels of complexity, concentrations and size of OM, e.g., the freshwater is constituted by 20% of simples molecules (amino acids, carbohydrates…) and 80% of hydrophobic and hydrophilic complex acids (humic and fulvic acids) (Perdue and Ritchie, 2003), the sewage sludge is constituted by particulate and soluble OM fractions which are composed by microorganisms, extracellular polymers and effluents polymers such as cellulose, humic acids and proteins (Nielsen et al., 2004). In the case of soils, the clay and silt contain particulate organic matter which is composed mainly by humic matter, fulvic acids, hydrophilic compounds and lipids, and the total OM corresponds to no more than 5% of the total soil composition (Riefer et al., 2011; Voroney, 2006). A mixture of green solid waste and sewage sludge (compost) is composed by hydrophobic (75%) and hydrophilic (25%) compounds. The hydrophobic OM is mainly constituted by hemicellulose, cellulose and lignin (Lashermes et al., 2012).

In most of these organic matrices that interact with OPs, it is possible to find a common organic substance. The humic acids (insoluble at pH<2 and soluble at higher pH) and fulvic acids (soluble at all pH), jointly named humic matter, are macromolecules amphiphilic with a molecular weight greater than 500 Da that constitute heterogeneous mixtures. Humic and fulvic acids have a low biodegradability and chemical reactivity and they present different properties. Humic acids have a greater molecular weight, aromaticity and carbon content and a lower oxygen content and acidity. The humic substances are the result of multiple stages of degradation of fresh OM and they are representative of the maturity of OM (Perdue and Ritchie, 2003).

Humic matter is usually considered as the constituent most influential in the transport and behavior of OPs present in organic matrices (Pan et al., 2008). However, this hypothesis is based on the fact that humic substances have been the most studied of the OM, and different studies have shown that they are not the only molecules that interact with the OPs (Akkanen et al., 2005; Kukkonen et al., 1990). Nowadays, the OM is being fully characterized in order to identify the major molecules involved in the OPs-OM interactions.

II.5.2 Characterization techniques

In this section the most important and innovative characterization techniques of sewage sludge (particulate and aqueous sludge fractions) and of solid matrices will be presented, with emphasis on functional, physical, physico-chemical and biochemical characterization. However, these characterization techniques will be classified in two main groups: separation techniques and OM analyses.

II.5.2.1 Separation techniques

II.5.2.1.1. Particulate fractionation

Van Soest biochemical fractions

The Van Soest characterization technique consists in series of successive extractions using different extraction solvents according to the different physico-chemical properties and biochemical groups of the sample. This technique separates solid organic samples obtaining different fractions from the more soluble to the less soluble fraction or from the more bioavailable to the less bioavailable fraction. Initially, a hot water soluble fraction is extracted, after an additional soluble fraction is extracted with a neutral detergent, and finally, the insoluble fractions hemicellulose-like, cellulose-like and lignin-like are sequentially extracted with a crude fiber extractor. Van Soest technique is usually used to characterize SOM from sewage sludge, green waste and compost (Lashermes et al., 2012).

EPS extraction from activated sludge

EPS from activated sludge are constituted by wide range of macromolecules, being the proteins and carbohydrates that have shown an important role in a functional and quantitative aspect. Some studies have demonstrated that EPS pool has enzyme activity with proteases as the most active enzymes. Additionally, it was demonstrated that protein content was linked to sludge processes, and that the types of proteins were rather linked to sludge settleability (Ras et al., 2008).

Methods for EPS extraction have been reviewed by Avella-Vasquez, (2010). They include physical methods such as centrifugation, thermal methods and sonication and chemical methods such as ion exchange resins, EDTA, sodium hydroxide and formaldehyde or glutaraldehyde. For example, Ras et al, (2008) proposed a multi-method extraction protocol based on mechanical, ionic and hydrophobic methods. Discontinuous sonication (3 x 2 min), Tween (0.25% 1 h) and EDTA (2% in Tris buffer, 1 h) extraction methods are combined. With this protocol optimal extracellular protein extraction yields (maximal protein release with minimal cell lysis) are obtained. Protocol repetition on the same sample shows that protein yields after each successive protocol fit an exponential curve model. The total amount of extractable proteins is evaluated by model predictions (Ras et al., 2008).

II.5.2.1.2. Aqueous phase fractionation

Ultrafiltration

The ultrafiltration is a type of membrane filtration where a solution flow passes through a membrane by pressurization. Industries such as chemical and pharmaceutical manufacturing, food and beverage processing, and wastewater treatment, employ ultrafiltration in order to recycle flow or add value to products.

With the ultrafiltration, it is possible to purify, separate, and concentrate target molecules either in the permeate or in the retentate, depending on the molecular weight cut off of the membrane used.

Asymmetrical flow field-flow fractionation (AF^4)

AF^4 is a field-flow fractionation (FFF) subtechnique that has an increasing application for the separation of polymeric samples, colloids and particulate samples from different origin and with a wide size range (1nm-100µm). This technique overcomes other separation techniques such as size exclusion chromatography, centrifugation, gel electrophoresis, GC, ultrafiltration etc. The combination of this molar mass selective separation with analytical systems capable of revealing specific molecular features allows to determine the polymers functionality as a function of molar masses. Thus the AF^4 coupled to a multiangle laser light scattering (LS) and differential refractive index (DRI) detectors has provided extensive information on a large number of polymer without calibration (Alasonati et al., 2007).

The principle of FFF is based on differences in the particle diffusion coefficients. The separation takes place in a thin ribbon-like separation channel (channel width 500 µm) in which a laminar carrier flow is exposed to a perpendicular cross-flow field resulting a parabolic flow velocity distribution (Figure II-17). Initially, under the action of a cross-flow field with a low laminar flow in the channel, the particles are driven to the bottom of the channel, while diffusion causes them to be distributed at characteristic heights above the channel wall. Thus, the diffusion coefficient (D) establishes the average height (l) of a particulate fraction and directly determines the average retention time tr. This initial step is named "focus". Further, during the elution time or fractionation time, the individual particle species are separated at different flow velocities due to the laminar and parabolic flow in the channel. The smaller particles, because of their higher diffusion coefficient, diffuse back into the channel faster than larger particles and, therefore, leave the channel earlier (Figure II-17 (b)) (Prestel et al., 2005).

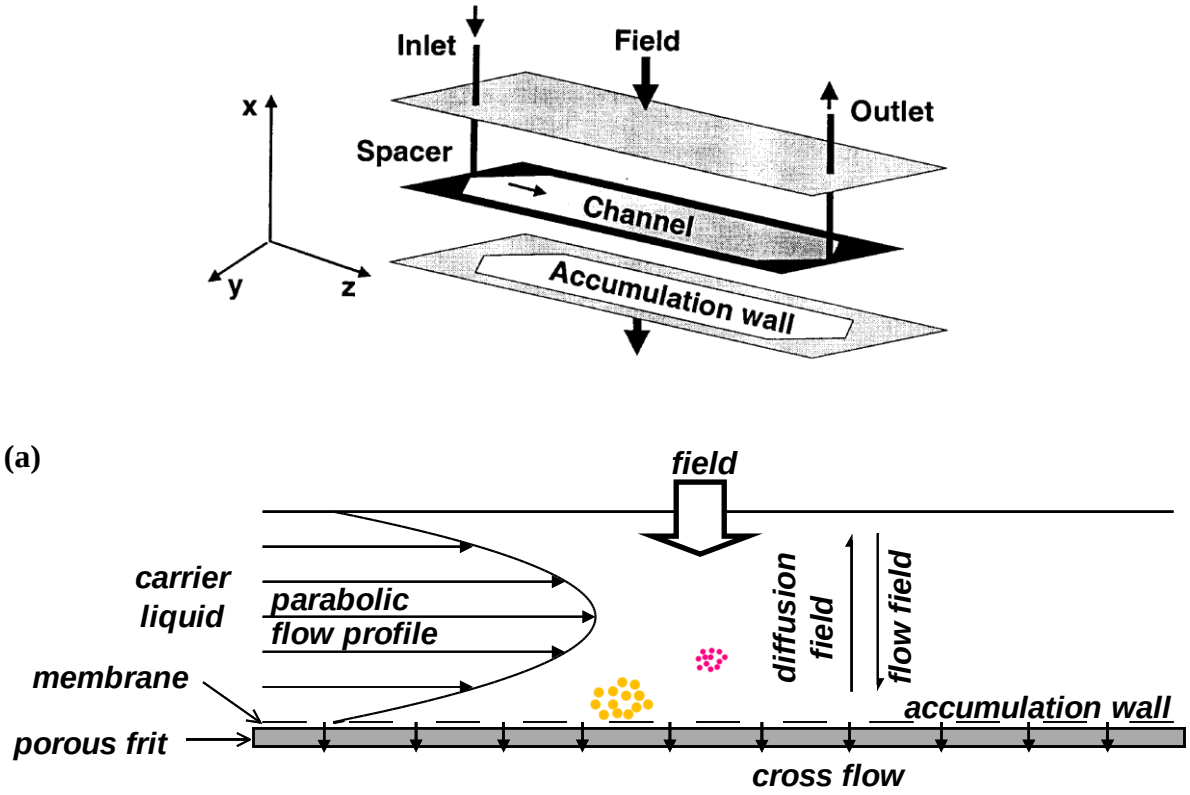

Figure II-17: AF^4 system. (a) Separation channel. (b) Separation principle.

Nowadays, AF^4 technology is used in the fractionation and characterization of the molar mass and size distribution of rivers samples, wastewater (Worms et al., 2010; Prestel et al., 2005), humic materials (Schimf and Petteys, 1997) and pharmaceutical molecules (Augsten and Mäder, 2008), and is commonly coupled to different characterization techniques such as plasma mass spectrometer (ICP-MS) (Prestel et al., 2005), 3D-fluorescence spectroscopy (Worms et al., 2010), etc., because this technique allows to get the different particle fractions to characterize individually each one.

II.5.2.2 Organic matter analyses

II.5.2.2.1. Solid matrices analyses

^{13}C nuclear magnetic resonance (NMR)

The nuclear magnetic resonance (NMR) spectroscopy is a technique that exploits the magnetic properties of certain atomic nuclei to determine physical and chemical properties of the molecules in which they are contained. It relies on the physical phenomenon of nuclear magnetic resonance in which the magnetic nuclei in a magnetic field absorb and re-emit electromagnetic radiation. This energy is at a specific resonance frequency which depends on the strength of the magnetic field and the magnetic properties of the isotope of the atoms.

^{13}C NMR spectroscopy is the application of NMR spectroscopy to carbon. It is analogous to proton NMR (^{1}H NMR) and allows the identification of carbon atoms in an organic molecule. ^{13}C NMR detects only the ^{13}C isotope of carbon, whose natural abundance is only 1.1% and is magnetically active with a spin quantum number of 1/2. The main carbon isotope, ^{12}C, is not detectable by NMR since it has a spin quantum number of zero and so is not magnetically active. ^{13}C NMR can provide detailed information about the chemical structure, dynamics and reaction state of environmental molecules.

^{13}C NMR spectroscopy has been widely used to characterize the SOM, especially in sewage sludge and soils to follow changes in chemistry over time. Using the ^{13}C NMR technique it is possible to identify different functional groups such as carboxyl, aryl (aromatic), o-alkyl and alkyl carbons, and, for example, comparing the functional composition of soils and sewage sludge; it was reported that sewage sludge is usually richer in alkyl carbon than soil OM (Smith et al., 2008). Additionally, ^{13}C NMR is used in the study of soil-bound residues of pesticides to better understand the fate of these compounds in the environment (Witte et al., 1998). A complication of this technique is that the quantitative reliability can be compromised by the presence of interfering, either paramagnetic species or lipids with a high degree of molecular mobility (Smith et al., 2008).

Thermally assisted hydrolysis and methylation-GC/MS

Nowadays, there is a great interest to know the molecular composition of sewage sludge and soils, because it was demonstrated that biochemical composition of the macromolecules (solid molecules) governs their reactivity and in the case of sewage sludge, its behavior once disposed on soils. Pyrolytic techniques coupled to mass spectrometry or gas chromatography-mass spectrometry (Py-GC/MS) are useful to get information on the biochemical composition of SOM at a molecular level, even if the pyrolysis products correspond only to a part of the insoluble organic fraction. A modification of the pyrolysis process is the high-temperature chemical reaction which provides additional chemical structure information not readily obtainable by conventional Py-GC/MS. The THM-GC/MS (thermally assisted hydrolysis and methylation-gas chromatography-mass spectrometer) has been applied to the biochemical characterization of a large number of matrices, mainly in the characterization of the humic substances from sediment or of organic macromolecules and or of sewage sludge (Jarde et al., 2003). Degradation products can be identified and related to original fractions present in the structure of the organic macromolecular matrix. In solid sewage sludge samples, three families have been identified: lignin-derived, lipid-derived and nitrogenous compounds. THM-GC/MS gives structural information and an organic signature of the organic insoluble fraction, allowing to compare the samples to one another (Jarde et al., 2003).

II.5.2.2.2. Aqueous phase analyses

3D-fluorescence spectroscopy

DOM is a heterogeneous mixture of aromatic and aliphatic organic compounds containing oxygen, nitrogen, and sulfur functional groups (e.g., carboxyl, phenol, enol, alcohol, carbonyl,

amine, and thiol). DOM is a ubiquitous constituent of river waters, between 40 and 60% of this natural DOM is fluorescent. This fluorescent material principally comprises protein and organic acids derived from the degradation of plant, animal matter and wastewater. Fluorescence occurs when an electron in a molecule is excited to a higher energy level by the absorption of energy, for example, a photon, and the fluorescence is generated when this energy is lost as light when the electron returns to its original energy level. Figure II-18 shows a representation of the energy transfer involved in the process of fluorescence. The wavelength at which absorption (excitation) and emission occur is specific to the molecule. Aromatic organic compounds have good fluorescence properties due to the unpaired electron structure of the carbon ring (Hudson et al., 2007). Recent advances in fluorescence spectroscopy allow the collection of fluorescence data from liquid samples at high optical resolution and the generation of excitation and emission data in the form of excitation emission wavelengths (Baker, 2001).

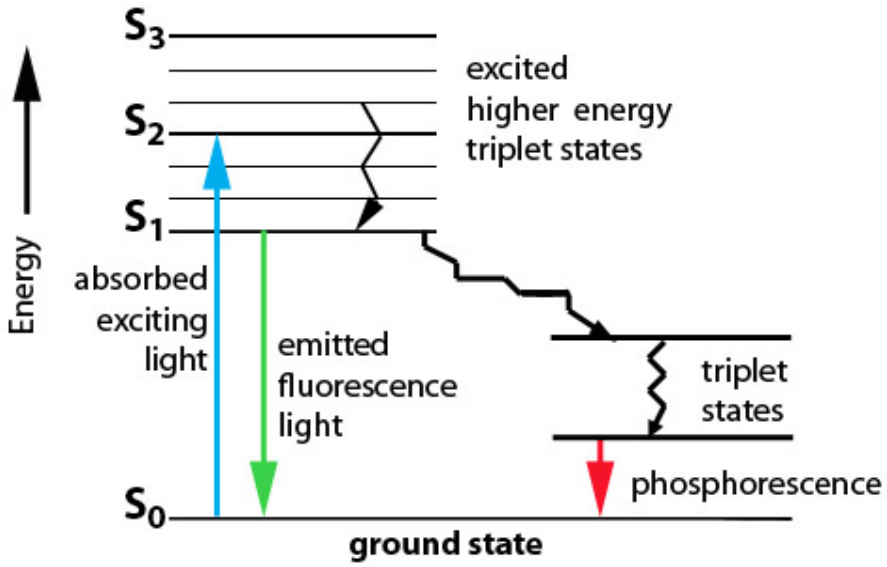

Figure II-18: Jablonski diagram

Excitation-emission matrix (EEM) fluorescence spectroscopy has been widely used to characterize DOM in water and soil. However, interpreting more than 10000 wavelength dependent fluorescence intensity data points represented in EEMs has posed a significant problematic. Fluorescence regional integration, a quantitative technique that integrates the volume beneath an EEM, has been developed to analyze EEMs. EEMs have been classified by different authors into four or five excitation-emission regions based on fluorescence of model compounds such as DOM fractions, marine waters, freshwaters and sewage sludge.

Figure II-18 presents an EEM fluorescence of the aqueous phase of a secondary sludge sample. Fluorescent organic matter exhibits different intensity peaks at known wavelengths. According to Baker (2001) and Chen et al. (2003), the Figure II-19 has been classified into four excitation-emission regions: tryptophan fluorescence (region A), fulvic-like fluorescence (region B), humic-like fluorescence (region C) and aromatic protein (region D). Fluorescence

intensities of these regions will predominantly depend on OM concentration, provided that other factors that affect fluorescence intensity (pH, metal ion interaction, etc.) remain relatively constant.

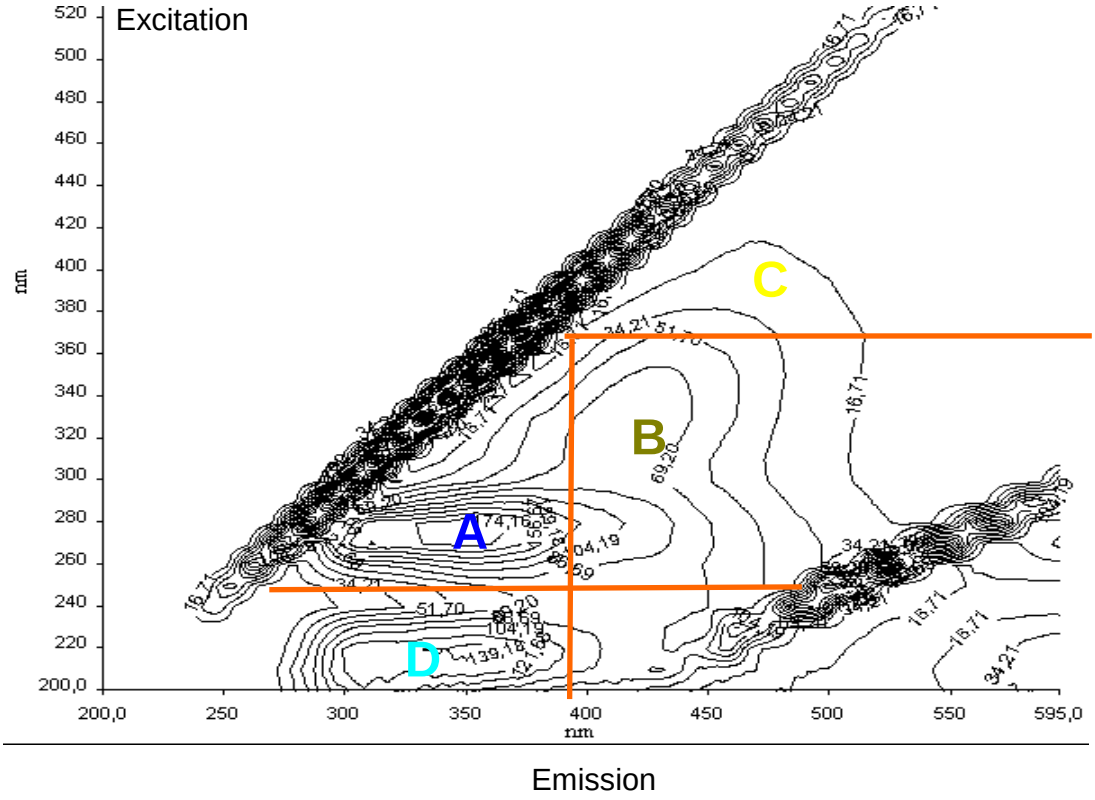

Figure II-19: Supernatant secondary sludge fluorescence excitation-emission matrix (EEM). Excitation wavelengths vary from 200 to 425 nm, and emission wavelengths vary from 250 to 550 nm. Four fluorescence peaks are identified as A-D. Tryptophan fluorescence (A) occurs at 275 nm excitation, 350 nm emission; fulvic-like fluorescence (B) at 320-340 nm excitation, 410-430 nm emission; humic-like fluorescence (C) at 370-390 nm excitation, 460-480 nm emission and aromatic protein (D) at 210-220 nm excitation, 300-350 nm emission (Baker, 2001; Chen et al., 2003).

Fluorescence analysis allows identifying the functional groups of DOM samples and has the potential to discriminate between DOM fractions and different DOM sources, indeed each fluorescent region may represent a signature of the sample origin.

Fluorescence spectroscopy has been used in the study of DOM in marine and estuarine waters, freshwater and wastewater (Hudson et al., 2007) to determine biological activity and associated protein fluorescence, characterization of DOM composition from different sources, determination of water source, photodegradation study, pH influence on DOM fluorescence, colloidal characterization and its role in metal distribution (Worms et al., 2010), characterization of EPS of sewage sludge (Sheng and Yu, 2006), and mixing of water bodies. In the case of wastewater, the study of DOM fluorescence has been used as a tool for water treatment process optimization, water quality assessment and pollution monitoring. Within the

WWTP, it was observed that the fluorescence intensity at 340 nm decreases with the sewage treatment and a strong correlation with the biological oxygen demand was observed (Baker, 2001; Hudson et al., 2007).

In recent years, another tool of the fluorescence spectroscopy has been developed: the three dimensional solid-phase fluorescence. Until now, this type of fluorescence spectroscopy has been used in the determination of physical and chemical quality of foods (Becker et al., 2003; Yaacoub et al., 2009). In environmental applications, only the detection of chlorophyll degradation by-products in marine sediments (Chen et al., 2000) and recently, the characterization of solid organic wastes such as solid sewage sludge, municipal solid waste and compost (Muller et al., 2011) have been reported. Moreover, laser induced fluorescence spectroscopy, a more sensitive version of solid-phase fluorescence spectroscopy, which uses laser as an excitation light source, has been used to characterize soil OM (Muller et al., 2011).

The characterization of solid organic wastes has become a crucial field of research in order to develop functional indicators for sustainable waste management. However, the solid organic waste characterization requires multiple characterization techniques that are tedious and time consuming. Solid-phase fluorescence constitutes a rapid, sensitive, selective and quantitative analytical method which only requires basic scientific skills as well as compact and inexpensive analytical equipments (Muller et al., 2011).

II.6. Conclusion

This literature review shows that in the context of OPs contaminated sewage sludge matrices, OPs behavior is conditioned by a series of complex interaction and feedbacks between different actors. Thus, a conceptual approach was developed by Barret (2009) in which a complex network of interactions between the three actors of the system, i.e. OP/ microorganisms/matrix, must be considered (Figure II-20).

On one hand, the pair matrix-microorganisms determine a basal metabolic pathway, i.e. the fluxes of carbon and energy, and in our case, the methanogenesis as final electron acceptor. Moreover, a direct link between the basal metabolism of the microorganisms and the biodegradation of OPs is the co-metabolism.

Furthermore, the physico-chemical interactions between OPs and the matrix, in terms of sorption, are likely to determine the bioavailability of OPs to the microorganisms, and consequently the biodegradation activity. However, these interactions may vary among different matrices origins and physical compartment (particulate and aqueous) which could generate different OPs behaviors within the system.

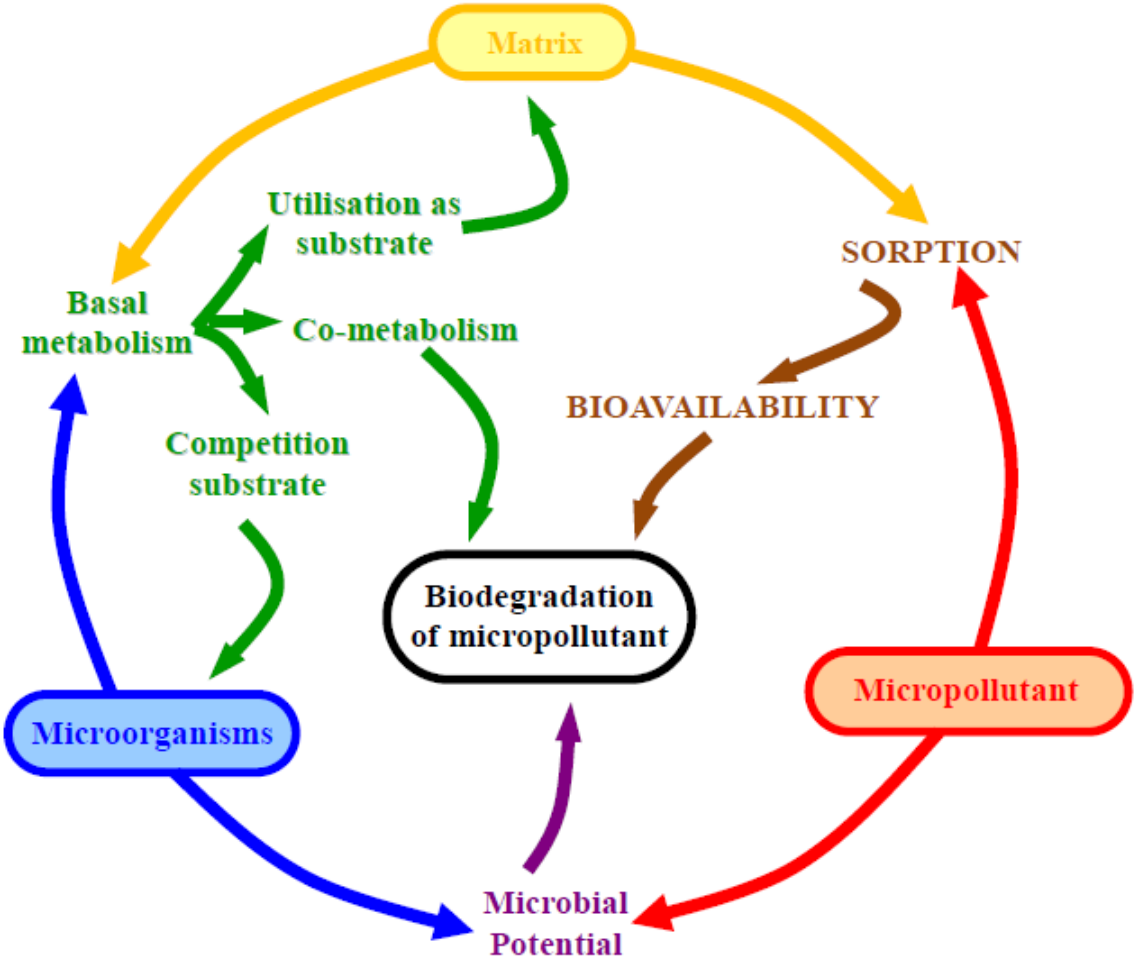

Figure II-20: Network of interactions between the three actors OP/matrix/microorganisms influencing the biodegradation of OPs during anaerobic digestion of contaminated sludge (Barret 2009).

Because of the OPs contained in aqueous phase are considered bioavailable, different authors have studied the OP-DOM interactions in order to identify the main molecules that govern the behavior of OPs in this environment. This suggests that the DOM could play an important role in the bioavailability of OPs (linked to the nature of DOM), as cometabolic substrate and in the distribution of OPs between the physical compartment of the matrix. Finally, the pair OP-microorganism defines a microbiological potential for the presence of organisms directly involved in the OPs anaerobic degradation under methanogenic conditions.

The main objective of this thesis will be focused on the study of the OP-matrix interactions, and more specifically the OPs distribution on the aqueous compartment, linking these interactions with the removal of OPs under methanogenic conditions. Due to that the matrix plays two different roles (cometabolism and bioavailability), the influence of each role may not be studied individually. However, this effect will be decreased with a full characterization of the matrix and thus it will be identify the most influential parameters on the OPs removals regarding the bioavailability approach.

III. MATERIALS AND METHODS

III.1. OPs solutions

PAH powder was obtained from Dr Ehrenstorfer GmbH. The compounds studied are listed in Table III-1. Each compound was separately dissolved in dichloromethane at 1 g/L. The pure 4 nonylphenol (NP) isomer mixture was purchased from Interchim. It was diluted in hexane to obtain 40 g/L. The spiking mix was prepared from these individual concentrated solutions to the final concentration of 100 mg/L, except for indeno(1,2,3,c,d)pyrene (20 mg/L) and nonylphenol (2 g/L). The 10 mg/L of PAHs in acetonitrile and the 100 mg/L of NP in hexane HPLC standard solutions were provided by Dr Ehrenstorfer GmbH. For quantification, the standard solutions were diluted to obtain 6 calibration levels from 10 to 1000 µg/L in acetonitrile for PAHs and from 500 to 5000 µg/L in hexane for NP. Standards were stored at -20 °C.

III.2. Sewage sludge samples

III.2.1. Continuous experiments

The continuous experiments were carried out using five different sludge samples: the primary sludge sample (PS), the thermally treated primary sludge sample (TTPS), a high loaded secondary sludge sample (HLSS), the cellulose secondary sludge sample (CSS) and the supernatant secondary sludge sample (SupSS). PS was collected at the outlet of the primary settling tank at a domestic WWTP treating 33 000 PE (Person Equivalent). A part of this sample was hydrolysed at 160 °C for 30 min in a Zipperclave reactor to obtain the TTPS. The HLSS came from the biological aerobic unit of a domestic plant treating 250 000 PE with a very low sludge retention time (0.4 day). The CSS sample was obtained by mixing HLSS with cellulose particles (20 µm, Sigma-Aldrich) at a chemical oxygen demand (COD) proportion of 50:50. Centrifugation of SS (10 000×rpm, 20min), followed by filtration at 1.2 µm (Whatman GF/C filter), was carried out to separate the particles from the supernatant, this latter containing the dissolved and colloidal matter (DCM). Finally, HLSS was diluted with its own supernatant at volumic proportions of 3:1 (sludge: supernatant) to provide the fifth sludge sample SupSS. Prior to their direct use, PS and SS were stored at -20 ◦C. All these samples were then diluted with deionized water to obtain 24 ± 5 g_{COD}/L and spiked at 5 µg/g_{DM} for each PCB and PAH, except for indeno(1,2,3,c,d)pyrene (1 µg/g_{DM}), and for NP (100 µg/g_{DM}), so that the spiked concentrations were similar to actual sewage sludge contamination levels.

III.2.2. Batch experiments

The batch experiments were carried out using three sludge samples: a low loaded secondary sludge (LLSS), the HLSS and a modified HLSS. The LLSS was sampled in the biological aerobic unit of a domestic plant treating 120 000 PE operated with a hydraulic retention time ranging from 3 to 5 days and a solid retention of approximately 20 d. The third sludge sample was made as followed: HLSS was centrifuged and filtrated at 1.2 µm. The supernatant was afterwards filtrated (PVDF membrane 0.1 µm) and ultrafiltrated using an Amicon ultrafiltration cell (Millipore) to yield the fractions below 1 kDa, using regenerated cellulose

membranes. This fraction was mixed with the initial particles to get a HLSS-1kDa sample. Prior to their direct use, HLSS and LLSS sludge samples were stored at -20°C.

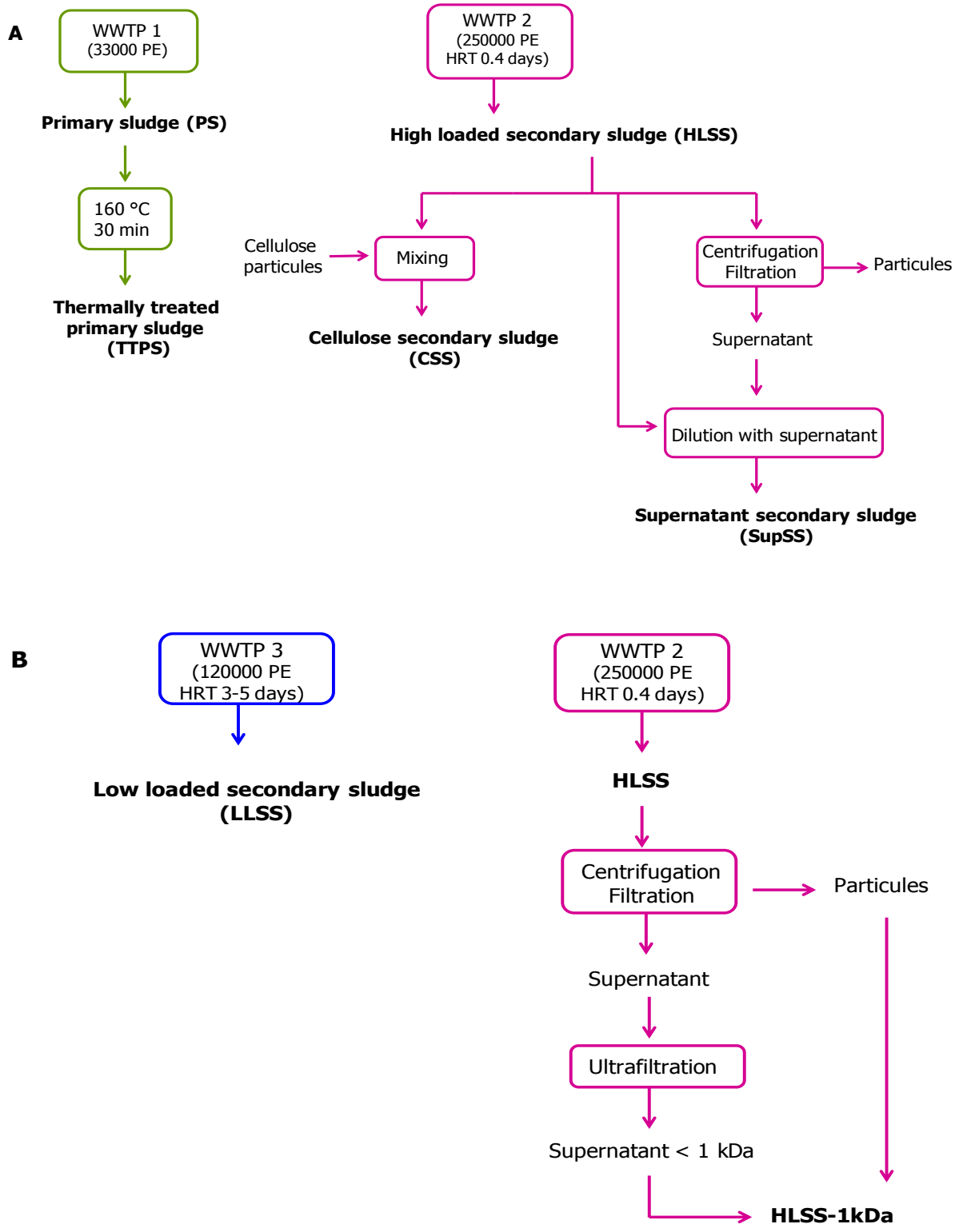

Figure III-1: Methology to obtain sludge samples for A: continuous experiments and B: batch experiments from different WWTP.

III.3. Anaerobic digestion of spiked sludge samples

III.3.1. Continuous reactors

The anaerobic digestion of the spiked sewage sludge was performed in stirred lab-scale reactors of 5 L (Figure III.1 (a)). The temperature was regulated at 35 °C thanks to hot water circulation in the external jacket. The feed, stored at 4 ◦C, was pumped six times per day into the reactor straight after the pumping out of the digested sludge. This latter was collected in tanks at 4 °C. Hence, the reactors were operated with a retention time of 20 days and an organic load of 1.2 ± 0.2 g_{COD}/L/day. For the start-up, they were filled with methanogenic sludge coming from an anaerobic mesophilic reactor adapted to PAH-polluted sludge, and directly fed at the normal operating conditions. The reactors were run during 4-5 retention times. The pH and the volumetric production of biogas were monitored on-line. Once a week, samples were taken from the feeding tank, the outlet tank and the gaseous phase to measure the particulate and supernatant chemical parameters and biogas composition. Removals were calculated when the steady state was achieved.

A sorbent cartridge (ORBO, Supelco) was placed at the gaseous outlet of the reactor fed with SupSS for 7 days, to quantify the volatilization of OPs.

Table III-1: Physico-chemical characteristics of the PAHs, NP and PCBs

Compound	Log Kow	M	log S	n5C	n6C	nCl	nOH
Fluorene	4.18	166	0,301	1	2	0	0
Phenanthrene	4.57	178	0,079	0	3	0	0
Anthracene	4.45	178	0,114	0	3	0	0
Fluoranthene	5.1	202	-0,585	1	3	0	0
Pyrene	5.32	202	-0,886	0	4	0	0
Benzo(a)anthracene	5.85	228	-1,959	0	4	0	0
Chrysene	5.89	228	-2,699	0	4	0	0
Benzo(b)fluoranthene	6.57	252	-1,921	1	4	0	0
Benzo(k)fluoranthene	6.84	252	-3,097	1	4	0	0
Benzo(a)pyrene	6.00	252	-2,523	0	5	0	0
Dibenzo(a,h)anthracene	6.70	278	-3,301	0	5	0	0
Benzo(g,h,i)perylene	6.73	276	-3,523	0	6	0	0
Indeno(1,2,3,c,d)pyrene	6.60	276	-1,208	1	5	0	0
Nonylphenol	5.76	220	0,778	0	1	0	1
PCB28	5.66	257	-0,64	0	2	3	0
PCB52	5.95	292	-0,904	0	2	4	0
PCB101	6.38	327	-1,475	0	2	5	0
PCB118	6.65	327	-1.575	0	2	5	0
PCB138	7.19	364	-2,137	0	2	6	0
PCB153	6.86	364	-1,959	0	2	6	0
PCB180	7.15	399	-2.167	0	2	7	0

Kow: octanol-water constant; M: molar mass (g/mol); S: solubility in water (mg/L); n5C: number of five carbon rings; n6C: number of six carbon rings; nCl: number of chlorines; nOH: number of hydroxyl substitutions.

III.3.2. Batch reactors

The anaerobic digestion of the sewage sludge in batch conditions was performed using 300 mL plasma bottles containing 250 mL of a defined mixture of sewage sludge (substrate) and inoculum (biomass). The bottles were stirred (100 rpm) and maintained at 35 °C. For these experiments, the sludge to inoculum ratio was equal to 0.5 g_{COD}/g_{OM}. The inoculum was concentrated from 8 to 18 g/L of dry matter (DM) to obtain a mixture with a total DM of 20 g/L. The mixture was spiked at three times the concentration of the continuous reactor (15 $\mu g_{PAH,PCB}/g_{DM}$, 3 $\mu g_{Ind}/g_{DM}$ and 300 $\mu g_{NP}/g_{DM}$) to improve OPs-degrading-microorganism activity. The inoculum was produced in a semi-continuous stirred lab-scale reactor fed with the spiked HLSS as it was described in the section III.3.1. Thus, an adapted-to-OPs digested sludge was obtained.

Each sludge condition was carried out in duplicate reactors series (Figure III.1 (b)). At different reaction times, two reactors were stopped to measure the total, free and aqueous OPs concentration over time. The initial OPs concentration was determined also in duplicate for all series. In parallel, several control reactors were realized with HLSS: not-spiked HLSS reactors and HLSS abiotic reactors. These abiotic control reactors were prepared by autoclaving the mixture containing plasma bottles at 121°C for 20 min.

Biogas volume was measured by liquid displacement and its composition was measured by gas chromatography. For all reactors, volumes of biogas were reported to the COD introduced in the bottle. In addition, volatile fatty acids (VFAs, g/L) production and DM removal were followed over time in all reactors series.

a

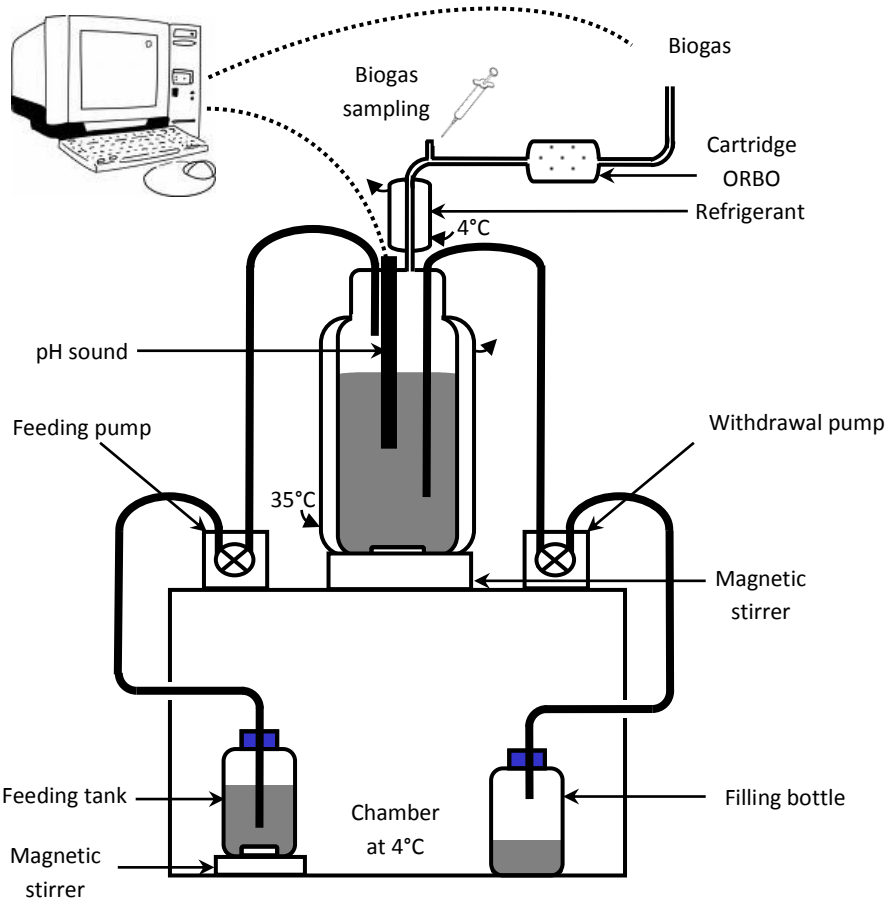

b

Figure III-2: (a) Continuous reactors setup. (b) Batch experiments.

III.4. Analytical methods

The scheme of the processes and the analytical methods that each type of sample was undergone are presented in the Figure III-3.

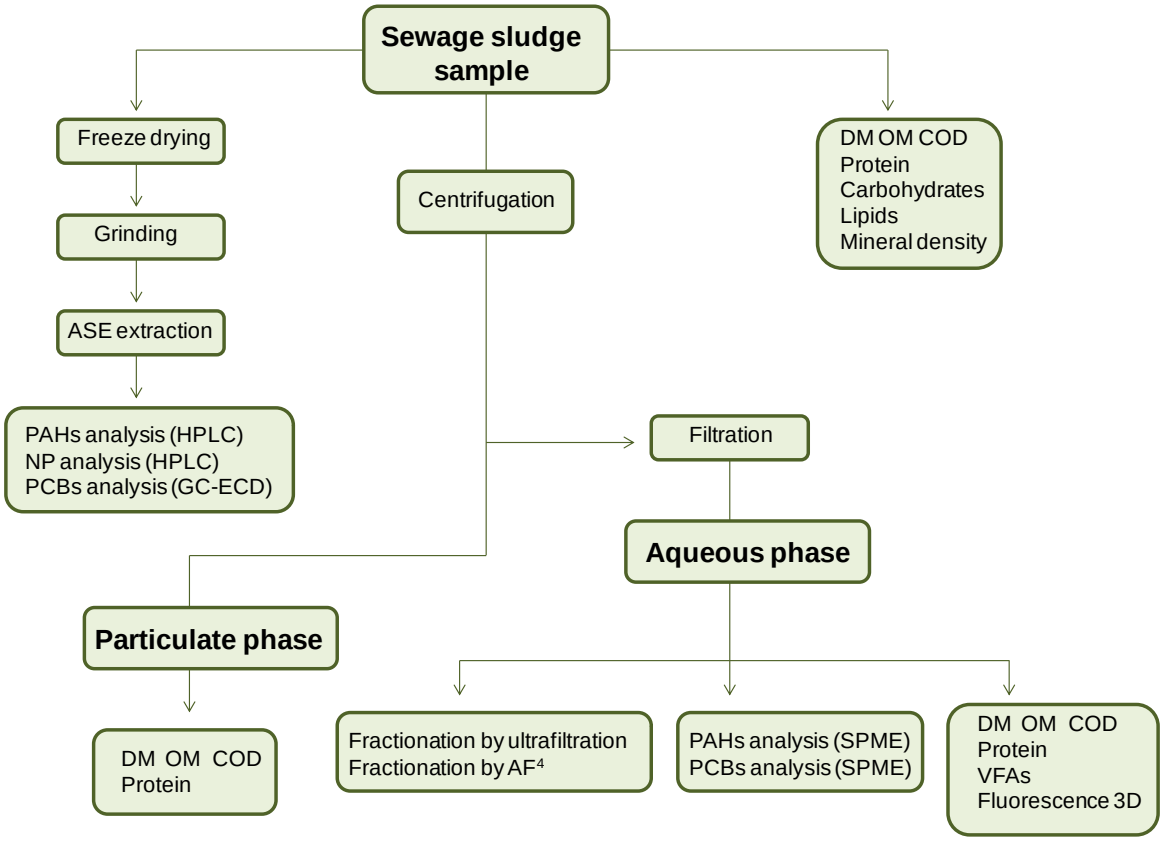

Figure III-3: Analytical, chemical and physical methodologies implemented in each type of sludge sample.

III.4.1. Samples preparation

III.4.1.1. Separation of particles from aqueous phase

The aqueous phase that contains the dissolved and colloidal matter was separated from the particulate phase by centrifugation (10 000×rpm, 20 min) followed by filtration at 1.2 µm (Whatman GF/C filter) in order to get rid of all the particles that are resuspended.

III.4.1.2. Freeze drying

300 mL of total sludge sample from continuous reactor or 100 mL from batch reactor were frozen at -20 °C. With the module HetoPowerDry PL 3000 (ThermoElectron Corporation), these samples were freeze dried. The walls of the ice trap were maintained at -55 °C, the vacuum was pushed to 1 mbar, and the shelves carrying the trays were equipped with heating resistors, in order to accelerate the sublimation of ice. The heating was programmed according to ranges of 2 h at -20 °C, -5 °C, 5 °C, 15 °C and then the samples were maintained at 25 °C until stop of the device. The freeze lasted about 20 h.

III.4.1.3. Grinding

Grinding was applied to freeze dried samples to reduce them to a fine powder and ensure sample homogeneity. For this, a microgrinder (Culatti) equipped with a 1 mm sieve was used. The grinding rotational speed was set at 3000 rpm.

III.4.2. Sludge analysis

III.4.2.1. Chemical characterization

Dry matter and organic matter determination

In a ceramic crucible (mass T), approximately 60 mL of sample was introduced. The crucible was then weighed (m_0), then placed in an oven at 105 °C for 24 h to evaporate the water and weighed again (m_{105}). Finally, the sample was placed in an oven at 550 °C for 2 h, and weighed again (M_{550}). The concentrations of dry matter (DM) and organic matter (OM) were obtained by the following calculations:

$$DM\,(g/kg) = \frac{m_{105}(g) - T(g)}{m_0(g) - T(g)} * 1000 \quad \text{and} \quad OM\,(g/kg) = \frac{m_{105}(g) - m_{550}(g)}{m_0(g) - T(g)} * 1000$$

The method error was 2% for liquid samples, and 5% for total sludge samples.

Chemical oxygen demand

The chemical oxygen demand (COD) of total sludge or aqueous sample was measured using kits Spectroquant (Merck), in accordance with ISO 15705. The commercial COD tubes, that contained an excess of potassium dichromate ($K_2Cr_2O_7$) in acidic conditions, catalyzed the complete oxidation of 2 mL of sample after 2h at 150 °C. The samples were diluted to be in the range 150–1500 mg_{O2}/L, and were measured by spectrophotometric detection. The method error was 5% for liquid samples, and reached 10% in the presence of particles due to the heterogeneity of the matrix and the small volume sampled.

Protein determination

The proteins contained in the total sludge or the aqueous phase were measured by the spectrophotometric method of Lowry (Lowry et al., 1951) based on the detection of peptide bonds. The reagents solution were a mixture of a basic solution (4 g_{NaOH}/L) of Na_2CO_3 (20 g/L), $CuSO_45H_2O$ (10 g/L) and a double tartrate solution of potassium and sodium (20 g/L), in volume proportions 100/1/1. Solutions of bovine serum albumin (BSA) at 20, 40, 60, 80 and 100 mg/L were prepared in order to build a calibration curve. In test tubes, 1 mL of sample or standard solution, 3 mL of reagents solution and 0.3 mL of Folin reagent were introduced and then placed in the dark for 2 h. In this alkaline medium, Cu^{2+} ions react with the nitrogen atoms of the peptide bonds, and are reduced to Cu^{+}. Cu^{+} ions then reduce the complex phosphotungsitic acid / phosphomolybdic acid content in the Folin reagent, giving a blue coloration to the reaction mixture. The absorbance at 750 nm was finally measured to

obtain the sample concentration g_{BSA}/L equivalents. The presence of particles increased the measurement error of 5 to 15%.

Carbohydrates determination

The determination of total carbohydrates in the sludge or the aqueous phase was based on their reaction with the anthrone reactive (Dreywood, 1946). The reagent solution was prepared by dilution of anthrone in sulfuric acid (98%) at 2 g/L. Calibration was performed with solutions of glucose at 20, 40, 60, 80 and 100 mg/L. 1 mL of sample or standard and 1 mL of reagent solution were placed in test tubes and then immersed in a water bath at 98 °C for 10 min. At this temperature and under acidic conditions, carbohydrates are dehydrated to give furan derivatives. These are condensed with the anthrone, generating a green color for hexoses. After cooling in ice, the absorbance at 625 nm was measured to obtain the sample concentration $g_{glucose}$/L equivalents. The method error was less than 10%.

Lipids determination

The determination of lipids in freeze-dried and ground samples was realized with the device ASE 200 (Dionex), in which the lipophilic compounds were extracted by petroleum ether at high temperature and pressure. ASE cells containing 1 g of dried sample and hydromatrix dispersant were heated to 105 °C and brought to a pressure of 67 bars to be fully filled with solvent. Cells were maintained under these conditions for 10 min and then the solvent was purged. Each cell underwent three cycles of this type. The extracts were collected in previously tared vials. The petroleum ether was evaporated in a Multivapor (Büchi) where the vials were stirred and heated to 45 °C under vacuum (500 mbar) condition, and then the petroleum ether was condensed at 4 °C. The remaining traces of solvent were then removed in an oven at 105 °C before weighing the vial. The difference compared to the tare weight was used to determine the mass of extractable petroleum ether compounds per unit of sample mass.

Volatile fatty acids determination

Volatile fatty acids (VFA) were determined by gas chromatography. 1 µL of a mixture 50/50 volume of sample (aqueous phase) and internal standard to 1 g/L (ethyl-2-butyric acid) were injected into the capillary column (FFAP Econocap; length/diameter/thickness: 15 m/0.53 mm/1.2 µm). The carrier gas was composed by nitrogen (25 bar), hydrogen (50 bar) and air (100 bar). The injector was maintained at 250 °C, the flame ionization detector at 275 °C, and the oven of the column had a gradient from 80 °C to 120 °C in 3 min. External standard at 1 g/L was used to quantify acetic acid (retention time t_R: 3.8 min), propionic acid (4.8 min), iso-butyric acid (5.2) min), butyric (6.3 min), iso-valeric (7.3 min) and valeric (9.2 min). The quantification limit was 0.1 g/L, and the measurement error was 2%.

Biogas analysis

The composition of the biogas produced by anaerobic digestion reactors was determined by gas chromatography. 1 mL of gas sample was injected. Two columns in series allowed the

separation of various gases. The first column Hayesep Q (Altech CTRI), filled with silica gel, allowed the separation of CO_2. The other gases were separated by the second column, which was a molecular sieve of 5 Å (Altech CTRI).

The carrier gas was argon at 2.8 bar. The detection was carried out using a catharometer whose current was set at 80 mA. The column oven was adjusted to 30 °C, while the injector and the detector operated at 100 °C. The composition of the sample was determined by external calibration. For this, a standard gas consisting of 25 % volume CO_2, 2 % O_2, 5 % H_2, 10 % N_2 and 58 % CH_4 was used.

III.4.2.2. Physical characterization

Aqueous phase fractionation

The criterion for the physical characterization of the aqueous phase (dissolved and colloidal matter) was the distribution in size fraction. Four fractions were defined: F1 for molecules between 0.1 and 1.2 µm, F2 between 10 kDa and 0.1 µm, F3 between 1 and 10 kDa and F4 below 1 kDa. The fractions were obtained using filtration and ultrafiltration techniques and the measurement of COD in the filtrates was chosen as the reference for this distribution due to the low volume that requires its analysis. Additionally, the particles that were retained on each membrane were taken for qualitative characterization.

The initial COD of the sample (COD <1.2 µm) was measured. The sample underwent a vacuum filtration through a PVDF membrane of 0.1 µm cutoff (Millipore), and COD of the filtrate (COD <0.1 µm) was measured. The filtrate underwent then an ultrafiltration at 3 bars in an Amicon cell (Millipore) with a regenerated cellulose membrane of 10 kDa pore size (Millipore). This ultra-filtrate (COD <10 kDa) was again ultra-filtered at 1 kDa pore size to give the fraction represented by COD <1kDa. F1, F2, F3 and F4 were calculated as follows:

$$F1 = \frac{COD_{<1.2\mu m} - COD_{<0.1\mu m}}{COD_{<1.2\mu m}} * 100 \qquad F2 = \frac{COD_{<0.1\mu m} - COD_{<10kDa}}{COD_{<1.2\mu m}} * 100$$

$$F3 = \frac{COD_{<10kDa} - COD_{<1kDa}}{COD_{<1.2\mu m}} * 100 \qquad F4 = \frac{COD_{<1kDa}}{COD_{<1.2\mu m}} * 100$$

Between each filtration, each membrane was rinsed with milliQ water under vacuum filtration or with pressure in the case of ultrafiltration in order to separate all the smaller particles that were still retained on the membrane. Further, the particles on the membrane were resuspended in a small volume of milliQ water and stored at -20 °C in amber glass vials. Thus, F1, F2, F3 and F4 (last ultra-filtrate) fractions were recovered. In order to normalize the characterization of these fractions, the dissolved organic carbon (DOC) of each fraction was measured.

Aqueous phase fractionation by AF^4 technology

The aqueous phase of sludge samples was separated using AF^4 (Figure III.3) and characterized using multiangle laser light scattering (LS), differential refractive index (DRI) and UV detectors. The AF^4 system was an Eclipse particle fractionators Wyatt Technology Europe. The characterization equipment consisted of the channel Eclipse F and the 18 angle scattering detector Dawn EOS from Wyatt Technology Europe. The DRI detector was a refractometer Optilab-rEX from Wyatt Technology Europe.

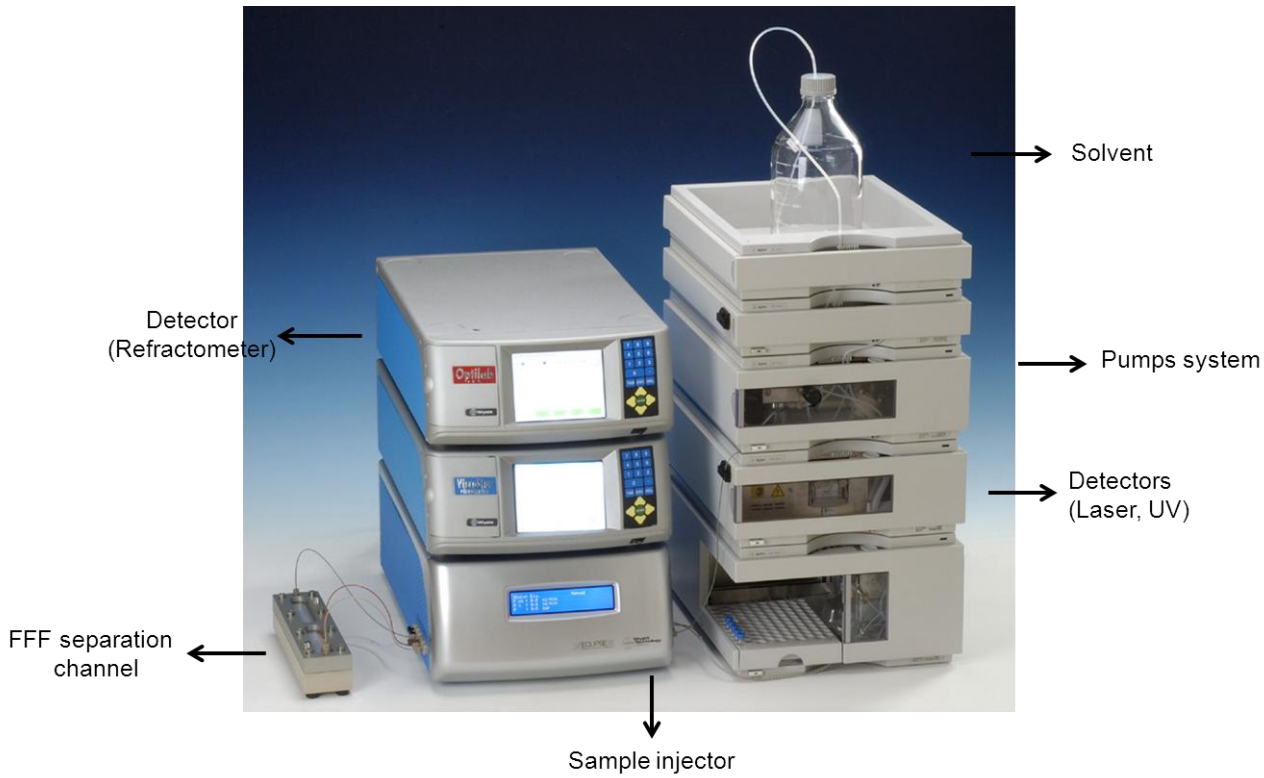

Figure III-4: AF^4 complete system

A channel spacer with a height of 350 µm and a regenerated cellulose membrane with a molecular weight cut-off of 1kDa were used. The following parameters were used for most of the separations: the detector flow was kept constant at 1 mL/min. After flow equilibrium, a volume of 100 µL of aqueous sludge sample (300 mg/L DOC) was injected at 0.2 mL/min for 2 min while focusing and it was focused further for 10 min with 2 mL/min focus flow (Figure III.4 (a)). During an elution time of 15 min, different cross flows (range from 0 to 3.5 ml/min) and cross flow rate gradients were tested in order to separate each aqueous sludge sample (Figure III.4 (b)). Finally, absorbance (UV detector), 90° LS response (V) and DRI response (V) v/s retention time (t_r) separation profile were obtained.

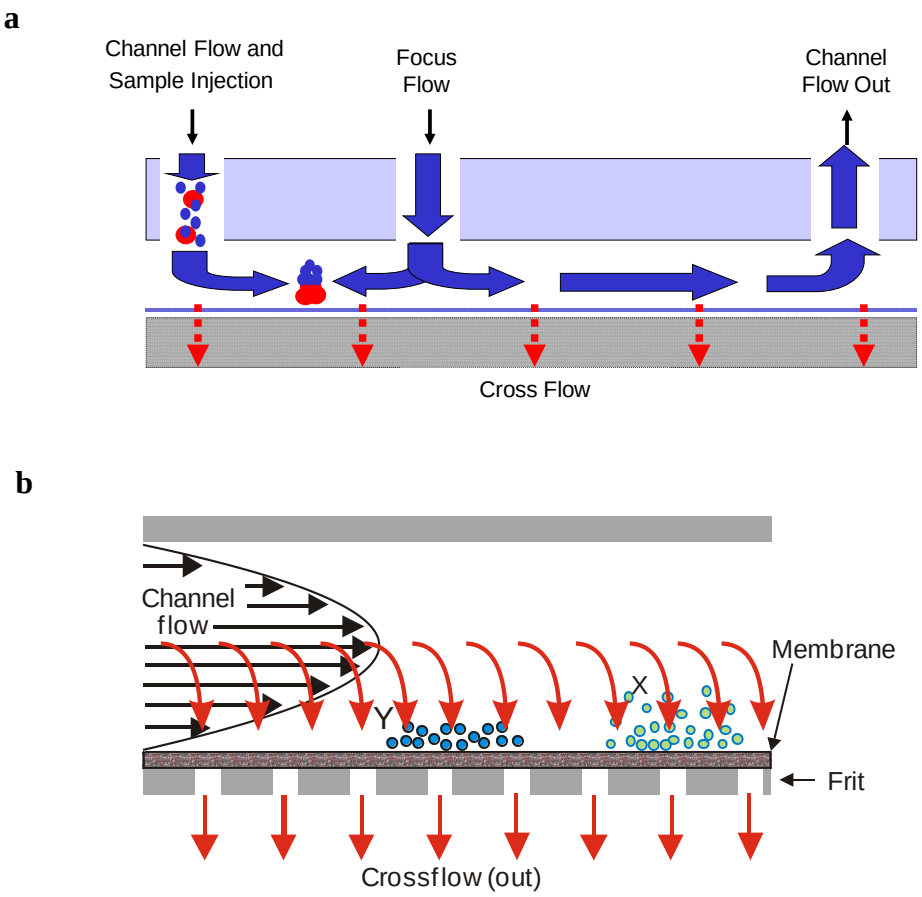

Figure III-5: (a) Focus technology. (b) AF^4 elution time. x: smaller particles; y: higher particles.

Mineral density

The mineral density of total sludge was measured on freeze dried and ground samples. In the case of mineral density, the total sludge was freeze dried, burned at 550 °C and finally ground.

In an Ultra Pycnometer 1000, a precise mass (≈1 g) of dried sample was introduced. Nitrogen was introduced into the sample chamber which the volume was known, until the pressure achieved 17 psi. The valve connecting the sample chamber to the expansion chamber (also with known volume) was then opened. The measured pressure difference between both chambers was directly related to the volume occupied by the sample. The ratio between the mass of a sample (g) and the occupied volume (mL) gived its density.

III.4.2.3. Functional characterization

3D-fluorescence characterization

Fluorescence EEMs were recorded on a spectrofluorimeter (LS55, Perkin Elmer, Courtaboeuf, France) using 500 µL of aqueous sludge sample in a 1 cm path length quartz cuvette. A xenon lamp emitted a pulsed radiation (20 kW for 8 µs) from 200 to 600 nm with 20 nm steps.

Fluorescence emission was recovered at a 90° angle from the excitation beam. Excitation and emission monochromator slit widths were set at 10 nm. Emission monochromator scan speed was 1200 nm s^{-1} so that fluorescence emission values were recorded each 0.5 nm from 200 to 600 nm.

The aqueous sludge samples were diluted with milliQ water at different dilution factors in order to measure the maximum emission intensity of each dilution at different excitation wavelengths. When a linear correlation between the diluted concentrations and their respective maximum emissions was obtained, a common dilution was chosen for all excitation wavelengths. In the linear range, the samples displayed a maximum emission intensity of 255 arbitrary units (AU).

Perkin Elmer FL Winlab 4.00.02 software was used to monitor the spectrofluorimeter and process the signals. To quantify the spectra an analytical approach termed fluorescence regional integration (FRI) was used (Cheng et al., 2003). This method consisted of a treatment of spectra 3D in image format using Image J software.

Initially, all spectra were transformed to .ASCII format using Winlab software in order to be treated with an algorithm (INRA-Cemagref) that generated a grey image in format .bmp using Matlab software. After, the image was treated with the plugin Sync measure 3D of the Image J software in order to get the fluorescence intensity (I) in AU, the area of the region (expressed as volume) and the X,Y/pixel: coordinates of barycenter. Finally, calculate the ratio (R_a) between the area of each region and the total area (sum of all regions) and then express the normalized intensity (NI) of each region using the following equations:

$$R_a = \frac{A_{i,region}}{A_t}$$

$$NI_{i,region} = \frac{I_{i,region}}{R_a \cdot DOC}$$

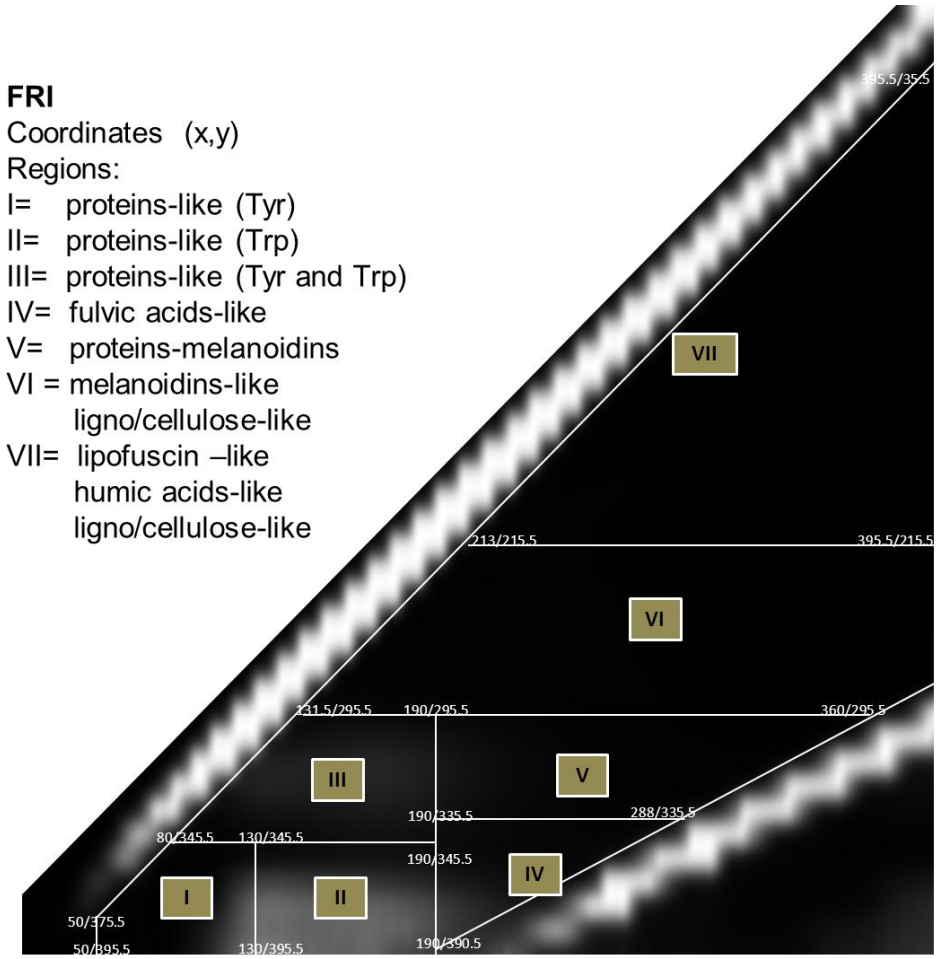

Figure III-6: Coordinates of fluorescent regions using Image J software and their respective functional groups.

III.5. PAHs/NPs/PCBs analysis

III.5.1. Extraction of PAHs/NPs/PCBs from the total sludge sample

The extraction of PAHs/NPs/PCBs from freeze dried and ground total sludge samples was realized by solvent accelerated extraction in ASE 200 (Dionex) extractor according to the methodology optimized by Trably et al., 2004.

ASE cells contained, in the bottom side, a glass fiber filter, and on it, 1 g of alumina (polar compound retention, Sigma Aldrich), 1 g of hydromatrix (dispersant, Varian) and 0.5 g (continuous reactors) or 0.1 g (batch reactors) of sample were introduced, and then the sample was mixed with the hydromatrix present. Finally, the rest of the volume was filled with hydromatrix.

The extraction solvent was a volumetric mixture (50/50) of hexane and acetone. Cells were fully filled with this mixture, and then heated to 120 °C and brought to a pressure of 100 bars. They were maintained 5 min under these conditions, and then the 60 % of solvent was purged and replaced by new solvent. This operation was repeated twice. Thus, two extractions per

cell were carried out, and were recovered in two separate vials. Evaporation of the solvent was carried out using the Multivapor (Büchi) and the complete drying of the extracts was obtained under nitrogen flow. Further, 2 mL of acetonitrile were added to each vial recovery. After agitation and repose, the two volumes of 2 mL more 1 mL of acetonitrile, used for additional rinsing, were collected in a tared vial. By weighing, the recovered exact amount was determined. The extracts were stored at -20 °C.

III.5.2. PAHs quantification

The ASE extracted PAHs were analyzed by HPLC that was composed by an autosampler (Waters 717 plus Autosampler), a peristaltic pump system (Waters 600 Controller) and a fluorescence detector (Waters 2475).

The C18 column (PAH Bakerbond^{TM} 16-Plus) was maintained at 25°Cusing an oven (CIL Cluzeau). After injection of 20 µL of sample, the pump system generated a first isocratic phase at 0.25 mL/min of acetonitrile/water mixture (60/40 v/v) for 30 min, then a gradient up achieve elution of acetonitrile to 100% after 35 min, maintained for 60 min and the flow was finally increased to 0.5 mL/min for the rinsing phase with acetonitrile/water mixture (60/40 v/v). The detection system optimized by Trably et al. (2004) was programmed to quantify each PAH with its optimal excitation wavelength (λex)/ emission wavelength (λem) (Table III-2).

Table III-2: Retention time (min) and PAH λex/λem (nm) pairs used for their detection by fluorimetry

HAP	Flu	Phe	Ant	Fluora	Pyr	BaA	Chr	BbF	BkF	BaP	DBA	BghiP	Ind
t_R	22	26	31	36	39	49	51	57	60	63	67	69	71
λ_{ex}	266	250	250	280	260	280	268	234	270	270	300	300	300
λ_{em}	312	370	400	430	410	430	384	420	400	400	407	407	500

Calibration was performed using six levels of PAH standard concentration (10 to 1000 mg/L) obtained by diluting a stock solution PAH Mix (CIL Cluzeau). Then, after each series of 10 samples, a standard was injected in order to check the stability of the signal over the injections.

III.5.3. NPs quantification

The ASE extracted NPs were analyzed using the method developed by Ahel et al. (2000). The HPLC device consisted of an ASI 100 autosampler (Dionex), a P580 pump system (Dionex) and a RF2000 fluorescence detector (Dionex).

First, 100 µl of the ASE acetonitrile extracts were evaporated under nitrogen flow and recovered in an appropriate volume of hexane (≈ 1 mL). Column LiChroCART Purospher® STAR® NH2 was maintained at 30 °C using an oven (CIL Cluzeau). The eluent used was a mixture of hexane/isopropanol (98.5/1.5 v/v). Elution was carried out in isocratic conditions

at 2 mL/min, and nonylphenol (t_R: 13 min) was detected at a λex/λem pair of 228/305 nm. From a commercial NP standard solution at 10 mg/L (CIL Cluzeau), four levels of concentrations were prepared (0.5, 1, 2 and 4 mg/L). The injected volume was 20 µL. A series of injection of these standard solutions was interposed between each series of 10 samples.

III.5.4. PCBs quantification

The ASE acetonitrile extracts were purified using micro-columns with acid silica and active copper in order to transfer and concentrate the pure composites (PCBs) in isooctane (quantification solvent).

The purification occurs in glass micro-columns as shown in the Figure III-6. The purification columns were built as follows: in the bottom, a small amount of fiberglass cotton was introduced in order to support the column; on the cotton, approximately 1cm of height of active copper was introduced and the rest of the column was filled with acid silica to top (Figure III.7).

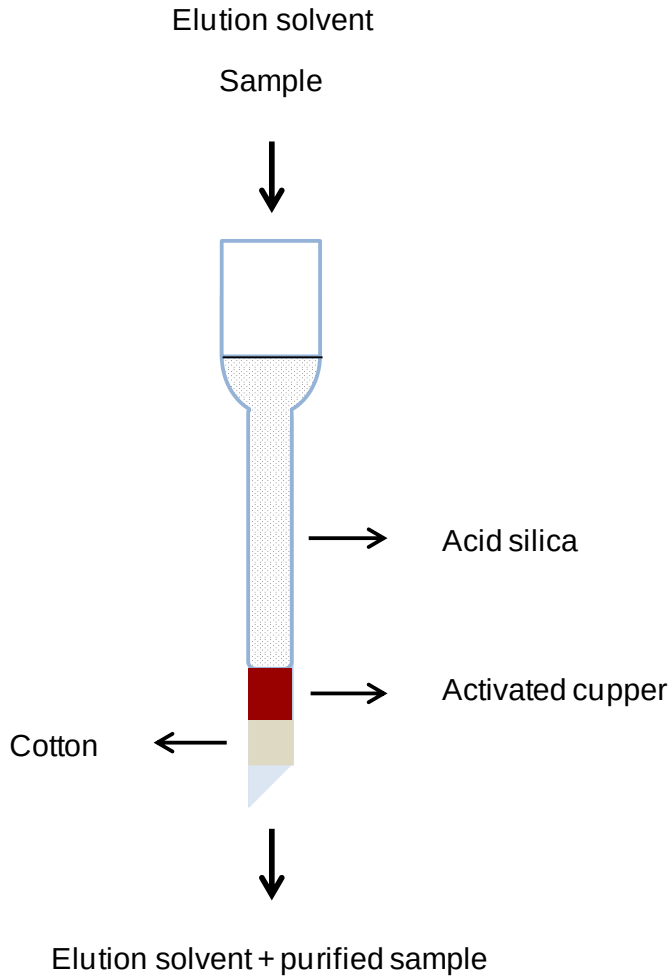

Figure III-7: Purification micro-columns system.

First, the columns were connected to a vacuum system and they were conditioned with 5 mL of n-pentane or the volume necessary to maintain the column wet. After, an exact volume of sample was introduced and then, it was eluted under vacuum condition with 3 x 5 mL of a mixture of n-pentane/dichloromethane (90/10 v/v). The elution mixture (15 mL) was recovered in glass vials. The vials were then evaporated under nitrogen flow, leaving approximately 1 mL of solution, and then 2 mL of isooctane were added and finally, the solution was again evaporated until reaching a final isooctane volume of 300 µL. Thus, the sample was ready for analysis by gas chromatography-electron capture detector (GC-ECD).

Fiberglass cotton preparation

Using a metal beaker, the cotton was immersed in dichloromethane and it was placed in an ultrasonic bath for 15 min. After, the cotton was dried under vacuum.

This procedure was performed three times, and after the third drying, the cotton was covered with foil (with some perforations), and then it was placed over the range hood one night.

Acid silica preparation

First, the silica was conditioned in the same way that the fiberglass cotton (previous paragraph).

An exact mass of conditioned silica was mixed with H_2SO_4 according to following equation:

$$V_{H_2SO_4} = \frac{(Silica\ mass \cdot 47)}{129}$$

$V_{H_2SO_4}$ is the volume of acid in mL and *Silica mass* is the mass of conditioned silica in g.

The silica and the acid were mixed until the lumps disappeared. After, the silica was stored in amber bottles and they were placed in an oven at 200 °C one night. The bottles were stored in a desiccator.

Active copper preparation

The copper (Aldrich, 40 mesh 99.5%) was mixed with dilute hydrochloric acid (dilution factor: 2) for 5 min or until the copper turned pink/red. After, the acid was dropped (without putting the copper in contact with air) and then, the copper was immersed in miliQ water and mixed again. This washing with miliQ water was repeated until the solution achieved a neutral pH.

Further, the miliQ water is dropped and copper was rinsed 5 times with acetone, and after this, the acetone was dropped and the copper was rinsed again 5 times with dichloromethane. Finally, the copper immersed in dichloromethane (completely covered with the solvent) was stored in a hermetic bottle.

III.5.5.PAHs and PCBs quantification by solid phase microextraction

III.5.5.1. Aqueous and free PAHs quantification

The spiked sludge aqueous samples were prepared as it was presented in the section III.4.1.1. SPME analyses of 9 mL of aqueous samples and spiked water were performed with commercially available PDMS (polydimethylsiloxane) 100µm coated fibers from Supelco (Bellefonte, USA). After the immersion of the fiber in the sample, it was immediately desorbed into GC injection port (GC-MS for PAHs and GC-ECD for PCBs). Analyses were performed in automated mode with a Combipal (CTC Analytics, Zwingen, Switzerland).

For PAHs quantification the GC was an Agilent 6890 model equipped with a mass selective detector, model 5972 with energy of ionization of 70eV. The column used was a HP-5MS ((5%-Phenyl)-methylpolysiloxane; 30 m x 0.25 mm i.d; 0.25 µm film; Agilent Technologies). Injection of SPME samples was performed in the pulsed splitless mode (30 psi of pulse pressure for 1 min, after 2 min, 55 mL/min of purge flow and after 15 min, the gas saver was set at 20 mL/min) and the inlet temperature was 250 °C. The carrier gas was helium with a constant flow rate of 1.3 mL/min and linear velocity of 42 cm/s. The column temperature was kept initially at 60 °C for 2 min, increased to 150 °C at 20 °C/min, then to 250 °C at 15 °C/min and to 310 °C at 10 °C/min and finally kept for 3 min. For the determination of PAHs, GC-MS was operated in the Selected Ion Monitoring (SIM) acquisition mode.

To quantify the free and aqueous PAHs concentrations (Figure III-7) by SPME-GC-MS, standards were made with spiked milliQ water at known concentrations of PAHs and their corresponding deuterated PAHs (d-PAHs) to calculate the response factor (Ki) and the quantification yields (Ci) of each PAH. Two standards were measured at the beginning, every 8 samples and at the end of each SPME-GC-MS sequence in order to determine the Ki and Ci evolution over the analysis. Additionaly, d-PAHs were added at known concentrations as internal standards in the spiked sludge aqueous samples. Aqueous PAHs concentrations were calculated using their respective Ki values, chromatography areas (PAHs and d-PAHs) and the d-PAHs concentrations. In the case of aqueous PAHs concentrations, Ki ranged between 0.62 and 0.96, and the Ci for each PAH ranged between 95 and 100 %. PAHs and d-PAHs (including naphthalene-d8) concentrations in standards were 26.4 and 148.87 ng/L respectively. To determine the free PAHs concentrations, naphthalene-d8 was chosen as internal standard (Hawthorne et al., 2005), because its response is the same with or without dissolved and colloidal matter (DCM). Thus, recalculating Ki and Ci using only naphthalene-d8 as internal standard for all PAHs, the free PAHs fraction in aqueous-phase sludge samples was determined.

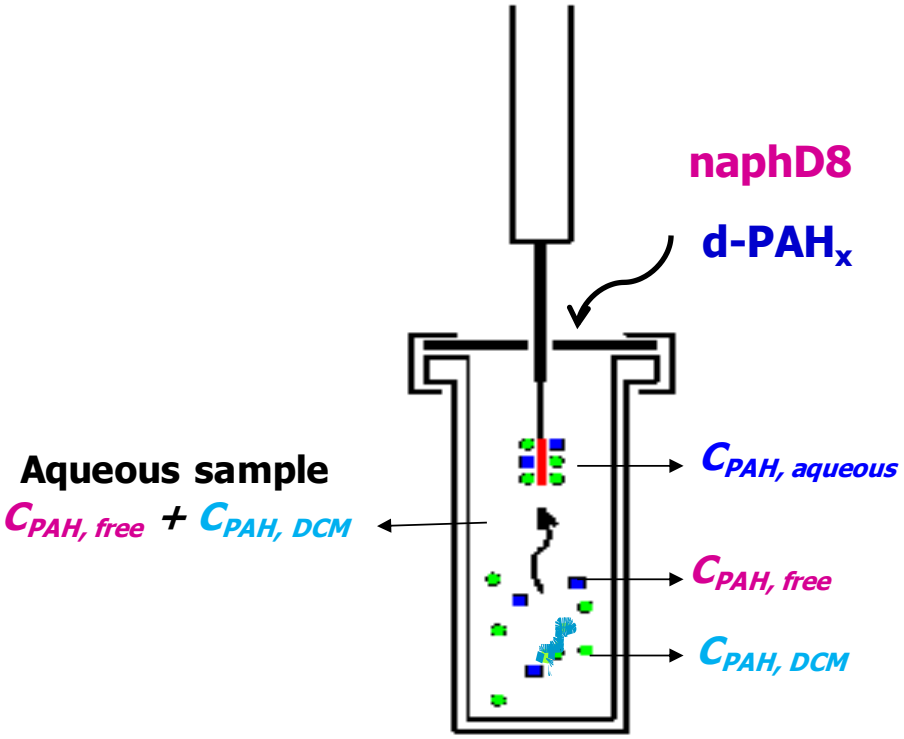

Figure III-8: SPME system. $C_{PAH,free}$: Free PAH concentration. $C_{PAH,DCM}$: Adsorbed to dissolved and colloidal matter PAH concentration. $C_{PAH,Aqueous}$: Aqueous PAH concentration.

Validation of quantification methodology

The quantification methodology was validated determining the Ki and Ci values in milliQ water and in DCM samples not previously spiked.

Six samples (three milliQ water and three DCM) of 9 mL were spiked at known concentrations of the targeted 13 PAHs with their corresponding d-PAHs. The samples were analyzed by SPME-GC-MS, determining the Ki for milliQ water and for DCM samples. Then, Ci were calculated in the DCM samples using the Ki values obtained in milliQ water, thus it was possible to know the matrix interferences on the aqueous PAHs quantification. If Ci values for each PAH are closed to 100%, the methodology is validated.

III.5.5.2. Aqueous PCBs quantification

To quantify the aqueous PCBs concentrations by SPME-GC-ECD, standards were made with spiked milliQ-water at known concentrations of PCBs and internal standards to calculate the response factors (Ki) and quantification yields (Ci). The PCBs internal standards were chosen according to a validation methodology that takes into account their similar molar mass to the targeted PCB and the obtained Ki values (close to 1) and Ci values (close to 100%). The Table III-3 shows the composition of the spiked milliQ-water with 7 PCBs and 10 internal standards. Two standards samples were measured at the beginning, every 8 samples and at the

end of each SPME-GC- ECD sequence in order to determine the Ki and Ci evolution over the analysis. Free PCBs concentrations were not quantified.

Table III-3: PCBs spiked water compositions

PCBs	PCBs concentration (ng/g solution)	Internal Standards	Standards concentration (ng/g solution)
PCB 28	11.5	PCB 20	22.59
PCB 52	12.3	PCB 30	7.36
PCB 101	9.7	PCB 103	6.43
PCB 118	10.5	PCB 155	6.72
PCB 153	7.2	PCB 79	18.64
PCB 138	7.3	PCB 77	22.20
PCB 180	13.2	PCB 87	21.05
		PCB 128	21.61
		PCB 159	15.01
		PCB 198	8.35

Validation of quantification methodology

The quantification methodology was validated determining the Ki and Ci values in milliQ water and in DCM samples not previously spiked.

Six samples (three milliQ water and three DCM) of 9 mL were spiked at known concentrations of the 7 targeted PCBs and of the 10 tested internal standards (Table III-3). The samples were analyzed by SPME-GC-MS, determining the Ki for milliQ water and for DCM samples. Then, Ci were calculated in the DCM samples using the Ki values obtained in milliQ water, thus it was possible to determine the matrix interferences on the aqueous PCBs quantification and to choose the apropriate internal standard for each PCB. If Ci values for each PCB are closed to 100%, the methodology is validated.

III.6. Data analysis

III.6.1. Removals calculation in continuous and batch reactors

The comparison of input and output parameters in continuous reactors and between t_0 and t_f in batch reactors permits to determine the total removals and removal rates, either for the macroscopic parameters of the reactor (dry matter, organic matter, COD ...) or for OPs.

In continuous reactors, the removals were calculated after reaching steady state, i.e. after 3 to 4 HRT, in our case, between 60 and 80 days of digestion. The removals of each parameter were calculated by the the removal average of the last 5 weeks.

$$removal = \frac{average(output) - average(input)}{average(input)} \times 100$$

With average (output), the average concentrations of output over the last 5 weeks and average (input), the average inlet concentrations over the last 5 weeks. Thus, the removal average and the corresponding standard deviation were obtained.

In batch reactors, OPs removal rates (r_{OPs}) were calculated using discrete points by difference of concentrations between two reactors and divided by their respective difference of reaction times. These parameters were expressed in µg/L/day. Methane production rate (r_{CH4}) and acetate accumulation rate ($r_{acetate}$) were calculated with the production of methane or accumulation of acetate in a range of time expressed in mL_{CH4}/g_{COD}/day and g/L/day respectively.

III.6.2. OPs partitioning coefficients calculation

OPs partitioning coefficients of DCM and particulate fractions were determined using the $C_{OP,free}$, $C_{OP,DCM}$ and C_{OPpart} that were quantified using the methodology presented in the sections III.5.2. and III.5.5. Thus, $K_{d,part}$ and $K_{d,DCM}$ values were calculated as following:

$$K_{d,part} = \frac{C_{OP,part}}{C_{OP,free}}$$

$$K_{d,DCM} = \frac{C_{OP,DCM}}{C_{OP,free}}$$

Using the DOC and POC as the concentrations of organic matter in the DCM and particulate fractions respectively, the partitioning coefficients are expressed as following:

$$K_{part} = \frac{K_{d,part}}{POC}$$

$$K_{DOC} = \frac{K_{d,DCM}}{DOC}$$

III.6.3 ANOVA

An ANOVA (Analysis of Variance, ANOVA) at one factor was performed to determine whether there was a statistical difference between two or more data samples. The data samples that were considered were small (often three individuals). We therefore could not verify that they followed a normal law or they had an identical variance.

The ANOVA was implemented through the utility analysis of Excel (Microsoft). The hypothesis tested (H_0) was that all samples had the same average. The alternative hypothesis was that at least one sample had an average different from the others. The test principle was to decompose the intra-class variance and inter-class and then calculate a coefficient F of Fisher. If $F_{observed}$ exceeded the $F_{critical}$, H_0 was rejected.

A second information was provided by the software: the p-value or critical probability. If the p-value was lower than 0.05, H_0 was rejected with a 5% risk. If it was greater than 0.05, the risk was too great to reject H_0, therefore the hypothesis was validated.

III.6.4 Multivariate linear regression by PLS

The linear regression partial least squares (PLS) is applied to explain or predict a variable (block Y) in function of several explicative variables or predictors (X block). The hypothesis is the existence of a linear regression between Y and each predictor (X).

This regression technique is based on the construction of factors (also called principal components) by minimizing the covariance between the block Y and the block X. The first factor contains the highest percentage of variance, and the following factors decreasing percentages. The number of factors to be included (dimension) is determined by using a cross-validation procedure. A multivariate regression of Y block in function of the factors, therefore the X block, is then performed. This technique has the advantage of considering related explicative variables.

PLS regressions were implemented either with the software R version 1.2.2 for Windows using PLS functions developed by Durand or with a demo version of the software Unscrambler 10.6, using NIPALS algorithm. This latter allows estimating missing variables from their coordinates during the construction of factors, which makes it possible to do predictions of Y from a X block that contained undetermined variables. Completed X Block was used to apply the model to predict the corresponding Y variable.

IV. STUDY OF THE COMETABOLISM AND BIOAVAILABILITY INFLUENCE ON THE ORGANIC MICROPOLLUTANTS REMOVAL

IV.1. Overview

OPs removals were measured in semi-continuous anaerobic digestion reactors fed with different types of sewage sludge. Sludge samples were selected in order to get various matrice types and jointly various reaction rates within the process. Indeed, the physicochemical characteristics of the digested sludge, and therefore the affinity of OPs for it, depend on the fed matrix. If we suppose that there is a link between sorption and bioavailability, this strategy will vary the OPs bioavailability.

Moreover, the rates of matrix transformation are also dependent on its composition, its accessibility and its biodegradability. The chosen strategy may potentially allow to vary the basal metabolism, and thus the cometabolism in the anaerobic digestion systems.

In order to get different sludge feed characteristics, two sewage sludge were sampled in industrial WWTP (PS and SS) and then these sludge were modified in order to build other three sludge samples. PS underwent a thermal pretreatment to obtain a TTPS. SS was mixed with particulate cellulose in equal proportions of COD, resulting CSS sludge. The cellulose is a fully biodegradable substrate, therefore CSS should induce a high cometabolism. Finally, the fifth sludge feed was made by diluting the SS with its own supernatant, in order to increase the proportion of DCM without changing the properties of both particles and DCM. The DCM is more easily biodegradable than particulate matter, and permits the displacement of OPs to the aqueous fraction by sorption, thus SupSS was designed to promote a strong cometabolism and high bioavailability.

To go further and to improve our understanding about the OPs removals driving mechanisms under anaerobic conditions, the approach "black box" will be tackled with the prediction of OPs fate from the reactors feed characteristics.

IV.2. Influence of feed characteristics on the removal of micropollutants during the anaerobic digestion of contaminated sludge

M. Barret, G. Cea Barcia, A. Guillon, H. Carrère, D. Patureau

Journal of Hazardous Materials 181 (2010) 241–247

Abstract

The removal of 13 polycyclic aromatic hydrocarbons, 7 polychlorobiphenyls and nonylphenol was measured during the continuous anaerobic digestion of five different sludge samples. The reactors were fed with one of the following: primary/secondary sludge (PS/SS), thermally treated PS, cellulose-added SS, or SS augmented with dissolved and colloidal matter (DCM). These various feeding conditions induced variable levels of micropollutant bioavailability (assumed to limit their biodegradation) and overall metabolism (supposed to be linked to

micropollutant metabolism throughout co-metabolism). On the one hand, overall metabolism was higher with secondary sludge than with primary and the same was observed for micropollutant removal. However, when overall metabolism was enhanced thanks to cellulose addition, a negative influence on micropollutant removal was observed. This suggests that either the co-metabolic synergy would be linked to a specific metabolism or co-metabolism was not the limiting factor in this case. On the other hand, micropollutant bioavailability was presumably diminished by thermal treatment and increased by DCM addition. In both cases, micropollutant removal was reduced. These results suggest that neither overall metabolism nor bioavailability would absolutely limit micropollutant removal. Each phenomenon might alternatively predominate depending on the feed characteristics.

IV.2.1. Introduction

Organic micropollutants such as polycyclic aromatic hydro-carbons (PAHs) and polychlorobiphenyls (PCBs) can be removed efficiently from wastewater: for example, 75% of PCBs are removed at a Wastewater Treatment Plant (WWTP) in Greece (Katsoyiannis and Samara, 2004) and at a WWTP in Paris, France, 76% and 98% of PCBs and PAHs, respectively (Blanchard et al., 2004). However, biodegradation only accounts for a small part of this removal. In fact, since PAHs and PCBs present very low water solubility and are highly hydrophobic, these properties favor their sorption to organic matter. As a consequence, sorption onto the solid effluent (sludge) has been demonstrated to be the main removal mechanism for PAHs and PCBs (Manoli and Samara, 1999; Byrns, 2001; Blanchard et al., 2004; Katsoyiannis and Samara, 2004). Thus, their concentration in sludge reaches 0.001-10 $\mu g_{PAH}/g_{DM}$ (Bodzek and Janoszka, 1999; Blanchard et al., 2004; Abad et al., 2005) and 0.01-1 $\mu g_{PCB}/g_{DM}$ (Blanchard et al., 2004; Katsoyiannis and Samara, 2004; Abad et al., 2005), depending on the influent and the characteristics of the WWTP.

Nonylphenol (NP) is produced within WWTP as a byproduct of the aerobic/anoxic biodegradation of long-chain ethoxylated nonylphenols (Di Corcia, 1998; Corvini et al., 2006). Due to its recalcitrance and hydrophobicity, NP accumulates in the biological process and is removed from wastewater through sorption to residual matter and subsequent clarification (Hung et al., 2004; Koh et al., 2005). NP occurs in sludge at a typical concentration of about 100 $\mu g_{NP}/g_{DM}$ (Fountoulakis et al., 2005; Aparicio et al., 2007).

Before its final disposal, sludge has to be stabilized. Among the available solutions, anaerobic digestion followed by spreading is the most sustainable option (Suh and Rousseaux, 2002). In addition, the anaerobic consortia involved in this bioprocess have been shown to partially remove PAHs (Trably et al., 2003; Dionisi et al., 2006; Bernal-Martinez et al., 2009), PCBs (Patureau and Trably, 2006; Bertin et al., 2007; El-Hadj et al., 2007) and NP (Chang et al., 2005b; Patureau et al., 2008). However, the comparison of published data reveals considerable variation in the anaerobic removal of micropollutants. Indeed, PCB removal ranged from 12% (Patureau and Trably, 2006) to 98% (El-Hadj et al., 2007) in continuous mode while NP removal varied from 0% in continuous mode (Hernandez-Raquet et al., 2007) to 40% in batch mode when operated with same retention times (Chang et al., 2005b). This

variability highlights a lack of understanding of the mechanisms which determine micropollutant removal. Nonetheless, several operational parameters have been shown to influence their removal, such as retention time (Benabdallah El-Hadj et al., 2006; El-Hadj et al., 2007) and temperature (Trably et al., 2003; Christensen et al., 2004; Benabdallah El-Hadj et al., 2006; El-Hadj et al., 2007). In addition to these operating conditions, the microbial population, bioavailability and cometabolism were also found to influence micropollutant removal. For example, an adapted inoculum is favourable (Trably et al., 2003), suggesting that the abundance of micropollutant degrading microorganisms is a crucial factor. Moreover, the poor bioavailability of micropollutants is usually assumed to limit their biodegradation (Chang et al., 2003; Patureau and Trably, 2006). Thus, when they are transferred to the aqueous phase thanks to surfactants, removal rates are higher (Chang et al., 2005b). PAHs, PCBs and NP are recalcitrant compounds and their biodegradation is only likely to occur thanks to co-metabolism and syntrophic interaction in conjunction with overall metabolism and the structure of the microbial population. Thus, an additional readily biodegradable carbon source can enhance micropollutant removal (Chang et al., 2005b; Dionisi et al., 2006), probably because it stimulates the overall metabolism. Finally, the anaerobic biodegradation of micropollutants is influenced by their physico-chemical properties (Chang et al., 2003; Benabdallah El-Hadj et al., 2006; Carballa et al., 2006). In this study, the removal by anaerobic digestion of PAHs, PCBs and NP was measured for different feed characteristics, in fixed operating conditions (retention time, temperature, inoculum, chemical oxygen demand and micropollutant load). The feed characteristics varied according to sludge origin, thermal treatment and the preparation of sludge composites obtained by mixing with cellulose or sludge supernatant. The objective was to identify both key parameters of the feed sludge along with the properties of the micropollutants which condition their removal and might help to predict their fate.

IV.2.2. Material and methods

IV.2.2.1 Chemicals

All solvents were purchased from J.T. Baker. The compounds studied are listed in Table IV-1. PAH and PCB powders were obtained from Dr Ehrenstorfer GmbH. Each compound was separately dissolved in dichloromethane at 1 g/L. The pure 4-nonylphenol (NP) isomer mixture was purchased from Interchim. It was diluted in hexane to obtain 40 g/L. The spiking mix was prepared from these individual concentrated solutions to the final concentration of 100 mg/L, except for indeno(1,2,3,c,d)pyrene (20 mg/L) and nonylphenol (2 g/L). The 10 mg/L standard solution of PAHs in acetonitrile, the 10 mg/L standard solutions of PCBs and of tetrachloronaphthalene (TCN) in hexane and the 100 mg/L of NP in hexane were all supplied by Dr EhrenstorferGmbH.For quantification, the standard solutions were diluted to obtain 6 calibration levels from 10 to 1000 µg/L in acetonitrile for PAHs, from 100 to 1000 µg/L in dichloromethane for PCBs and from 500 to 5000 µg/L in hexane for NP. Standards were stored at -20 ◦C.

Table IV-1: Physicochemical characteristics of the PAHs, NP and PCB180

Compound	log K_{ow}	M	log H	n5C	n6C	nCl	nOH
Fluorene	4.18	166	1.64	1	2	0	0
Phenanthrene	4.57	178	1.03	0	3	0	0
Anthracene	4.45	178	2.34	0	3	0	0
Fluoranthene	5.1	202	0.40	1	3	0	0
Pyrene	5.32	202	0.87	0	4	0	0
Benzo(a)anthracene	5.85	228	0.81	0	4	0	0
Chrysene	5.89	228	0.69	0	4	0	0
Benzo(b)fluoranthene	6.57	252	-1.15	1	4	0	0
Benzo(k)fluoranthene	6.84	252	-0.16	1	4	0	0
Benzo(a)pyrene	6.00	252	0.09	0	5	0	0
Dibenzo(a,h)anthracene	6.70	278	-0.08	0	5	0	0
Benzo(g,h,i)perylene	6.73	276	-0.61	0	6	0	0
Indeno(1,2,3,c,d)pyrene	6.60	276	-0.40	1	5	0	0
Nonylphenol	5.76	220	1.04	0	1	0	1
PCB 28	5.66	257	1.57	0	2	3	0
PCB 52	5.95	292	2.21	0	2	4	0
PCB 101	6.38	327	1.71	0	2	5	0
PCB 118	6.65	327	1.58	0	2	5	0
PCB 138	7.19	364	1.33	0	2	6	0
PCB 153	6.86	364	1.77	0	2	6	0
PCB 180	7.15	399	1.60	0	2	7	0

M: molar mass (g/mol); H: Henry's law constant (Pa.m^3/mol); n5C: number of five carbon rings;n6C: number of six carbon rings; nCl: number of chlorines; nOH: number of hydroxyl substitutions

IV.2.2.2. Sludge samples

The experiments were carried out using five different sludge samples. The primary sludge sample (PS) was collected at the outlet of the primary settling tank at a domestic WWTP treating 33 000 PE (Person Equivalent). A part of this sample was hydrolysed at 165 ◦C for 30 min in a Zipperclave reactor to obtain the thermally treated primary sludge sample (TTPS). The secondary sludge sample (SS) came from the biological aerobic unit of a domestic plant treating 250 000 PE with a very low sludge retention time (0.4 day). The CSS sample was obtained by mixing SS with cellulose particles (20 µm, Sigma-Aldrich) at a chemical oxygen demand (COD) proportion of 50:50.

Centrifugation of SS (10 000 × g, 20 min), followed by filtration at 1.2 µm (Whatman GF/C filter), was carried out to separate the particles from the supernatant, this latter containing the dissolved and colloidal matter (DCM). Finally, SS was diluted with its own supernatant at volumic proportions of 3:1 (sludge: supernatant) to provide the fifth sludge sample SupSS. Prior to their direct use or to composite preparation, PS and SS were stored at -20 °C. All these samples were then diluted with deionised water to obtain 24 ± 5g_{COD}/L and spiked at 5 µg/g_{DM} for each PCB and PAH, except for indeno(1,2,3,c,d)pyrene (1 µg/g_{DM}), and for NP (100 µg/g_{DM}), so that the spiked concentrations were similar to actual contamination levels.

IV.2.2.3. Experimental setup

The anaerobic digestion of PS, TTPS, SS, CSS and SupSS was performed in stirred lab-scale reactors of 5L. Temperature was regulated at 35 °C thanks to hot water circulation in the external jacket. The feed, stored at 4 °C, was pumped six times per day into the reactor straight after the pumping out of the digested sludge. This latter was collected in tanks at 4 °C. Hence, the reactors were operated with a retention time of 20 days and an organic load of 1.2 ± 0.2 g_{COD}/L/day. For the start-up, they were filled with methanogenic sludge coming from an anaerobic mesophilic reactor adapted to PAH-polluted sludge, and directly fed at the normal operating conditions. The reactors were run during 4-5 retention times.

The pH and the volumetric production of biogas were monitored on-line. Once a week, 7-day composite samples were taken from the feeding tank, the outlet tank and the gaseous phase. Removals were calculated when a steady state was achieved. A sorbent cartridge (ORBO, Supelco) was placed at the gaseous outlet of the reactor fed with SupSS for 7 days, to quantify the volatilization of micropollutants.

IV.2.2.4. Analytical methods

The phase containing dissolved and colloidal matter was separated from the total sludge samples by centrifugation (10 000 × g, 20 min) followed by filtration at 1.2 µm. The dry matter (DM, g_{DM}/L) in total sludge and in the dissolved/colloidal phase was measured by weighing the sample after heating at 105 °C during 24 h. The proteins and carbohydrates in total sludge samples were analyzed according to the Lowry (Lowry et al., 1951) and anthrone (Dreywood, 1946) methods, respectively. The standard curves 20-100 mg/L were obtained

with bovine serum albumin (BSA) for proteins (expressed in g_{eqBSA}/L) and with glucose for carbohydrates (g_{eqGlu}/L). The chemical oxygen demand in total sludge (COD, g_{O2}/L) was determined using Merck Spectro-quant kits, in accordance with ISO 15 705. The samples were diluted to be in the range 150-1500 mg_{COD}/L. To determine the concentrations of volatile fatty acids (VFA) acetate, propionate, iso-butyrate, butyrate, iso-valerate and valerate in the dissolved/colloidal phase, 0.5 µL were injected at 250 °C into a capillary column Econocap FFAP (Altech), Varian 3900 gas chromatograph. The carrier gas was composed of N_2 (25 bar), H_2 (50 bar) and air (100 bar). The detection by flame ionisation was carried out at 275 °C.

A fraction of each sludge sample was freeze-dried and ground in order to quantify the lipids and the micropollutants. The lipid content was defined as the matter extractible with petroleum ether (PEEM). The extraction was performed with an Accelerated Solvent Extractor (Dionex) operating at 70 bar and 105 °C. PAHs, PCBs and NP were extracted from the ORBO cartridge using a Soxhlet setup operating for 16 h at 60 °C, with 200 mL of hexane/acetone (50:50, v:v). Extraction from inlet and outlet sludge samples and quantification in all extracts were performed in accordance with Barret et al. (2009b).

The composition of biogas was measured by gas chromatog-raphy (Shimadzu GC-8A), with argon as the carrier gas (2.8 bar). A 1 mL volume was injected at 100 °C. Separation was performed using two columns: a Hayesep Q (Altech CTRI) and a 5 Å molecular sieve (Altech CTRI), both maintained at 30 °C. CO_2, CH_4, O_2, N_2 and H_2 were quantified with a catharometer operating at 80 mA.

IV.2.2.5. PLS regression

The partial least-squares (PLS) technique is based on con-structing PLS factors by minimizing the covariance between the dependant variable (Y block) and the explicative variables (X block). The prediction of Y block is then calculated with a multivariable linear regression on the X block using the software R version 1.2.2 for Windows and by using PLS functions developed elsewhere (Durand). The first PLS factor accounts for the highest percentage of variance and the following factors for decreasing amounts of variance. The num-ber of PLS factors (dimension, dim) of the models was determined by minimizing the mean squared predictions error (predicted residual sum of squares, PRESS) through a cross-validation procedure.

This technique was used to model the removal of PAHs, PCB180 and NP in the five reactors. X block was composed of micropollutant characteristics (Table IV-1) and of inlet sludge characteristics (Table IV-2), whereas Y block consisted of the removal values as percentage.

IV.2.3. Results and discussion

IV.2.3.1. Suitability of the operating conditions

VFAs did not accumulate within the five reactors (Table IV-2), indicating that the biodegradation was complete and that the organic load was appropriate. Moreover, the

methane content of the biogas was about 70%, except for the reactor fed with CSS which will be discussed later (Figure IV-1). 70% of methane in the biogas is typical for the anaerobic digestion of sludge (Benabdallah El-Hadj et al., 2007; Bougrier et al., 2008). The reactors thus ran in favorable methanogenic conditions.

Table IV-2: Average value and standard deviation of the feed characteristics and removals measured for the five operated reactors (calculated from 5 measurements performed at steady state). For each parameter, the p-value between the 5 sets of measurements is indicated in italic. Characteristics and removals can be considered as statistically different for p-value below 0.05.

Feeding	COD	DM	DCM	Proteins	Carbohydrates (from cellulose)	Lipids	VFA
				Feed characteristics			
	g_{O2}/L	g_{DM}/L	*% of total DM*	g_{eqBSA}/g_{DM}	g_{eqGlu}/g_{DM}	g_{PEEM}/g_{DM}	g_{VFA}/g_{DM}
PS	28 ± 4	24 ± 2	5 ± 1	0,27 ± 0.03	0.29 (0.00) ± 0.09	0.13 ± 0.01	0.03 ± 0.02
TTPS	27 ± 3	20 ± 2	11 ± 2	0.32 ± 0.10	0.29 (0.00) ± 0.15	0.15 ± 0.02	0.04 ± 0.01
SS	22 ± 2	19 ± 1	4 ± 4	0.25 ± 0.02	0.30 (0.00) ± 0.05	0.10 ± 0.01	0.04 ± 0.03
CSS	27 ± 2	21 ± 4	8 ± 7	0.16 ± 0.03	0.66 (0.46) ± 0.15	0.06 ± 0.04	0.02 ± 0.04
SupSS	19 ± 2	16 ± 2	14 ± 2	0.29 ± 0.05	0.26 (0.00) ± 0.06	0.10 ± 0.05	0.10 ± 0.02
p-value	***0.0004***	***0.0002***	***0.0003***	***<0.0001***	***<0.0001***	***0.001***	***0.03***
				Removal (%)			
PS	57 ± 7	49 ± 9	-	38 ± 12	88 ± 1	79 ± 7	93 ± 3
TTPS	64 ± 10	60 ± 10	-	51 ± 15	84 ± 10	83 ± 8	100 ± 5
SS	67 ± 7	58 ± 10	-	41 ± 16	81 ± 14	79 ± 5	97 ± 3
CSS	83 ± 4	79 ± 5	-	53 ± 11	98 ± 1	nm	100 ± 5
SupSS	62 ± 5	52 ± 11	-	49 ± 9	90 ± 3	nm	100 ± 4
p-value	***0.0001***	***0.0002***	***-***	***0.35***	***0.02***	***-***	***0.01***

nm: not measured

IV.2.3.2. Apparent removal vs. biodegradation of micropollutants

The removals of PAHs, NP and PCBs are presented in Figure IV-2. Since PAH volatilisation was undetectable in the reactor fed with SupSS, the calculated removals include two main mechanisms: biodegradation and sequestration. An analysis of variance was performed for each micropollutant between the removals measured in the 3 or 5 reactors (PCB removal was not measured in reactors fed with CSS and SupSS). For most compounds, removals in the different reactors were statistically different.

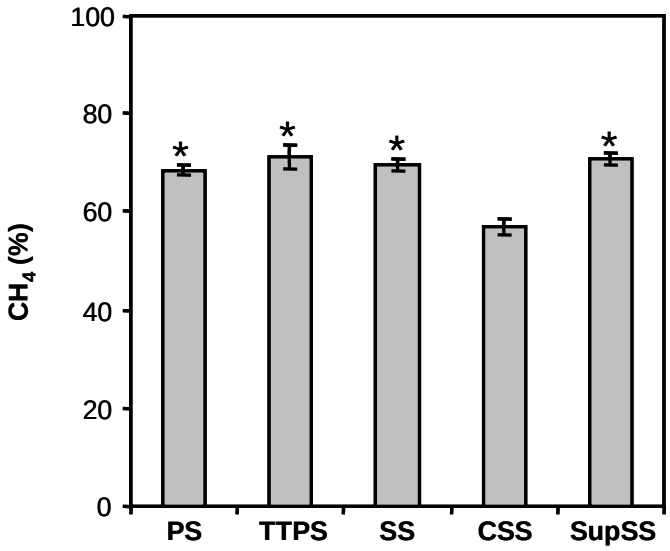

Figure IV-1: Average methane percentage of the biogas produced under the different feeds. Means labelled with a star are not significantly different (p-value=0.05).

Slightly substituted PCBs exhibited lower removals (Figure IV-2). Indeed, PCB anaerobic degradation is initiated by reductive dechlorination (Smidt and de Vos, 2004). Hence, the apparent removal of slightly substituted PCBs may result from their degradation and from their formation by dechlorination of highly substituted PCBs. Two cascade reactions could have occurred:

PCB180 → PCB153 → PCB101 → PCB52

PCB180 → PCB138 → PCB118 → PCB28

As we were not able to determine whether such reactions actually occurred, we only considered the fate of PCB180.

IV.2.3.3. Influence of sludge origin on micropollutant removal

Both primary sludge (PS) and secondary sludge (SS) presented a similar composition (Table 2). As the SS was sampled in an aerated tank with a very low retention time, it was not stabilized, which explains the slight differences with the PS. PS and SS differed slightly in protein and lipid content: both were higher in the PS. As microbial cells and exopolymeric substances structuring sludge flocs are mainly constituted of proteins (Sponza, 2003), the

measurement of proteins may be an indicator of poorly biodegradable matter. Higher lipid content suggests a higher proportion of hydrophobic material, poorly accessible during anaerobic digestion. These slight differences are probably responsible for the lower COD and DM removal with the PS feed. The removal of all micropollutants was also lower with the PS feed. Benabdallah El-Hadj et al. (2007b) observed contradictory results for NP degradation using primary and secondary sludge feed, with respective removals of 27% and 20%. However, information given by the authors about the origin and characteristics of their sludge samples was not complete. If their secondary sludge sample originated from a WWTP with the most common retention time (several days), its biodegradability would be lower than the SS used in this study (Bougrier et al., 2008), and also lower than PS (Gavala et al., 2003), which would explain the lower NP removal observed in secondary sludge than in primary sludge. Hence, a link may exist between the biodegradation of sludge matter and micropollutant removal. Nevertheless, the origin of sludge is not the determining factor: the characteristics of the sludge matter and its biodegradability are likely to be more reliable indicators.

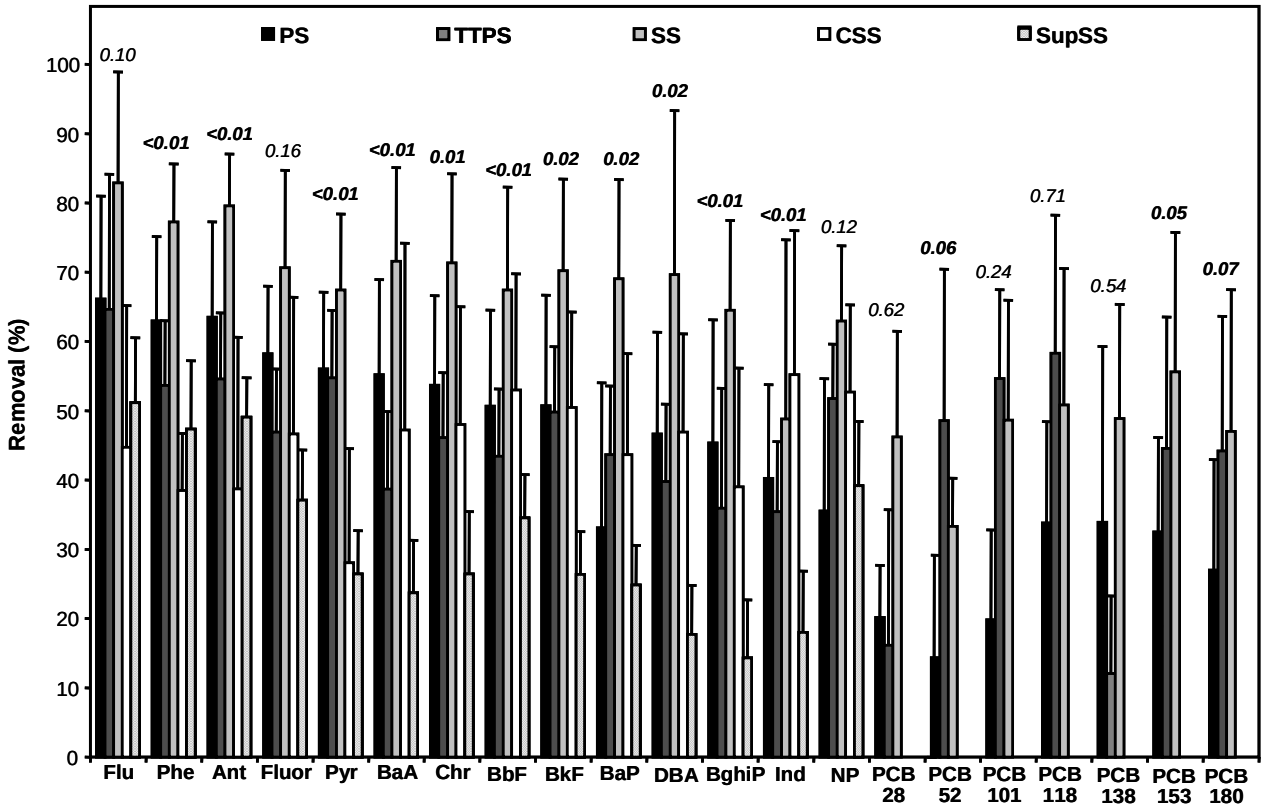

Figure IV-2: Micropollutant removal with PS, TTPS, SS, CSS and SupSS feeds. For each compound, the p-value between the 5 (3 for PCBs) sets of measurements is indicated in italic. Removal can be considered as statistically different for p-value below 0.05.

IV.2.3.4. Influence of thermal treatment of sludge on micropollutant removal

To investigate more thoroughly the link between sludge characteristics, sludge degradation and micropollutant removal, thermal treatment was applied to the PS to obtain TTPS. This

pre-treatment improved the removal of dry matter from 49% to 60% (Table IV-2), which is in accordance with results in the literature. Indeed, thermal pre-treatment, as well as ozone and ultrasound pre-treatments, have all been previously shown to solubilise sludge matter and to enhance sludge biodegradability and methane production (Gavala et al., 2003; Graja et al., 2005; Bougrier et al., 2006; Bougrier et al., 2007). Bougrier et al. (2008) established that the higher the initial biodegradability, the lower the pre-treatment effect. This may explain the positive but limited effect of thermal treatment in our case (11% enhancement), since the raw PS exhibited a high removal rate. In contrast, micropollutant removal was slightly reduced by thermal pre-treatment (Figure IV-2). Studies concerning the impact of such pre-treatment on the fate of organic micropollutants are scarce. Whereas ozonation was demonstrated to solubilise PAHs (Benabdallah El-Hadj et al., 2007b), probably because of PAH sorption to the solubilised dissolved and colloidal matter, no PAH transfer into the aqueous phase was detected after thermal treatment (Benabdallah El-Hadj et al., 2007b), or the aqueous fraction was found to decrease in both feed sludge and digested sludge on account of the denaturing of the dissolved and colloidal matter (Barret et al., 2009b). Usually, the aqueous fraction of micropollutants is assumed to be bioavailable to microorganisms (Artola-Garicano et al., 2003; Ivashechkin et al., 2004; Dionisi et al., 2006). According to this hypothesis, the bioavailability of micropollutants should decrease with thermal pre-treatment.

Furthermore, the second widely postulated hypothesis is that the biodegradation of micropollutants is limited by their bioavailability (Chang et al., 2003; Patureau and Trably, 2006). According to this view, thermal pre-treatment should decrease micropollutant biodegradation, as a result of a decrease in the bioavailability. The fact that no impact or, indeed, a negative impact was previously detected on NP (Benabdallah El-Hadj et al., 2007), pharmaceuticals and personal care products (Carballa et al., 2006) and linear alkylbenzene sulphonates (Carballa et al., 2009) tend to corroborate the hypotheses. The poorer removal of micropollutants after thermal pre-treatment observed in this study is thus consistent with the previously published data and might be explained by lower bioavailability after such pre-treatment.

In addition to bioavailability, co-metabolism is known to influence micropollutants metabolism. However, in spite of higher overall metabolism, as proven by higher DM removal (Table IV-2), micropollutant removal was not improved, indicating that the co-metabolic interactions were not linked to the overall metabolism. Either a specific metabolism is involved in co-metabolic interactions or the biodegradation of micropollutants is limited by other phenoma such as bioavailability.

IV.2.3.5. Influence of the addition of cellulose on micropollutant removal

As a readily biodegradable particulate compound, cellulose was added to SS in order to obtain a high level of overall co-metabolism. Cellulose is a polymer of glucose. The mass balance of monomeric pattern conversion (Symons and Buswell, 1933) predicts the production of a biogas composed of 50% of methane during cellulose degradation:

$C_6H_{10}O_5 + H_2O \rightarrow 3CH_4 + 3CO_2$

This explains why the methane content in the reactor fed with CSS decreased (57 ± 2%) in comparison to the reactor fed with SS (69 ± 1%, Figure IV-1). The extent of the enhancement of COD and DM removal (Table IV-2), as well as the low carbohydrate content in digested CSS (not statistically different from digested SS), suggests that all the cellulose was metabolized (100% removal). The degradation rates for cellulose and sludge matter could thus be calculated. In fact, the overall metabolism was found to be stimulated with CSS (1.1 g_{COD}/L/day removed with CSS, in contrast to 0.7 g_{COD}/L/day with SS), whereas the metabolism of the specific sludge matter was divided by a 2-fold factor compared to the SS feed (0.4 g_{COD}/L/day with CSS in contrast to 0.7 g_{COD}/L/day with SS). However, micropollutant removal did not increase: on the contrary, it decreased by a factor of 1.6 ± 0.4 (Figure IV-2). The addition of readily biodegradable substrates, such as yeast extract, molasses and cellulose, had already been performed in several batch experiments. The results were contradictory: in some cases, the removal rate of PAHs, NP and PCBs increased (Chang et al., 2004; Chang et al., 2005b; Dionisi et al., 2006; Chang et al., 2008) whereas the removal of PCBs (Bertin et al., 2007) and of brominated micropollutants (Gerecke et al., 2006) was not affected. Such discrepancies might be ascribed to different physico-chemical and microbial sludge properties. Depending on the microbial population, overall metabolic stimulation might or might not concern the microorganisms involved in micropollutant degradation.

IV.2.3.6. Influence of the addition of dissolved and colloidal matter on micropollutant removal

In SupSS, the proportion of dissolved and colloidal matter was multiplied by a 3-fold factor, in comparison to SS (Table IV-2). As particulate disintegration and hydrolysis are assumed to limit sludge methanisation, higher COD and DM removal was expected for SupSS than for SS. In fact, quite the opposite occurred: COD and DM removal was reduced by approximately 10% (Table IV-2). This slight decrease in the overall metabolism might be due to the effect of concentration: SupSS contained 19 g_{COD}/L, whereas SS contained 22 g_{COD}/L (Table IV-2). An inhibitory effect might also have occurred: VFA concentration reached 1.6 g/L in SupSS (Table IV-2), in which acetate accounted for 44%. Nonetheless, VFAs were totally removed (Table IV-2): they were not responsible for the inhibition of the methanogenic consortium. The hypothetical inhibition may have been caused by an unidentified constituent of DCM.

As a result of the decrease in overall metabolism, the potential co-metabolic effect on micropollutant removal would be expected to be negative. Micropollutants were, in fact, less efficiently removed (Figure IV-2). The high acetate concentration in feed might contribute to lower their biodegradation, as polyaromatic hydrocarbons biodegradation is supposed to produce acetate and hydrogen (Christensen et al., 2004). The acetate metabolic fluxes modification caused by high acetate load might cause the modification of micropollutant metabolism.

In SupSS, DCM proportion was enhanced without the denaturing phenomenon reported for thermal treatment Barret et al., 2010b. According to the bioavailability hypotheses previously

mentioned in Section IV.4.4., micropollutant bioavailability may have been increased. Insofar as micropollutant removal decreased, the decrease in overall metabolism or inhibitory effects might be predominant in comparison to the increase of bioavailability.

IV.2.3.7. Regression model

The presumable effect on bioavailability level (based on the usual hypotheses presented in Section IV.4.4.), the presumable effect on co-metabolism (in reference to the measured overall metabolism) and the measured micropollutant removal were summarized in Table IV-3. The anaerobic digestion performance with PS, TTPS, SS, CSS and SupSS tends to show that co-metabolism and bioavailability predominate alternately and limit micropollutant removal. The predominant phenomenon may be determined by the feed characteristics.

Table IV-3. Comparison of the different feeds and confrontation of micropollutant removal to the relative bioavailability (according to the usual hypotheses) and co-metabolism (assumed to be linked to overall metabolism). The "+" symbol indicates an enhancement, "-" symbol a diminution and "?" indicates that, in the light of the present and literature data, no assumption can be formulated about the effect.

Feed comparison	Presumable effect on bioavailability	Presumable effect on co-metabolism	Measured effect on micropollutant removal
SS with PS	?	+	+
TTPS with PS	-	+	-
CSS with SS	?	+	-
SupSS with SS	+	-	-

The feed characteristics differed statistically one from the others in different parameters (Table IV-2) so that conclusions were difficult to draw about the individual effect of each parameter. To accurately pinpoint the effect of each one, a PLS multivariate linear regression was performed. The regression led to the following model (dimension 6):

$$REMOVAL = 151 + 0.41 \log Kow - 0.077M - 1.94n5C - 3.08n6C - 1.86nCl - 11.8nOH + 0.08 \log H + 131DCM - 24.0Proteins - 45.7Carbo - 336Lipids - 54.2Cellulose - 577VFA$$

The modelled removal corresponded well with the actual measured removal for each of the 71 individual cases studied (Figure IV-3). This indicates that the representation by the selected predictors of removal variability was good. Model accuracy was not improved by including data on COD, DM, protein and carbohydrate removal (data not shown), suggesting that the relevant information is to be found in the feed characteristics. The relative importance of the feed and micropollutant characteristics could be assessed by comparison of the centered and

reduced regression coefficients (Figure IV-4). The VFA content was found to be the most influential parameter. This was due to the lesser removal of micropollutants reported with the SupSS feed, rich in VFAs. A possible direct inhibition by VFAs was mentioned in the previous paragraph, but the inhibition may have been caused by an undetermined compound. The effect of such an inhibitor would be linked to the presence of VFAs. Lipid content was the second most important parameter. In the first place, hydrophobic material may not be readily accessible for microorganisms, and thus it lowers the overall co-metabolism. Furthermore, it favours the sorption of micropollutants to particles (Barret et al., 2010b) and may thus lower bioavailability. Both these effects may account for the strong negative impact of lipids. The presence of cellulose, the third most important negative parameter, was shown to increase overall metabolism but to decrease the metabolism of sludge matter, resulting in a drop inmicropollutant removal.

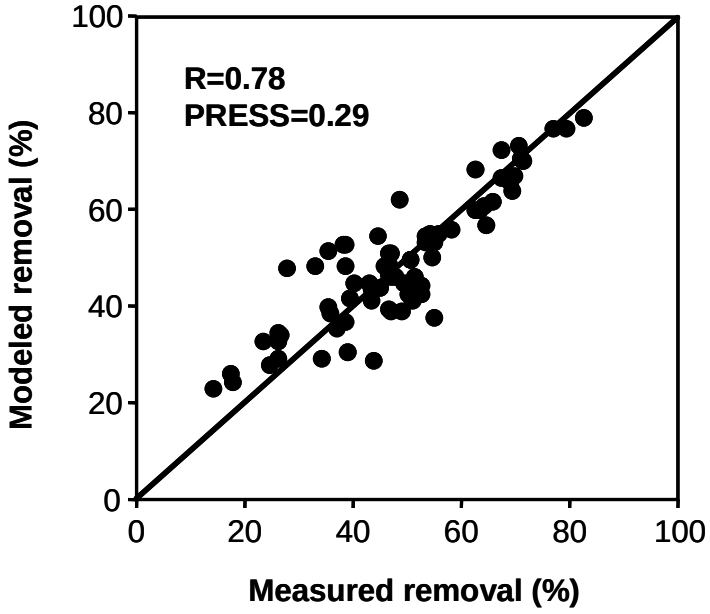

Figure IV-3: Modelled vs measured values of the removal of PAHs, NP and PCB180 during the anaerobic digestion with PS, TTPS, SS, CSS and SupSS.

The only positive parameter of the feed was the proportion of DCM, probably because it determined the aqueous and bioavailable fraction of micropollutants, and because DCM is a readily bioaccessible substrate.

The characteristics of micropollutants also account for differences in removal rates. The number of 6 carbon rings had the most negative effect. Indeed, the higher the aromaticity, the more recalcitrant to biodegradation (Benabdallah El-Hadj et al., 2006; Chang et al., 2003). The influence of Henry's law constant (logH) was negligible, which confirms the very low removal through volatilisation.

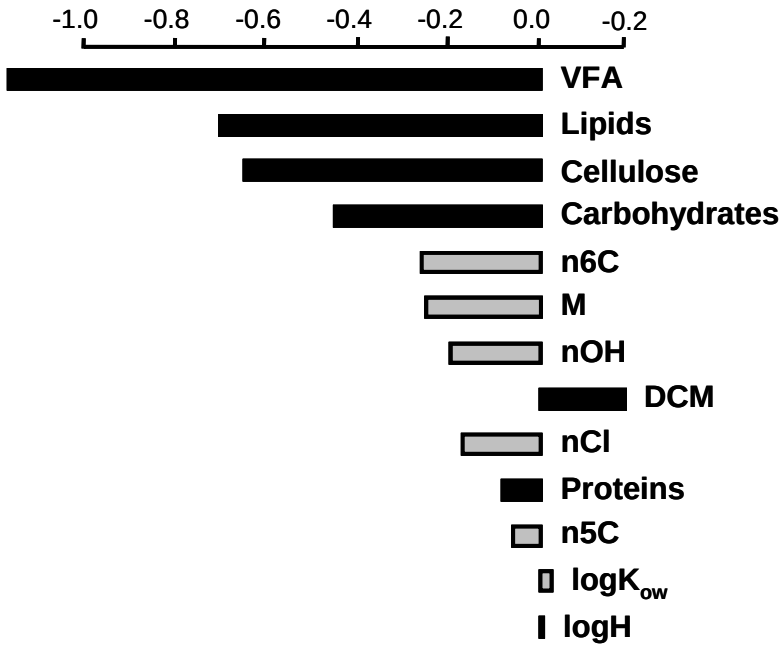

Figure IV-4: Centered and reduced regression coefficients. Coefficients related to the characteristics of the sludge feed are black coloured, whereas those related to micropollutants are represented in grey.

IV.2.4. Conclusion

The removal of PAHs, NP and PCBs by anaerobic digestion varied greatly as a function of feed sludge characteristics. The sample of primary sludge was slightly richer in proteins and lipids than the sample of secondary sludge. These differences may account for the slightly lower removal from PS of COD and micropollutants. The thermal treatment applied to the PS diminished the removal of micropollutants, while at the same time it stimulated the overall metabolism. When cellulose was added, micropollutant removal did not increase despite higher overall metabolism. These results demonstrate that co-metabolic synergy with the metabolism of micropollutants is not determined by the overall metabolism. Such synergy might be linked to a more specific metabolism or cometabolism did not limit micropollutant removal in these cases. In contrast, the overall metabolism in the reactor fed with a high proportion of DCM dropped while the bioavailability of micropollutants was hypothetically enhanced, resulting in lower micropollutant removal. In this case, limitation due to co-metabolism was likely to have predominated over limitation caused by bioavailability.

Depending on the reactor, greater or lesser removal might be explained either by variations in co-metabolism or by different levels of bioavailability. This suggests that no one mechanism can be identified as the absolute limiting factor. More research is needed to investigate and accurately quantify both mechanisms and determine their relative significance. Nonetheless,

the results suggest that a detailed characterization of the feed may help to predict the removal of micropollutants.

IV.3. Chapter conclusion

These results suggest that a fully characterization is necessary to better understand the role of the OP-matrix interaction on the OPs removals. For this, other different substrates will be tested coupled to a the study of the OP-matrix interactions of each physical compartment (aqueous and particulate) using separation techniques, functional characterization, sorption studies and the determination of the OPs concentration among the physical compartments (free, DCM and particulate OPs concentrations).

V. KINETICS OF ORGANIC MICROPOLLUTANT REMOVAL UNDER ANAEROBIC CONDITIONS IN SEWAGE SLUDGE

V.1. Overview

As it was discussed in the previous chapter, the removal of OPs by anaerobic digestion varied strongly as a function of feed sludge characteristics, suggesting that a detailed characterization of the feed may help to predict the removal of OPs. Additionally, this study reveals the importance of the nature of DCM fraction on the OPs removals, showing that although an increment in the proportion of this fraction did not affect significantly the overall metabolism (methane production), an important decrease in the OPs total removals was observed. This behavior may be explained by either the presence of additional compounds such as acetate that can produce an inhibition of the OPs metabolism (Christensen et al., 2004; Dolfing et al., 2009) or a displacement of the equilibrium constants K_{part} and K_{DCM} (Figure V-1) due to the increase of DCM constituents that may affect the OPs bioavailability.

In another study with sewage sludge, OPs removals were higher in the reactors fed with primary sludge than those fed with a mixture of primary and secondary sludge (Larsen et al., 2009). The characterization showed that the COD and VS concentrations in primary sludge were significantly lower than in the sludge mixture. This study supports our results, demonstrating that the sludge characteristics generate different levels of OPs bioavailability and consequently, different OPs removals. However, as it was showed in our study and subsequently validated by Barret et al. (2010c), OPs biodegradation resulted from a combination of bioavailability and cometabolism, being difficult to dissociate these two phenomena.

Additionally, Barret et al. (2010c) demonstrated experimentally that the aqueous fraction (Figure V-1) corresponds to the bioavailable sludge compartment. Taking into account this result and our first study, OPs removals were tested in batch reactors fed with different sludge compositions, inoculated with the same OPs-adapted anaerobic inoculum in order to better understand the influence of the bioavailability on the removals of OPs through the study of the role of the DCM concentration and nature on the distribution of OPs among the three physical compartments.

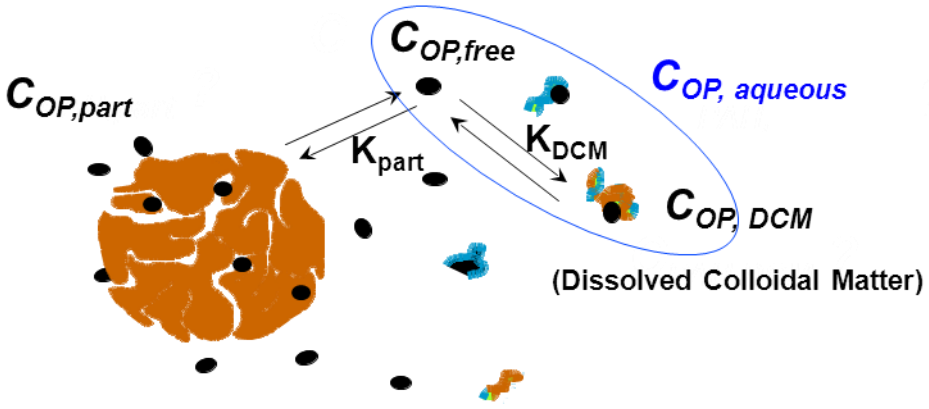

Figure V-1: Representation of the three-compartment system of an OP in sewage sludge (Barret et al. 2010a).

The ideas of choosing batch versus continuous reactors are:

- the high reaction times required for each continuous experience makes it difficult to test different substrates, besides in continuous systems the assessment of OPs removals through the different stages of anaerobic digestion is not possible,
- possibility of measurement of initial removal rates in batch reactor, using an adapted OPs anaerobic inoculum and a low ratio substrate/inoculum, with the hypothesis that the overall metabolism and the cometabolism will be the same in each experiment.

In this context, to measure the OPs removal rate over time jointly to the DCM role, five reactors series were carried out in duplicate using various sludge samples as substrates. A highly loaded secondary sludge (HLSS), a lowly loaded secondary sludge (LLSS) and the same HLSS with a modified DCM compartment (presence of colloids inferior to 1kDa) were used in order to get various OPs distributions (Figure V-2).

In addition to the total OPs concentration, aqueous and free OPs concentrations were measured all along the experiments using SPME technique. Thus, the OPs removal kinetics of the three physical compartments were obtained for each sludge mixture.

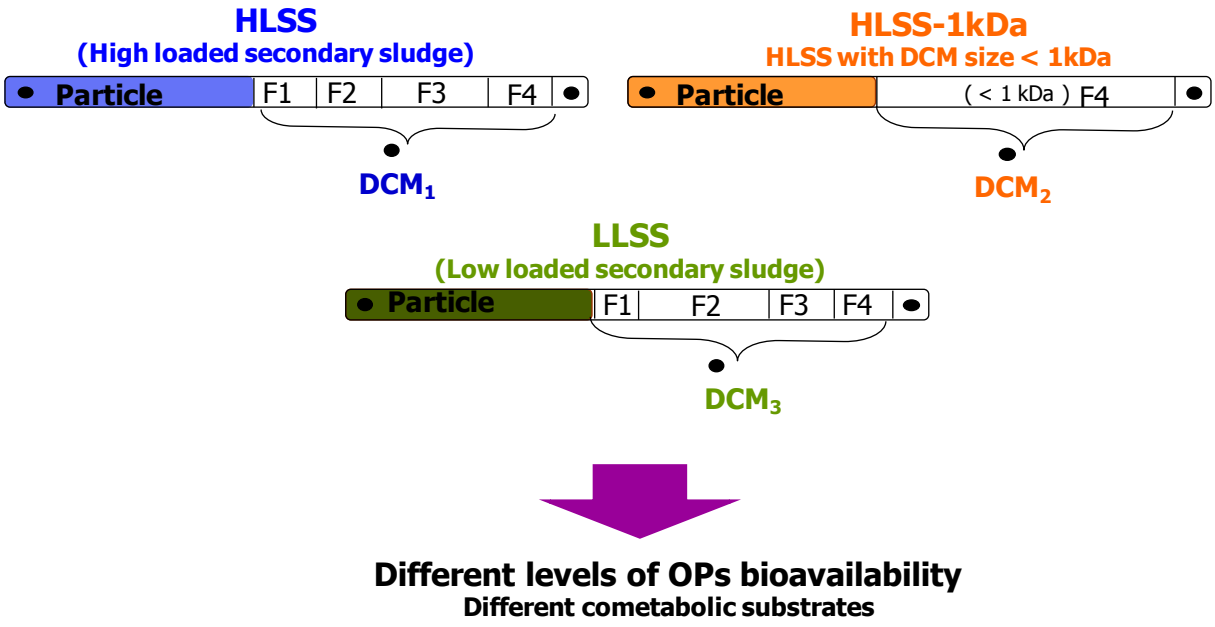

Figure V-2: Representation of the sludge physical compartments classified according to the particle size and the schema of confrontation between the different sludge mixtures.

The mixtures were prepared in such a way that:

- they contain enough concentration of DM for OPs analysis,

- a substrate to inoculum ratio is appropriate to get good performances of the anaerobic digestion.

To achieve these conditions, the mixtures were constituted around by an 80/20 % w/w of concentrated inocula and of substrate. Such substrate/inoculum proportion suggests that the OPs performance of the inoculum may be similar between the different sludge mixtures. However, such substrate/inoculum proportion may also not change significantly the affinity of the OPs for the DCM fraction (K_{DCM}) among the sludge mixtures. To verify this assumption a simplified version of a PLS model estimating the log K_{DCM} as a function of the sludge and OPs characteristics proposed by Barret et al. (2010b) was used in order to estimate the values of K_{DCM} for each mixture before to carry out the experiments. For this, COD, proteins and F_4 fraction, which are the parameters that presented the highest influences on K_{DCM} prediction, were measured in the DCM fractions of the sludge mixtures (HLSS and LLSS) beside the mineral density of the total mixtures, and then, with these data and the OPs characteristics, the K_{DCM} values were estimated.

The Figure V-3 shows the PLS model of Barret et al. (2010b) to predict K_{DCM} as a function of OPs and DCM characteristics (COD, proteins, F_4, mineral density). K_{DCM} values of HLSS and LLSS mixtures were predicted by PLS regression using the program Unscrambler 10.6. The predicted K_{DCM} are well correlated with the PLS model of Barret et al. (2010b) and, for a certain OP, the K_{DCM} values are different between the sludge mixtures. This result shows that different levels of bioavailability can be obtained with the chosen substrate/inoculum proportion.

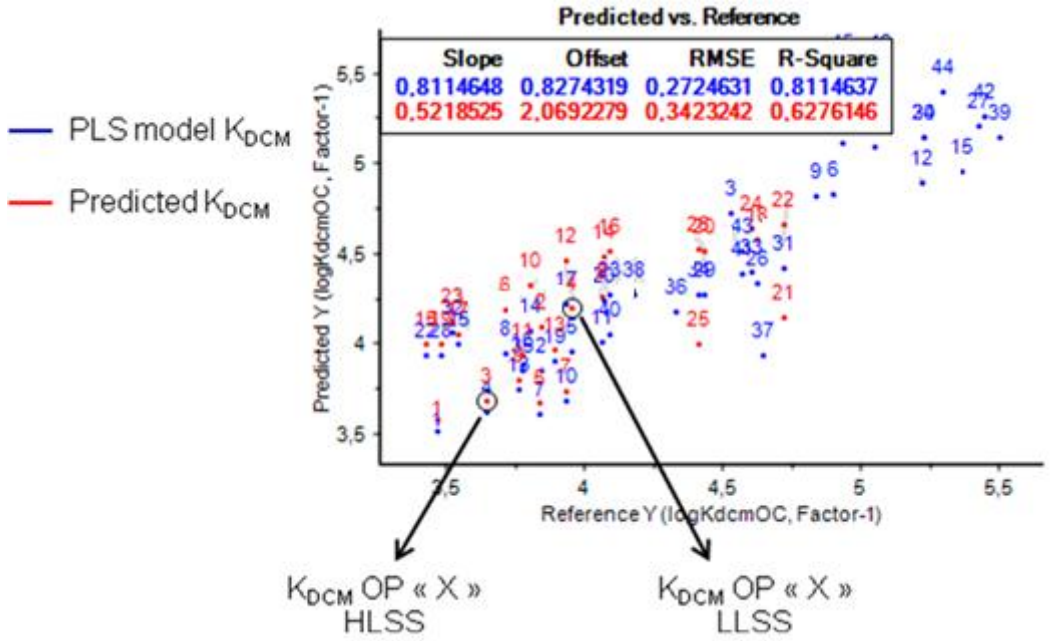

Figure V-3: K_{DCM} values of the PLS model of Barret et al. (2010) (Blue) and predicted K_{DCM} values for HLSS and LLSS mixtures (red) using the program Unscrambler 10.6.

In the following sections, the results of three HLSS, one LLSS and one HLSS-1kDa reactors series will be presented.

First, the PAH, NP and PCBs totals removals of the three sludge mixtures will be presented.

Afterwards, the kinetics results of the three HLSS reactors series will be presented. Mainly, this section will tackle the link between the OPs removals and the steps of anaerobic digestion, topic that will be presented in journal format.

Finally, the OPs distribution among the three physical compartments over time and their partition coefficient (Kpart and K_{DOC}) linked to the OPs removals and the macroscopic anaerobic parameters will be presented for each sludge mixture with their respective discussion.

V.2. OPs total removals in batch reactors under anaerobic conditions

V.2.1. PAHs and NP total removals

PAHs and NP total removals were quantified in three HLSS, one LLSS and one HLSS-1kDa batch reactors series. In all reactors, production of methane and DM removal were observed (Figures V-4A, V-4B) with a concomitant PAHs and NP removals in HLSS reactors (Figures V-4C, V-4D). The HLSS presented higher methanogenic performances than LLSS. This can be explained by the presence of a really stabilized organic matter in LLSS (due to the high HRT and SRT on the WWTP) by comparison to HLSS. In the HLSS-1kDa, the aqueous compartment contained only small dissolved compounds implying thus a higher COD concentration in the particles in order to have the same initial organic load. The PAH and NP removals followed the DM removal, with lowest removals with LLSS and HLSS-1kDa. The three sludge samples behave differently which may be explained by their various biochemical compositions and their various OPs distribution in the sludge compartments.

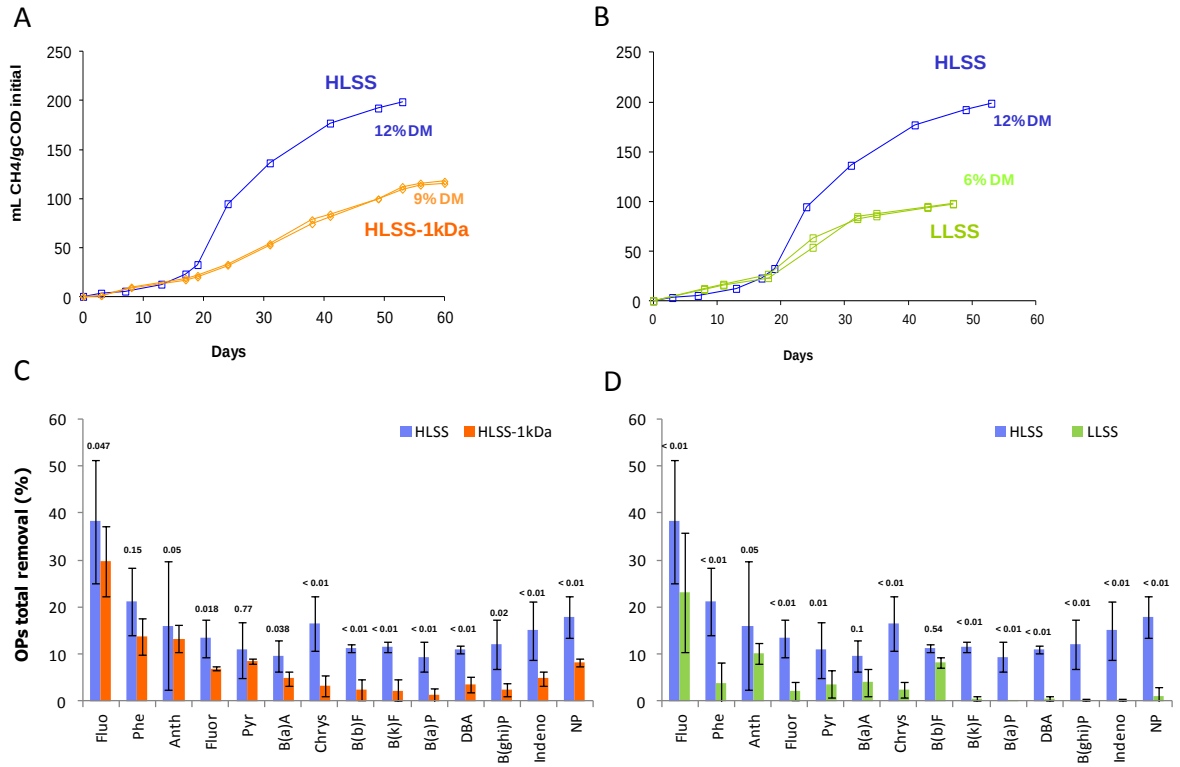

Figure V-4: Methane production and DM removal (A and B) and total PAHs and NP removals (C and D) for the three sludge samples HLSS, HLSS-1kDa and LLSS. For each compound, the p-value between the 2 sets of measurements is indicated in black. Removal can be considered as statistically different for p-value below 0.05.

V.2.2. PCBs total removals

The total removals of the sum of 7 PCBs (28, 52, 101, 118, 153, 138, 180) in HLSS, LLSS and HLSS-1kDa are shown in the Figure V-5. The three total removals are not statistically different, which means that PCB removals are not affected by the DM removal and the various level of compounds availability created by the various sludge samples. PCBs behave differently than PAHs which removal is hardly linked to the overall metabolism. Indeed PCBs anaerobic degradation is initiated by reductive dechlorination (Smidt and de Vos, 2004) where PCBs are considered as electron acceptors. Hence, the removal of slightly substituted PCBs results from their degradation and production by dehalogenation of highly substituted PCBs. It is thus important to carefully interpret the total and individual removals. Thus discussions will focus on the most substituted molecule PCB180 which is not produced from dehalogenation of other molecules. PCB180 presents the highest removals with no statistical differences between the three conditions.

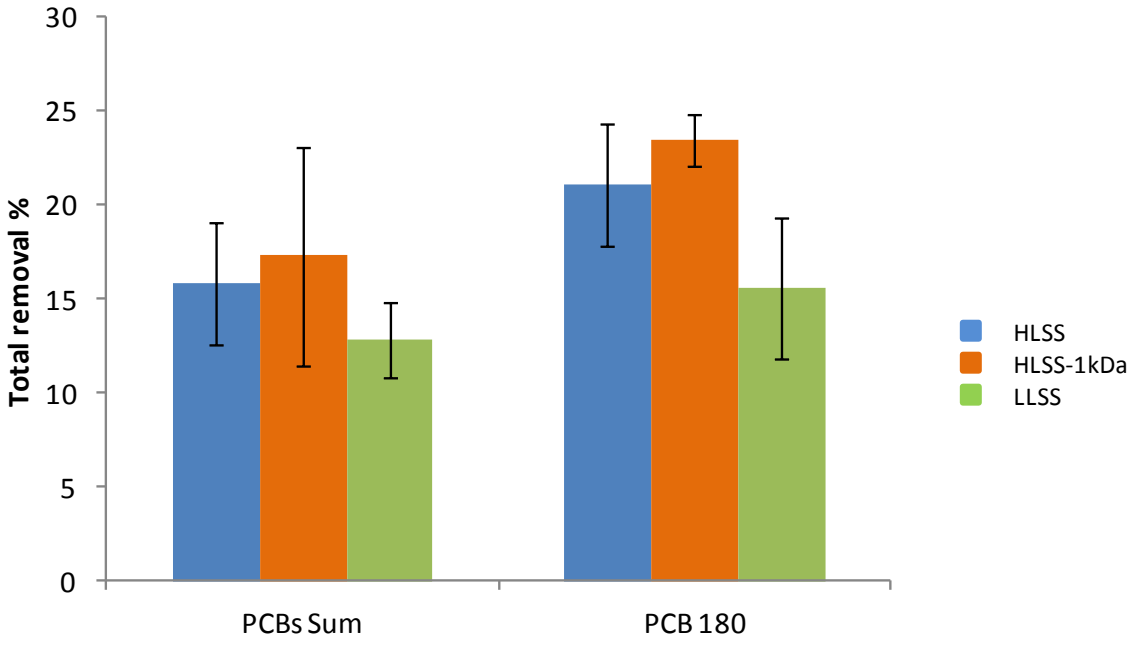

Figure V-5: Total removals of the sum of PCBs, PCB 180 and PCB 28 after 53 days of reaction.

V.3. Evidence for PAH and NP removal coupled to the first steps of anaerobic digestion in sewage sludge

Chemosphere, Submitted January 2012

Abstract

Anaerobic degradation of Polycyclic Aromatic Hydrocarbons and Nonylphenol has been brought to the fore, but information on removal kinetics and anaerobic degrading bacteria is still lacking. In order to explore the organic micropollutants removals kinetics under anaerobic conditions in regard to the methane production kinetics, the removal rate of 12 Polycyclic Aromatic Hydrocarbons and Nonylphenol was measured in two anaerobic batch reactors series fed with a highly loaded secondary sludge as growth substrate. The results underscore that organic micropollutants removals is coupled to the initial stages of anaerobic digestion (acidogenesis and acetogenesis). In addition, the organic micropollutants kinetics suggest that the main removal mechanisms of these hydrophobic compounds are biodegradation and/or sequestration depending of the compounds.

V.3.1 Introduction

Polycyclic Aromatic Hydrocarbons (PAHs) are nowadays looked as environmental pollutants by environmental and health agencies because of their toxic, mutagenic and carcinogenic effect on living organisms (Samanta et al., 2002). PAHs are mainly formed during human activities such as crude oil spillage, fossil fuel combustion and gasoline leakage. Through the air and runoff after rainy events, the PAHs can deposit to soil, water bodies and sewage system (Wada et al., 2005; Welker 2005). Nonylphenol (NP) is a degradation product of nonylphenol polyethoxylates (NPE) used in the formulation of a large variety of lubricants, paints, detergents, pesticides and resins (Tolls et al., 1994). NPE end up to the sewage treatment plants system and they are efficiently removed during biological wastewater treatment. However, the overall yield of biodegradation is limited due to the formation of biorefractory metabolites, including NP, nonylphenol mono- and diethoxylates (NP1EO, NP2EO) and nonylphenoxy carboxylic acids (NPEC) (Ahel et al., 1994; Corvini et al., 2006). NP has been shown to have a toxic and endocrine disrupting effect on wild life organisms and humans (Soto et al., 1991). Due to their low water solubility and high octanol-water partition coefficients, these organic micropollutants (µP) are mainly associated with hydrophobic compartments such as the organic matter in sewage sludge and river sediments or the lipids in biota, with levels between 0.001 to 10 $\mu g/g_{DM}$ for PAHs (Abad et al., 2005; Blanchard et al., 2004; Bodzek and Janoszka, 1999) and around 100 $\mu g/g_{DM}$ for NP (Aparicio et al., 2007; Fountoulakis et al., 2005). µP can be also sorbed irreversibly in a short time scale to the organic matter. This phenomenon named sequestration has been reported by different authors as one of the abiotic mechanisms of µP removal in digested sewage sludge and soils (Barret et al., 2010a; Northcott and Jones, 2001; Semple et al., 2003).

PAHs and NP are known to be biodegraded under aerobic conditions (Corvini et al., 2006; Lu et al., 2011; Yuan et al., 2000). However, most contaminated environments are anaerobic. In these environments, the anaerobic digestion can occur. Anaerobic digestion is a process whereby organic matter is broken down in absence of oxygen into methane and carbon dioxide by naturally occurring microorgsnisms. The anaerobic digestion consists of four stages where different microbial populations participate: (1) hydrolysis, (2) acidogenesis, (3) acetogenesis, and (4) methanogenesis. The digestion process begins with the hydrolysis of insoluble organic polymers into monomers that are available for microorganisms. Acidogenesis is the step where these monomers are converted to carbon dioxide, hydrogen, and volatile fatty acids (acetic, propionic, butyric acids, etc) by fermentative bacteria and then, in the acetogenesis stage, these metabolites are converted to acetic acid, hydrogen and carbon dioxide by three different groups of *Bacteria* (hydrogenic, homoacetogenic and sulfatoreductive). Finally, the methanogenic microorganisms (strict anaerobic *Archaea*) convert the acetic acid, hydrogen and carbon dioxide into methane (Ahring, 2003; Batstone et al., 2002).

Recent results demonstrated that some PAHs (Bernal-Martinez et al., 2009; Chang et al., 2003; Dionisi et al., 2006; Trably et al., 2003) and NP (Chang et al., 2005; Patureau et al., 2008) can be degraded under anaerobic conditions. It appears that this biodegradation is

mainly coupled to methanogenic terminal oxidation processes (Chang et al., 2006; Jones et al., 2008). A recent thermodynamic landscape study showed that the biodegradation of PAHs under methanogenic conditions is an exergonic process, it indicated also that PAHs could be degraded to acetate and H_2 coupled to the conversion of these substrates to methane as the optimal pathway (Dolfing et al., 2009). In addition, observations that bromoethanesulfonic acid, an inhibitor of methanogenesis, inhibited partially the degradation of naphthalene and phenanthrene with the total elimination of methanogenic *Archaea* and some *Bacteria*, suggested that the PAHs degradation could be associated not only to the methanogenesis stage but also to the first stages of anaerobic digestion (Chang et al., 2006).

On the other hand, microbial population and cometabolism pathway were found to influence µP removal. Indeed, an adapted inoculum is favorable to quantify µP degradation (Trably et al., 2003), suggesting that the abundance and diversity of µP degrading microorganisms and their associated metabolic routes are essential. PAHs and NP are recalcitrant compounds, but their biodegradation is possible if combined with other substrate degradation and if syntrophic interactions occurr. These interactions can thus be stimulated by the addition of a readily biodegradable growth substrate (Chang et al., 2005; Dionisi et al., 2006; Zhong et al., 2007). In fact, in the case where the sewage sludge is the growth substrate, it was demonstrated that the removal of PAHs by anaerobic digestion strongly varies as a function of sludge characteristics (Barret et al., 2010a).

In order to further explore the µP biodegradation kinetics under anaerobic conditions in regard to the methane production kinetics, both total removal and removal rate of 12 PAHs and NP were measured in different batch reactors series fed with secondary sludge as growth substrate.

V.3.2. Materials and Methods

V.3.2.1. Chemicals

All solvents were purchased from J.T.Baker. Fluorene (Fluo), phenanthrene (Phe), fluoranthene (Fluor), pyrene (Pyr), benzo(a)anthracene (B(a)A), chrysene (Chrys), benzo(b)fluoranthene (B(b)F), benzo(k)fluoranthene (B(k)F), benzo(a)pyrene (B(a)P), dibenzo(a,h)anthracene (DBA), benzo(g,h,i)perylene (B(ghi)P) and indeno(1,2,3,c,d)pyrene (Ind) were obtained from Dr Ehrenstorfer GmbH. The 4 nonylphenol (NP) isomer mixture was purchased from Interchim. The spiking mix at 100 mg/L was prepared in acetonitrile except for indeno(1,2,3,c,d)pyrene (20 mg/L) and for nonylphenol (2 g/L). The 10 mg/L HPLC standard solution of PAHs in acetonitrile and the 100 mg/L of NP in hexane were provided by Dr Ehrenstorfer GmbH. For quantification, the standard solutions were diluted to obtain 6 calibration levels from 10 to 1000 µg/L in acetonitrile for PAHs and from 500 to 5000 µg/L in hexane for NP. Standards were stored at – 20 °C.

V.3.2.2. Sludge samples

The experiments were carried out using a highly loaded secondary sludge sample (HLSS) which was sampled in the biological aerobic unit of a domestic plant treating 250 000 person equivalent (PE) with a very low sludge retention time (0.4 day); it was therefore not stabilized. Prior to their direct use, HLSS was stored at -20°C.

V.3.2.3. µP-adapted anaerobic inoculum

The inoculum was produced in a semi-continuous stirred lab-scale reactor of 5 L. It was fed with HLSS diluted with deionized water to reach 24 ± 5 g_{COD}/L and spiked at 5 µg/g_{DM} for each PAH except for indeno(1,2,3,c,d)pyrene (1 µg/g_{DM}), and at 100 µg/g_{DM} for NP. This reactor was inoculated with a digested sludge coming from a mesophilic anaerobic industrial reactor adapted to PAH-polluted sludge. Temperature was regulated at 35°C using hot water circulation in the external jacket. The feed was stored at 4°C. The reactor was operated at a retention time of 20 days and an organic load of 1.2 ± 0.2 g_{COD}/L/day. The pH and the biogas volumetric production were monitored on line. Once a week, composite samples were taken from the feeding and outlet tanks to measure the chemical parameters and µP concentrations. The adapted-to-µP digested sludge was kept at 35°C until its use for batch experiments as inoculum.

V.3.2.4. Batch experiments

The anaerobic digestion of HLSS in batch conditions was performed using 300 mL plasma bottles containing 250 mL of a defined mixture of sewage sludge (substrate) and inoculum (biomass). The bottles were stirred (100 rpm) and maintained at 35 °C. For these experiments, the sludge to inoculum ratio was equal to 0.5 $g_{COD}/g_{Organic\ Matter}$. The inoculum was concentrated from 8 to 18 g/L of dry matter (DM) to obtain a mixture with a total DM of 20 g/L. The mixture was spiked at three times the concentration of the continuous reactor (15 $\mu g_{PAH}/g_{DM}$, 3 $\mu g_{Ind}/g_{DM}$ and 300 $\mu g_{NP}/g_{DM}$) to improve µP-degrading-microorganism activity.

Two reactors series (A and B) were carried out. The series A was performed in order to observe the overall activities with DM removal, biogas production and µP removal. Based on the results of series A, indicating that µP removals occur before the production of methane, the series B was latter undergone. This series was carried out in duplicate to accurately analyze the concomitant evolution of µP and acetate during the first steps of the anaerobic digestion. At different reaction time, one reactor (series A) or two reactors (series B) were stopped to measure the total µP concentration over time. Indeed, to quantify the µP, it is necessary to get a large amount of dry matter to extract them in duplicate. The two series were conducted under the same initial conditions, but for the series B, sampling frequency was higher in order to observe more precisely the µP kinetics and the anaerobic digestion kinetics. The initial µP concentration was determined also in duplicate for both series. In parallel, several control reactors were realized (one per series): not-spiked HLSS reactors and HLSS abiotic reactors. These abiotic control reactors were prepared by autoclaving the mixture-containing plasma bottles at 121°C for 20 min.

Biogas volume was measured by liquid displacement and its composition was measured by gas chromatography. For all reactors, volumes of biogas were reported to the COD introduced in the bottle. In addition, volatile fatty acids (VFAs, g/L) production was followed in all reactors series.

V.3.2.5. Analytical methods

Chemical oxygen demand (COD, g_{O2}/L), dry matter (DM, g_{DM}/L) and organic/volatile matter (OM, g_{OM}/L) were determined both at the beginning and end of the experiments. DM in total mixtures was measured by weighing the sample after heating at 105°C during 24 h and the OM after heating at 550°C during 2 h. The chemical oxygen demand COD was determined thanks to Merck Spectroquant kits, according to the ISO 15 705. The samples were diluted to be in the range 0 - 1 500 mg_{COD}/L. The VFAs acetate, propionate, isobutyrate, butyrate, iso-valerate and valerate concentrations were determined in dissolved/colloidal phase by gas chromatography (GC800, Fisons Instruments).

At different reaction time, the total volume of each pair of reactors was freeze-dried in order to extract the PAHs and NP according to the method developed by Trably et al. (2004). The extractions were done in duplicate. The PAHs quantification in the extracts was previously described (Trably et al., 2004). The method used to quantify NP is described by Ahel et al. (2000) and Hernandez-Raquet et al. (2007). These measurements gave the total µP concentration in $\mu g_{\mu P}/g_{DM}$.

V.3.2.6. Data analysis

The µP removal rates and the accumulation rates of methane and acetate were used to correlate the µP removal kinetics to the anaerobic digestion steps. µP removal rates ($r_{\mu P}$) were calculated using discrete points by difference of concentrations between two reactors (series A) or two pairs of reactors (series B) and divided by their respective difference of reaction times. These parameters were expressed in µg/L/day. In the case of series B, the $r_{\mu P}$ were plotted in a boxplot graph wich is a descriptive representation of independent data. Methane production rate (r_{CH4}) and acetate accumulation rate ($r_{acetate}$) were calculated with the production of methane or accumulation of acetate in a range of time expressed in mL_{CH4}/g_{COD}/day and g/L/day respectively. The methane production first order kinetic constant (k_{CH4}, day^{-1}), was determined according to Eq. (1) ($V_{CH4}(t)$, methane volume; $V_{CH4}(t_f)$, maximum methane production; k_{CH4}, first order constant; t, time).

$$V_{CH4}(t) = V_{CH4}(t_f)(1-exp(-k_{CH4}\, t)) \quad (1)$$

The total µP concentrations (µg/L) were calculated using the measured concentrations ($\mu g/g_{DM}$) and the DM concentrations of each reactor. µP removals were calculated on the basis of mass balance between the initial reactors (day 0) and the reactors stopped at different reaction times. For the abiotic reactors, the µP removals were calculated on the basis of mass balance between the initial reactors (day 0) and the reactors stopped at the end of incubation.

V.3.3. Results and discussion

V.3.3.1. Production of µP-adapted anaerobic digested sludge

The continuous anaerobic digestion of spiked HLSS was carried out to produce a homogeneous µP-adapted inoculum for the batch experiments. All the results were previously published by Barret et al. (2010a). During the anaerobic digestion, total COD and DM were reduced by 67 ± 7% and 58 ± 10% respectively. µP removals for all compounds are shown in Table 1. Since µP volatilization was undetectable in the reactor, it was assumed that the calculated removals included biodegradation and sequestration (Barret et al., 2010a; Semple et al., 2003); therefore a µP-adapted inoculum was obtained.

V.3.3.2. Removal of µP in HLSS anaerobic batch reactors

In order to know the µP removal kinetics under anaerobic conditions, the total µP concentrations, DM and OM concentrations, biogas production and composition were measured over time using one HLSS batch reactors series spiked at three times the concentration of the continuous reactor (series A) and its corresponding not-spiked HLSS reactor.

In both reactors, the anaerobic digestion was stable with methane content in biogas about 80% and pH 7. In the case of spiked reactors series, the lag phase lasted approximately twice as long the lag phase of not-spiked reactors (Figure V-6). This could indicate that there was an effect of the µP concentrations on the microbial population adaptation. However, the maximum volume of biogas was similar in both spiked reactors series and not-spiked reactor, which means that there was no inhibitory effect of the µP on the overall metabolism of anaerobic digestion. In contrast, a recent study showed that the anaerobic digestion in continuous reactors of wastewaters from industrial processes that contain very high concentrations of µP (included PAHs) is inhibited with concentrations around 16 g_{COD}/L (Puyol et al., 2011). This result suggests that a certain µP level could have an inhibitory effect on the anaerobic digestion. To compare, in our case, the initial COD concentration was 1 $mg_{COD,PAH}$ /L and 19 $mg_{COD,NP}$/L, which are much lower than the µP level of Puyol et al. (2011).

Therefore, even if no inhibition occurred on the overall metabolism, the methane first order constant (k_{CH4}) decreased by 44% in the case of spiked reactors (Figure V-6). The k_{CH4} values of not-spiked reactors are 40% lower than those calculated using the methane production of a secondary sludge in batch conditions published by Mottet et al., (2009). These results show that the presence of µP slows down the overall methanogenic kinetic but leads to the same methane potential. This may be due to either the expression of different metabolic routes to degrade the substrate and the µP, to the deviation of electron fluxes towards µP or to the µP toxicity/inhibition on some microbial groups.

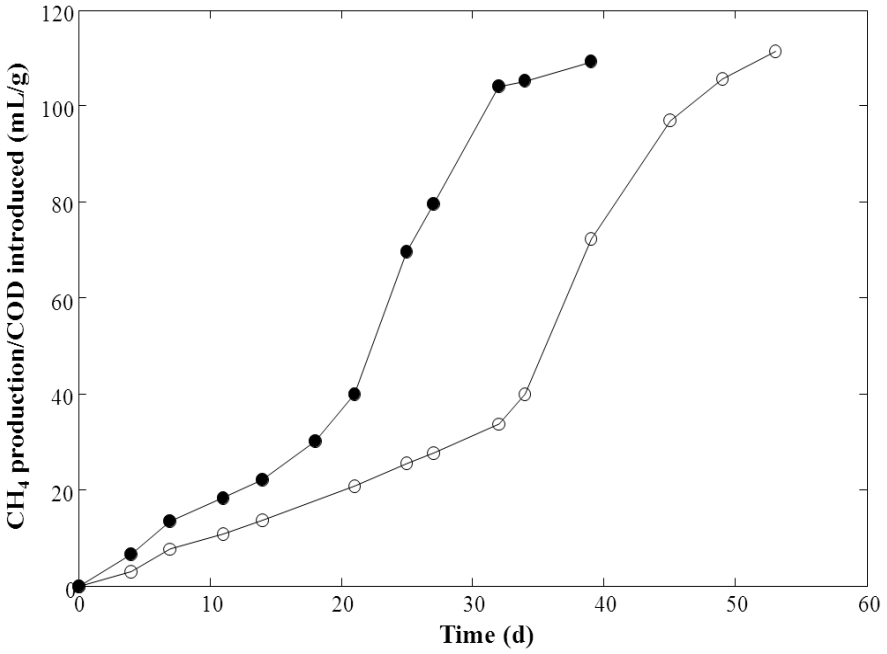

Figure V-6: Methane production over time in un-spiked and spiked HLSS reactors. ● HLSS not-spiked, k_{CH4} 0.12 day^{-1}. ○ HLSS spiked, k_{CH4} 0.067± 0.003 day^{-1}.

Moreover, the total µP removals at the end of the exponential phase (53 days) were considerably lower than those in continuous conditions (Table V-1) but in accordance with the average DM removal (13 ± 0,72%). May be explain/hypothesis why such difference in batch and continuous cultures. This result it was already obtained for previous batch system (Barret, 2009).

Table V-1: µP total removals in biotic and abiotic HLSS reactors at 53 days of reaction time. Comparison with the µP removals calculated in the continuous reactors at steady states (Barret et al., 2010a).

Compound	**Biotic HLSS removal (%)**	**Abiotic HLSS r**emoval (%)	**Continuous reactors r**emoval (%)
Fluorene	44 ± 10	33 ± 0.6	83 ± 15
Phenantrene	25 ± 5	8 ± 1	77 ± 8
Fluoranthene	18 ± 2	3 ± 2	71 ± 13
Pyrene	17 ± 3	-12 ± 2	67 ± 14
Benzo(a) anthracene	13 ± 3	-2 ±2	72 ± 6
Chrysene	16 ± 3	-4 ± 2	71 ± 9
Benzo(b) fluoranthene	13 ± 3	2 ± 1	67 ± 8
Benzo(k) fluoranthene	14 ± 2	3 ± 0.8	70 ± 7
Benzo(a) pyrene	13 ± 4	-5 ± 2	69 ± 19
Dibenzo (a,h) anthracene	12 ± 3	2 ± 0.2	70 ± 16
Benzo(g,h,i) perylene	12 ± 3	2 ± 2	65 ± 8
Indeno (1,2,3,c,d)pyrene	13 ± 3	-9 ± 1	49 ± 7
Nonylphenol	15 ± 3	11 ± 0.6	62 ± 16

The higher removals were found for compounds with the lowest logKow (Fluo, Phe, Fluor and Pyr), therefore less hydrophobic. The results obtained by Chang et al. (2003) on spiked batch reactors with municipal sludge in 60 days incubation period, showed a lower Fluo removal (28%) and higher Phe and Pyr removals (67% and 60%, respectively). This behavior could be explained by the high concentration of suspended solid (around 20 g/L) used in our study in contrast with the one used in the cited experiment (5 g/L). In fact, Chang et al. (2003) also studied the effect of suspended solid on µP removal rates, and it was observed that, when concentration of suspended solids was doubled, removal rates of Fluo, Phe and Pyr decreased by 92%, 75% and 90% respectively. The total NP removals were also lower than those published by Chang et al. (2004) (100%) obtained on spiked batch reactors with a defined medium and in their case without suspended solid.

Fluor, DBA and NP removals rates (r_{Fluor}, $r_{DBA,}$ r_{NP}) together with methane production rate (r_{CH4}) over time are presented in Figure V-7. In all cases, the µP removal rates increase during the first 39 days of reaction and then, decrease to zero. This period includes the lag phase and the beginning of the exponential phase. This behavior was also found for the other 10 PAHs, and most of them have the same profile as DBA, where the $r_{\mu P}$ decreased to zero after 45 days. However, negative values of $r_{\mu P}$ were obtained at 45 and 53 days. This could be due to concentration variability between each reactor.

These results suggest that the reduction of µP concentration is not only linked to methanogenesis or may be only due to abiotic processes at the beginning of the lag phase such as volatilization, adsorption to internal glass surface of the bottles and/or sequestration (Bamforth and Singleton, 2005; Semple et al., 2003). Considering these results, abiotic reactors and a second HLSS reactors series were carried out to know the µP degradation kinetics during the early stages of anaerobic digestion.

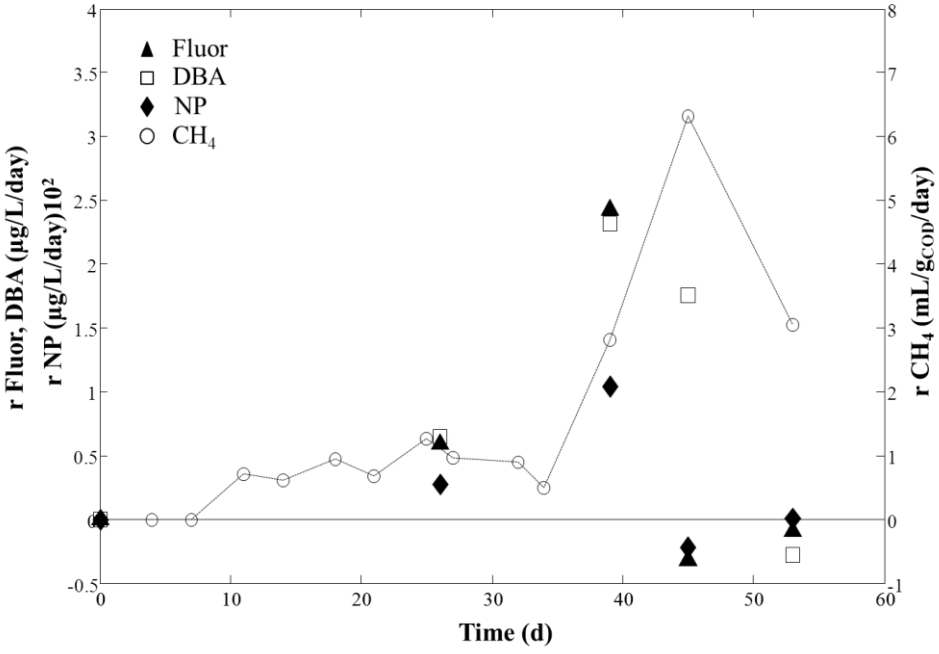

Figure V-7: Removal kinetics of Fluor, DBA and NP coupled to methane production kinetic in HLSS reactors, (series A). The initial µP concentration was measured in duplicate. One reactor was stopped at different sampling times.

V.3.3.3. µP degradation kinetics in HLSS anaerobic batch reactors

A second HLSS reactors series (series B) was carried out according to section *V.3.2.4.* to know the µP removal kinetics until the beginning of the exponential phase of methane production.

The VFAs concentration and methane production were followed in each reactor. Both VFAs and methane kinetics were similar in all reactors. For most of the µP, their concentrations were approximately constants until day 8 with no significant differences between each pair of reactors, finding the highest standard deviations in Chrys, B(ghi)P and NP. In the case of Fluo, Phe, Fluor and NP, important losses were found during the first 8 days mainly at day 1 of incubation as shown in Figure V-8 for NP. In this period, no important acetate and methane productions were observed, indicating that these compounds could have been removed by abiotic processes like volatilization and sequestration. This behavior was confirmed by the abiotic reactors results. All abiotic controls had a very low methane and VFAs production indicating no microbial activity. The most important abiotic losses were found for Fluo, Phe, Fluor and NP (Table V-1). These resultas are in agreement with those of Chang et al. (2003, 2004), who found abiotic losses after 60 and 84 days of incubation with spiked batch reactors of 7% Fluo, 5% Phe, 4% Pyr and 11% NP.

Regarding the physicochemical characteristics of these compounds and according to the model proposed by Barret et al. (2010b), in the case of Fluo and Phe, their higher volatility and low logKow (4.18 and 4.57) (PHYSPROP Database) suggest that the main removal mechanism at day 1 of incubation could be the volatilization. However, the methane production at day 1 is negligible, and thus the liquid-gas transfer is low. This suggests that the drop in the concentration is not only due to volatilization but also to sequestration. Fluor has a higher logKow (5.1) indicating that the sorption to the sludge and sequestration could be more important than volatilization. In contrast, in the case of NP, even if it has a high volatility, its high logKow (5.76) and ambivalent properties, with both hydrophilic and hydrophobic moieties, suggest that physicochemical interactions between the molecule and the sludge matrix are favored; therefore the phenomenon that could better explain the decrease in the NP concentration in the abiotic controls is the sequestration.

Different $r_{\mu P,}$ r_{CH4} and $r_{acetate}$ were calculated according to section *V.3.2.6.* $r_{\mu P}$ ranged from 4 ± 2 µg/L/day (Fluo) to 1 ± 0.5 µg/L/day (Ind) for PAHs and 160 ± 34 µg/L/day for NP. Maximal $r_{acetate}$ were 0.039 ± 0.006 g_{COD}/L/day and are comparable to values found in literature (Mottet et al., 2009). Figure V-8 shows that the kinetics of r_{DBA} and r_{NP} are coupled to those of $r_{acetate}$ and r_{CH4}. Indeed, r_{DBA} and r_{NP} begin to increase after 13 days of reaction and decrease after the exponential phase started. $r_{acetate}$ increased from day 0 to day 18 and then decreased slowly until the methanogenesis started (between day 30 and 34) where it fell down sharply.

These results reveal a relation between the first stages of anaerobic digestion (acidogenesis/acetogenesis) and the removal of µP. The maximum r_{DBA} and r_{NP} were reached when the $r_{acetate}$ was also the maximum. This behavior was also found for most of the compounds. In the case of Pyr, $r_{\mu P}$ started to increase after 18 days. Furthermore, Fluor, Phe, Chrys, B(a)A, B(a)P and Ind maintained maximum values of $r_{\mu P}$ even at the beginning of the exponential phase; however, in the series A, all of them had the same behavior as shown in Figure V-7.

The kinetic of NP was different from the PAH kinetics. After 8 days, the concentrations in both reactors increased significantly with a maximum production rate of -157 ± 40 µg/L/day at day 13, and then the concentrations decreased with a maximum removal rate of 178 ± 27 µg/L/day at day 18. This behavior can be explained by the presence of non-spiked NP parent compounds (NP1EO, NP2EO and NPEC) in the sewage sludge (Ahel et al., 1994; Giger et al., 1984). Indeed, in wastewater treatment systems, the NPE are partially converted under aerobic and anaerobic conditions into NP1,2EO and NPEC. According to Ahel et al.(2009), secondary wastewater treatment effluents such as treated water and sewage sludge can contain, in the soluble phase, hydrophilic NP intermediates (NPEC) and parents (NPE) compounds. NPE concentrations vary depending on the type and efficiency of secondary treatment, but the main hydrophilic recalcitrant compounds found in secondary effluents are the NPEC. Thus, NPEC and NPE might be present in the substrate used in this experiment (HLSS) and consequently in the initial mixture. Moreover, the most hydrophobic intermediates, NP1,2EO, are concentrated in the sewage sludge. The transformation of these metabolites into NP is strongly favored under anaerobic conditions (Corvini et al., 2006; Giger et al., 1984). In fact, the NP1EO in the initial mixture was quantified at a concentration of 816 ± 14 µg/L. The NP1EO was removed until the NP concentration increased and then the concentration remained constant until the end of the experiment. The total NP1EO removal accounted for 17% of the NP production, meaning that other NPE by-products were present. However, the method used to quantify NP, described in the section *V.3.2.5.*, did not include the extraction of hydrophilic compounds previously described by Ahel et al. (2000), hence it was not possible to validate the presence of NPEC and NPE in the initial mixture. Their presence could explain the rest of the NP production under anaerobic conditions. Anyway, after 13 days, NP was degraded during the remaining time of experiment (series B), obtaining a total removal at 53 days (series A) higher than the total abiotic removal at the same time (Table V-1). The production and removal of NP are also concomitant to the first steps of the anaerobic digestion.

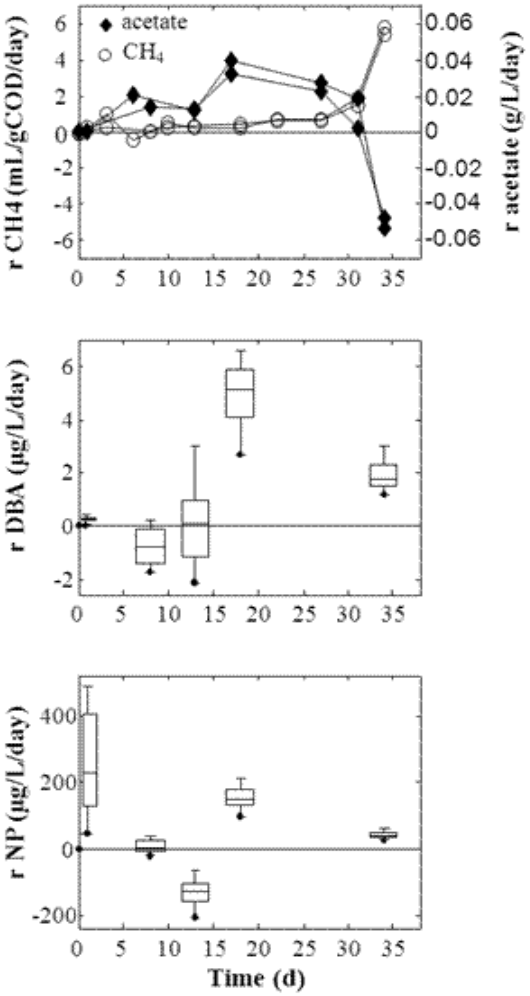

Figure V-8: Removal kinetics of DBA and NP coupled to methane production kinetic and acetate accumulation kinetic during the anaerobic digestion of HLSS (series B). The initial µP concentrations were measured in duplicate. Two reactors were stopped at different sampling times.

V.3.4. Conclusions

The anaerobic degradation of PAHs and NP in sewage sludge has already been studied but mainly under simplified batch experiments or using complex medium in continuous reactors. Unlike the continuous reactors, our methodology allows to observe the different steps of anaerobic digestion and to link these steps to the removal of µP. The results show a strong evidence of relation between initial stages of anaerobic digestion (acidogenesis and acetogenesis) and µP removal in HLSS reactors. This relation was demonstrated determining $r_{\mu P}$ and $r_{acetate}$. The results also suggest the role of methanogenesis as terminal electron acceptor in order to prevent an inhibition of the first stages of anaerobic digestion. In the other hand, no complete inhibition of methanogenesis was observed in the presence of µP with a production of methane similar with and without µP but lag phases occurred implying microorganisms adaptation and the methane production kinetic was slightly slowed down.

The evidence of microorganisms adaptation to µP concentrations supports the results that linked the first stages of anaerobic digestion with the µP removal. In the same way, the NP kinetics also showed that its production as well as its degradation under anaerobic condition, are mainly linked to the acidogenesis and acetogenesis stages. In addition, the results show that the µP removals are also linked to two important abiotic processes depending of the compounds: volatilization (mainly the low molecular weight PAHs) and sequestration. This work provided important outcomes to better understand the PAHs and NP anaerobic removal, to know their kinetics and to identify the most important parameters for optimizing their depletion.

V.4. Role of the dissolved and colloidal matter on the distribution and the removal of OPs in sewage sludge

After the study of the removal kinetics of OPs under anaerobic conditions, additional information is needed to better understand the role of the DCM compartment in terms of concentration and nature on the distribution and the removal of OPs. PAHs were chosen to measure their distribution between the free and aqueous compartments and PCBs to measure their aqueous concentrations using SPME technique.

V.4.1. Validation of aqueous PAHs quantification by SPME

In order to know if it is feasable to quantify by SPME the aqueous and free PAHs concentration in aqueous sludge samples (matrix with high concentrations of organic matter) without matrix interferences, a validation was carried out. The validation methodology was described in the section III.5.5.1. All values of Ki and Ci for milliQ water, the aqueous sludge compartment (DCM) and DCM samples are ploted in the appendix B.

The average values of Ki determined in milliQ water and DCM samples, and the PAHs quantification yields (Ci) in DCM using the Ki values in milliQ water are presented in the Table V-2. Ci values near to 100 % were obtained for 11 PAHs with similar Ki values in milliQ water and DCM, validating the SPME technique to quantify these compounds. In contrast, the Ci values obtained for the lowest molecular weight PAHs (fluorene and phenanthrene) were higher than 100 % (Table V-2) with significant differences in both Ki values. This result shows an interference of the aqueous sludge matrix on the quantification of these two compounds resulting in an overestimation of the aqueous concentrations.

Table V-2: Ki and Ci average values obtained in the validation of the SPME technique for PAH analysis.

Compound	Ki milliQ water	Ki DCM	Ki milliQ water Ci DCM
Fluorene	**0.59**	**0.42**	**134**
Phenanthrene	**0.74**	**0.41**	**171**
Anthracene	0.65	0.63	100
Fluoranthene	0.74	0.71	97
Pyrene	0.67	0.70	95
Benzo(a)anthracene	0.68	0.82	82
Chrysene	0.71	0.75	90
Benzo(b)fluoranthene	0.68	0.78	84
Benzo(k)fluoranthene	0.76	0.79	90
Benzo(a)pyrene	0.64	0.77	84
Dibenzo(a,h)anthracene	0.64	0.58	90
Benzo(g,h,i)perylene	0.75	0.86	84
Indeno(1,2,3,c,d)pyrene	0.66	0.66	86

V.4.2. PAHs distribution between the sludge compartments and kinetics

The PAHs distribution in the free and aqueous compartments of the three initial mixtures is shown on the Figure V-9. Whatever the sludge sample, the aqueous compartment was always very low (Figures V-9C, V-9D), inferior to 1.5% for LLSS, 1% for HLSS and 0.5% for HLSS-1kDa, excepted for the fluorene around 2.5%. In this aqueous compartment, the low molecular weight PAHs are mainly present in the free fraction and a little bit in the DCM fraction whereas the high molecular weight PAHs were only present in the DCM fraction. The fact that fluorene has the highest free concentration could be related with its higher water solubility (Table III-1). The PAHs distribution is significantly different from one sludge to another: the free and aqueous fractions of HLSS-1kDa are the lowest whereas the DCM fraction of LLSS is the highest. For example chrysene has a free and DCM concentrations of 251 and 867 ng/L respectively in HLSS-1kDa against 671 and 5188 ng/L in LLSS with a total chrysene concentration of 373701 ng/L (Table V-3).

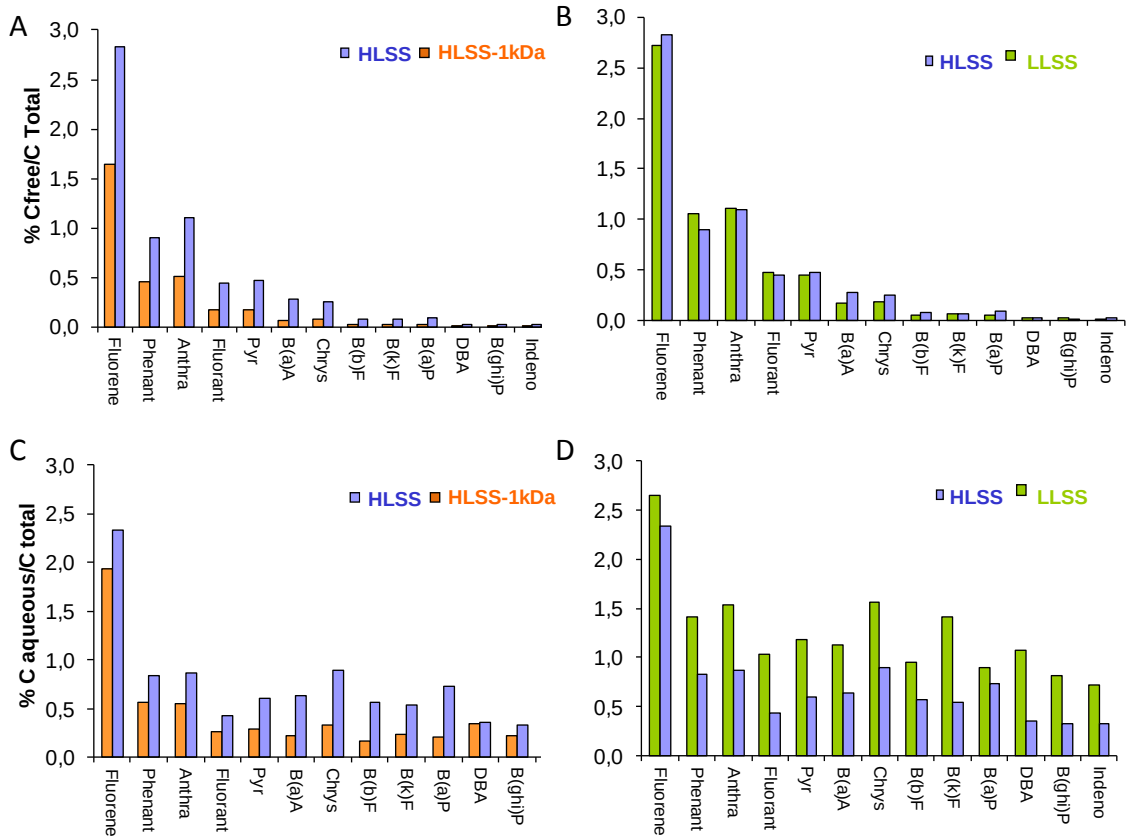

Figure V-9: PAHs distribution in the sludge compartments of the initial mixture. A and B, ratio Cfree/Ctotal, C and D ratio Caqueous/Ctotal.

Table V-3: Pyrene, chrysene and indeno(1,2,3,c,d)pyrene distribution in the sludge compartments of the initial mixture in ng/L.

Sludge mixture	$C_{PAH,free}$			$C_{PAH,DCM}$			$C_{PAH,aqu}$		
	Pyr	Chrys	Indeno	Pyr	Chrys	Indeno	Pyr	Chrys	Indeno
HLSS	1871	926	36	497	2289	401	2368	3215	437
HLSS-1kDa	727±24	251±13	12±2	540	867	281	1266±32	1127±254	293±98
LLSS	2117±62	671±11	30±6	3460	5188	1012	5578±402	5859±81	1042±169

Barret et al. (2010c), based on a modeling of PAHs sorption in sludge, estimated the $C_{PAH,free}$, $C_{aqu,PAH}$ and $C_{PAH,part}$ in different sludge samples. This model determined percentages from 10 to 30% for $C_{PAH,aqu}$ and from 5 to 11% for the $C_{PAH,free}$, depending of the PAHs. Compared to our measured distribution, this model overestimates the PAHs distribution, mainly for the $C_{aqu,PAH}$.

Regarding the $C_{PAH,free}$, $C_{PAH,DCM}$ and $C_{PAH,total}$ kinetics of both HLSS-1kDa and LLSS (Figures V-10 and V-11), in the case of low molecular weight PAHs, it is possible to observe removals in all fractions during the first 20 days, the free fraction presenting the highest removal. The middle molecular weight PAHs have a combined effect of $C_{PAH,free}$ and $C_{PAH,DCM,}$ both fractions being removed. In contrast, in the case of high molecular weight PAHs, the free fraction has only a very slight removal, whereas the $C_{PAH,DCM}$ governs the removal in the aqueous fraction. The large difference between the $C_{PAH,total}$ and $C_{PAH,DCM}$ and the very low totals removals obtained hinder to observe the decrease of the $C_{PAH,total}$ over time.

Moreover, if the total removals and initial distributions of PAHs in HLSS and HLSS-1kDa are compared, it is possible to observe that the larger removals differences are found for the high molecular weight PAHs from chrysene to indeno(1,2,3,c,d)pyrene, with higher removals in HLSS (Figure V-4 C). If the initial distributions are compared for these PAHs, it is observed that the PAH-DCM concentration are higher in HLSS than in HLSS-1kDa, suggesting that the PAH-DCM interactions improve the bioavailability of the high molecular weight PAHs, and consequently reveals the importance of the level of these concentrations in the overall dynamics of these compounds. Additionally, the cometabolism is also different in HLSS-1kDa, this latter presents a lower concentration of COD in the aqueous phase, and with different nature to HLSS. This modification on the overall metabolism is evidenced by the modification of the DM removal and the methane potential between HLSS and HLSS-1kDa (Figure V-4). In contrast, if the same high molecular weight PAHs removals are compared between HLSS and LLSS, the total removals are higher in HLSS even if the PAH-DCM concentrations are lower. In this case, cometabolism influence is higher than the bioavailability influence. Indeed, LLSS presented a lower cometabolic flux (lower DM removal) than HLSS, explained by either different concentrations of the cometabolic substrate or differences in the nature of the matrix. These differences could be explained by a more detailed physico-chemical and functional characterization of the matrix.

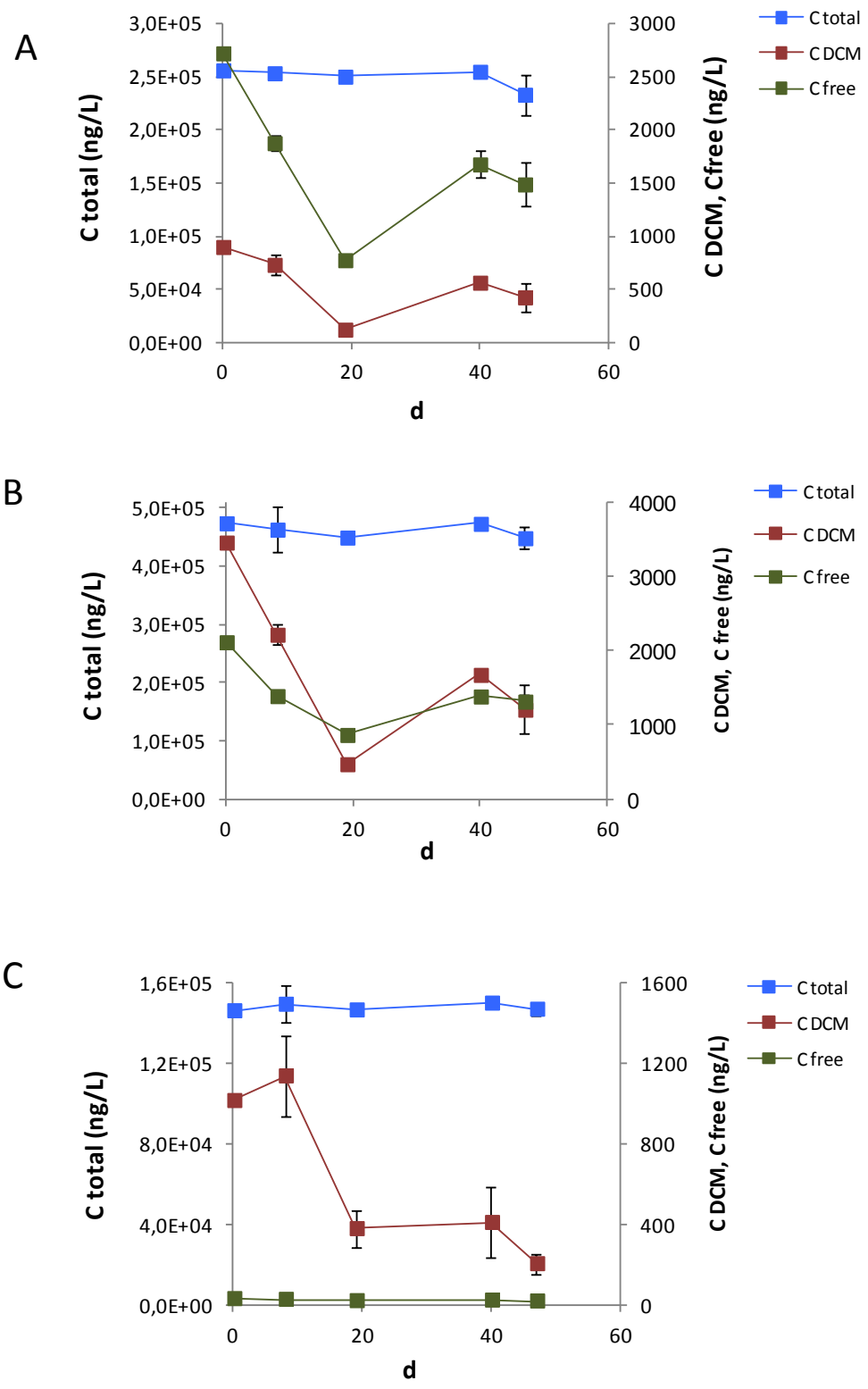

Figure V-10: Kinetics of $C_{PAH,free}$, $C_{PAH,DCM}$ and $C_{PAH,total}$ in LLSS. A: Phenantrene (low molecular weight). B: Pyrene (middle molecular weight). C: Indeno(1,2,3,c,d)pyrene (high molecular weight). Standard deviations correspond to the two different reactors.

A mass balance done in each time interval reveals that even if the highest removals are reached in the aqueous phase, between 80 and 98 % of the total removal corresponds to the particulate fraction, except for the high molecular weight PAHs in LLSS with a 70 % of the total removal occurring in the aqueous fraction. This may be explained by the organic composition of LLSS. Indeed this sludge sample may be more stabilized than the HLSS sample due to the high HRT on the sampling site. As a consequence, we observe a low DM total removal (6 %) in the batch test with a low methane potential. For PAHs, the aqueous compartment seems to be more consumed than the particulate one which suggests that the degradation in this latter compartment depends of a good cometabolic flux and of the nature of the cometabolic substrate : the hydrolysis step may be slowed down influencing the bioavailability of the PAH sorbed to the particles and consequently the overall PAH removal. A PAHs removal model proposed by Barret el al. (2010), which takes into account combined influences of bioavailability and cometabolism, identified the aqueous phase as the bioavailable fraction and the DM removal rate as the most relevant cometabolic flux. In the same way as this model, our results suggest that the aqueous fraction corresponds to the bioavailable fraction, however the results demonstrate also that the particulate compartment is also implied in the PAH removal (either directly consumed or through transfer to the other compartments) but not with the same levels of bioavailability among the sludge mixtures.

In both HLSS-1kDa and LLSS kinetics, the initial removal is observed during the first 20 days in all PAHs fractions with the same profile of HLSS kinetics presented in the section V.3. (Figure V-10 and V-11). Although the concentrations of VFAs were not measured (unlike the HLSS kinetics), the COD DCM and methane kinetic coupled well to the PAHs kinetic in each physical fraction: this supports the hypothesis that the removals of PAHs are linked to the first stages of the anaerobic digestion.

This initial removal stage is followed by a stage of refilling of the aqueous fraction from the particulate fraction. This phenomenon is due to the fact that the batch configuration is not at equilibrium state. Indeed, under batch experiments, what we observe is the results of dynamic evolution of the parameters, meaning that an increase in concentration results in highest production than consumption, and inversely. Additionally, this refilling stage could suggest that the removal mechanism in the particulate compartment is linked to a PAH transfer to the aqueous phase generated by the hydrolysis of the particulate fraction or by desorption phenomena from the particulate phase. This behavior can be observed in the Figure V-11. The highest removal rates in the particulate compartment are reached during the first stages of anaerobic digestion where PAHs transfer and degradation occur simultaneously. During the methanogenic stage, the PAHs removals rates decrease, predominating the transfer of $C_{PAH,part}$ to the aqueous phase.

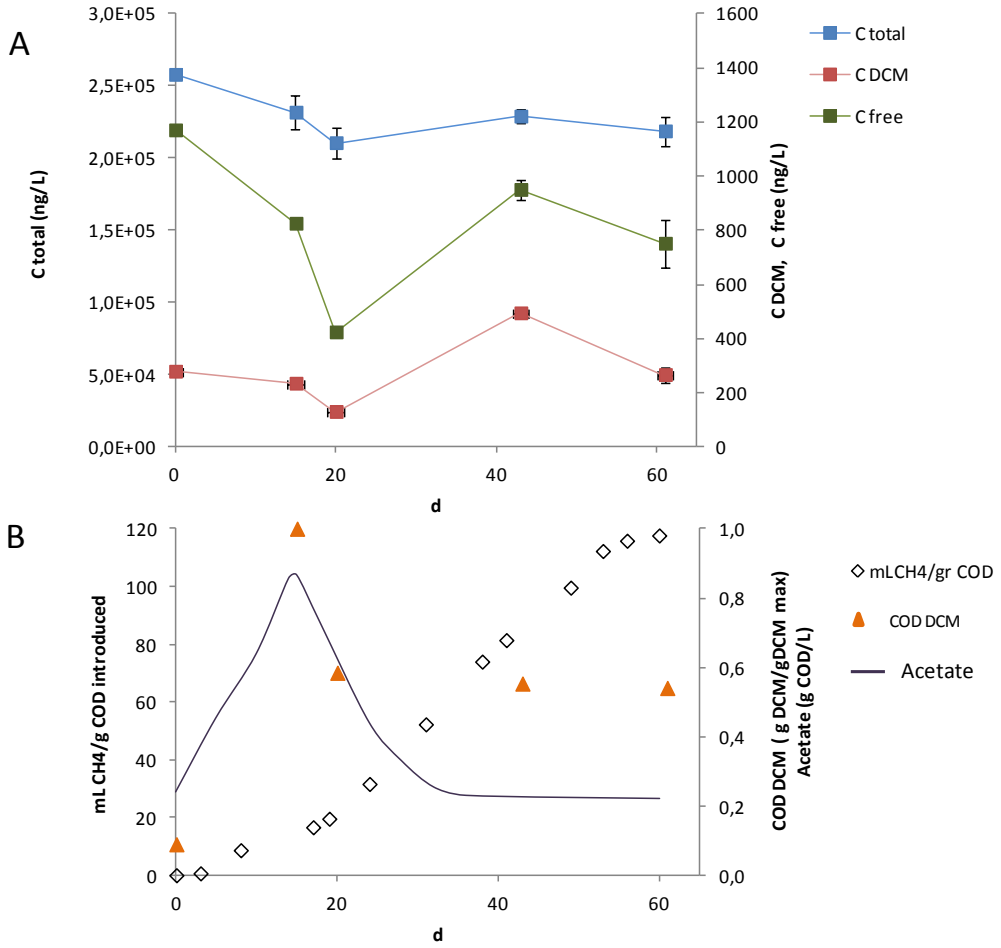

Figure V-11: Kinetics of $C_{PAH,free}$, $C_{PAH,DCM}$ and $C_{PAH,total}$ in HLSS-1kDa. A: Phenanthrene. B: Anaerobic digestion kinetics (acetate kinetic was estimated with the values obtained in HLSS kinetics presented in the section V.3.3.3)

V.4.3. Determination of PAHs K_{DOC} and K_{part} values

Additionally, the DOC was measured in all aqueous fractions in order to quantify the DCM concentration. With these values it was possible to determine the DCM/free partitioning coefficients (K_{DOC}) and the particulate/free partitioning coefficients (K_{part}) to study the interactions between PAHs and the organic fractions from the different sludge mixtures. K_{DOC} and K_{part} were calculated with the equations presented in the section III.6.2. Comparing the three initial sludge mixtures, PAHs have a higher affinity for the DCM fractions of LLSS and HLSS-1kDa than HLSS (Figure V-12). However, at the end of the experiments, the values of K_{DOC} in LLSS and HLSS-1kDa are significantly lower than those of HLSS that remained at the same levels. Regarding the K_{part} values, HLSS and LLSS have similar affinity for the particulate fractions in contrast with HLSS-1kDa that has higher values. At the end of the experiments, all K_{part} values increased (Figure V-13). According to Barret et al. (2010b), both K_{DOC} and K_{part} values for PAHs in secondary and thermally treated secondary sludge increase after anaerobic digestion in continuous reactors. For one OP, the increase or decrease of its

affinity for the sludge matrix could be linked to the modification of the physico-chemical characteristics of the matrix, generating a modification of the OP-matrix interactions.

In the case of HLSS, the concentration sorbed to DCM fraction of fluorene, phenanthrene, anthracene and fluoranthene were not detected.

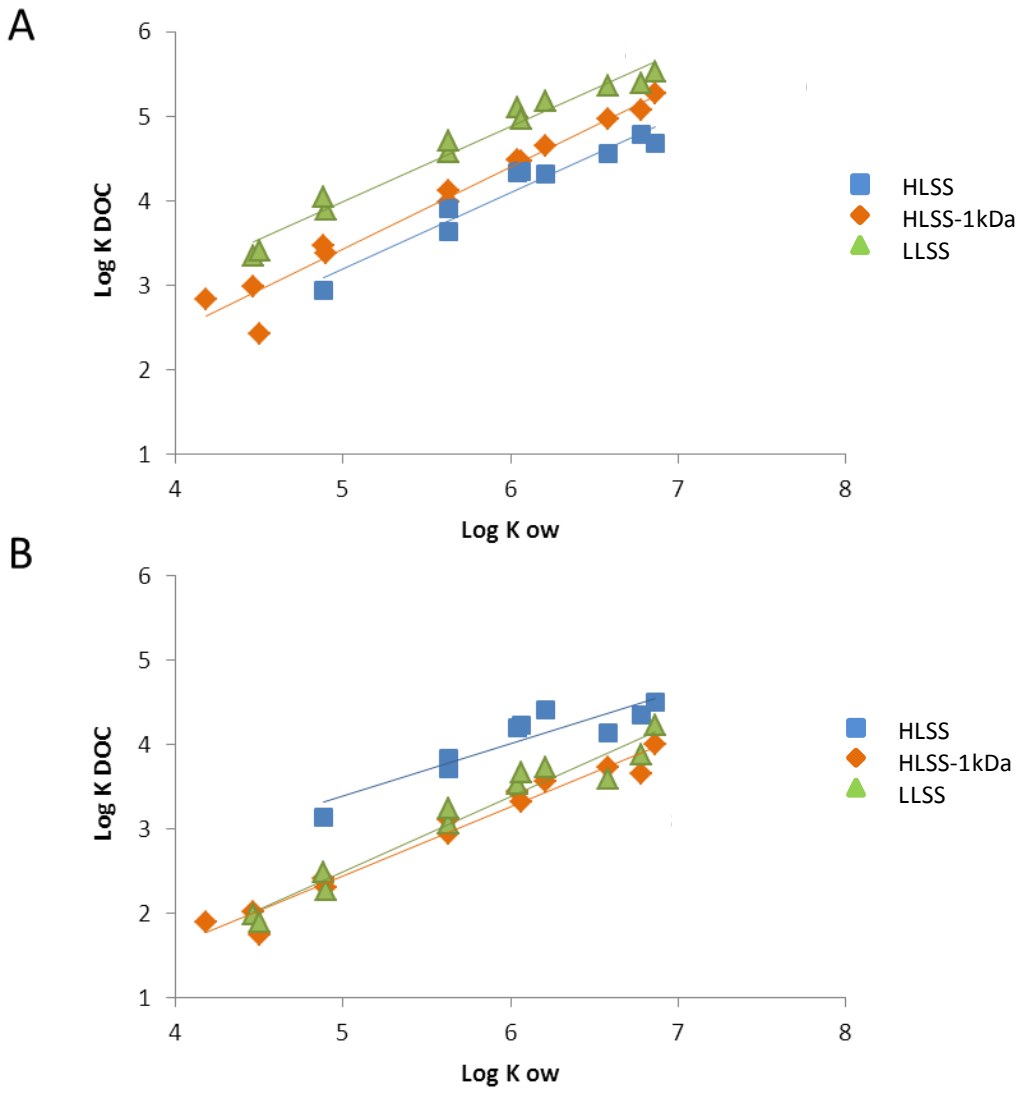

Figure V-12: Log K_{DOC} of PAHs. A: initial mixture. B: Final mixture after 53 days of reaction.

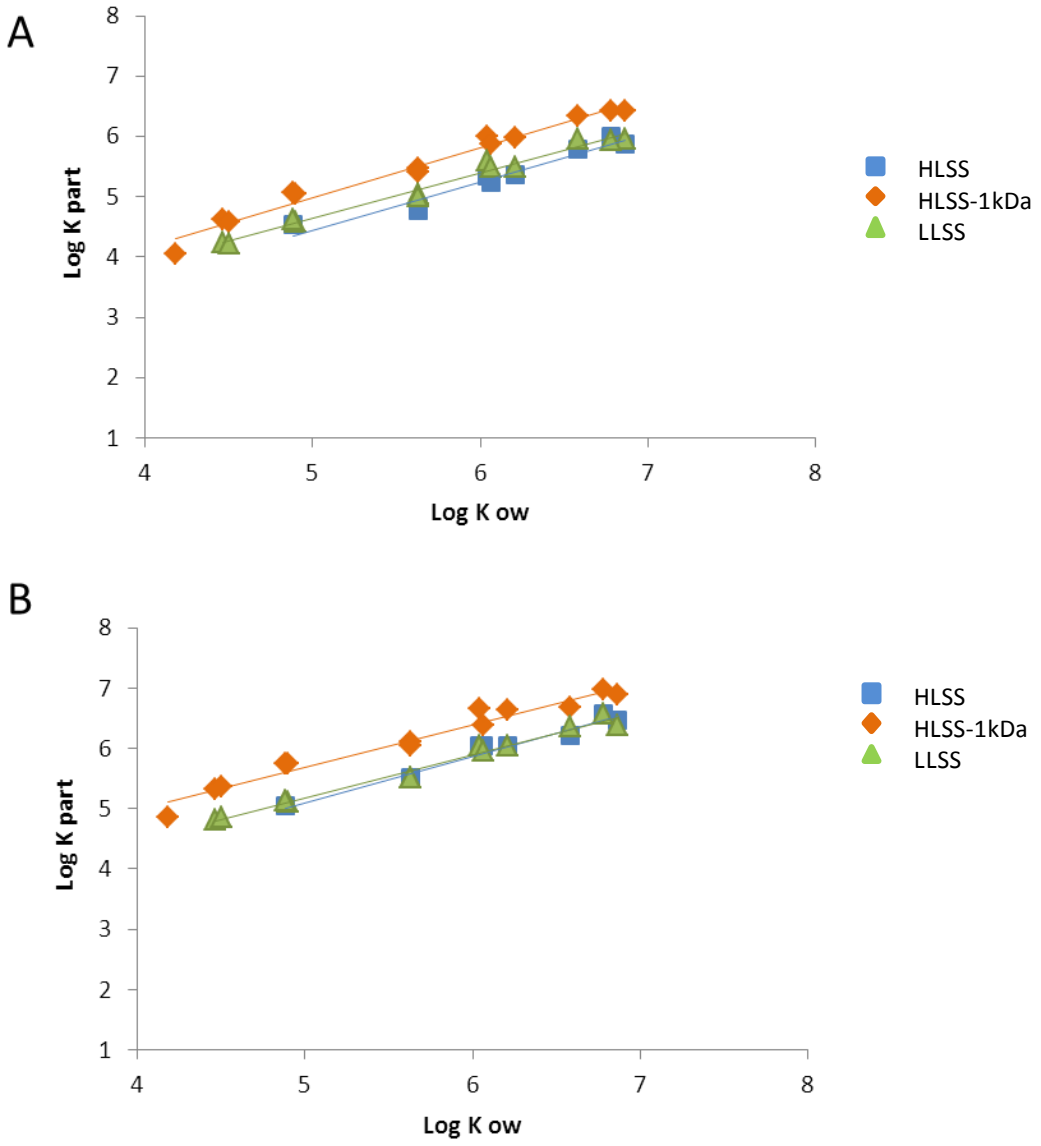

Figure V-13: Log K_{part} of PAHs. A: initial mixture. B: Final mixture after 53 days of reaction.

In the case of LLSS, initial K_{DOC} and K_{part} values explain the higher aqueous PAHs concentrations obtained in contrast with those of HLSS. However, although the K_{DOC} values of HLSS-1kDa are also higher than those of HLSS, its low DOC concentration and consequently, its high POC concentrations, govern the distribution between compartments.

V.4.4. Validation of aqueous PCBs quantification by SPME

The validation methodology to quantify the aqueous PCBs concentration by SPME was described in the section III.5.5.2. The values of Ki determined in milliQ water and DCM, the PCBs quantification yields (Ci) in DCM using the Ki values in milliQ water and the internal standard chosen for each compound are presented in the Table V-4. Ci values close to 100 %

were obtained for all PCBs with similar Ki values in milliQ water and DCM, validating the SPME thechnique to quantify these compounds.

Table V-4: Ki and Ci values of PCBs quantification and their respective internal standard

Compound	Ki milliQ water	Ki DCM	Ki milliQ water Ci DCM	Internal Standard
PCB28	0.95±0.056	0.97±0.006	98±6.5	PCB20
PCB52	0.98±0.07	1.04±0.009	98±2.6	PCB20
PCB101	1.13±0.28	1.36±0.12	89±23	PCB155
PCB118	1.06±0.07	1.05±0.04	103±8.3	PCB87
PCB153	1.02±0.03	1.12±0.06	90±1.1	PCB87
PCB138	1.01±0.06	0.9±0.03	118±2.93	PCB128
PCB180	1.42±0.09	1.56±0.09	99±19.9	PCB198

V.4.5. Aqueous PCBs concentrations and kinetics

The Figure V-14 shows the kinetics of the total and aqueous concentrations of PCB 180 in HLSS-1kDa and LLSS. Both kinetics have similar profiles and the highest aqueous PCBs removals were found in LLSS.

In the same way as PAH-aqueous kinetics, PCBs removals occur during the first stage of the anaerobic digestion followed by a stage of sorption/removal (Figure V-11) where the sorption phenomena govern the PCB-aqueous behavior.

A mass balance done during the first 20 days reveals that even if the highest removals are reached in the aqueous phase (85% HLSS-1kDa and 90% LLSS), between 99 (HLSS-1kDa) and 92 % (LLSS) of the total removal corresponds to the particulate fraction.

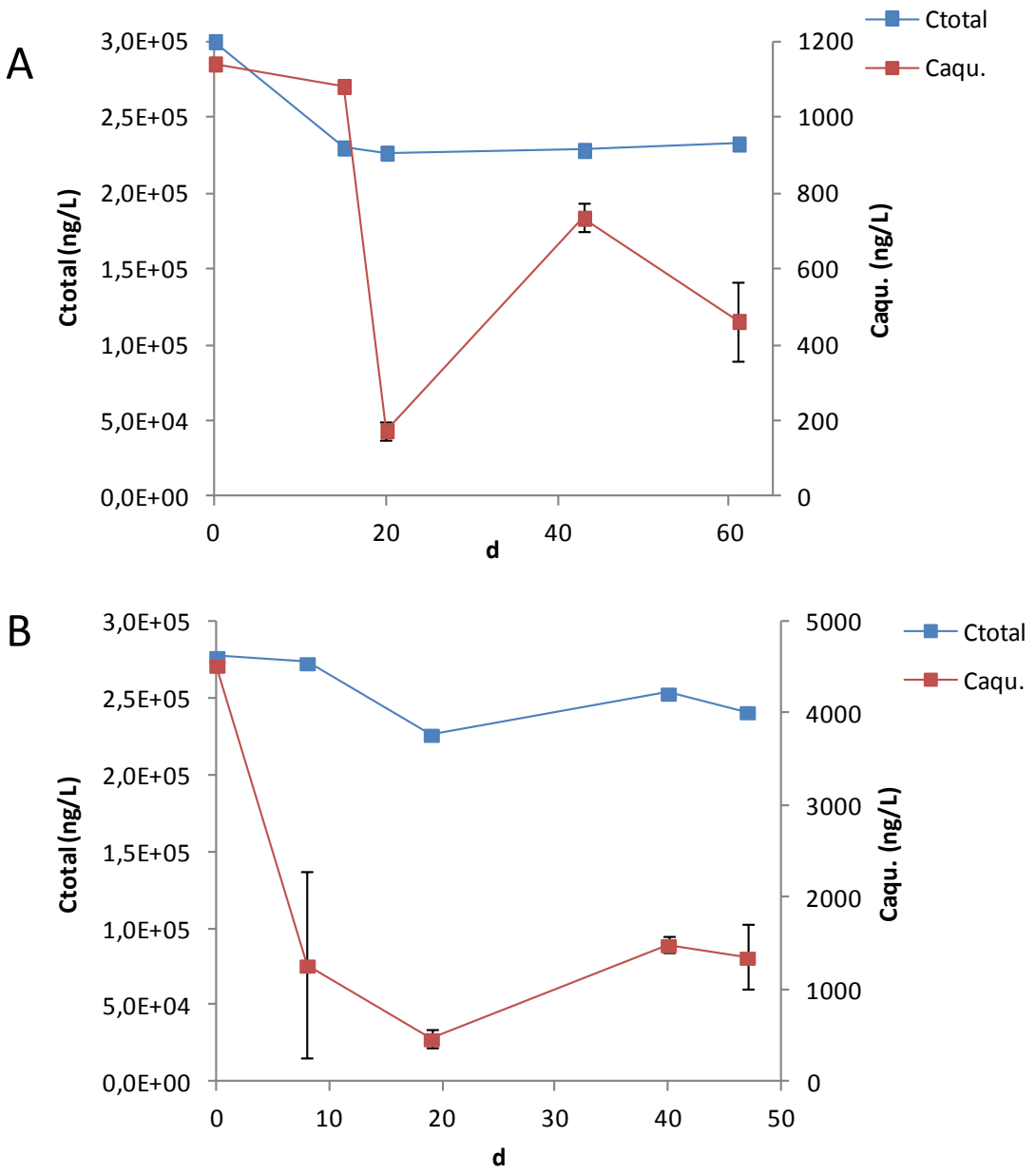

Figure V-14: Kinetics of total and aqueous PCB 180 concentration. A: HLSS-1kDa, B: LLSS. Standard deviations correspond to two different reactors.

V.5. Chapter conclusion

The OPs removal kinetics ($C_{OP,free}$, $C_{OP,DCM}$ and $C_{OP,part}$) in batch reactors series demonstrated that OPs removals are coupled to the first step of the anaerobic digestion, jointly to a OPs transfer from the particulate compartment to the aqueous compartment which is generated by the degradation of the particulate fraction. This OPs transfer allows the apparent removal of the $C_{OP,part}$, $C_{OP,free}$ and $C_{OP,DCM}$ simultaneously.

Additionally, it was highlighted the importance of the DCM fraction on the removal of the high molecular weight PAHs which is directly related with the initial $C_{PAH,DCM}$. This link could be due to the nature of the OP-DCM interactions and also to the cometabolic contribution of this DCM, phenomenon that was evidenced in the LLSS and HLSS-1kDa reactors. However, not only the $C_{PAH,DCM}$ and the nature of this interaction govern the total OPs removals. Indeed, LLSS reactors demonstrated that even if the highest initial $C_{PAH,DCM}$ are linked with the highest $C_{PAH,DCM}$ removals, $C_{OP,part}$ removals are governed by the cometabolism flux from the particulate compartment and by transfer phenomena.

Different values of K_{DOC} were found among the three initial sludge mixtures and different evolutions through the degradation process were observed. This result suggests that a detailed characterization of the DCM fraction could explain this behavior and mainly, both K_{DOC} values and characterization could help to predict the total OPs removals.

VI. SLUDGE MATRIX CHARACTERIZATION AND LINK WITH THE ORGANIC MICROPOLLUTANTS REMOVAL

VI.1. Overview

As it was shown in the previous chapters, different sludge matrices generate different OPs removals and different OPs distributions among the physical compartments. Additionally, it was shown that the OPs have different affinities among themselves for one matrix and among different sludge matrices. According to these results a more detailed characterization of the three initial mixtures was performed, mainly in the aqueous compartment; indeed, this compartment is the one with the highest changes among the mixtures, and this study is focused on elucidating the role of the aqueous compartment on OPs bioavailability and removal.

In order to highlight the role of the aqueous compartment on OPs bioavailability and removals, a chemical, physical and functional characterization was performed in all initial mixtures and at the end of each batch reactors series as it was shown in the section III.4.

First, 3D fluorescence spectra were acquired in the aqueous phase of the initial and final sludge mixtures using the protocol described in the section III.4.2.3. Seven normalized intensities (NI) regions were measured for each sludge sample. NI values jointly with the chemical and physical characterization at the initial and the end of the experiences (after 53 days of reaction), and the initial OPs distribution between compartments were used to explain and predict the variation of K_{DCM} and Kpart, shown in the section V.6.1., using a statistical analysis (PLS).

In addition, the aqueous compartment of the initial sludge mixtures was fractionated by filtration/ultrafiltration and AF^4 as it was described in the section III.4.2.2. These physicals separation techniques were carried out in order to know the size distribution of the aqueous compartment and the OPs distribution among the different aqueous sub-fractions. AF^4 technique allows getting a profile of the different groups of sizes colloids contained in the initial aqueous sludge samples. Moreover, ultrafiltration allows separating the samples using known cutting off sizes and, as it was described in the III.4.2.2., different aqueous colloid sub-fractions can be recuperated (F1, F2, F3 and F4) in order to be further analyzed. Ultrafiltration was coupled to SPME technique in order to determine the free and aqueous OPs concentrations among the different aqueous colloid sub-fractions and thus to quantify the OPs affinity and distribution according to this different aqueous colloid sub-fractions.

The detailed characterization of the sludge matrices and the OPs distribution with SPME helped to better explain and understand the OP-OM interactions through sorption. These data, representing the bioavailability, combined to the substrate removals representing the cometabolism effect, were also used to explain the OPs removals. Finally, predictive models of total and aqueous OPs removals were constructed from the initial matrix characteristics and OPs distribution, using PLS regression analysis.

PLS regression technique is based on constructing PLS factors (also called principal components) by minimizing the covariance between the dependent variables (Y block: OPs removals or K_{part} and K_{DCM}) and the explicative variables (X block: matrix and molecules

characteristics, NI and OPs distribution). Then, the prediction of the Y block was calculated with a multivariable linear regression on X block through NIPALS algorithm using the software Unscrambler 10.6. The algorithm constructs orthogonal PLS factors in each block by minimizing the covariance between the X and Y blocks. The first PLS factor contains the highest percentage of variance, and the following factors account for decreasing amounts of variance. A leave-one-out cross-validation procedure was used to choose the dimension of the predictive model. The RMSEC/MAX value (the root mean square error of calibration divided by the maximal value) was used to know the accuracy of the model.

VI.2. K_{part} and K_{DOC} explanatory models using PLS regression analysis

As it was shown in the section V.6.1., K_{part} and K_{DOC} values fit a linear correlation with the OPs physico-chemical characteristics (Kow), being only displaced by a change in the matrix composition. In order to understand this displacement of the lines, either by an increase or decrease of K_{part} and K_{DOC} values, two explanatory models were constructed taking into account the variation of the 3D fluorescence spectra (RI-RVII) and the sludge characteristics of the initial matrices and the end of the experiences (after 53 days of reaction). The study of K_{part} with aqueous fluorescence spectra is based on the assumption that the aqueous phase is a representation of the particulate phase.

The explicative variables (X block) to explain the K_{DOC} and K_{part} values are shown in the Tables VI-1 and VI-2. $C_{OP,free}$, $C_{OP,DCM}$ and $C_{OP,part}$ were not included in the X variables because K_{part} and K_{DOC} are directly calculated from these concentrations. 13 PAHs were chosen to construct the models. In the appendix A the values of the X block and Y block variables of each model are presented.

The equation 1 obtained (centered and reduced) for the dependent variables (Y block) K_{DOC} is the following:

(eq.1) $$LogK_{DOC} = -1.68 + 0.25LogK_{OW} + 0.46M - 0.11LogS - 0.18RI - 0.17RII - 0.38RIII + 0.18RIV + 0.13RV + 0.38RVI + 0.55RVII$$

The R^2 coefficient is equal to 0.96 (cross-validation) confirming the good explanatory capability of this model. The RMSEC/MAX value (the root mean square error of calibration divided by the maximal value) is equal to 0.2/5.53=0.03, indicating a very good accuracy of 3% of the predictive model.

Figure VI-1 shows the weighted regression coefficient of the Log K_{DOC} model. Log Kow, M, RIII, RVI and RVII fluorescence regions present the highest weights, with relative values of 0.25, 0.46, 0.38, 0.38 and 0.55, indicating that they were the most influential variables on K_{DOC} values variation. According to section III.4.2.3, RIII corresponds to a protein-like (Tyr and Trp) region. As much as the RIII, all other indicators of proteins (RI and RII) have negative and positive effects (Figure VI-1) on the K_{DOC} values not being significative explicative variables. In contrast, RVI and RVII which correspond to melanoidin-like, ligno-cellulose-like and humic acid-like fluorescence regions have a positive effect on the K_{DOC}

values. These results are consistent with literature that identifies the humic acids (RVII) as the molecules that have stronger interaction with hydrophobic contaminants in aqueous matrices (Lee and Farmer, 1989; Perminova et al., 1999). However, the uncertain effect of the proteins is contradictory with the results of Barret et al., 2010 who, also with a PLS analysis, found a positive effect of the proteins content on the K_{DOC} values. However, in this paper the standard deviation of the weighted regression coefficients were not calculated and no fluorescence data were provided. These latter are more precise because they give an idea of the functional groups present in the aqueous sample. The colorimetric method provides general information about all types of molecules that contain amino-acids in contrast with the fluorescence analysis where only fluorescent proteins are taken into account. Moreover, fluorescence data provide information on molecules complexity.

Table VI-1: PLS variables of K_{DOC} model. X block: explicative variables. Y block: measured K_{DOC} values of the 13 PAHs in each sludge mixture.

Sludge matrix	**X block**		**Y block**
	OPs characteristics	Matrix characteristics	
HLSS t_0	Log Kow	RI	
HLSS-1kDa t_0	M	RII	
LLSS t_0	Log S	RIII	
HLSS t_f		RIV	
HLSS-1kDa t_f		RV	K_{DOC}
LLSS t_f		RVI	
		RVII	

t_0: initial time; t_f: final time; RI-RVII: NI regions.

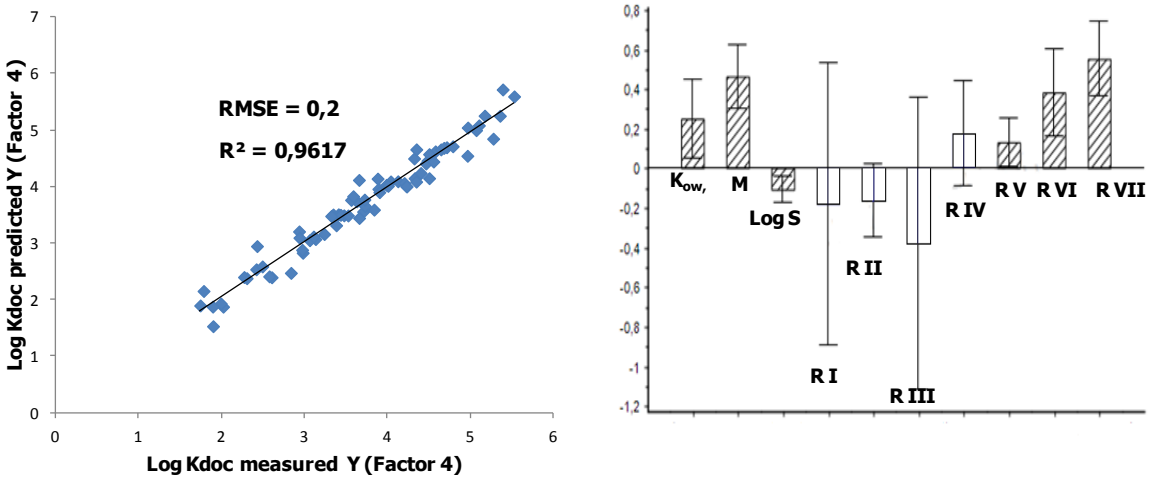

Figure VI-1: LogK_{DOC} explanatory model Left: Measured K_{DCM} values versus predicted K_{DCM} values. Cross-validation factor 4. Right: Weighted regression coefficient.

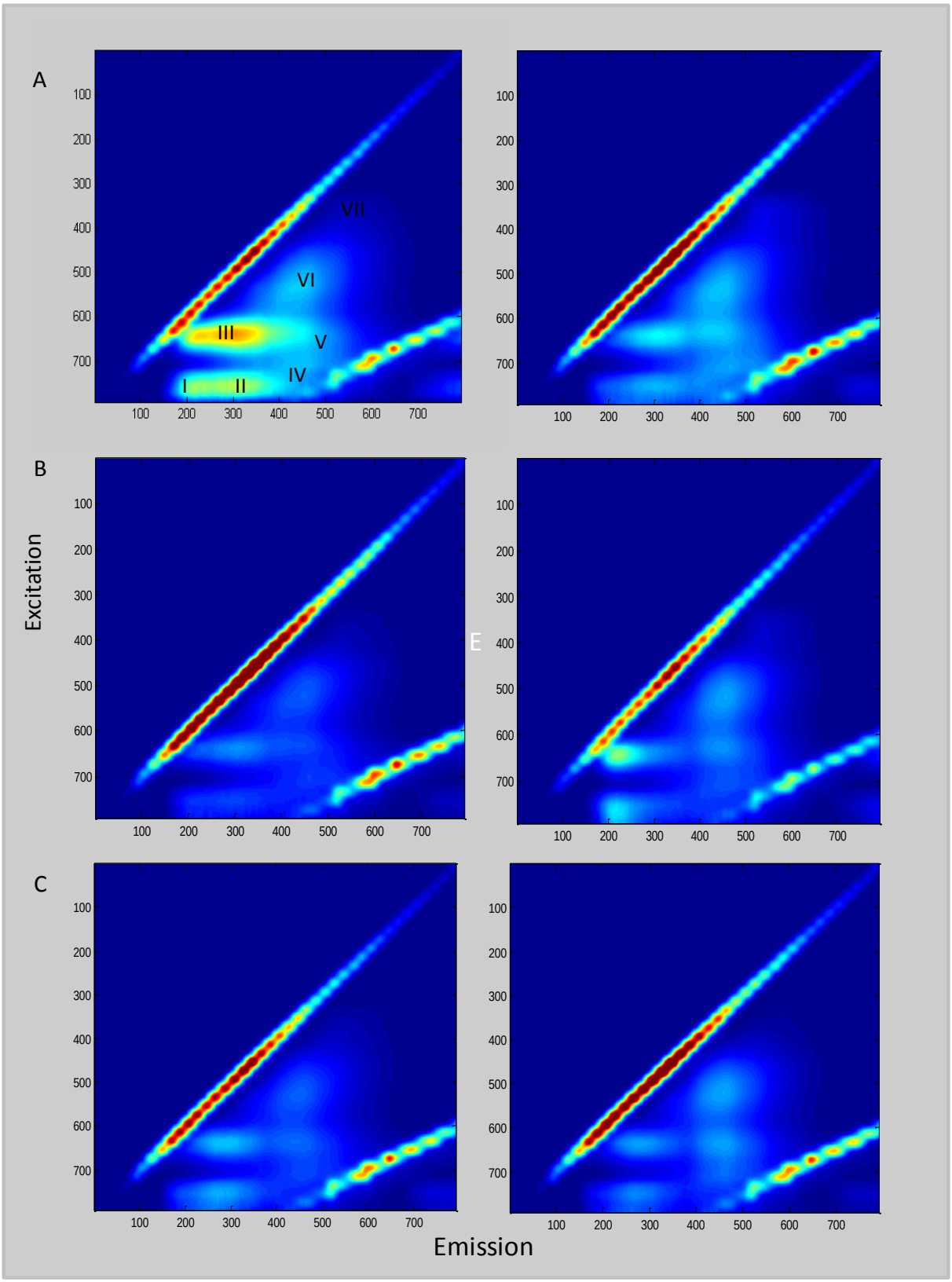

Figure VI-2: 3D Fluorescence spectra and regions of aqueous sludge samples. t_0 (left) and t_f (right). A: HLSS. B: HLSS-1kDa. C: LLSS.

In the Figure V-12 (chapter V), we can observe that the K_{DOC} values of HLSS are similar at initial and final reaction times whereas for HLSS-1kDa and LLSS the K_{DOC} values at the initial time are higher than those at the final time. This behavior can be explained with the values of RVII fluorescence. In HLSS, RVII intensity decreased by 62% after 53 days of reaction against 91% in HLSS-1kDa and 94% in LLSS (appendix A). Additionally, if only the fluorescence of the initial mixtures is taken into account, LLSS presents the highest RVII and RVI intensities (appendix A and Figure VI-2) which explains the highest K_{DOC} values found in LLSS at the initial time. LLSS is a more stabilized sludge sampled in a low organic load WWTP which explains its high content of more recalcitrant and complex molecules as melanoidins (condensed carbohydrates and amino acids) and humic acids. In the initial LLSS sample (Figure VI-2 C), fluorescence is observed in the RV, unlike HLSS and HLSS-1kDa, which corresponds to a mixture of proteins and melanoidins that are indicators of a more mature matrix.

Initially, K_{part} PLS model was constructed with the 13 PAHs and the functional and chemical characterization of the matrices. However, this model showed that the K_{part} values depend only of the physic-chemical characteristics of the OPs (R^2= 0.93 and RMSE/max= 2.9%). As it was shown in the section V.2.1., PAHs present different behaviors according to their M and physico-chemical properties, being possible classify in low, middle and high molecular weight PAHs (Table VI-2). Thus, the construction of three different models divided by PAHs molecular weight was tested.

Table VI-2: Classification of PAHs according to their molecular weights and physico-chemical properties.

PAHs		Log Kow	M
Low	Fluorene	4.18	166
	Phenanthrene	4.57	178
	Anthracene	4.45	178
Middle	Fluoranthene	5.1	202
	Pyrene	5.32	202
	Benzo(a)anthracene	5.85	228
	Chrysene	5.89	228
High	Benzo(b)fluoranthene	6.57	252
	Benzo(k)fluoranthene	6.84	252
	Benzo(a)pyrene	6.00	252
	Dibenzo(a,h)anthracene	6.70	278
	Benzo(g,h,i)perylene	6.73	276
	Indeno(1,2,3,c,d)pyrene	6.60	276

The three PLS models were carried out using the variables presented in the Table VI-3. It was found that the matrix characteristics only explain the behavior of the low and middle molecular weight PAHs separately. In contrast, the matrix characteristics do not explain the behavior of the high molecular weight PAHs being the OPs characteristics that take the highest weighted regression coefficient.

The equations obtained for the Y block (K_{part}) for the low (eq. 2) and middle (eq. 3) molecular weight PAHs are the following:

(eq.2) $LogK_{part} = 40.54 - 0.012LogK_{OW} + 0.15M - 0.07LogS - 0.15n5C + 0.15n6C - 3.21RI - 6.71RII + 10.12RIII + 0.39RIV - 3.27RV - 0.57RVI + 4.57RVII - 2.40eqBSA - 2.93COD_{total} + 1.83DM$

(eq.3) $LogK_{part} = 36.38 + 0.28LogK_{OW} + 0.47M + 0.31LogS + 0.016n5C - 0.016n6C - 3.92RI - 7.77RII + 10.80RIII + 0.56RIV - 3.58RV - 0.29RVI + 5.64RVII - 2.57eqBSA - 3.03COD_{total} + 1.99DM$

The R^2 coefficient for (eq. 2) is equal to 0.98 (cross-validation) confirming the good explanatory capability of this model. The RMSEC/MAX value (the root mean square error of calibration divided by the maximal value) is equal to 0.05/5.36=0.009, indicating a good accuracy of 0.9% of the predictive model. Equation 3 has a R^2 of 0.92 and a RMSEC/MAX of 0.13/6.09=0.02 indicating a good accuracy of 2%.

Figure VI-3 shows the weighted regression coefficients of the K_{part} model for the low molecular weight PAHs. Similar weighted regression coefficients and influence were obtained for the middle molecular weight PAHs. RI, RII, RIII and RVII fluorescence regions present the highest weights, with relative values of -3.21, -6.71, 10.12 and 4.57 respectively, indicating that they were the most influential variables on K_{part} values variation. Although the indicators of proteins (RIII protein-like, Tyr and Trp; RI and RII amino acids-like) RI, RII and $eqBSA_{total}$ have a negative effect on the K_{part} values, RIII has a positive effect, contrary as it was shown for K_{DOC} values. This suggests that the OPs affinity for the particulate compartment is governed by the presence of bigger protein structures that have a higher biodegradability potential (less mature structures) which present a fluorescence in RIII (Baker, 2001). Moreover, as for K_{DOC}, RVII presents a positive effect on the K_{part} values, confirming the importance of humic acids on the OP-matrix interactions.

Observing the Figure V-12 (chapter V), all K_{part} values increased after 53 days of reaction. This can be explained indirectly by the combined effect of RI, RII, RIII and RVII. Indeed, during the anaerobic reaction time, proteins containing particules hydrolysis with a concomitant proteins condensing (cell growth, EPS production) are observed. It results in the presence of fluorescence massif on the right of the spectra (more complex and condensed molecules), implying higher affinity for PAHs.

Table VI-3: PLS variables of K_{part} model. X block: explicative variables. Y block: measured K_{part} values of the 13 PAHs in each sludge mixture.

Sludge matrix	X block		Y block
	OPs characteristics	Matrix characteristics	
HLSS t_0	Log Kow	RI	
HLSS-1kDa t_0	M	RII	
LLSS t_0	Log S	RIII	
HLSS t_f	n5C	RIV	
HLSS-1kDa t_f	n6C	RV	K_{part}
LLSS t_f		RVI	
		RVII	
		eqBSAt	
		CODt	
		DM	

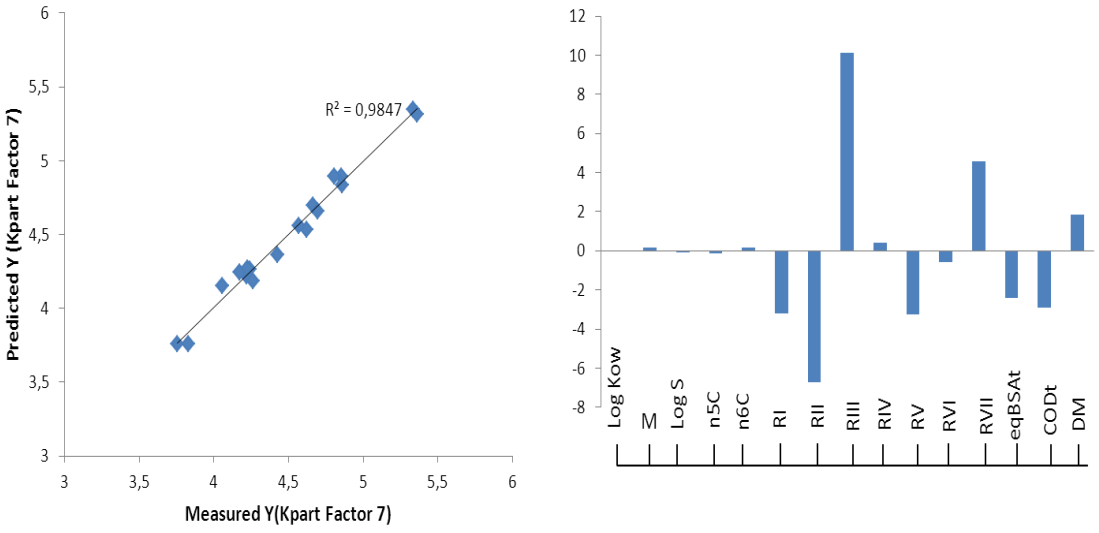

Figure VI-3: Log K_{part} explanatory model of the low molecular weight PAHs. Left: Measured K_{part} values versus predicted K_{part} values. Cross-validation factor 7. Right: Weighted regression coefficient.

The equations 4 obtained for the Y block (K_{part}) for the high molecular weight PAHs is the following:

(eq.4) $$LogK_{part} = 36.38 + 0.19LogK_{OW} + 0.30M + 0.013LogS - 0.013n5C + 0.15n6C - 0.1RI - 0.1RII - 0.1RIII - 0.08RIV - 0.085RV - 0.064RVI - 0.061RVII - 0.0091eqBSAt_t - 0.15COD_t - 0.14DM$$

The R^2 coefficient is equal to 0.8 (cross-validation). The RMSEC/MAX value is equal to 0.19/6.97=0.027, indicating a good accuracy of 2.7% of the model.

The K_{part} values of the high molecular weight PAHs are not correlated with the matrix characteristics (Figure VI-4), being only the COD_t and the DM which present the higher influences. K_{part} are more explained by their physico-chemical characteristics. This result suggests that the 3 D fluorescence of the aqueous phase is not a real and complete image of the particulate phase which may interact differently with the high molecular weight PAHs. The fact that a correlation was found for the low and middle molecular weight PAHs could be that these OPs interact with the organic matter present as much in the particulate phase as in the aqueous phase i.e. with the less complex molecules. This hypothesis can be supported also by the contrary effect of RIII in K_{DOC} and K_{part}. RIII (protein-like) is present in both aqueous and particulate phases with only an important positive role in the particulate phase where it may have an important role in the flocs structure (EPS).

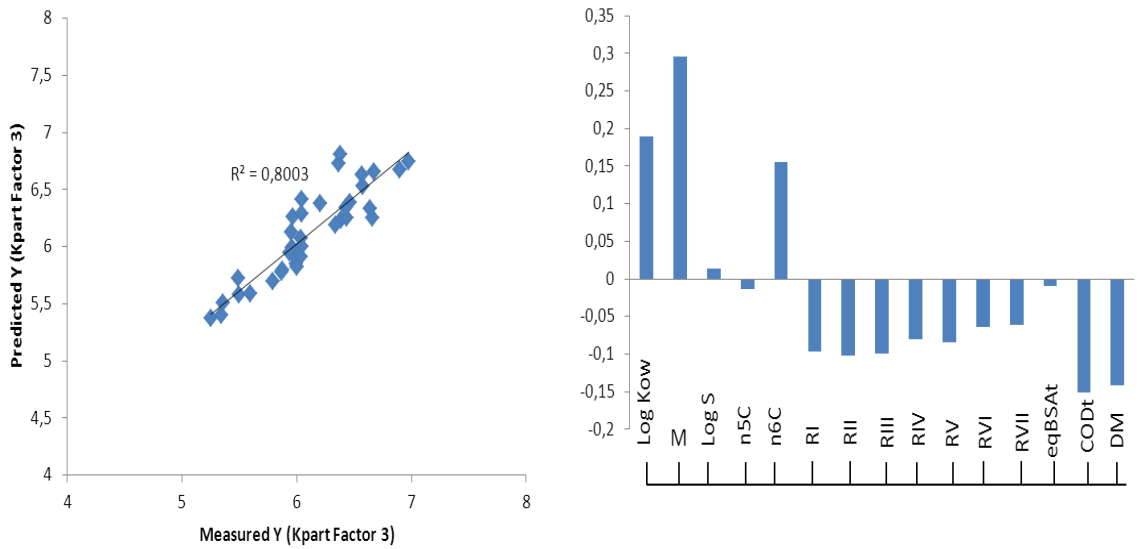

Figure VI-4: Log K_{part} explanatory model of the high molecular weight PAHs. Left: Measured K_{part} values versus predicted K_{part} values. Cross-validation factor 3. Right: Weighted regression coefficients.

VI.3. Fractionation of the aqueous compartment by filtration/ultrafiltration coupled to OPs quantification by SPME

The aqueous compartment of HLSS was fractionated by filtration/ultrafiltration following the protocol shown in the section III.4.2.2. F_1 to F_4 fractions were analyzed by SPME jointly to the determination of the DOC in order to calculate the K_{DOC} of the 13 PAHs in each independent sub-fraction.

The Figure VI-5 shows the K_{DOC} values of the 13 PAHs for each aqueous fraction. In the fractions F3 and F4 it was not possible to calculate the K_{DOC} values of fluorene to pyrene because the concentrations sorbed to the DCM of these compounds were not detected in these aqueous sub-compartments.

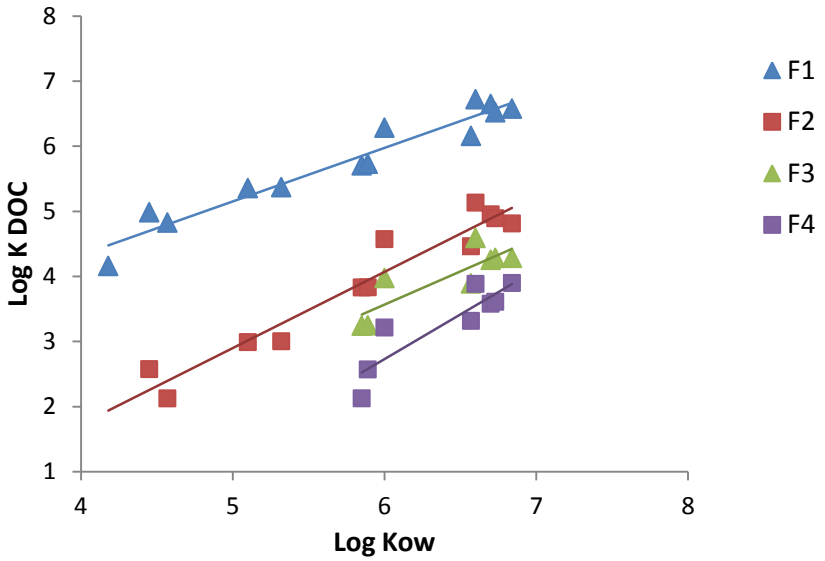

Figure VI-5: Log K_{DOC} of PAHs in each aqueous fraction of HLSS. F1: 0.1-1.2 µm, F2: 10 kDa-0.1 µm, F3: 1-10 kDa and F4: < 1 kDa.

We observe that the OPs present the highest affinities for F1 fraction where the higher size colloids are contained. In general, the smaller is the colloid size, lower is the OPs affinity for the DCM fraction, being the F4 fraction (< 1kDa) which presents the lowest OPs affinity. This result agrees with that obtained by Barret et al. (2010b) where it was shown that K_{DOC} values decrease significantly with high percentage of F4 fraction.

VI.4. Fractionation of the aqueous compartment by AF^4

AF^4 fractionation of the three aqueous initial samples (HLSS, HLSS-1kDa and LLSS) was carried out as it was described in the section III.4.2.2. Absorbance v/s retention time (t_r) separation profiles were obtained for the three sludge samples using a total elution time from22 to 25 min with an initial cross flow (Cx) of 3.5 mL/min from 2 to 5 min, and then

with a Cx gradient from 3.5 to 0 mL/min for 20 min. These parameters of separation were chosen testing different Cx gradients and elution times in order to obtain the best separation profile. The Cx initial constant stage allows separating the smallest colloids from the rest of colloids size groups.

Figure VI-6 shows the HLSS, HLSS-1kDa and LLSS aqueous separation profiles. It is possible to distinguish different colloids size groups among the aqueous samples.

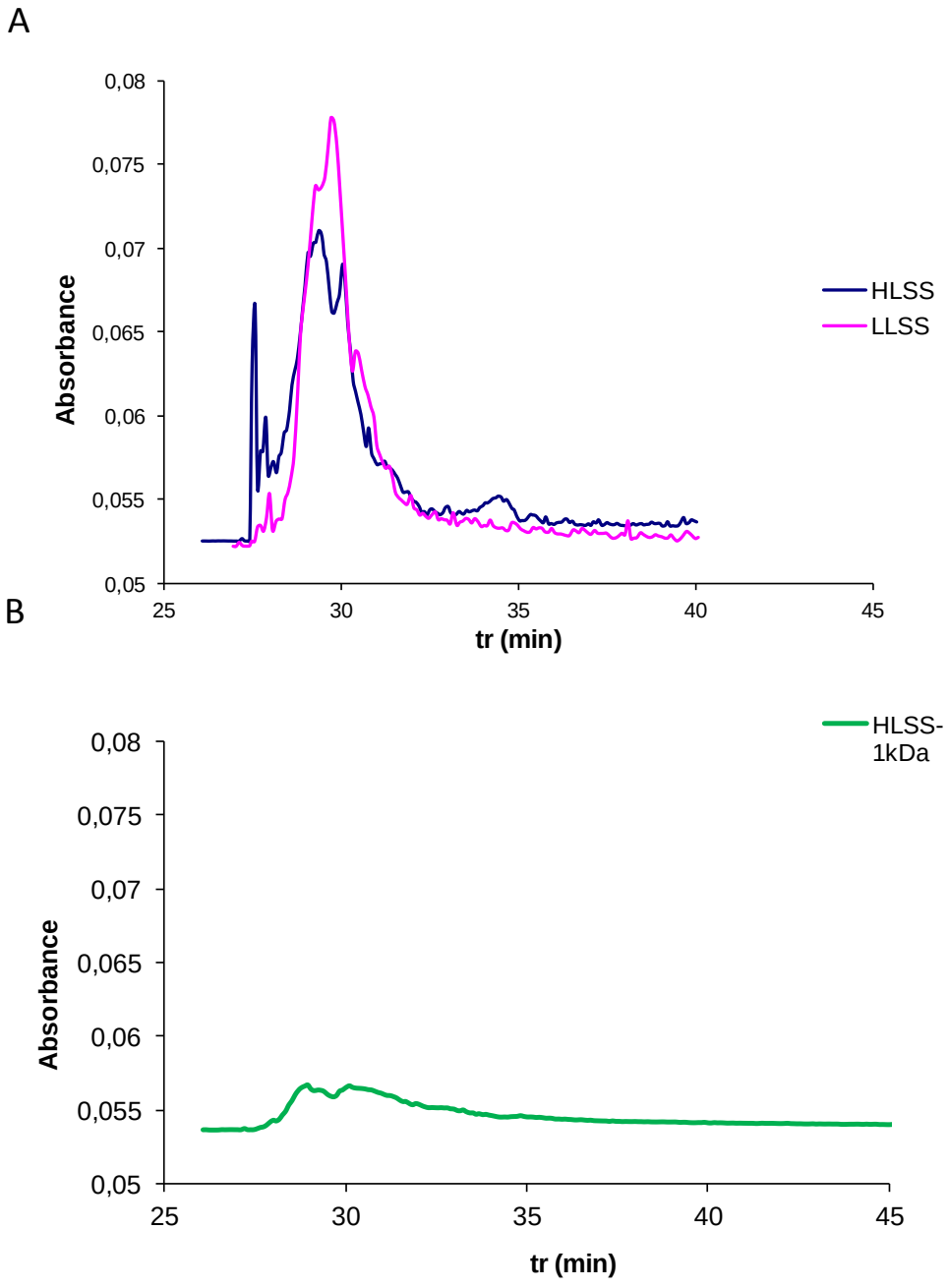

Figure VI-6: Separation profile of the aqueous sludge samples using AF^4 technology. A: Cx: 3.5 mL/min, elution: 2 min; Cx: 3.5-0 mL/min, elution: 20 min. B: Cx: 3.5 mL/min, elution: 5 min; Cx: 3.5-0 mL/min, elution: 20 min.

In the Figure VI-6 A, during the initial 2 min of elution time (from 27-29 min), it is possible to observe a group of colloids that corresponds to the smaller one that are contained mostly in HLSS. After, two groups of colloids are present in both HLSS and LLSS, LLSS presenting the higher intensity of the bigger group (30 min). These differences of absorbance intensities could be due to groups with the same colloid size but with different nature or compositions. After 30 min, HLSS and LLSS present different colloids size group profiles. HLSS have two additional groups (31.5 and 34.5 min), while LLSS has only one additional group (31 min). All these last groups correspond to highest colloids size.

Regarding the HLSS-1kDa sample (Figure VI-6 B), it is possible to find two colloids size groups at 30 min, however this sample cannot be compared with the 2 others due to that different parameters of separation were used.

VI.5. OPs total removals explanatory model

In order to better understand the OPs removals in sewage sludge under anaerobic conditions, an explanatory PLS model was constructed. Considering that the main removal mechanisms that govern the OPs removals are the cometabolism and the bioavailability (Barret et al., 2010c), different parameters representing these two mechanisms were taken into account to construct the model. Cometabolism effect was represented by the substrate removals and the OPs bioavailability was represented by K_{part} and $K_{DOC,}$ and the initial OPs distribution among the physical compartments ($C_{OP,free}$ and $C_{OP,DCM}$).

The PLS model was constructed with a X block of 13 PAHs and the cometabolic variables listed in the Table VI-3. Regarding the bioavailability influence, when the PLS analysis was carried out, K_{part} and K_{DOC} values showed a very low influence on the total OPs removals (Y block) in contrast with the OPs distribution that showed the highest influence, thus the OPs initial distribution was chosen as the explicative variable that represents the bioavailability.

Table VI-4: PLS variables of total OPs removals explanatory model. X block: explicative variables. Y block: measured OPs removals of 13 PAHs in each sludge mixture.

Sludge Matrix	X block			Y block
	OPs characteristics	Substrate removals (%)	Initial OPs repartition (%)	
HLSS	Log Kow	DM	$C_{OP,free}$	
HLSS-1kDa	M	OM	$C_{OP,DCM}$	
LLSS	Log S	Carbohydrates		
	n5C	eqBSAt		Total OPs removals
	n6C	eqEEPt		(%)
		CODdcm		

The equation 5 obtained for the explanation of total OPs removal (Y block) is the following:

$$(eq.5) \quad OPsR_{total} = 76.68 - 0.11LogK_{OW} + 0.08M + 0.27LogS + 0.06n5C + 0.11n6C + 0.12COD_{DCM} + 0.09Carbohydrates + 0.18eqBSA + 0.17OM + 0.18MS + 0.23eqEEP + 0.35C_{free,OP} + 0.14C_{DCM,OP}$$

The R^2 coefficient was equal to 0.83 (cross-validation). The RMSEC/MAX value is equal to 3.55/32.3=0.11, indicating an accuracy of 11% of the predictive model.

The Figure VI-7 shows the weighted regression coefficients of the total OPs removal explanatory model. The model shows that all cometabolic variables have a positive effect on the OPs removals jointly to the bioavailability variables $C_{OP,free}$ and $C_{OP,DCM}$, the $C_{OP,free}$ presenting the higher positive effect (0.35). Moreover, OPs solubility in water (Log S) has also a significant positive effect, which can be linked to the key role of $C_{OP,free.}$ This tends to confirm that the bioavailable fraction corresponds to the aqueous compartment.

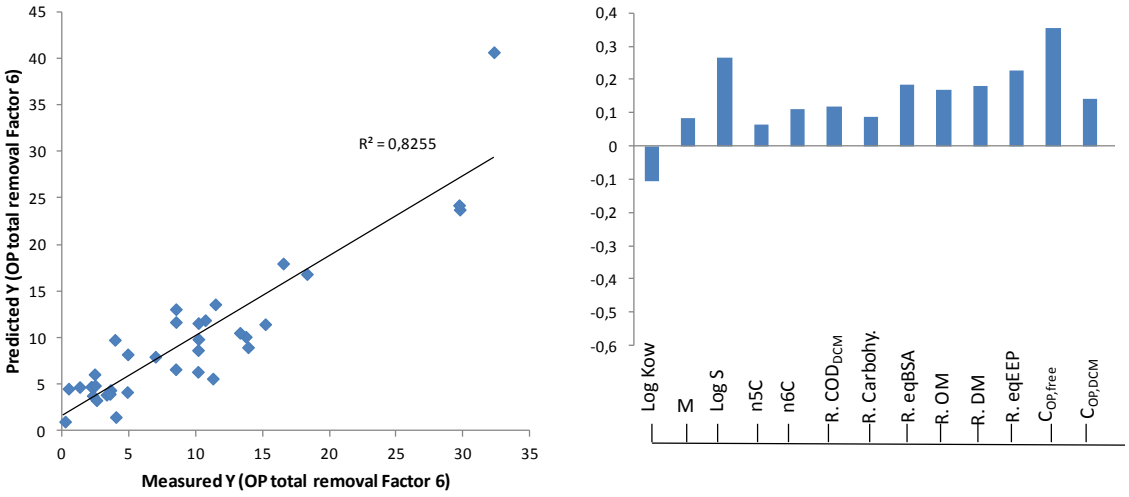

Figure VI-7: Total OPs removal explanatory model. Left: Measured OPs removals versus predicted OPs removals. Cross-validation factor 6. Right: Weighted regression coefficient.

VI.6. OPs aqueous removal predictive model

As it was shown in the section V.6.1, aqueous removals were significantly higher than the particulate removals, with an important role of the $C_{OP,free}$ on the low molecular weight PAHs removals and $C_{OP,DCM}$ on the high molecular weight PAHs removals. In order to understand and predict the OPs aqueous removals, a PLS model was constructed taking into account the initial matrix characteristics, mainly in the aqueous phase and the initial OPs bioavailability parameters. X block and Y block variables are listed in the Table VI-4. The initial OPs distribution among the compartment was chosen as the OPs bioavailability. Considering that both $C_{OP,free}$ and $C_{OP,DCM}$ play an important role in the OPs aqueous removal, PLS analysis was carried out using the $C_{aqu,\ OP}$ as explicative variable.

Initially, PLS was carried out with the 13 PAHs, and a very low accurate model was obtained. After, it was carried out using only the low and middle molecular weight PAHs, thus improving the accuracy of the model. The highest accuracy was obtained using only 5 PAHs (the low more 2 middle molecular weight PAHs). In contrast, no accurate model was found for the high molecular weight PAHs.

Table VI-5: PLS variables of OPs aqueous removals predictive model. X block: explicative variables. Y block: measured aqueous OPs removals of fluorene, phenanthrene, anthracene, fluoranthene and pyrene in each sludge mixture.

Sludge Matrix	X block			Y block
	OPs characteristics	Matrix initial characteristics	Initial OPs repartition (%)	
HLSS HLSS-1kDa LLSS	Log Kow M Log S n5C n6C	$eqBSA_{part}$ $eqBSA_{DCM}$ COD_{DCM} VFAs F4 RI RII RIII RIV RV RVI RVII	$C_{OP,aqu}$	Aqueous OPs removals (%)

The equation 6 obtained for the prediction of the aqueous OPs removals of 5 lower PAHs is the following:

$$(eq.6)\quad OPR_{aqueous} = 24.44 - 0.12LogK_{OW} - 0.12M + 0.1LogS + 0.04n5C - 0.10n6C - 0.007COD_{DCM} + 0.11eqBSA_{part} + 0.046eqBSA_{DCM} - 0.038VFAs + 0.0009F_4 + 0.16C_{OP,aqu} + 0.039RI + 0.027RII - 0.02RIII + 0.056RIV + 0.053RV + 0.092RVI + 0.10RVII$$

The R^2 coefficient is equal to 0.711 (cross-validation). The RMSEC/MAX value is equal to 9.36/63.7=0.15, indicating an accuracy of 15% of the predictive model.

The Figure VI-8 shows the weighted regression coefficients of the aqueous OPs removal predictive model. The parameters with the higher influence are the OPs physico-chemical characteristics, $C_{OP,aqu}$, particulate proteins and RVI and RVII. The OPs characteristics show that the low molecular weight PAHs present the highest aqueous removal that is directly

linked with their higher solubility and consequently their high $C_{OP,free}$. The positive effect of $C_{OP,aqu}$ confirms that the aqueous compartment is the bioavailable one and the determination of the initial $C_{OP,aqu}$ and the OPs characteristics could predict the aqueous OPs removal. Both particulate and DCM proteins have a positive influence. This influence could be related with the cometabolic mechanism, being the proteins of the particulate fraction the main cometabolic flux.

Additionally, this cometabolic flux from the particulate fraction could play an important role in the phenomena of the OPs transfer from the particles to the aqueous compartment. RVI and RVII that correspond to the melanoïdin-like and humic-like present a positive influence on the aqueous OPs removals. This positive influence was also observed for the K_{DOC} values. This result suggests that the removals of the $C_{OP,aqu}$ are govern by both the $C_{OP,free}$ and the OPs sorbed to these type of molecules which could play an important role on their availability to the microorganisms. Interestingly, this model was constructed with the 5 lower PAHs for which were not detected in F3 and F4 fractions. This may suggest that, in addition to the free compartment, the bioavailable fraction may be mainly linked to F1 and F2 fractions. This assumption, which needs to be confirmed, would explain the low OPs removals observed in HLSS-1kDa sludge.

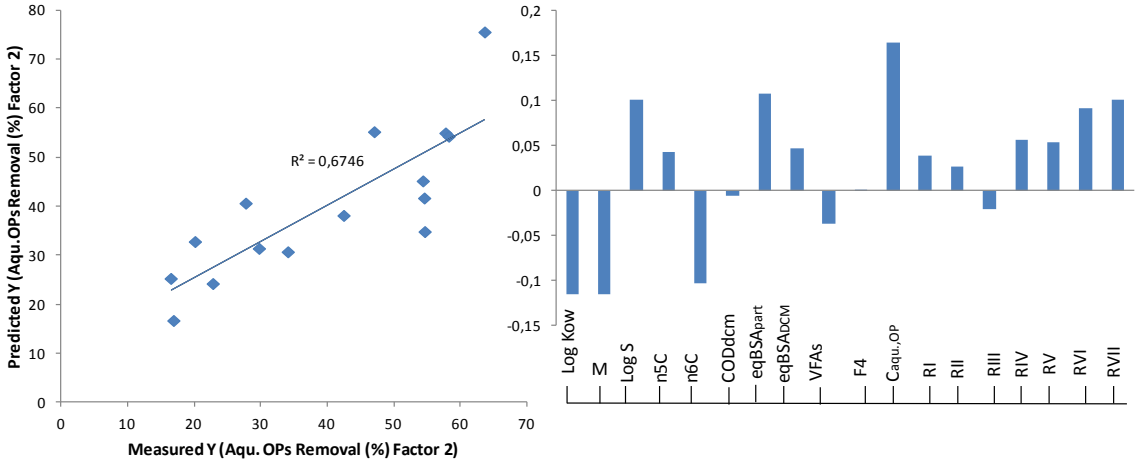

Figure VI-8: Aqueous OPs removal predictive model of 5 PAHs (Fluorene to Pyrene). Left: Measured OPs removals versus predicted OPs removals. Cross-validation factor 2. Right: Weighted regression coefficient.

However, the low R^2 and the low accuracy (15%) suggest that more explicative variables or more sludge matrices are necessary to construct a more accurate model. Additionally, no enough variables that explain the OPs transfer from the particles to the aqueous phase were considered in the model, which could explain its low accuracy.

VI.7. OPs total removal predictive model

In order to predict the OPs removals in sewage sludge under anaerobic conditions a predictive PLS model was constructed from the initial matrix characteristics. Unlike the predictive

model showed in the section IV.4.7., this model was constructed with a more detailed initial characterization and considering the initial OPs distribution among the physical compartments. X block and Y block variables are listed in the Table VI-5. Chemical initial characterization was not considered because of their low influence in the model in contrast with fluorescence intensities and OPs distribution.

Table VI-6: PLS variables of OPs total removals predictive model. X block: explicative variables. Y block: measured OPs removals of the 13 PAHs in each sludge mixture.

Sludge Matrix	**X block**			**Y block**
	OPs characteristics	Matrix initial characteristics	Initial OPs repartition ($\mu g_{OP}/g_{TOC}$)	
HLSS	Log Kow	RI	$C_{OP,free}$	
HLSS-1kDa	M	RII	$C_{OP,DCM}$	
LLSS	Log S	RIII		
	n5C	RIV		Total OPs removals (%)
	n6C	RV		
		RVI		
		RVII		

The equation 7 obtained for the prediction of the total OPs removals is the following:

$$(eq.7)\quad OP_{r\,total} = 3.28 - 0.17LogK_{OW} + 0.05M + 0.14LogS + 0.079n5C + 0.022n6C + 0.74C_{OP,free} + 0.37C_{OP,DCM} + 0.028RI + 0.11RII + 0.4RIII - 0.087RIV - 0.069RV - 0.36RVI - 0.44RVII$$

The R^2 coefficient is equal to 0.8 (cross-validation). The RMSEC/MAX value is equal to 3.69/32.3=0.11, indicating an accuracy of 11% of the predictive model.

The Figure VI-9 shows the weighted regression coefficients of the total OPs removal predictive model. The parameters with the higher influence are $C_{OP,free}$, $C_{OP,DCM}$, RIII, RVI and RVII.

The respective positive influence of $C_{OP,free}$ and $C_{OP,DCM}$ that represent the bioavailability influence confirm the tendency showed in the section VI.3 identifying the aqueous compartment as the bioavailable one.

Regarding the influence of the fluorescence spectra RIII, RVI and RVII in the case of OPs removals, it may be linked to the cometabolism influence. The positive influence of RIII shows that the proteins-like substances, indicators of more biodegradable matters (Baker, 2001), may have an important cometabolism influence on the OPs removals. In contrast RVI and RVII fluorescence regions, indicators of more recalcitrant matters (melanoidins-like, ligno-cellulose-like and humic acid-like), have a negative effect on the total OPs removals, may be because they generate a lower cometabolic flux.

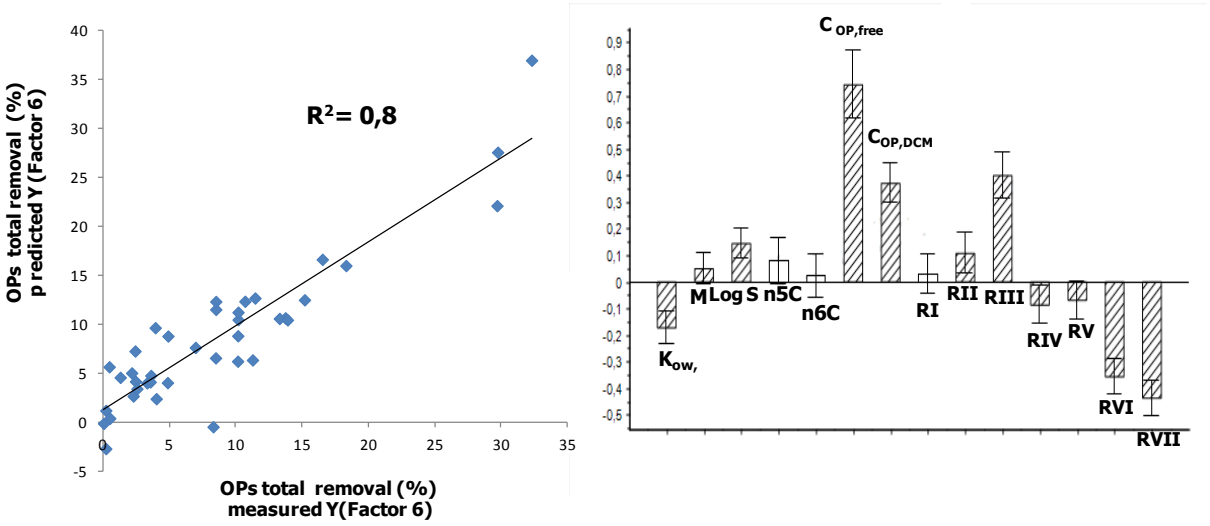

Figure VI-9: Total OPs removals predictive model. Left: Measured OPs removals versus predicted OPs removals. Cross-validation factor 6. Right: Weighted regression coefficient.

If this predictive model is compared to the first model presented in the section IV.4.7., it is possible to observe that this is an improved predictive model of the total OPs removals (R^2 0.8 against 0.78 and lower RMSEC/MAX). Additionally, in the first predictive model, it was not possible to identify important positive parameters that predict the total OPs removal in contrast with this new model that identifies two important predictive parameters: $C_{OP,aqu}$ and RIII.

VI.8. Chapter conclusion

3 D fluorescence coupled to SPME technique allowed to get a more detailed PLS model that help to explain the OP-organic matrix interaction linking the functional characterization of the aqueous fraction with the determination of the K_{part} and K_{DOC} values. However, this functional characterization of the aqueous phase was not enough to explain the interactions between the high molecular weights PAHs and the particulate fraction, suggesting that the aqueous compartment is not representative of the complex interactions between particules and OPs and that it would be necessary to get a more detailed characterization of this particulate fraction.

Additionally, filtration/ultrafiltration and AF^4 separations techniques showed, on the one hand, that within the same aqueous sample it is possible to find different OPs affinities and that these affinities increase with the colloids size, and on the other hand, that it is feasible to characterize the aqueous sludge fraction according to its different colloids size, obtaining different profiles among the sludge samples. Additionally, it was possible to calibrate the AF^4 technique to separate aqueous sewage sludge samples, this technique being mainly used to characterize low loaded organic matter sample.

Explicative and predictive PLS models of the total OPs removal were constructed. The explicative model confirmed that the cometabolism and the bioavailability govern the OPs removals, showing the aqueous compartment as the bioavailable one. The predictive PLS model was constructed from a more detailed initial sludge characterization and taking into account the bioavailability influence. Bioavailable and cometabolic parameters were identified as positive parameters influencing the OPs removals, resulting in a more accurate predictive model than the one presented in the chapter IV.

VII. CONCLUSIONS AND PERSPECTIVES

The objective of this work was to identify the key driving mechanisms of the OPs bioavailability in order to optimize their removal under anaerobic conditions. The global strategy is based on the following cascade hypothesis: various sludges in composition imply various OPs affinities for the matter compartments and thus various distribution/sorption/bioavailability and thus various removals. The strategy consists in a deep characterization of the sludge matter combined to (1) the measurement of the OPs distribution in the sludge compartments and (2) the measurement of OPs removals for various types of sludge. First of all, the results demonstrate that partial removal of OPs present in sludge matrices is possible under anaerobic conditions whatever the two tested configurations, continuous and batch. However, the continuous reactors give the highest removals but in this configuration it is difficult to identify the mechanisms that influence the OPs removals. Indeed, the removal of PAHs, NP and PCBs under continuous anaerobic digestion varies greatly as a function of feed sludge characteristics. **Depending on the feeding, greater or lesser removal might be explained either by variations in cometabolism or by different levels of bioavailability.** This suggests that none of the mechanisms can be identified as the absolute limiting factor of the OPs removals. These results suggest that (i) it would be interesting to work at constant metabolic flux with a high biomass concentration and measure an initial OP removal rate according to various types of sludge like in batch configuration and (ii) a full characterization of the sludge matrix is necessary to better understand the role of the OP-matrix interactions on the OPs removals.

Batch kinetics, realized on three various sludge samples, show that (i) **OPs removals are coupled to the first steps of the anaerobic digestion,** and (ii) jointly to these removals, OPs transfers occur from the particles to the aqueous compartment as shown by the evolution of the OPs in the various compartments by SPME. Indeed, this technique was successfully applied on the aqueous fraction of sludge matrix to quantify the free and aqueous concentrations of PAHs, i.e. to get the PAHs distribution in the three (free, DCM and particules) compartments. The results show that the free and DCM compartments represent less than 2% of the total concentration but this distribution is different from one sludge sample to another. Moreover, the kinetics in each compartments are different. Indeed, **the OPs are simultaneously removed from the three physical compartments (free, DCM and particles).** It is also highlighted the importance of the DCM fraction on the removal of the high molecular weight PAHs which is directly linked with the initial $C_{OP,DCM}$. However, even if the highest initial $C_{OP,DCM}$ is linked to the highest $C_{OP,DCM}$ removal, the total OPs removal is not only governed by this DCM compartment but is also driven by the cometabolism flux generated by the global matrix properties and by OP transfer phenomena from particulate to aqueous compartments.

In order to study the OP-organic matrix interactions, K_{DOC} and K_{part} partition coefficients, i.e. OPs affinities for respectively the DCM and particulate compartments, were calculated using the SPME results. These coefficients are well correlated with the OPs Kow but are different from one sludge to another. They were thus used to construct an explicative and predictive model of these OP-organic matrix interactions with partial least square regression (PLS) using

a functional characterization by 3D fluorescence of the aqueous fraction. It was found that **the humic acid-like and the melanoidins-like have a great role in the OP-organic matrix interactions in the aqueous phase.** The aqueous 3D fluorescence characterization was also used to explain and predict the OPs affinity to the particulate compartment**. For this compartment, additionally to the humic acid-like, the complex proteins govern the OPs-matrix interactions.** However, this functional characterization of the aqueous phase is not enough to explain the interactions between the high molecular weights PAHs and the particulate fraction, making necessary a more detailed characterization of the particulate fraction to determine which type of particulate organic matter interacts with OPs. However, the K_{DOC} model predicts with a good accuracy the OPs affinity for the aqueous compartment using a simple, non-destructive, functional characterization method.

Finally, explanatory and predictive PLS models of total OPs removals were constructed. It was concluded that **OPs removals are favored by all cometabolic parameters (substrates removals) jointly to the aqueous OPs concentration which tends to confirm that this compartment corresponds to the bioavailable one.** The predictive PLS model was constructed from a more detailed initial characterization and taking into account the bioavailability influence. **The initial OPs distributions (free andDCM) were identified as the most important variables that predict the total OPs removals**, with a positive influence of free and DCM concentrations. **From the sludge characterization, the protein-like, humic acid-like and melanoidins-like presented the higher influences.** These matrix parameters may influence either the bioavailability through various OPs affinities to matrix compartments or indirectly the cometabolism flux.

In general, two main parameters participate in the **OP-organic matrix interactions**: the nature and the size of the molecules. This last one was evidenced by the filtration/ultrafiltration-SPME analysis. It was shown that big size colloids contribute mainly in the OPs sorption in the aqueous compartment. With respect to the nature of the molecules, **three functional groups play an important role on the OP-organic matrix interactions as well as on the cometabolic influence: protein-like, humic acid-like and melanoidins-like** (Figure VII-1)**.** Moreover, these OP-organic matrix interactions govern mainly the removals of the high molecular weight PAHs demonstrating that the bioavailability of these compounds depends directly of their interactions with the organic matter (metabolic substrate). However, **the OPs transfer from the particles to the aqueous compartment is identified as the main limiting factor of the total OPs removals which depends mainly on the cometabolic flux from the particulate fraction and the sorption/desorption phenomena.**

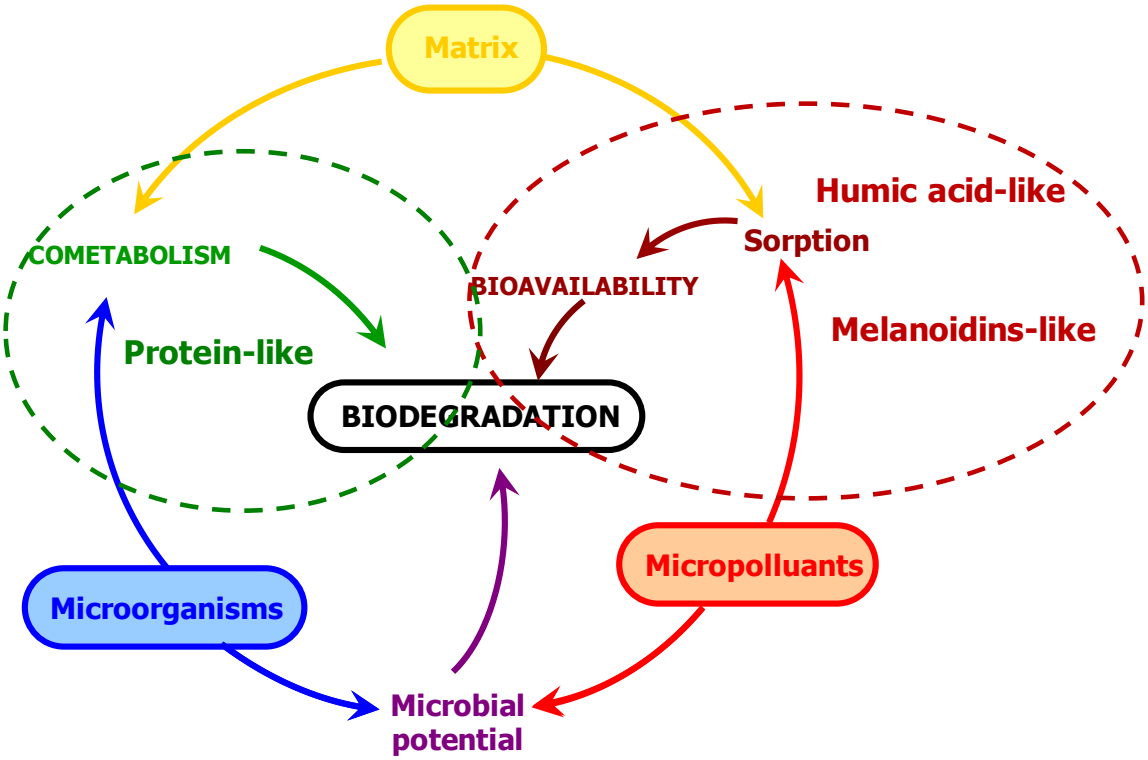

Figure VII-1: Functional groups involved on the interactions between the three actors: OP/matrix/microorganisms.

Additionally, in this study, two innovating techniques were tested that have not been used previously in sewage sludge: SPME and AF^4. Indeed, these two techniques are usually applied to low load organic aqueous samples like rivers and lakes. They were successfully applied to our aqueous samples with a high concentration of organic matter with, in the case of SPME, the measurement of $C_{OP,free}$ and $C_{OP,free}$ and in the case of AF^4, the possible separation of the colloids according to their size. Regarding the AF^4, further methodology development and combination are necessary to extract more information. Indeed, it would be interesting to analyze each independent colloids group in order to identify its composition, functional groups (3D fluorescence) and $C_{OP,free}$ and $C_{OP,DCM}$ by SPME. In the same way, it would be important to link the filtration/ultrafiltration-SPME analysis with a functional characterization of the fraction in order to know in detail all OP-organic matrix interactions.

This study contributes to better understand the OPs distribution among the sludge compartments and its role in the fate and removal of the compounds, to predict this distribution through matter functional characterization and to propose strategies in order to optimize the OPs removals under anaerobic conditions.

VIII. Bibliography

Abad E, Martinez K, Planas C, Palacios O, Caixach J, Rivera J. 2005. Priority organic pollutant assessment of sludges for agricultural purposes. Chemosphere 61(9):1358-1369.

Ahel M, Giger W, Koch M. 1994. Behavior of Alkylphenol Polyethoxylate Surfactants in the Aquatic Environment .1. Occurrence and Transformation in Sewage-Treatment. Water Research 28(5):1131-1142.

Ahel M, Senta I, Terzic S. 2009. Occurrence and Behavior of Polar Organic Contaminants in Croatian Municipal Wastewaters. Progress in Environmental Science and Technology, Vol Ii, Pts a and B. Beijing: SCIENCE PRESS BEIJING. p 1104-1112.

Akkanen J, Lyytikainen M, Tuikka A, Kukkonen JVK. 2005. Dissolved organic matter in pore water of freshwater sediments: Effects of separation procedure on quantity, quality and functionality. Chemosphere 60(11):1608-1615.

Alasonati E, Benincasa MA, Slaveykova VI. 2007. Asymmetrical flow field-flow fractionation coupled to multiangle laser light scattering detector: Optimization of crossfIlow rate, carrier characteristics, and injected mass in alginate separation. Journal of Separation Science 30(14):2332-2340.

Andreadakis AD. 1993. PHYSICAL AND CHEMICAL-PROPERTIES OF ACTIVATED-SLUDGE FLOC. Water Research 27(12):1707-1714.

Aparicio I, Santos JL, Alonso E. 2007. Simultaneous sonication-assisted extraction, and determination by gas chromatography-mass spectrometry, of di-(2-ethylhexyl)phthalate, nonylphenol, nonylphenol ethoxylates and polychlorinated biphenyls in sludge from wastewater treatment plants. Analytica Chimica Acta 584(2):455-461.

Aparicio I, Santos JL, Alonso E. 2009. Limitation of the concentration of organic pollutants in sewage sludge for agricultural purposes: A case study in South Spain. Waste Management 29(5):1747-1753.

Arthur CL, Pawliszyn J. 1990. SOLID-PHASE MICROEXTRACTION WITH THERMAL-DESORPTION USING FUSED-SILICA OPTICAL FIBERS. Analytical Chemistry 62(19):2145-2148.

Artola-Garicano E, Borkent I, Hermens JLM, Vaes WHJ. 2003. Removal of two polycyclic musks in sewage treatment plants: Freely dissolved and total concentrations. Environmental Science & Technology 37(14):3111-3116.

Augsten C, Mader K. 2008. Characterizing molar mass distributions and molecule structures of different chitosans using asymmetrical flow field-flow fractionation combined with multi-angle light scattering. International Journal of Pharmaceutics 351(1-2):23-30.

Avella-Vasquez A C. 2010. Substances polymeriques extracellulaires dans le procedes de traitement des eaux usees. l'INPL, RP2E, Laboratoire environnement et minéralurgie.

Baker A. 2001. Fluorescence excitation-emission matrix characterization of some sewage-impacted rivers. Environmental Science & Technology 35(5):948-953.

Bamforth SM, Singleton I. 2005. Bioremediation of polycyclic aromatic hydrocarbons: current knowledge and future directions. Journal of Chemical Technology and Biotechnology 80(7):723-736.

Barret M, Carrere H, Delgadillo L, Patureau D. 2010a. PAH fate during the anaerobic digestion of contaminated sludge: Do bioavailability and/or cometabolism limit their biodegradation? Water Research 44(13):3797-3806.

Barret M, Carrere H, Latrille E, Wisniewski C, Patureau D. 2010b. Micropollutant and Sludge Characterization for Modeling Sorption Equilibria. Environmental Science & Technology 44(3):1100-1106.

Barret M, Patureau D, Latrille E, Carrere H. 2010c. A three-compartment model for micropollutants sorption in sludge: Methodological approach and insights. Water Research 44(2):616-624.

Batstone DJ, Keller J, Angelidaki I, Kalyuzhnyi SV, Pavlostathis SG, Rozzi A, Sanders WTM, Siegrist H, Vavilin VA. 2002. The IWA Anaerobic Digestion Model No 1 (ADM1). Water Science and Technology 45(10):65-73.

Benabdallah El-Hadj T, Dosta J, Torres R, Mata-Alvarez J. 2007. PCB and AOX removal in mesophilic and thermophilic sewage sludge digestion. Biochemical Engineering Journal 36(3):281-287.

Bernal-Martinez A, Carrere H, Patureau D, Delgenes JP. 2005. Combining anaerobic digestion and ozonation to remove PAH from urban sludge. Process Biochemistry 40(10):3244-3250.

Bernal-Martinez A, Patureau D, Delgenes JP, Carrere H. 2009. Removal of polycyclic aromatic hydrocarbons (PAH) during anaerobic digestion with recirculation of ozonated digested sludge. Journal of Hazardous Materials 162(2-3):1145-1150.

Blanchard M, Teil MJ, Ollivon D, Legenti L, Chevreuil M. 2004. Polycyclic aromatic hydrocarbons and polychlorobiphenyls in wastewaters and sewage sludges from the Paris area (France). Environmental Research 95(2):184-197.

Bodzek D, Janoszka B. 1999. Comparison of polycyclic aromatic compounds and heavy metals contents in sewage sludges from industrialized and non-industrialized region. Water Air and Soil Pollution 111(1-4):359-369.

Buffle J, Wilkinson KJ, Stoll S, Filella M, Zhang JW. 1998. A generalized description of aquatic colloidal interactions: The three-colloidal component approach. Environmental Science & Technology 32(19):2887-2899.

Carlstrom CJ, Tuovinen OH. 2003. Mineralization of phenanthrene and fluoranthene in yardwaste compost. Environmental Pollution 124(1):81-91.

Chang BV, Chang IT, Yuan SY. 2008. Biodegradation of phenanthrene and pyrene from mangrove sediment in subtropical Taiwan. Journal of Environmental Science and Health Part a-Toxic/Hazardous Substances & Environmental Engineering 43(3):233-238.

Chang BV, Chang SW, Yuan SY. 2003. Anaerobic degradation of polycyclic aromatic hydrocarbons in sludge. Advances in Environmental Research 7(3):623-628.

Chang BV, Chiang F, Yuan SY. 2005a. Biodegradation of nonylphenol in sewage sludge. Chemosphere 60(11):1652-1659.

Chang BV, Chiang F, Yuan SY. 2005b. Anaerobic degradation of nonylphenol in sludge. Chemosphere 59(10):1415-1420.

Chang BV, Yu CH, Yuan SY. 2004. Degradation of nonylphenol by anaerobic microorganisms from river sediment. Chemosphere 55(4):493-500.

Chang W, Um Y, Holoman TRP. 2006. Polycyclic aromatic hydrocarbon (PAH) degradation coupled to methanogenesis. Biotechnology Letters 28(6):425-430.

Chen RF, Jiang Y, Zhao M. 2000. Solid-phase fluorescence determination of chlorins in marine sediments. Organic Geochemistry 31(12):1755-1763.

Chen W, Westerhoff P, Leenheer JA, Booksh K. 2003. Fluorescence excitation - Emission matrix regional integration to quantify spectra for dissolved organic matter. Environmental Science & Technology 37(24):5701-5710.

Christensen N, Batstone DJ, He Z, Angelidaki I, Schmidt JE. 2004. Removal of polycyclic aromatic hydrocarbons (PAHs) from sewage sludge by anaerobic degradation. Water Science and Technology 50(9):237-244.

Clara M, Strenn B, Gans O, Martinez E, Kreuzinger N, Kroiss H. 2005. Removal of selected pharmaceuticals, fragrances and endocrine disrupting compounds in a membrane bioreactor and conventional wastewater treatment plants. Water Research 39(19):4797-4807.

Cornelissen G, Rigterink H, Ferdinandy MMA, Van Noort PCM. 1998. Rapidly desorbing fractions of PAHs in contaminated sediments as a predictor of the extent of bioremediation. Environmental Science & Technology 32(7):966-970.

Corvini PFX, Schaffer A, Schlosser D. 2006. Microbial degradation of nonylphenol and other alkylphenols - our evolving view. Applied Microbiology and Biotechnology 72(2):223-243.

Criddle CS. 1993. THE KINETICS OF COMETABOLISM. Biotechnology and Bioengineering 41(11):1048-1056.

Cuypers C, Pancras T, Grotenhuis T, Rulkens W. 2002. The estimation of PAH bioavailability in contaminated sediments using hydroxypropyl-beta-cyclodextrin and Triton X-100 extraction techniques. Chemosphere 46(8):1235-1245.

Dean JR, Scott WC. 2004. Recent developments in assessing the bioavailability of persistent organic pollutants in the environment. Trac-Trends in Analytical Chemistry 23(9):609-618.

Degrémont, 1989. Mémento technique de l'eau. Tomme1 Rueil-Malmaison: Degrémont

Delbes C, Moletta R, Godon JJ. 2000. Monitoring of activity dynamics of an anaerobic digester bacterial community using 16S rRNA polymerase chain reaction - single-strand conformation polymorphism analysis. Environmental Microbiology 2(5):506-515.

Denys S. 2011. Vers une intégration de la biodisponibilité dans l'estimation des expositions humaines aux contaminants des sols. l'INPL, RP2E.

Dionisi D, Bertin L, Bornoroni L, Capodicasa S, Papini MP, Fava F. 2006. Removal of organic xenobiotics in activated sludges under aerobic conditions and anaerobic digestion of the adsorbed species. Journal of Chemical Technology and Biotechnology 81(9):1496-1505.

Dolfing J, Xu A, Gray ND, Larter SR, Head IM. 2009. Thermodynamic constraints on methanogenic PAH degradation. Geochimica Et Cosmochimica Acta 73(13):A298-A298.

Doll TE, Frimmel FH, Kumke MU, Ohlenbusch G. 1999. Interaction between natural organic matter (NOM) and polycyclic aromatic compounds (PAC) - comparison of fluorescence quenching and solid phase micro extraction (SPME). Fresenius Journal of Analytical Chemistry 364(4):313-319.

Dou JF, Liu X, Ding AZ. 2009. Anaerobic degradation of naphthalene by the mixed bacteria under nitrate reducing conditions. Journal of Hazardous Materials 165(1-3):325-331.

Dreywood R. (1946. Qualitative test for carbohydrates material. Industrial and Engineering Chemistry Analytical Edition 18:499.

During RA, Krahe S, Gath S. 2002. Sorption Behavior of nonylphenol in terrestrial soils. Environmental Science & Technology 36(19):4052-4057.

Ekelund R, Bergman A, Granmo A, Berggren M. 1990. BIOACCUMULATION OF 4-NONYLPHENOL IN MARINE ANIMALS - A REEVALUATION. Environmental Pollution 64(2):107-120.

El-Hadj TB, Dosta J, Mata-Alvarez J. 2006. Biodegradation of PAH and DEHP micro-pollutants in mesophilic and thermophilic anaerobic sewage sludge digestion. Water Science and Technology 53(8):99-107.

Eriksson M, Sodersten E, Yu ZT, Dalhammar G, Mohn WW. 2003. Degradation of polycyclic aromatic hydrocarbons at low temperature under aerobic and nitrate-reducing conditions in enrichment cultures from northern soils. Applied and Environmental Microbiology 69(1):275-284.

Fountoulakis M, Drillia P, Pakou C, Kampioti A, Stamatelatou K, Lyberatos G. 2005. Analysis of nonylphenol and nonylphenol ethoxylates in sewage sludge by high performance liquid chromatography following microwave-assisted extraction. Journal of Chromatography A 1089(1-2):45-51.

Fountoulakis MS, Stamatelatou K, Batstone DJ, Lyberatos G. 2006. Simulation of DEHP biodegradation and sorption during the anaerobic digestion of secondary sludge. Water Science and Technology 54(4):119-128.

Frolund B, Palmgren R, Keiding K, Nielsen PH. 1996. Extraction of extracellular polymers from activated sludge using a cation exchange resin. Water Research 30(8):1749-1758.

Fuchedzhieva N, Karakashev D, Angelidaki I. 2008. Anaerobic biodegradation of fluoranthene under methanogenic conditions in presence of surface-active compounds. Journal of Hazardous Materials 153(1-2):123-127.

Gabriel FLP, Heidlberger A, Rentsch D, Giger W, Guenther K, Kohler HPE. 2005. A novel metabolic pathway for degradation of 4-nonylphenol environmental contaminants by Sphingomonas xenophaga Bayram - ipso-hydroxylation and intramolecular rearrangement*. Journal of Biological Chemistry 280(16):15526-15533.

Galushko A, Minz D, Schink B, Widdel F. 1999. Anaerobic degradation of naphthalene by a pure culture of a novel type of marine sulphate-reducing bacterium. Environmental Microbiology 1(5):415-420.

Ghasemi Y, Rasoul-Amini S, Fotooh-Abadi E. The Biotransformation, Biodegradation, and Bioremediation of Organic Compounds by Microalgae. Journal of Phycology 47(5):969-980.

Gibson J, Harwood CS. 2002. Metabolic diversity in aromatic compound utilization by anaerobic microbes. Annual Review of Microbiology 56:345-369.

Gibson RW, Wang MJ, Padgett E, Lopez-Real JM, Beck AJ. 2007. Impact of drying and composting procedures on the concentrations of 4-nonylphenols, di-(2-ethylhexyl)phthalate and polychlorinated biphenyls in anaerobically digested sewage sludge. Chemosphere 68(7):1352-1358.

Giger W, Brunner PH, Schaffner C. 1984. 4-Nonylphenol in Sewage-Sludge - Accumulation of Toxic Metabolites from Nonionic Surfactants. Science 225(4662):623-625.

Haitzer M, Hoss S, Traunspurger W, Steinberg C. 1998. Effects of dissolved organic matter (DOM) on the bioconcentration of organic chemicals in aquatic organisms - A review. Chemosphere 37(7):1335-1362.

Hawthorne SB, Grabanski CB, Miller DJ, Kreitinger JP. 2005. Solid-phase microextraction measurement of parent and alkyl polycyclic aromatic hydrocarbons in milliliter sediment pore water samples and determination of K-DOC values. Environmental Science & Technology 39(8):2795-2803.

Hudson N, Baker A, Reynolds D. 2007. Fluorescence analysis of dissolved organic matter in natural, waste and polluted waters - A review. River Research and Applications 23(6):631-649.

Jarde E, Mansuy L, Faure P. 2003. Characterization of the macromolecular organic content of sewage sludges by thermally assisted hydrolysis and methylation-gas chromatography-mass spectrometer (THM-GC/MS). Journal of Analytical and Applied Pyrolysis 68-9:331-350.

Jones DM, Head IM, Gray ND, Adams JJ, Rowan AK, Aitken CM, Bennett B, Huang H, Brown A, Bowler BFJ and others. 2008. Crude-oil biodegradation via methanogenesis in subsurface petroleum reservoirs. Nature 451(7175):176-U6.

Jorgensen A, Giessing AMB, Rasmussen LJ, Andersen O. 2008. Biotransformation of polycyclic aromatic hydrocarbons in marine polychaetes. Marine Environmental Research 65(2):171-186.

Katsoyiannis A, Samara C. 2004. Persistent organic pollutants (POPS) in the sewage treatment plant of Thessaloniki, northern Greece: occurrence and removal. Water Research 38(11):2685-2698.

Kavlock RJ, Daston GP, DeRosa C, FennerCrisp P, Gray LE, Kaattari S, Lucier G, Luster M, Mac MJ, Maczka C and others. 1996. Research needs for the risk assessment of health and environmental effects of endocrine disruptors: A report of the US EPA-sponsored workshop. Environmental Health Perspectives 104:715-740.

Kawasaki N, Araki M, Nakamura T, Tanada S. 2001. Inclusion behavior of 4-nonylphenol into cyclodextrin derivatives. Journal of Colloid and Interface Science 238(1):215-218.

Kocamemi BA, Cecen F. 2010. Cometabolic degradation and inhibition kinetics of 1,2-dichloroethane (1,2-DCA) in suspended-growth nitrifying systems. Environmental Technology 31(3):295-305.

Kohli J, Lee HB, Peart TE. 2006. Organic contaminants in Canadian municipal sewage sludge. Part II. Persistent chlorinated compounds and polycyclic aromatic hydrocarbons. Water Quality Research Journal of Canada 41(1):47-55.

Kukkonen J, McCarthy JF, Oikari A. 1990. BINDING AND BIOAVAILABILITY OF ORGANIC MICROPOLLUTANTS IN NATURAL-WATERS - EFFECT OF THE QUALITY AND THE QUANTITY OF DISSOLVED ORGANIC-CARBON. Abstracts of Papers of the American Chemical Society 199:177-ENVR.

Larsen SB, Karakashev D, Angelidaki I, Schmidt JE. 2009. Ex-situ bioremediation of polycyclic aromatic hydrocarbons in sewage sludge. Journal of Hazardous Materials 164(2-3):1568-1572.

Lashermes G, Barriuso E, Le Villio-Poitrenaud M, Houot S. 2012. Composting in small laboratory pilots: Performance and reproducibility. Waste Management 32(2):271-277.

Lashermes G, Houot S, Barriuso E. 2010. Sorption and mineralization of organic pollutants during different stages of composting. Chemosphere 79(4):455-462.

Laspidou CS, Rittmann BE. 2002. A unified theory for extracellular polymeric substances, soluble microbial products, and active and inert biomass. Water Research 36(11):2711-2720.

Lead JR, Wilkinson KJ. 2006. Aquatic colloids and nanoparticles: Current knowledge and future trends. Environmental Chemistry 3(3):159-171.

Lee DY, Farmer WJ. 1989. DISSOLVED ORGANIC-MATTER INTERACTION WITH NAPROPAMIDE AND 4 OTHER NONIONIC PESTICIDES. Journal of Environmental Quality 18(4):468-474.

Lehto KM, Vuorimaa E, Lemmetyinen H. 2000. Photolysis of polycyclic aromatic hydrocarbons (PAHs) in dilute aqueous solutions detected by fluorescence. Journal of Photochemistry and Photobiology a-Chemistry 136(1-2):53-60.
Lei L, Khodadoust AP, Suidan MT, Tabak HH. 2005. Biodegradation of sediment-bound PAHs in field contaminated sediment. Water Research 39(2-3):349-361.
Leutwein C, Heider J. 1999. Anaerobic toluene-catabolic pathway in denitrifying Thauera aromatica: activation and beta-oxidation of the first intermediate, (R)-(+)-benzylsuccinate. Microbiology-Sgm 145:3265-3271.
Liu HC, Hwu CS, Chu KC, Lu CJ. 2010. Estimation of bioavailability and potential risks of naphthalene in soils with solid phase microextraction. World Journal of Microbiology & Biotechnology 26(7):1311-1316.
Liu HC, Hwu CS, Hung JM, Lai HY, Chang HY, Lu CJ. 2011. Reliability of solid phase microextraction in estimating bioavailability of pyrene in soil. Journal of Environmental Biology 32(3):319-323.
Lowry OH, Rosenbrough NJ, Fan AL, Randall R. 1951. Protein measurement with the folin phenol reagent. Journal of Biological Chemestry 193:265-271.
Lu XY, Zhang T, Fang HHP. Bacteria-mediated PAH degradation in soil and sediment. Applied Microbiology and Biotechnology 89(5):1357-1371.
Lu XY, Zhang T, Fang HHP. 2011. Bacteria-mediated PAH degradation in soil and sediment. Applied Microbiology and Biotechnology 89(5):1357-1371.
Lucio M, Schmitt-Kopplin P. 2006. Modelling the binding of triazine herbicides to humic substances using capillary electrophoresis. Environmental Chemistry Letters 4(1):15-21.
Manoli E, Samara C. 1999. Occurrence and mass balance of polycyclic aromatic hydrocarbons in the Thessaloniki sewage treatment plant. Journal of Environmental Quality 28(1):176-187.
Metcalf and Eddy. 1991. Wastewater engineering : treatment, disposal, and reuse. New York : McGraw-Hill.
McCarthy JF, Jimenez BD. 1985. INTERACTIONS BETWEEN POLYCYCLIC AROMATIC-HYDROCARBONS AND DISSOLVED HUMIC MATERIAL - BINDING AND DISSOCIATION. Environmental Science & Technology 19(11):1072-1076.
McCarthy JF, Zachara JM. 1989. SUBSURFACE TRANSPORT OF CONTAMINANTS - MOBILE COLLOIDS IN THE SUBSURFACE ENVIRONMENT MAY ALTER THE TRANSPORT OF CONTAMINANTS. Environmental Science & Technology 23(5):496-502.
McNally DL, Mihelcic JR, Lueking DR. 1998. Biodegradation of three- and four-ring polycyclic aromatic hydrocarbons under aerobic and denitrifying conditions. Environmental Science & Technology 32(17):2633-2639.
Miquel Becker E, Christensen J, Frederiksen CS, Haugaard VK. 2003. Front-face fluorescence spectroscopy and chemometrics in analysis of yogurt: rapid analysis of riboflavin. Journal of dairy science 86(8):2508-15.
Muller M, Milori D, Deleris S, Steyer JP, Dudal Y. 2011. Solid-phase fluorescence spectroscopy to characterize organic wastes. Waste Management 31(9-10):1916-1923.
Musat F, Galushko A, Jacob J, Widdel F, Kube M, Reinhardt R, Wilkes H, Schink B, Rabus R. 2009. Anaerobic degradation of naphthalene and 2-methylnaphthalene by strains of marine sulfate-reducing bacteria. Environmental Microbiology 11(1):209-219.
Natarajan MR, Wu WM, Sanford R, Jain MK. 1999. Degradation of biphenyl by methanogenic microbial consortium. Biotechnology Letters 21(9):741-745.

Nielsen PH, Thomsen TR, Nielsen JL. 2004. Bacterial composition of activated sludge - importance for floc and sludge properties. Water Science and Technology 49(10):51-58.

Northcott GL, Jones KC. 2001. Partitioning, extractability, and formation of nonextractable PAH residues in soil. 1. Compound differences in aging and sequestration. Environmental Science & Technology 35(6):1103-1110.

Pakou C, Kornaros M, Stamatelatou K, Lyberatos G. 2009. On the fate of LAS, NPEOs and DEHP in municipal sewage sludge during composting. Bioresource Technology 100(4):1634-1642.

Pan B, Ghosh S, Xing BS. 2008. Dissolved organic matter conformation and its interaction with pyrene as affected by water chemistry and concentration. Environmental Science & Technology 42(5):1594-1599.

Pan YL, Pinnick RG, Hill SC, Rosen JM, Chang RK. 2007. Single-particle laser-induced-fluorescence spectra of biological and other organic-carbon aerosols in the atmosphere: Measurements at New Haven, Connecticut, and Las Cruces, New Mexico. Journal of Geophysical Research-Atmospheres 112(D24).

Patureau D, Delgenes N, Delgenes JP. 2008. Impact of sewage sludge treatment processes on the removal of the endocrine disrupters nonylphenol ethoxylates. Chemosphere 72(4):586-591.

Patureau D, Trably E. 2006. Impact of anaerobic and aerobic processes on PolyChloroBiphenyl removal in contaminated sewage sludge. Biodegradation 17(1):9-17.

Perminova IV, Grechishcheva NY, Kovalevskii DV, Kudryavtsev AV, Petrosyan VS, Matorin DN. 2001. Quantification and prediction of the detoxifying properties of humic substances related to their chemical binding to polycyclic aromatic hydrocarbons. Environmental Science & Technology 35(19):3841-3848.

Perminova IV, Grechishcheva NY, Petrosyan VS. 1999. Relationships between structure and binding affinity of humic substances for polycyclic aromatic hydrocarbons: Relevance of molecular descriptors. Environmental Science & Technology 33(21):3781-3787.

Pieper DH, Seeger M. 2008. Bacterial metabolism of polychlorinated biphenyls. Journal of Molecular Microbiology and Biotechnology 15(2-3):121-138.

Poerschmann J, Kopinke FD, Pawliszyn J. 1997. Solid phase microextraction to study the sorption of organotin compounds onto particulate and dissolved humic organic matter. Environmental Science & Technology 31(12):3629-3636.

Prestel H, Schott L, Niessner R, Panne U. 2005. Characterization of sewage plant hydrocolloids using asymmetrical flow field-flow fractionation and ICP-mass spectrometry. Water Research 39(15):3541-3552.

Quantin C, Joner EJ, Portal JM, Berthelin J. 2005. PAH dissipation in a contaminated river sediment under oxic and anoxic conditions. Environmental Pollution 134(2):315-322.

Ras M, Girbal-Neuhauser E, Paul E, Lefebvre D. 2008. A high yield multi-method extraction protocol for protein quantification in activated sludge. Bioresource Technology 99(16):7464-7471.

Reid BJ, Stokes JD, Jones KC, Semple KT. 2000. Nonexhaustive cyclodextrin-based extraction technique for the evaluation of PAH bioavailability. Environmental Science & Technology 34(15):3174-3179.

Riefer P, Klausmeyer T, Schwarzbauer J, Schaffer A, Schmidt B, Corvini PFX. 2011. Rapid incorporation and short-term distribution of a nonylphenol isomer and the herbicide MCPA in soil-derived organo-clay complexes. Environmental Chemistry Letters 9(3):411-415.

Ritchie JD, Perdue EM. 2003. Proton-binding study of standard and reference fulvic acids, humic acids, and natural organic matter. Geochimica Et Cosmochimica Acta 67(1):85-96.

Rockne KJ, Chee-Sanford JC, Sanford RA, Hedlund BP, Staley JT, Strand SE. 2000. Anaerobic naphthalene degradation by microbial pure cultures under nitrate-reducing conditions. Applied and Environmental Microbiology 66(4):1595-1601.

Rockne KJ, Strand SE. 1998. Biodegradation of bicyclic and polycyclic aromatic hydrocarbons in anaerobic enrichments. Environmental Science & Technology 32(24):3962-3967.

Safinowski M, Meckenstock RU. 2006. Methylation is the initial reaction in anaerobic naphthalene degradation by a sulfate-reducing enrichment culture. Environmental Microbiology 8(2):347-352.

Samanta SK, Singh OV, Jain RK. 2002. Polycyclic aromatic hydrocarbons: environmental pollution and bioremediation. Trends in Biotechnology 20(6):243-248.

Schlebaum W, Badora A, Schraa G, Van Riemsdijk WH. 1998. Interactions between a hydrophobic organic chemical and natural organic matter: Equilibrium and kinetic studies. Environmental Science & Technology 32(15):2273-2277.

Semple KT, Doick KJ, Jones KC, Burauel P, Craven A, Harms H. 2004. Defining bioavailability and bioaccessibility of contaminated soil and sediment is complicated. Environmental Science & Technology 38(12):228A-231A.

Semple KT, Doick KJ, Wick LY, Harms H. 2007. Microbial interactions with organic contaminants in soil: Definitions, processes and measurement. Environmental Pollution 150(1):166-176.

Semple KT, Morriss AWJ, Paton GI. 2003. Bioavailability of hydrophobic organic contaminants in soils: fundamental concepts and techniques for analysis. European Journal of Soil Science 54(4):809-818.

Sheng GP, Yu HQ. 2006. Characterization of extracellular polymeric substances of aerobic and anaerobic sludge using three-dimensional excitation and emission matrix fluorescence spectroscopy. Water Research 40(6):1233-1239.

Shuttleworth KL, Cerniglia CE. 1995. ENVIRONMENTAL ASPECTS OF PAH BIODEGRADATION. Applied Biochemistry and Biotechnology 54(1-3):291-302.

Smidt H, de Vos WM. 2004. Anaerobic microbial dehalogenation. Annual Review of Microbiology 58:43-73.

Smith MTE, Smernik RJ, Merrington G, Tibbett M. 2008. Changes in sewage sludge carbon forms along a treatment stream. Chemosphere 72(6):981-985.

Sobeck DC, Higgins MJ. 2002. Examination of three theories for mechanisms of cation-induced bioflocculation. Water Research 36(3):527-538.

Soto AM, Justicia H, Wray JW, Sonnenschein C. 1991. PARA-NONYL-PHENOL - AN ESTROGENIC XENOBIOTIC RELEASED FROM MODIFIED POLYSTYRENE. Environmental Health Perspectives 92:167-173.

Suh YJ, Rousseaux P. 2002. An LCA of alternative wastewater sludge treatment scenarios. Resources Conservation and Recycling 35(3):191-200.

Tay JH, Liu QS, Liu Y. 2001. Microscopic observation of aerobic granulation in sequential aerobic sludge blanket reactor. Journal of Applied Microbiology 91(1):168-175.

Tolls J, Kloeppersams P, Sijm D. 1994. SURFACTANT BIOCONCENTRATION - A CRITICAL-REVIEW. Chemosphere 29(4):693-717.

Trably E, Patureau D. 2006. Successful treatment of low PAH-contaminated sewage sludge in aerobic bioreactors. Environmental Science and Pollution Research 13(3):170-176.

Trably E, Patureau D, Delgenes JP. 2003. Enhancement of polycyclic aromatic hydrocarbons removal during anaerobic treatment of urban sludge. Water Science and Technology 48(4):53-60.

Trably E, Delgenes N, Patureau D, Delgenes JP. 2004. Statistical tool for the optimization of a highly reproductive method for the analysis of polycyclic aromatic hydrocarbons in sludge samples. International Journal of Environmental Analytical Chemistry 84:995-1008.

Urase T, Kikuta T. 2005. Separate estimation of adsorption and degradation of pharmaceutical substances and estrogens in the activated sludge process. Water Research 39(7):1289-1300.

Van Aken B, Correa PA, Schnoor JL. 2010. Phytoremediation of Polychlorinated Biphenyls: New Trends and Promises. Environmental Science & Technology 44(8):2767-2776.

Vasilyeva GK, Strijakova ER. 2007. Bioremediation of soils and sediments contaminated by polychlorinated biphenyls. Microbiology 76(6):639-653.

Weissenfels WD, Beyer M, Klein J. 1990. DEGRADATION OF PHENANTHRENE, FLUORENE AND FLUORANTHENE BY PURE BACTERIAL CULTURES. Applied Microbiology and Biotechnology 32(4):479-484.

Wijayaratne RD, Means JC. 1984. AFFINITY OF HYDROPHOBIC POLLUTANTS FOR NATURAL ESTUARINE COLLOIDS IN AQUATIC ENVIRONMENTS. Environmental Science & Technology 18(2):121-123.

Wijnja H, Pignatello JJ, Malekani K. 2004. Formation of pi-pi complexes between phenanthrene and model pi-acceptor humic subunits. Journal of Environmental Quality 33(1):265-275.

Wilson SC, Jones KC. 1993. BIOREMEDIATION OF SOIL CONTAMINATED WITH POLYNUCLEAR AROMATIC-HYDROCARBONS (PAHS) - A REVIEW. Environmental Pollution 81(3):229-249.

Witte EG, Philipp H, Vereecken H. 1998. Binding of (13)C-labelled 2-aminobenzothiazoles to humic acid as derived from (13)C NMR spectroscopy. Organic Geochemistry 29(5-7):1829-1835.

Worms IAM, Szigeti ZAG, Dubascoux S, Lespes G, Traber J, Sigg L, Slaveykova VI. 2010. Colloidal organic matter from wastewater treatment plant effluents: Characterization and role in metal distribution. Water Research 44(1):340-350.

Yan S, Rodenburg LA, Dachs J, Eisenreich SJ. 2008. Seasonal air-water exchange fluxes of polychlorinated biphenyls in the Hudson River Estuary. Environmental Pollution 152(2):443-451.

Yuan SY, Chang BV. 2007. Anaerobic degradation of five polycyclic aromatic hydrocarbons from river sediment in Taiwan. Journal of Environmental Science and Health Part B-Pesticides Food Contaminants and Agricultural Wastes 42(1):63-69.

Yuan SY, Chang JS, Yen JH, Chang BV. 2001. Biodegradation of phenanthrene in river sediment. Chemosphere 43(3):273-278.

Yuan SY, Wei SH, Chang BV. 2000. Biodegradation of polycyclic aromatic hydrocarbons by a mixed culture. Chemosphere 41(9):1463-1468.

Yuan SY, Yu CH, Chang BV. 2004. Biodegradation of nonylphenol in river sediment. Environmental Pollution 127(3):425-430.

Zhang XM, Young LY. 1997. Carboxylation as an initial reaction in the anaerobic metabolism of naphthalene and phenanthrene by sulfidogenic consortia. Applied and Environmental Microbiology 63(12):4759-4764.

Zhong Y, Luan TG, Wang XW, Lan CY, Tam NFY. 2007. Influence of growth medium on cometabolic degradation of polycyclic aromatic hydrocarbons by Sphingomonas sp strain PheB4. Applied Microbiology and Biotechnology 75(1):175-186.

Appendix A:

X Bolck and Y Block for K_{DOC} PLS Model

	X Block												Y Block
Sludge samples	LogKow	M	logS	n5C	n6C	Fluo 3D RI	Fluo 3D RII	Fluo 3D RIII	Fluo 3D RIV	Fluo 3D RV	Fluo 3D RVI	Fluo 3D RVII	Log Kdcm
HLSS t0	4.18	166	0.301	1	2	704587	1281971	1604343	1051252	859074	452286	88705	
HLSS-1kDa t0	4.18	166	0.301	1	2	354667	643002	779376	715232	561065	368160	74081	2,83
LLSS t0	4.18	166	0.301	1	2	802083	1371549	1386117	1228053	1002895	602396	130381	
HLSS t0	4.18	166	0.301	1	2	126106	255770	269981	287073	229380	137154	34115	1,78
HLSS-1kDa t0	4.18	166	0.301	1	2	41119	51361	68061	58553	50487	33027	6773	1,90
LLSS t0	4.18	166	0.301	1	2	39570	71013	73901	81387	70889	44901	7368	
HLSS t0	4.57	178	0.079	0	3	704587	1281971	1604343	1051252	859074	452286	88705	
HLSS-1kDa t0	4.57	178	0.079	0	3	354667	643002	779376	715232	561065	368160	74081	2,98
LLSS t0	4.57	178	0.079	0	3	802083	1371549	1386117	1228053	1002895	602396	130381	3,34
HLSS t0	4.57	178	0.079	0	3	126106	255770	269981	287073	229380	137154	34115	2,60
HLSS-1kDa t0	4.57	178	0.079	0	3	41119	51361	68061	58553	50487	33027	6773	2,02
LLSS t0	4.57	178	0.079	0	3	39570	71013	73901	81387	70889	44901	7368	1,99
HLSS t0	4.45	178	0.114	0	3	704587	1281971	1604343	1051252	859074	452286	88705	
HLSS-1kDa t0	4.45	178	0.114	0	3	354667	643002	779376	715232	561065	368160	74081	2,43
LLSS t0	4.45	178	0.114	0	3	802083	1371549	1386117	1228053	1002895	602396	130381	3,41
HLSS t0	4.45	178	0.114	0	3	126106	255770	269981	287073	229380	137154	34115	2,57
HLSS-1kDa t0	4.45	178	0.114	0	3	41119	51361	68061	58553	50487	33027	6773	1,74
LLSS t0	4.45	178	0.114	0	3	39570	71013	73901	81387	70889	44901	7368	1,89
HLSS t0	5.1	202	-0.585	1	3	704587	1281971	1604343	1051252	859074	452286	88705	
HLSS-1kDa t0	5.1	202	-0.585	1	3	354667	643002	779376	715232	561065	368160	74081	3,38
LLSS t0	5.1	202	-0.585	1	3	802083	1371549	1386117	1228053	1002895	602396	130381	3,89

HLSS t0	5.1	202	-0.585	1	3	126106	255770	269981	287073	229380	137154	34115	2,97
HLSS-1kDa t0	5.1	202	-0.585	1	3	41119	51361	68061	58553	50487	33027	6773	2,30
LLSS t0	5.1	202	-0.585	1	3	39570	71013	73901	81387	70889	44901	7368	2,27
HLSS t0	5.32	202	-0.886	0	4	704587	1281971	1604343	1051252	859074	452286	88705	2,93
HLSS-1kDa t0	5.32	202	-0.886	0	4	354667	643002	779376	715232	561065	368160	74081	3,47
LLSS t0	5.32	202	-0.886	0	4	802083	1371549	1386117	1228053	1002895	602396	130381	4,04
HLSS t0	5.32	202	-0.886	0	4	126106	255770	269981	287073	229380	137154	34115	3,13
HLSS-1kDa t0	5.32	202	-0.886	0	4	41119	51361	68061	58553	50487	33027	6773	2,42
LLSS t0	5.32	202	-0.886	0	4	39570	71013	73901	81387	70889	44901	7368	2,49
HLSS t0	5.85	228	-1.959	0	4	704587	1281971	1604343	1051252	859074	452286	88705	3,63
HLSS-1kDa t0	5.85	228	-1.959	0	4	354667	643002	779376	715232	561065	368160	74081	3,99
LLSS t0	5.85	228	-1.959	0	4	802083	1371549	1386117	1228053	1002895	602396	130381	4,58
HLSS t0	5.85	228	-1.959	0	4	126106	255770	269981	287073	229380	137154	34115	3,71
HLSS-1kDa t0	5.85	228	-1.959	0	4	41119	51361	68061	58553	50487	33027	6773	2,94
LLSS t0	5.85	228	-1.959	0	4	39570	71013	73901	81387	70889	44901	7368	3,06
HLSS t0	5.89	228	-2.699	0	4	704587	1281971	1604343	1051252	859074	452286	88705	3,90
HLSS-1kDa t0	5.89	228	-2.699	0	4	354667	643002	779376	715232	561065	368160	74081	4,12
LLSS t0	5.89	228	-2.699	0	4	802083	1371549	1386117	1228053	1002895	602396	130381	4,71
HLSS t0	5.89	228	-2.699	0	4	126106	255770	269981	287073	229380	137154	34115	3,84
HLSS-1kDa t0	5.89	228	-2.699	0	4	41119	51361	68061	58553	50487	33027	6773	3,11
LLSS t0	5.89	228	-2.699	0	4	39570	71013	73901	81387	70889	44901	7368	3,24
HLSS t0	6.57	252	-1.921	1	4	704587	1281971	1604343	1051252	859074	452286	88705	4,33
HLSS-1kDa t0	6.57	252	-1.921	1	4	354667	643002	779376	715232	561065	368160	74081	4,48
LLSS t0	6.57	252	-1.921	1	4	802083	1371549	1386117	1228053	1002895	602396	130381	5,10
HLSS t0	6.57	252	-1.921	1	4	126106	255770	269981	287073	229380	137154	34115	4,20
HLSS-1kDa t0	6.57	252	-1.921	1	4	41119	51361	68061	58553	50487	33027	6773	3,43
LLSS t0	6.57	252	-1.921	1	4	39570	71013	73901	81387	70889	44901	7368	3,52
HLSS t0	6.84	252	-3.097	1	4	704587	1281971	1604343	1051252	859074	452286	88705	4,32
HLSS-1kDa t0	6.84	252	-3.097	1	4	354667	643002	779376	715232	561065	368160	74081	4,64

LLSS t0	6.84	252	-3.097	1	4	802083	1371549	1386117	1228053	1002895	602396	130381	5,17
HLSS t0	6.84	252	-3.097	1	4	126106	255770	269981	287073	229380	137154	34115	4,40
HLSS-1kDa t0	6.84	252	-3.097	1	4	41119	51361	68061	58553	50487	33027	6773	3,56
LLSS t0	6.84	252	-3.097	1	4	39570	71013	73901	81387	70889	44901	7368	3,73
HLSS t0	6	252	-2.523	0	5	704587	1281971	1604343	1051252	859074	452286	88705	4,35
HLSS-1kDa t0	6	252	-2.523	0	5	354667	643002	779376	715232	561065	368160	74081	4,46
LLSS t0	6	252	-2.523	0	5	802083	1371549	1386117	1228053	1002895	602396	130381	4,97
HLSS t0	6	252	-2.523	0	5	126106	255770	269981	287073	229380	137154	34115	4,23
HLSS-1kDa t0	6	252	-2.523	0	5	41119	51361	68061	58553	50487	33027	6773	3,32
LLSS t0	6	252	-2.523	0	5	39570	71013	73901	81387	70889	44901	7368	3,66
HLSS t0	6.7	278	-3.301	0	5	704587	1281971	1604343	1051252	859074	452286	88705	4,68
HLSS-1kDa t0	6.7	278	-3.301	0	5	354667	643002	779376	715232	561065	368160	74081	5,27
LLSS t0	6.7	278	-3.301	0	5	802083	1371549	1386117	1228053	1002895	602396	130381	5,53
HLSS t0	6.7	278	-3.301	0	5	126106	255770	269981	287073	229380	137154	34115	4,50
HLSS-1kDa t0	6.7	278	-3.301	0	5	41119	51361	68061	58553	50487	33027	6773	4,00
LLSS t0	6.7	278	-3.301	0	5	39570	71013	73901	81387	70889	44901	7368	4,23
HLSS t0	6.73	276	-3.523	0	6	704587	1281971	1604343	1051252	859074	452286	88705	4,79
HLSS-1kDa t0	6.73	276	-3.523	0	6	354667	643002	779376	715232	561065	368160	74081	5,07
LLSS t0	6.73	276	-3.523	0	6	802083	1371549	1386117	1228053	1002895	602396	130381	5,39
HLSS t0	6.73	276	-3.523	0	6	126106	255770	269981	287073	229380	137154	34115	4,35
HLSS-1kDa t0	6.73	276	-3.523	0	6	41119	51361	68061	58553	50487	33027	6773	3,66
LLSS t0	6.73	276	-3.523	0	6	39570	71013	73901	81387	70889	44901	7368	3,88
HLSS t0	6.6	276	-1.208	1	5	704587	1281971	1604343	1051252	859074	452286	88705	4,55
HLSS-1kDa t0	6.6	276	-1.208	1	5	354667	643002	779376	715232	561065	368160	74081	4,96
LLSS t0	6.6	276	-1.208	1	5	802083	1371549	1386117	1228053	1002895	602396	130381	5,35
HLSS t0	6.6	276	-1.208	1	5	126106	255770	269981	287073	229380	137154	34115	4,50
HLSS-1kDa t0	6.6	276	-1.208	1	5	41119	51361	68061	58553	50487	33027	6773	3,72
LLSS t0	6.6	276	-1.208	1	5	39570	71013	73901	81387	70889	44901	7368	3,59

Appendix B:

PAHs response factor (Ki) and quantification yield (Ci) in milliQ water and DCM.

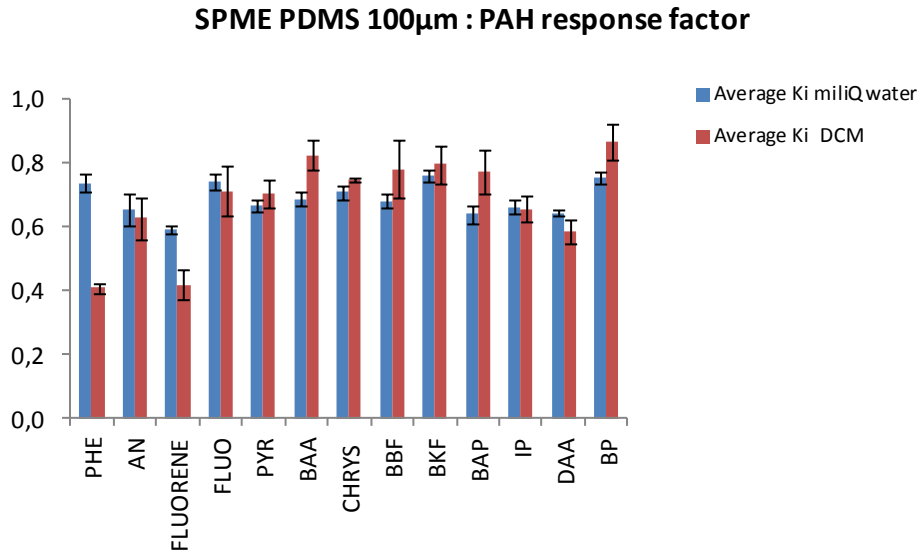

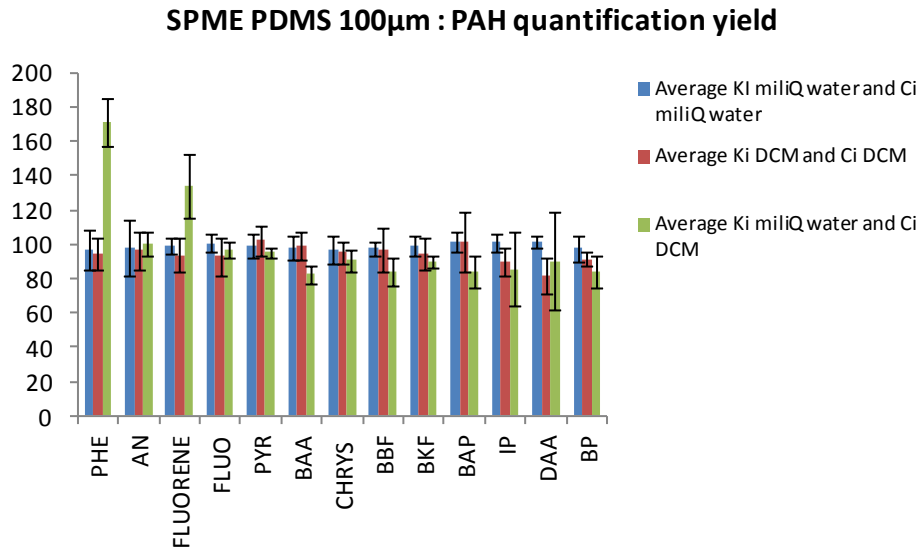

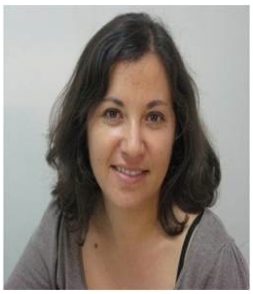

Abstract

Organic micropollutants (OPs) such as PAHs, NP and PCBs, are endocrine disrupters that, within the environment, can deposit to soil, water bodies and sewage system. Anaerobic digestion has been shown as a potential biological process for removing these compounds from sewage sludge. The two main mechanisms that govern their anaerobic removals are the cometabolism and the bioavailability. In this work, cometabolism and bioavailability influences were evaluated focusing mainly on the study of the OP-organic matrix interactions, the determination of the OPs distribution among the physical compartments (free, sorbed to dissolved and colloidal matter (DCM) and sorbed to particles) combined with a detailed physical, chemical and functional matrix characterization. It was found that the OPs removals varied greatly as a function of sludge characteristics. Additionally, kinetics demonstrated that OPs removals are coupled to the first step of the anaerobic digestion, jointly to the OPs transfer from the particles to the aqueous compartment. The OPs are simultaneously removed from the three physical compartments (free, DCM and particles). KDOC and Kpart partition coefficients were calculated to study the OP-organic matrix interactions coupled to a functional characterization by 3D fluorescence of the matrix in order to construct an explicative and predictive model of the OP-organic matrix interactions using partial least square regression (PLS). It was found that the humic acid-like compartment has a great role in the OP-organic matrix interactions mainly in the aqueous phase. Finally, explanatory and predictive PLS models of total OPs removals were constructed. It was concluded that OPs removals are favored by all cometabolic parameters jointly to the aqueous OPs concentration. The predictive model based on the initial sludge characteristics, identified the initial OPs concentrations (free and DCM), representing the bioavailability, and the protein-like, representing the cometabolism influence, as the most important variables that predict the total OPs removals. This study contributes to better understand the OPs distribution among the sludge compartments and its role in the fate and removal of the compounds, to predict this distribution through matter functional characterization and to propose strategies in order to optimize the OPs removals under anaerobic conditions. **(PhD thesis in English)**

Defended on May 29th, 2012 at : UNIVERSITÉ MONTPELLIER 2 SCIENCES ET TECHNIQUES

with the financial support of : CONICYT Ministerio de Educación Gobierno de Chile — UNIVERSITÉ MONTPELLIER 2 SCIENCES ET TECHNIQUES

INRA

INSTITUT NATIONAL DE LA RECHERCHE AGRONOMIQUE

Laboratoire de Biotechnologie de l'Environnement UR50

Avenue des Etangs F-11100 NARBONNE – France

Tel. +00 33 (0)468 425 151 · Fax +00 33 (0) 468 425 160 Email: lbe.contact@supagro.inra.fr

http://www.montpellier.inra.fr/narbonne/